Temporal Progression of *Drosophila* Neural Stem Cell Promoting Neuronal Diversity

by

Noah Robert Dillon

A dissertation accepted and approved in partial fulfillment of the
requirements for the degree of
Doctor of Philosophy
in Biology

Dissertation Committee:

Dr. Adam Miller, Chair

Dr. Chris Doe, Advisor

Dr. Tory Herman, Core Member

Dr. Kryn Stankunas, Core Member

Dr. Matt Smear, Institutional Representative

University of Oregon

Fall 2024

Dissertation Abstract

Noah Robert Dillon

Doctor of Philosophy in Biology

Title: Temporal Progression of *Drosophila* Neural Stem Cells Promoting Neuronal Diversity

How are complex nervous systems generated? During development, a small pool of neural stem cells generates a diverse array of cell type diversity that forms a functional brain. Remarkably, this neuronal diversity is generated in a predictable order. In this dissertation, I report my work in understanding how neural stem cells of the developing *Drosophila melanogaster*, known as neuroblasts, are temporally patterned. My work has established a single-cell RNA sequencing atlas of the early larval stages of neurogenesis that identified key regulators of how neuroblasts progress from a quiescent to a proliferative state. My subsequent studies focused on neuroblast lineages that generate the central brain of the adult. I show that the transcription factor Seven-up is required for switching the production of early to late neuron identities and progressing Type 2 neuroblasts to the end of their lineage (i.e. death). Finally, I show the temporal transcription factor Castor is required for specifying neuron identities born in early larval Type 2 neuroblast lineages. My work shows significant advancements in understanding how the fly brain is generated and provides fruitful future directions to pursue.

This dissertation includes previously published and unpublished co-authored material.

Curriculum vitae

Name of author: Noah Robert Dillon

Graduate and undergraduate schools attended:

University of Oregon, Eugene, OR

University of Puget Sound, Tacoma, WA

Degrees awarded:

Doctor of Philosophy, Biology, 2024, University of Oregon

Bachelor of Science, Biology, 2020, University of Puget Sound

Areas of special interest:

Developmental Biology

Neurogenetics

Stem cells

Professional experience:

Graduate Researcher, University of Oregon, 2021-2024

Laboratory of Dr. Chris Q. Doe

Graduate Employee – Teaching Assistant, University of Oregon, 2020-2021

Associate Editor – Elements magazine, University of Puget Sound 2019-2020

Lab Accessibility and Biology Instructor Assistant, University of Puget Sound 2018-2020

Undergraduate Research Intern, University of Puget Sound, 2017-2020

Laboratory of Dr. Oscar Sosa, 2019-2020

Laboratory of Dr. Siddhartha Ramakrishnan, 2018-2019

Laboratory of Dr. Alyce DeMarais, 2017-2019

Museum Docent, Puget Sound Natural History Museum, 2016-2020

Director Dr. Peter Wimberger

Grants, awards, and honors:

Talk Platform Prize, Seven-up acts in neuroblasts to specify adult *Drosophila* central complex neuron identity and initiate neuroblast decommissioning, Society for Developmental Biology, 2024

Developmental Biology Training Grant, University of Oregon / National Institute of Child Health and Human Disease, 2021-2024

University Enrichment Committee Funds for Research, University of Puget Sound, 2018

Mellam Independent Research Scholarship, University of Puget Sound, 2018

LIASE: Biodiversity in Borneo, Henry Luce Foundation, 2018

Publications

Dillon, N. R. and Doe, C. Q. (2024). Castor is a temporal transcription factor that specifies early born central complex neuron identity. 2024.08.22.609207. *Under review at Development*.

Dillon, N. R., Manning, L., Hirono, K. and Doe, C. Q. (2024). Seven-up acts in neuroblasts to specify adult central complex neuron identity and initiate neuroblast decommissioning. *Development* 151, dev202504.

Epiney, D., Chaya, G. N. M., Dillon, N. R., Lai, S.-L. and Doe, C. Q. (2023). Transcriptional complexity in the insect central complex: single nuclei RNA sequencing of adult brain neurons derived from type 2 neuroblasts. *bioRxiv.* 2023.12.10.571022.

Dillon, N., Cocanougher, B., Sood, C., Yuan, X., Kohn, A. B., Moroz, L. L., Siegrist, S. E., Zlatic, M. and Doe, C. Q. (2022). Single cell RNA-seq analysis reveals temporally-regulated and quiescence-regulated gene expression in Drosophila larval neuroblasts. *Neural Development* 17, 7.

Acknowledgements

My adventure into the sciences has been an unexpected but marvelous journey. My original inspiration for pursing biology came from reading books by Sean B. Carroll and Richard Dawkins while ditching school in rural Wyoming. I have my high school science teachers to thank for keeping me from dropping all my classes. I am grateful to have found a home in the Pacific Northwest for the past eight years attending the University of Puget Sound and then the University of Oregon. My mentors during undergrad were gracious enough to steer me towards a path in scientific research. I am indebted to Dr. Alyce DeMarais, Dr. Siddhartha Ramakrishnan, Dr. Oscar Sosa, Dr. Peter Wimberger, and Dr. Joel Elliott (just to name a few).

I thank Dr. Chris Q. Doe for his mentorship and guidance during my dissertation as I have worked in his lab pursing projects built on a passion for understanding developmental biology. The Doe Lab members (Sarah Ackerman, Nathan Anderson, Elena Barth, Ben Brissette, Arnaldo Carreira-Rosario, Kasey Drake, Derek Epiney, Katie Fisher, Josmarie Graciani, Janet Hanawalt, Emily Heckman, Keiko Hirono, Sen-Lin Lai, Kristen Lee, Laurina Manning, Gonzalo Morales Chaya, Jordan Munroe, Peter Newstein, Heather Pollington, Megan Radler, Tyler Ramos, Natalie Rico Carvajal, Rishi Sastry, Austin Seroka, Alanna Sowles, and Chundi Xu) have, over the past four years, been an incredible support structure that I have cherished in helping me produce work that I am proud to publish. I also thank Dr. Adam Miller, and the Miller Lab, for guidance when I first joined the program in setting me up for success the moment I started at the University of Oregon. I extend gratitude to the rest of my dissertation advisory committee members Dr. Tory Herman, Dr. Matt Smear, and Dr. Kryn Stankunas for their guidance.

For the work in Chapter II, I thank Dr. Sen-Lin Lai, Dr. Cheng-Yu, and Dr. Sarah Ackerman for comments on the manuscript. Funding for this work was provided by NIH Training Grant 5-T32-HD07348, NIH HD27056, and Howard Hughes Medical Institute (Noah Dillon and Chris Doe). I thank my co-authors: Ben Cocanougher, Chhavi Sood, Xin Yuan, Andrea Kohn, Leonid Moroz, Dr. Sarah Siegrist, and Dr. Marta Zlatic for their help in making this work possible. Funding in part was also covered by NIH R35 GM141886 (Sarah Siegrist).

For work in Chapter III, I thank Dr. Kristen Lee, Peter Newstein, Dr. Megan Radler, and Dr. Chundi Xu for internal comments on the manuscript. I also thank Dr. Josie Clowny, Dr. Tzumin Lee and Dr. Mubarak Syed for feedback on the project. Funding for this work was provided by NIH Training Grant 5-T32-HD07348, NIH HD27056, and Howard Hughes Medical Institute (Noah Dillon and Chris Doe). I thank my co-authors Laurina Manning and Keiko Hirono as it was a privilege to work with these gifted scientists.

For work in Chapter IV, I thank Dr. Tory Herman, Derek Epiney and Gonzalo Morales Chaya for comments on the manuscript. I thank Laurina Manning and Jordan Munroe for assistance on the EdU experiments and Dr. Sen-Lin Lai for advice on antibodies. Funding for this work was provided by NIH Training Grant 5-T32-HD07348, NIH HD27056, and Howard Hughes Medical Institute. I thank Chris Doe for motivating me in getting this last paper ready in record time.

I would like to acknowledge the resource centers that make doing high quality science possible: FlyBase (http://flybase.org/) for a wonderful repository of *Drosophila* genetic information; Developmental Studies Hybridoma Bank, created by the NICHD of the NIH and maintained at the University of Iowa, Department of Biology, Iowa City, IA for antibodies; Bloomington Drosophila Stock Center (NIH P40OD018537); and Vienna Drosophila Resource Center for fly stocks; Institute of Molecular Biology Media Room at the University of Oregon for prepping the abundance of fly food used to maintain stocks and for cleaning the lab glassware.

This work was only made possible by the contributions of many in supporting the pursuit of knowledge. I will forever be grateful and indebted to the people who have shown me kindness and respect through my scientific career.

Table of Contents

List of Figures

List of Tables

Chapter I

An introduction to generating neuronal diversity and a complex brain in *Drosophila*

Patterning during *Drosophila* neurogenesis creates neural diversity

Animal behaviors require complex neural circuits, which requires a diverse set of neuronal cell types, to function. An open question in developmental neurobiology remains: How are diverse neurons generated from a small pool of neural stem cells? The primary focus of this chapter will be on the developing *Drosophila* central nervous system. The secondary focus will shift briefly to the matured adult central brain and how it is generated during development. Primary attention is placed on the developing ventral nerve cord and brain lobes with brief mentions of the optic lobes when relevant. The following chapters will cover my contributions to the field. The last chapter will discuss future directions and connect work done in *Drosophila* to mammalian neural development.

An introduction to neuroblasts and the developing nervous system

The neural stem cells in *Drosophila* are known as neuroblasts (NBs). NBs delaminate from the neuroectoderm with each NB having a distinct identity (Broadus et al., 1995; Doe, 1992; Hartenstein and Campos-Ortega, 1984; Wheeler, 1891; Wheeler, 1893) (reviewed in: Hartenstein and Wodarz, 2013; Skeath and Thor, 2003). Early lineage tracing studies show that each NB generates distinct and reproducible cell lineages (Bossing et al., 1996; Doe, 1992; Schmid et al., 1999; Schmidt et al., 1997). The identity of each NB in the ventral nerve cord is controlled by spatial factors that impart a unique molecular profile based on a 'column and row' logic (reviewed in Skeath and Thor, 2003) (Fig 1.1). For example, the row factor Gsb is required for row 5 NB identities (Bhat, 1996; Skeath et al., 1995) (Fig 1.1). The column factor Msh is required for the lateral most column of NB identities (Isshiki et al., 1997) (Fig 1.1). Recent work has shown these combinations of spatial factors to establish NB identity-specific chromatin accessibility (Sen et al., 2019). It remains to be seen if this NB identity chromatin profile is required for establishing unique cell lineages. Similar spatial patterning mechanisms have been seen in the optic lobe NBs (reviewed Rossi et al., 2021). These findings established the first level of generating diverse neuronal cell types in that each NB has a unique identity and produces a

distinct lineage with a defined set of cell types.

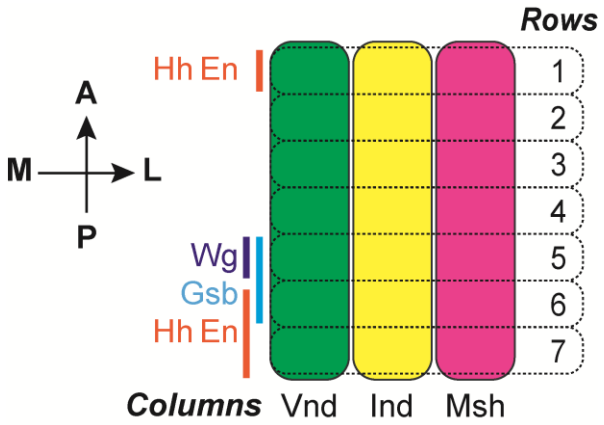

Fig. 1.1 Spatial patterning of neuroblasts in a single hemisegment of the developing *Drosophila* embryonic ventral nerve cord. Neuroblasts have unique spatial identities determined by cross-regulating spatial factors in a row and column logic. Row spatial factors include: Hh, En, Wg, and Gsb (Bhat, 1996; Chu-LaGraff and Doe, 1993; Deshpande et al., 2001; Matsuzaki and Saigo, 1996; McDonald and Doe, 1997; Skeath et al., 1995). Column spatial factors include: Vnd, Ind, and Msh (Isshiki et al., 1997; McDonald et al., 1998; von Ohlen and Doe, 2000; Weiss et al., 1998). A, Anterior; P, Posterior; M, Medial; L, Lateral.

All NBs undergo asymmetric cell divisions to generate smaller progeny while self-renewing for subsequent divisions. There are three NB division patterns (Fig 1.2). Type 0 NBs produce a progeny cell that directly differentiates into its postmitotic neuronal fate (Baumgardt et al., 2014) (Fig 1.2, left). These Type 0 divisions have not been extensively studied and therefore will not be discussed further. Type 1 NBs (T1NBs) produce a transitional progeny cell type known as a ganglion mother cell (GMC) that will divide once to produce a pair of postmitotic cells, neurons or glia (Fig 1.2, middle). Type 2 NBs (T2NBs) have a more complex division with each NB division generating an intermediate neural progenitor (INP) that will asymmetrically divide to produce 4-6 GMCs that each will divide once to produce a pair of postmitotic cells (Bello et al., 2008; Boone and Doe, 2008; Bowman et al., 2008) (Fig 1.2, right). Thus, T2NBs have more neurogenic potential from a single stem cell as each T2NB division will generate a total of 8-12 postmitotic cells compared to the 2 cells generated each T1NB division.

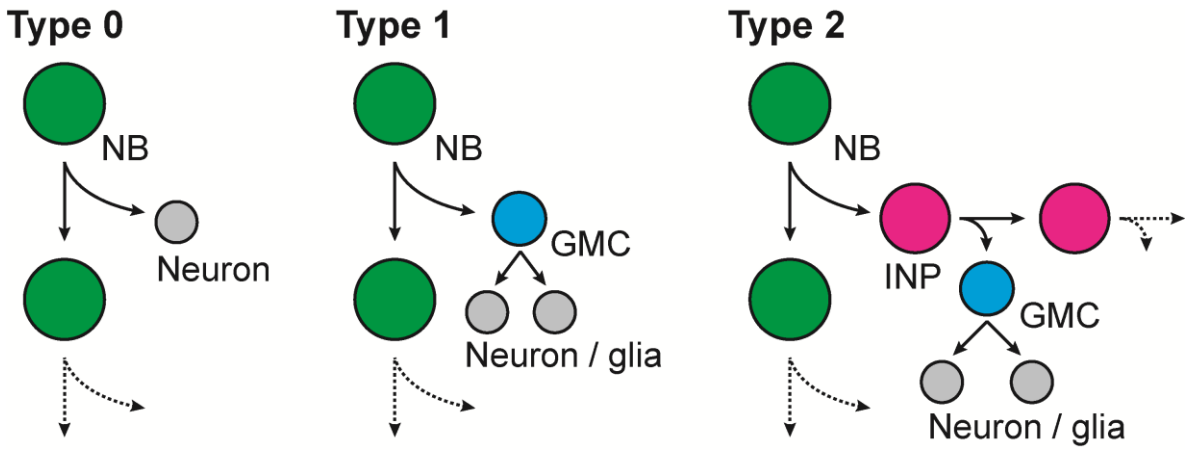

Fig. 1.2 Division patterns of *Drosophila* neuroblasts. Type 0 division (left) is a mode of direct neurogenesis with the NB producing one progeny cell per division. Type 1 division (middle) is indirect neurogenesis with the NB producing one GMC that will divide once to produce two progeny cells per NB division. Type 2 division (right) has the most neurogenic potential with the production of INPs that produces 4-6 GMCs that in total generate 8-12 progeny cells per T2NB division. NB, Neuroblast; GMC, Ganglion Mother Cell; INP, intermediate neural progenitor.

T1NBs have been extensively studied as they comprise the majority of NB lineages in the central nervous system. The ventral nerve cord is divided into 14 repeated segments known are hemisegments that are bilaterally symmetrical across the midline and contain ~30 NBs each for a total of ~420 NBs per ventral nerve cord (Broadus et al., 1995; Hartenstein and Campos-Ortega, 1984; Hartenstein et al., 1994). The central brain lobes contain ~100 T1NBs (Pereanu and Hartenstein, 2006; Younossi-Hartenstein et al., 1996). The optic lobes contain >800 NBs (Bertet et al., 2014; Li et al., 2013; Yasugi et al., 2008). These T1NB lineages generate most of the *Drosophila* central nervous system; thus, it is no surprise that these NB lineages have been the most studied.

T2NBs have been recently discovered and offer an exciting division pattern that closely resembles some primate cortical neural stem cell lineages (reviewed in El-Danaf et al., 2023; Holguera and Desplan, 2018) (discussed more in Chapter V). There are 8 T2NB lineages localized to each central brain lobe; each having a unique spatial identity with 6 lineages that are dorsal medial and 2 lineages dorsal lateral (Bello et al., 2008; Boone and Doe, 2008; Bowman et al., 2008) (Fig 1.3, left). Each T2NB produces a unique cell lineage with morphologically distinct progeny cells that populate the adult brain (Andrade et al., 2019; Pereanu and

Hartenstein, 2006; Riebli et al., 2013; Yang et al., 2013). Moreover, each progenitor cell type within the Type 2 lineages have been identified to express unique markers (Fig 1.3, right; Table 1.1). Thus, the Type 2 lineage has proven to be an excellent model for precise lineage manipulations for understanding the development of neural stem cells and neurons (Bayraktar and Doe, 2013; Dillon et al., 2024; Hamid et al., 2024; Li et al., 2016; Li et al., 2017b; Munroe et al., 2022; Rives-Quinto et al., 2020; San-Juán and Baonza, 2011; Sullivan et al., 2019; Syed et al., 2017; Zhu et al., 2011; Zhu et al., 2012). Type 2 lineages will be discussed in length below and are the focus in Chapters III and IV.

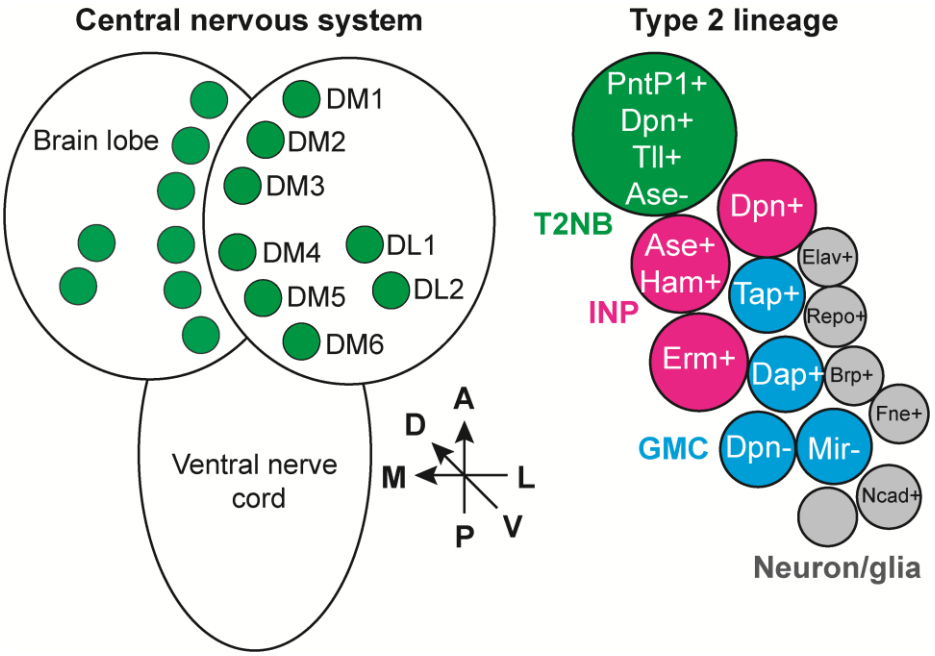

Fig. 1.3 Spatial positioning of Type 2 neuroblast and cell lineage markers. The eight Type 2 neuroblast lineages are bilaterally symmetrical with stereotyped spatial positions in the brain lobes (left). Type 2 neuroblasts generate identifiable lineage clusters of cell types (right). See Table 1.1 for references. A, Anterior; P, Posterior; M, Medial; L, Lateral; D, Dorsal; V, Ventral; DM, Dorsal-medial; DL; Dorsal-lateral; T2NB, Type 2 Neuroblast; INP, Intermediate Neural Progenitor; GMC, Ganglion Mother Cell. PntP1, Pointed; Dpn, Deadpan; Tll, Tailless; Ase, Asense; Ham, Hamlet; Erm, Earmuff; Tap, Target of poxn; Dap, Dacapo; Mir, Miranda; Elav, Rmbryonic lethal abnormal vision; Repo; Reverse polarity; Brp, Bruchpilot; Fne, Found in neurons; Ncad, Neural cadherin.

Table 1.1 Markers distinguishing the Type 2 neuroblast lineage progenitor cell types.

Cell type	Marker	References
Type 2 neuroblast (T2NB)	Deadpan (Dpn) +	(Bello et al., 2008; Bier et al., 1992; Boone and Doe, 2008; Bowman et al., 2008; Rives-Quinto et al., 2020; Zhu et al., 2011)
	Pointed (Pnt) +	
	Tailless (Tll) +	
	Asense (Ase) -	
Intermediate neural progenitor (INP)	Deadpan (Dpn) +	(Bello et al., 2008; Boone and Doe, 2008; Bowman et al., 2008; Li et al., 2016; Rives-Quinto et al., 2020; Zhu et al., 2011)
	Asense (Ase) +	
	Hamlet (Ham) +	
	Earmuff (Erm) +	
Ganglion mother cell (GMC)	Target of Poxn (Tap) +	(Ikeshima-Kataoka et al., 1997; Lane et al., 1996; Michki et al., 2021)
	Dacapo (Dap) +	
	Deadpan (Dpn) -	
	Miranda (Mir) -	
Glia	Reverse polarity (Repo) +	(Campbell et al., 1994; Xiong et al., 1994)
Neuron	Embyonic lethal abnormal vision (Elav) +	(Robinow and White, 1991; Samson and Chalvet, 2003; Wagh et al., 2006; Young and Armstrong, 2010)
	Bruchpilot (Brp) +	
	Found in neurons (Fne) +	
	Neural cadherin (Ncad) +	

The discovery of temporal transcription factors

In addition to the spatial factors determining the unique NB identities, temporal patterning within the lineages have been extensively studied as a mechanism for generating neuronal diversity. Embryonic NBs were first observed to sequentially express a series of transcription factors that were hypothesized to regulate temporal fate decisions (Brody and Odenwald, 2000; Kambadur et al., 1998). Isshiki et al. first discovered the canonical embryonic temporal transcription factor (TTF) cascade where narrow windows of transiently expressed factors, TTFs, in the NBs are required and sufficient to specify individual neuron identities (Isshiki et al., 2001) (Fig 1.4). Subsequent work has shown this TTF cascade to be a widely used mechanism across most embryonic T1NB lineages, persists in larval NBs, and is cross-regulating (Almeida and Bray, 2005; Baumgardt et al., 2014; Benito-Sipos et al., 2011; Cenci and Gould, 2005; Cleary and Doe, 2006; Grosskortenhaus, 2006; Grosskortenhaus et al., 2005; Meng et al., 2019; Meng et al., 2020; Moris-Sanz et al., 2014; Novotny et al., 2002; Pearson and Doe, 2003; Seroka and Doe, 2019; Tran and Doe, 2008) (Fig 1.4).

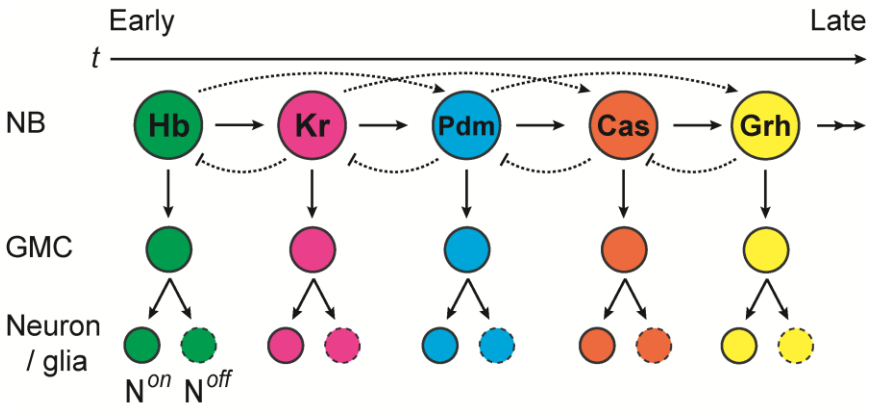

Fig. 1.4 The canonical temporal transcription factor cascade of embryonic Type 1 neuroblasts in the ventral nerve cord. Most embryonic T1NBs of the ventral nerve cord will transiently express the series of Hb, Kr, Pdm, Cas, and Grh. Variations of this temporal cascade is seen across some NB lineages (reviewed in: Doe, 2017; Pearson and Doe, 2004; Pollington et al., 2023). Hemilineages are formed during the GMC division when one daughter cell receives a N^{on} cue and the other cell a N^{off} signal. Dashed lines indicate cross-regulatory relationship between the TTFs. Hb, Hunchback; Kr, Krüppel; Pdm, POU Domain protein; Cas, Castor; Grh, Grainyhead; NB, Neuroblast; GMC, Ganglion Mother Cell; N, Notch; TTF, Temporal Transcription Factor.

The most extensively studied T1NB lineage for understanding TTFs has been NB 7-1 with the earliest TTF Hb studied the most within this lineage (Grosskortenhaus et al., 2005; Hirono et al., 2017; Isshiki et al., 2001; Kanai et al., 2005; Kohwi et al., 2011; Meng et al., 2019; Meng et al., 2020; Pearson and Doe, 2003; Seroka and Doe, 2019; Seroka et al., 2020; Seroka et al., 2022) (reviewed in Doe, 2017; Pollington et al., 2023). Hb was reported to be required and sufficient for specifying the first two neuron cell fates born from NB 7-1, motor neurons U1 and U2 (Isshiki et al., 2001). Recent studies have demonstrated that Hb is required for proper U motor neuron dendritic morphology and targeting to body wall muscles (Meng et al., 2019; Meng et al., 2020; Seroka and Doe, 2019). Interestingly, after more than 20 years since its discovery as a TTF, a mechanism for Hb in specifying the U1 and U2 motor neurons has not been identified (i.e., U1/U2 specific identity genes activated by Hb). Previous work has shown that Hb binds differentially across NB lineages 5-6 and 7-4 due to a difference in lineage-specific chromatin accessibility imparted by spatial factors (Sen et al., 2019). These studies suggest that determining the DNA-binding targets of TTFs across NB lineages will provide insight into the mechanism for specifying diverse cell fates. It remains an open question how any TTF acts within any NB lineage to specify unique identities.

Larval INPs, derived from T2NBs, display a similar temporal patterning progression as embryonic T1NBs. INPs express a series of cross-regulatory TTFs as INPs age (Bayraktar and Doe, 2013; Tang et al., 2022) (Fig 1.5). Most INP TTFs have been validated for being required to specify neuronal fates based on molecular markers and adult neuron morphology (Bayraktar and Doe, 2013; Sullivan et al., 2019). Neurons derived from INPs express markers tied to their INP temporal window. Young INP derived neurons generally express Dichaete, Runt, or Bsh (Bayraktar and Doe, 2013; Sullivan et al., 2019) (Fig 1.5). Old INP derived glia express Repo and the neurons Toy (Bayraktar and Doe, 2013) (Fig 1.5). It remains unknown if some of these markers are maintained from the larval to adult stages. Interestingly, the glia (Repo+) are restricted to an early T2NB window and Bsh+ neurons to a late T2NB window (Bayraktar and Doe, 2013). These data suggest that the temporal patterning in INPs can act in combination with temporal patterning of T2NBs to generate significant cell type diversity (discussed below). It remains unknown if Type 2 GMCs produce N^{on} and N^{off} hemilineages, as seen in the embryonic T1NB lineages. If hemilineages exist in the Type 2 lineage, this would provide a fourth mechanism (1 - Spatial, 2 – T2NB temporal, 3 - INP temporal, 4 - hemilineage) for generating the neuronal diversity seen in the adult brain.

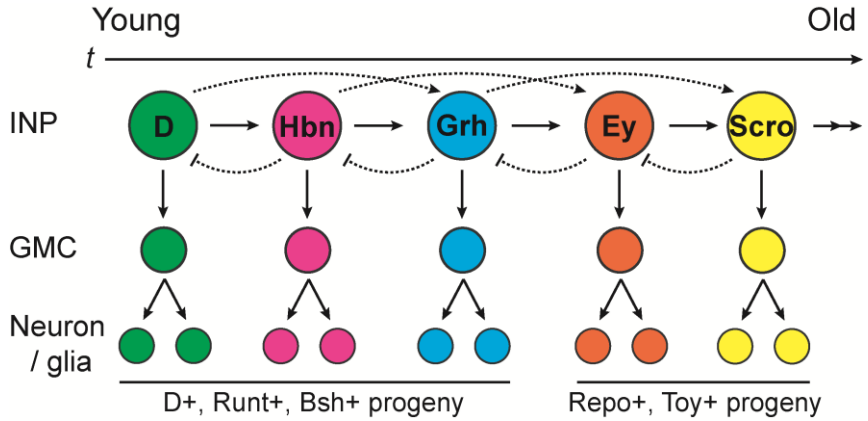

Fig. 1.5 The temporal transcription factor cascade of larval Type 2 intermediate neural progenitors. Larval INPs express a series of TTFs as they age from young (recently derived from the T2NB) INPs that produce D+, Runt+, and Bsh+ progeny to old (final divisions for the INP) INPs that produce Repo+ and Toy+ progeny (Bayraktar and Doe, 2013; Sullivan et al., 2019; Tang et al., 2022). Dashed lines indicate cross-regulatory relationship between the TTFs. D, Dichaete; Hbn, Homeobrain; Grh, Grainyhead; Ey, Eyeless; Scro, Scarecrow; INP, Intermediate Neural Progenitor; GMC, Ganglion Mother Cell; N, Notch; TTF, Temporal Transcription Factor.

Temporal progression in the larval neuroblasts

Most late-stage embryonic T1NBs and T2NBs will enter quiescence, cell cycle arrest when the NB does not divide, and reactivate ~12-24h after larval hatching (Munroe et al., 2022; Prokop and Technau, 1991; Truman and Bate, 1988) (Fig 1.6). The reactivation of larval NBs requires insulin signaling with quiescent NBs shown to be primed to respond to Insulin-like peptides to reactive proliferation (Chell and Brand, 2010; Dillon et al., 2022; Otsuki and Brand, 2018; Sousa-Nunes et al., 2011) (Fig 1.6; see Chapter II). Additionally, glia secrete the signaling molecules Ana and Trol to inhibit NB proliferation and promote NB proliferation, respectively, to temporally control neurogenesis in the early larvae (Datta, 1995; Datta, 1999; Ebens et al., 1993) (Fig 1.6). Quiescent NBs have been shown to repress Artichoke (Atk) and reactivate proliferation based on a dorsal-ventral positioning due to a heterogeneity in arrested cell stated of G_0 or G_2 (Otsuki and Brand, 2018; Otsuki and Brand, 2019). Additionally, Hh has been suggested to play a role in regulating quiescence downstream of the embryonic TTF cascade (Chai et al., 2013). Recent work has shown that the RNA-binding protein IGF-II mRNA-binding protein (Imp) is required for T2NBs to exit from quiescence (Munroe et al., 2022). It remains to be seen if this cue is also required for other NB lineages. Ongoing work aims to understand the mechanisms controlling the reactivation of NBs in the larval stages with the transcription factor Foxo suspected to be an essential regulator (see Dr. Sarah Siegrist's lab: https://siegristlab.org/research/; personal communication). See Chapter V for further discussion.

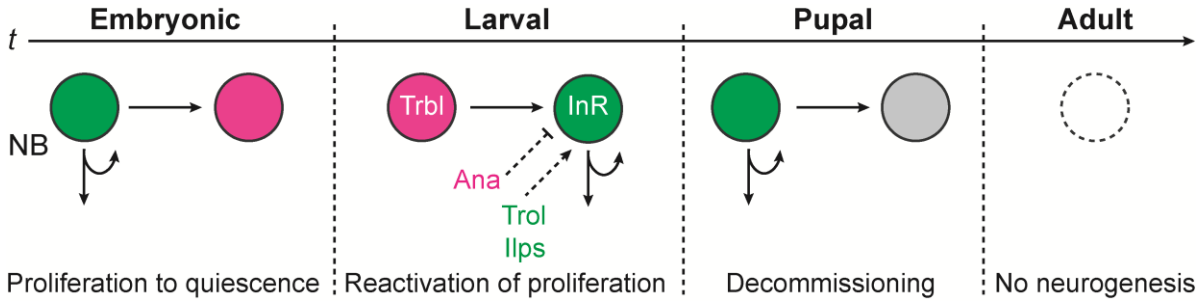

Fig. 1.6 Neuroblast progression of neurogenesis across fly development. Embryonic NBs proliferate until late stages when most lineages enter quiescence. Larval NBs express Trbls during quiescence with Ana secreted by glia to inhibit proliferation (Datta, 1995; Datta, 1999; Ebens et al., 1993). NBs express InR and are reactivated by signaling molecules Trol and Ilps (Chell and Brand, 2010; Datta, 1995; Datta, 1999; Dillon et al., 2022; Sousa-Nunes et al., 2011). Green indicates proliferating NB, magenta a quiescent NB, and grey a

decommissioning NB. Dashed lines indicate regulatory inputs. NB, Neuroblast; Trbl, Tribbles; Ana, Anachronism; InR, Insulin Receptor; Trol, Terribly reduce optic lobes; Ilps, Insulin like peptides.

Larval NBs, excluding the optic lobes, have been less studied than embryonic NBs with an open question remaining about how temporal patterning occurs during larval stages. Mushroom body T1NBs have been shown to express opposing temporal gradients of the RNA-binding proteins Imp and Syncrip that are required for proper specification of neuronal fates (Liu et al., 2015). Imp is expressed at high levels in early larval NBs and decreases in expression level as Syncrip increases in expression level during later stages (Liu et al., 2015). The temporal gradient of Imp and Syncrip has been seen in the T2NB lineages (Ren et al., 2017; Syed et al., 2017) (Fig 1.7). This suggests that larval NB lineages may use the broad protein gradients as a mechanism for temporal patterning instead of the narrow windows of TTF expression. This is supported by several studies showing that Imp and Syncrip gradients in the T2NBs and INPs are required for specifying some neuronal fates (Hamid et al., 2024; Munroe and Doe, 2023; Ren et al., 2017; Syed et al., 2017). Alternatively, candidate TTFs have been identified as temporally expressed within T2NBs and may be required to specify neuronal identities, similar to the embryonic T1NB lineages (Bayraktar and Doe, 2013; Ren et al., 2017; Syed et al., 2017). Recent unpublished studies indicate the these candidate TTFs are indeed necessary for specifying neuronal identities (Wani et al., 2023 preprint) (Dillon and Doe, 2024, preprint; see Chapter IV). Regardless of the mechanism, the temporal progression in T2NBs is required for specifying birth order-dependent neuronal identities (Dillon et al., 2024). These data suggest that both protein gradients and TTFs regulate temporal patterning in the larval T2NBs.

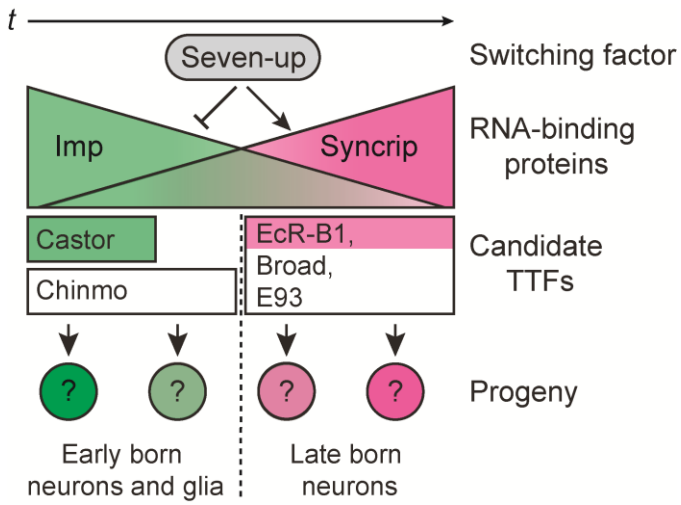

Fig. 1.7 Temporal patterning of the Type 2 neuroblast in larval stages. T2NBs express opposing gradients of the RNA-binding proteins Imp and Syncrip (Ren et al., 2017; Syed et al., 2017). Seven-up is known to be required for switching the temporal progression from early-to-late (Dillon et al., 2024; Ren et al., 2017; Syed et al., 2017). Candidate TTFs are hypothesized to specify neuronal fates (Bayraktar and Doe, 2013; Dillon et al., 2024; Ren et al., 2017; Syed et al., 2017). Green indicates a relationship to an early temporal fates and magenta a relationship to a late temporal fates (Bayraktar and Doe, 2013; Dillon et al., 2024; Hamid et al., 2024; Ren et al., 2017; Syed et al., 2017) (Dillon and Doe, 2024, preprint). White indicates an unvalidated relationship. T2NB, Type 2 Neuroblast; Imp, IGF-II mRNA-binding protein; EcR-B1, Ecdysone Receptor isoform 1B; E93, Ecdysone induced protein 93; TTF, Temporal Transcription Factor.

The mechanism for temporal progression in proliferating larval NBs remains unknown. Recent work has shown that the early factor Imp is required for reactivation of proliferation (Munroe et al., 2022). Additionally, the Imp and Syncrip gradients are cross-regulatory for the early-to-late progression (Liu et al., 2015; Ren et al., 2017). The switching factor Seven-up has been identified as being required for regulating this transition and the T2NB production switch from early-to-late identity neurons (Dillon et al., 2024; Ren et al., 2017; Syed et al., 2017) (Fig 1.7). This role for Seven-up as a switching has also been seen in the embryonic and larval T1NBs (Benito-Sipos et al., 2011; Kanai et al., 2005; Kohwi et al., 2011; Maurange et al., 2008; Mettler et al., 2006). The ecdysone receptor isoform B1 (EcR-B1) is also required for initiating the early-to-late switch and acts downstream of Seven-up in T2NBs (Syed et al., 2017). These data suggest that both intrinsic (Imp, Syncrip, and Seven-up) and extrinsic (EcR-B1 and ecdysone signaling) are required for temporal progression in proliferating T2NBs. It remains unknown what other factors are involved. See Chapter V for further discussion.

Larval NBs go through decommissioning, a process where the NB will stop proliferating to either differentiate into a postmitotic cell fate or undergo cell death (Fig 1.6). Most larval NBs decommission in the late larval or early pupal stages (Homem et al., 2014; Ito and Hotta, 1992; Maurange et al., 2008; Narbonne-Reveau et al., 2016; Siegrist et al., 2010; Yang et al., 2017). This process in the T1NBs is initiated by the Imp-to-Syncrip transition with atypically high Imp expression sustaining mushroom body NBs to continue proliferating longer than other T1NB lineages (Yang et al., 2017). Thus, it is no surprise that Seven-up is required for T1NB and T2NB lineages to initiate the timely onset of decommissioning as this switching factor acts upstream of the Imp-to-Syncrip transition (Dillon et al., 2024; Maurange et al., 2008; Narbonne-Reveau et al., 2016). Interestingly, the expression of Seven-up is early in the larval T2NBs at ~24h yet decommissioning occurs in the early pupal stages, days after Seven-up is no longer expressed (Bayraktar and Doe, 2013; Dillon et al., 2024; Homem et al., 2014; Ren et al., 2017; Syed et al., 2017). It remains unknown how Seven-up acts to initiate temporal progression for the onset of decommissioning in T2NB. See Chapter V for further discussion.

Establishing complexity within the *Drosophila* central brain

As discussed in the previous section, neurogenesis in the developing *Drosophila* central nervous system produces diverse neuronal cell types. The integration of spatial patterning of distinct NB lineages and the subsequent temporal patterning provide a robust framework for understanding neurogenesis that has been extensively reviewed (reviewed in Doe, 2017; El-Danaf et al., 2023; Pearson and Doe, 2004; Pollington et al., 2023; Rossi et al., 2021; Skeath and Thor, 2003). The result of these 5 days of neurogenesis leads to the adult fruit fly that contains the complex neural circuitry to allow context-dependent behavior. This section will focus on the adult central brain with brief mentions of some circuits. The cell type diversity and function of the larval nervous system will not be discussed here.

The diversity and function of the Central Complex

An extensively studied region of the adult *Drosophila* brain is the Central Complex (CX). The CX is comprised of four neuropils, regions of high synaptic connectivity, known as the Protocerebral Bridge (PB), Fan-shaped Body (FB), Ellipsoid Body (EB), and Noduli (NO) (Hanesch et al., 1989) (Fig 1.8, left). The main two classes of neurons in the CX are the tangential neurons that are transversally oriented and the columnar neurons that are longitudinally oriented (Hanesch et al., 1989). These broad neuron classes have distinct functions in the CX and arise from distinct NB lineages.

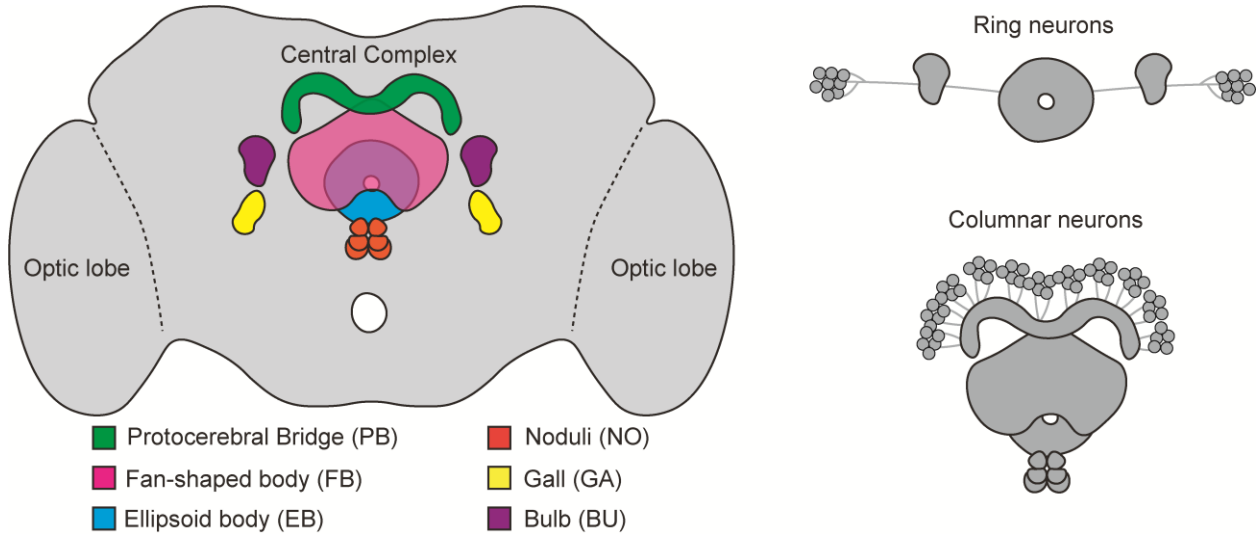

Fig. 1.8 The adult Central Complex neuropils and neurons. The CX is comprised of four main neuropils: PB, FB, EB, and NO. Other neuropils to note are the GA and BU (left). Most

studied neurons of the CX include the tangential Ring neurons and the columnar neurons (right). CX, Central Complex; PB, Protocerebral Bridge; FB, Fan-shaped Body; EB, Ellipsoid Body; NO, Noduli; GA, Gall; BU, Bulb. Figure diagrams inspired and adapted from: Wolff and Rubin, 2018; Seeling and Jayaraman 2013.

Ring neurons have been the most studied of the tangential neurons. These neurons bridge the anterior optic tubercle, the dominant visual input region, to columnar neurons to form the anterior visual pathway circuit (Omoto et al., 2017; Seelig and Jayaraman, 2013). Importantly, Ring neurons provide spatially organized visual information to the CX circuitry (Omoto et al., 2017; Timaeus et al., 2020). These Ring neurons are characterized by their unique morphology in targeting the Bulb (BU), their concentric rings within the EB, and laterally located cell bodies (Renn et al., 1999; Young and Armstrong, 2010) (Fig 1.8, right). The Ring neurons are derived from two T1NB lineages with other tangential neurons derived from both T1NB and T2NB lineages (Bridi et al., 2019; Larsen et al., 2009; Omoto et al., 2017; Wong et al., 2013; Yang et al., 2013). One lineage tracing study has demonstrated that Ring neuron subtypes are born in a birth order-dependent manner with unique molecular markers across embryonic, larval, and pupal stages (Bridi et al., 2019). It will be important work investigating the mechanisms behind the specification of tangential neurons. Interest should be placed in the Ring neurons as they provide a system of two T1NB lineages that generate a diverse class of neurons across all of *Drosophila* neurogenesis.

The majority of the CX is generated from T2NBs starting from late-stage embryo and into the pupal stages (Riebli et al., 2013; Walsh and Doe, 2017). The four T2NB lineages DM1-4 (Fig 1.3, left) generate all the adult columnar neurons (Andrade et al., 2019; Ito and Hotta, 1992; Pereanu and Hartenstein, 2006; Riebli et al., 2013; Yang et al., 2013) These columnar neurons are characterized by their apical cell body location with the majority innervating the PB, a subset of other CX neuropils, and occasionally neuropils outside of the CX (reviewed in Pfeiffer and Homberg, 2014) (Fig 1.8, right). Lineage tracing studies have shown that columnar neuron subtypes are born in a birth order-dependent manner (Andrade et al., 2019; Riebli et al., 2013; Walsh and Doe, 2017). Thus, columnar neurons provide an excellent model for understanding temporal patterning in the T2NB that give rise to this unique class of neurons.

Due to the diversity in CX neuron morphology, these neurons are named after the neuropils they innervate for a dendrite-axon naming convention (Wolff and Rubin, 2018; Wolff et al., 2015). For example, E-PG neurons are named for their dendrite targeting to the EB and axonal targeting to the PB and GA. Similarly, P-EN neurons are named for their dendritic targeting of the PB and axonal targeting to the EB and NO. Connectomes of the CX show hundreds of morphologically distinct neuron subtypes with complex synaptic connectivity (Franconville et al., 2018; Hulse et al., 2021; Scheffer et al., 2020; Zheng et al., 2018). Studies in other insect specicies has shown conserved and evolutionarily divergent neuroarchitecture with the *Drosophila* CX (reviewed in Pfeiffer and Homberg, 2014). These studies show that the CX is primed as a model for understanding not only developmental biology but also probe questions about evolution and systems neuroscience.

Research on the circuitry of the CX has focused on the integration of visual sensory input and the locomotor output with some recent work aiming to understand the CX's role in sleep (reviewed in: Fisher, 2022; Helfrich-Förster, 2018; Strauss, 2002; Turner-Evans and Jayaraman, 2016). The most studied role of the CX has been in navigational behavior. The EB can be considered the fly's compass as the directional heading of the adult fly is encoded in the EB and can be maintained even in the absence of a visual stimulus (Green et al., 2017; Green et al., 2019; Seelig and Jayaraman, 2013; Turner-Evans et al., 2017; Turner-Evans et al., 2020). The two columnar identities of E-PG and P-EN neurons are integrated to maintain and continuously update directional heading from sensory cues (Green et al., 2017; Green et al., 2019; Turner-Evans et al., 2017; Turner-Evans et al., 2020). Surprisingly, the P-EN neurons were found to contain two subtypes, P-ENa and P-ENb neurons, based on behavioral differences (Green et al., 2017). Subsequent EM reconstructions have identified morphological differences in synaptic connectivity initially missed by light microscopy (Scheffer et al., 2020; Turner-Evans et al., 2020; Wolff et al., 2015). The visual inputs for the directional heading circuit is encoded by the Ring neurons (discussed above), and other similar neuron classes not discussed here, connecting the visual system to the CX via the EB (Omoto et al., 2017; Seelig and Jayaraman, 2013; Timaeus et al., 2020). It remains an open question how these CX circuits are initially formed and if there is an underlining developmental mechanism that connects these neuron subtypes. For example: Are the CX neurons that are wired together born in the same temporal windows and are

their identities specified by shared temporal factors? See Chapters III and IV for studies on the development of E-PG and P-EN neurons and Chapter V for further discussion.

Tools for accessing the Central Complex

While connectomes of the CX provide unparallel access to the morphology and connectivity of neurons, they fail to provide data on the genetic programs underlining the brain's development. Recent single-cell/ single-nuclei RNA sequencing (scRNAseq) datasets of the adult *Drosophila* brain demonstrate that neurons are equally diverse in their transcriptomes as they are in morphology (Abruzzi et al., 2017; Croset et al., 2018; Davie et al., 2018; Epiney et al., 2023, preprint; Janssens et al., 2021; Li et al., 2017a). The Doe lab (https://www.doelab.org/) has ongoing work with a comprehensive dataset on adult neurons and glia derived from the T2NB lineages (Epiney et al., 2023, preprint). This work has identified unique molecular markers that distinguish CX neuron identities and provide support that combinatorial expression patterns define diverse neuronal cell types (Epiney et al., 2023, preprint). Importantly, these data sets provide access to the transcriptomes of individual neuronal subtypes. These data support a model similar to that found in *C. elegans* where combinations of homeodomain transcription factors delineate all neuronal cell types (Reilly et al., 2020). It remains to be seen if this is consistent across NB lineages in *Drosophila* much less vertebrate nervous systems, both of which contain significantly more neuronal diversity. These large transcriptomic datasets are valuable tools for understanding neuron diversity and building testable hypotheses prior to running experiments.

One of the greatest genetic tools in *Drosophila* neurobiology has been the development and wide use of the UAS/Gal4 and LexA/LexAop systems (Brand and Perrimon, 1993; Fischer et al., 1988; Lai and Lee, 2006; Szüts and Bienz, 2000). These tools allow selective expression of genetic constructs in cell-specific patterns to provide spatial and temporal control, a geneticist's dream. Combined with the recent advancements in CRISPR/Cas9 tools to use in flies, tissue-specific genetic knockouts offer a tool to study null mutations with precision of the affected cell types (Ewen-Campen et al., 2017; Port and Bullock, 2016; Port et al., 2020). Most relevant for the CX has been the extensive Gal4 and LexA lines that label hundreds of CX neuron types (Jenett et al., 2012; Wolff and Rubin, 2018; Wolff et al., 2015). These genetic stocks have allowed for the precise labeling of CX neuron molecular identity (i.e., pattern of Gal4 and LexA

expression) and labeling of neuron morphology. In addition to these genetic markers, several studies have identified unique transcription factors for CX cell types that can be identified through immunohistochemistry (Bayraktar and Doe, 2013; Dillon et al., 2024; Epiney et al., 2023; Sullivan et al., 2019) (Dillon and Doe, 2024, preprint). The tools described approve have been used extensively throughout the following work to investigate the development of the CX.

Bridge

This chapter covered the development of the *Drosophila* central nervous system starting at the delamination of the NB from embryonic neuroectoderm. I describe how NBs are spatially patterned to produce unique NBs identities and how each NB identity generates unique cell lineages. I focused on how temporal patterning by TTFs are required for generating neuronal diversity in embryonic T1NB lineages. It remains an open question whether temporal protein gradients or TTFs act as temporal patterning mechanisms in the larval T1NB and T2NB lineages. Furthermore, it is unknown how the larval NB lineages temporally progress in exiting from quiescence to proliferating and eventually decommissioning. I shifted focus to discuss how the adult CX is comprised of diverse cell types that are apart of important behavioral neural circuits. I finished the chapter by discussing the available tools used to study the CX.

In the following chapters, I present my previously published and unpublished work investigating the development of the *Drosophila* central nervous system. Chapter II will cover my 2022 publication that investigated a large scRNAseq dataset across multiple stages of early larval development. Chapter III will cover my 2024 publication that shows Seven-up is required in T2NB lineages for important temporal progression of a) switching production from early-to-late neuron identities and b) initiating T2NB decommissioning. Chapter IV covers my recent work, under review at Development, on how Castor acts as a TTF in T2NBs to specify early born CX identities. The last chapter, Chapter V, will discuss future directions from my work and others. Additionally, I will cover the similarities and differences between neurogenesis in the fly and mammalian brains.

References

Abruzzi, K. C., Zadina, A., Luo, W., Wiyanto, E., Rahman, R., Guo, F., Shafer, O. and Rosbash, M. (2017). RNA-seq analysis of Drosophila clock and non-clock neurons reveals neuron-specific cycling and novel candidate neuropeptides. *PLOS Genet.* 13, e1006613.

Almeida, M. S. and Bray, S. J. (2005). Regulation of post-embryonic neuroblasts by Drosophila Grainyhead. *Mech. Dev.* 122, 1282–1293.

Andrade, I. V., Riebli, N., Nguyen, B.-C. M., Omoto, J. J., Cardona, A. and Hartenstein, V. (2019). Developmentally Arrested Precursors of Pontine Neurons Establish an Embryonic Blueprint of the Drosophila Central Complex. *Curr. Biol.* 29, 412-425.e3.

Baumgardt, M., Karlsson, D., Salmani, B. Y., Bivik, C., MacDonald, R. B., Gunnar, E. and Thor, S. (2014). Global Programmed Switch in Neural Daughter Cell Proliferation Mode Triggered by a Temporal Gene Cascade. *Dev. Cell* 30, 192–208.

Bayraktar, O. A. and Doe, C. Q. (2013). Combinatorial temporal patterning in progenitors expands neural diversity. *Nature* 498, 449–455.

Bello, B. C., Izergina, N., Caussinus, E. and Reichert, H. (2008). Amplification of neural stem cell proliferation by intermediate progenitor cells in Drosophila brain development. *Neural Develop.* 3, 5.

Benito-Sipos, J., Ulvklo, C., Gabilondo, H., Baumgardt, M., Angel, A., Torroja, L. and Thor, S. (2011). Seven up acts as a temporal factor during two different stages of neuroblast 5-6 development. *Development* 138, 5311–5320.

Bertet, C., Li, X., Erclik, T., Cavey, M., Wells, B. and Desplan, C. (2014). Temporal patterning of neuroblasts controls Notch-mediated cell survival through regulation of Hid or Reaper. *Cell* 158, 1173–1186.

Bhat, K. M. (1996). The patched signaling pathway mediates repression of gooseberry allowing neuroblast specification by wingless during Drosophila neurogenesis. *Dev. Camb. Engl.* 122, 2921–2932.

Bier, E., Vaessin, H., Younger-Shepherd, S., Jan, L. Y. and Jan, Y. N. (1992). deadpan, an essential pan-neural gene in Drosophila, encodes a helix-loop-helix protein similar to the hairy gene product. *Genes Dev.* 6, 2137–2151.

Boone, J. Q. and Doe, C. Q. (2008). Identification of *Drosophila* type II neuroblast lineages containing transit amplifying ganglion mother cells. *Dev. Neurobiol.* 68, 1185–1195.

Bossing, T., Udolph, G., Doe, C. Q. and Technau, G. M. (1996). The Embryonic Central Nervous System Lineages of*Drosophila melanogaster*. *Dev. Biol.* 179, 41–64.

Bowman, S. K., Rolland, V., Betschinger, J., Kinsey, K. A., Emery, G. and Knoblich, J. A. (2008). The Tumor Suppressors Brat and Numb Regulate Transit-Amplifying Neuroblast Lineages in Drosophila. *Dev. Cell* 14, 535–546.

Brand, A. H. and Perrimon, N. (1993). Targeted gene expression as a means of altering cell fates and generating dominant phenotypes. *Dev. Camb. Engl.* 118, 401–415.

Bridi, J. C., Ludlow, Z. N. and Hirth, F. (2019). Lineage-specific determination of ring neuron circuitry in the central complex of *Drosophila*. *Biol. Open* 8, bio045062.

Broadus, J., Skeath, J. B., Spana, E. P., Bossing, T., Technau, G. and Doe, C. Q. (1995). New neuroblast markers and the origin of the aCC/pCC neurons in the Drosophila central nervous system. *Mech. Dev.* 53, 393–402.

Brody, T. and Odenwald, W. F. (2000). Programmed transformations in neuroblast gene expression during Drosophila CNS lineage development. *Dev. Biol.* 226, 34–44.

Campbell, G., Göring, H., Lin, T., Spana, E., Andersson, S., Doe, C. Q. and Tomlinson, A. (1994). RK2, a glial-specific homeodomain protein required for embryonic nerve cord condensation and viability in Drosophila. *Dev. Camb. Engl.* 120, 2957–2966.

Cenci, C. and Gould, A. P. (2005). Drosophila Grainyhead specifies late programmes of neural proliferation by regulating the mitotic activity and Hox-dependent apoptosis of neuroblasts. *Dev. Camb. Engl.* 132, 3835–3845.

Chai, P. C., Liu, Z., Chia, W. and Cai, Y. (2013). Hedgehog Signaling Acts with the Temporal Cascade to Promote Neuroblast Cell Cycle Exit. *PLoS Biol.* 11, e1001494.

Chell, J. M. and Brand, A. H. (2010). Nutrition-Responsive Glia Control Exit of Neural Stem Cells from Quiescence. *Cell* 143, 1161–1173.

Chu-LaGraff, Q. and Doe, C. Q. (1993). Neuroblast specification and formation regulated by wingless in the Drosophila CNS. *Science* 261, 1594–1597.

Cleary, M. D. and Doe, C. Q. (2006). Regulation of neuroblast competence: multiple temporal identity factors specify distinct neuronal fates within a single early competence window. *Genes Dev.* 20, 429–434.

Croset, V., Treiber, C. D. and Waddell, S. (2018). Cellular diversity in the Drosophila midbrain revealed by single-cell transcriptomics. *eLife* 7, e34550.

Datta, S. (1995). Control of proliferation activation in quiescent neuroblasts of the Drosophila central nervous system. *Development* 121, 1173–1182.

Datta, S. (1999). Activation of neuroblast proliferation in explant culture of the Drosophila larval CNS. *Brain Res.* 818, 77–83.

Davie, K., Janssens, J., Koldere, D., De Waegeneer, M., Pech, U., Kreft, Ł., Aibar, S., Makhzami, S., Christiaens, V., Bravo González-Blas, C., et al. (2018). A Single-Cell Transcriptome Atlas of the Aging Drosophila Brain. *Cell* 174, 982-998.e20.

Deshpande, N., Dittrich, R., Technau, G. M. and Urban, J. (2001). Successive specification of Drosophila neuroblasts NB 6-4 and NB 7-3 depends on interaction of the segment polarity genes wingless, gooseberry and naked cuticle. *Dev. Camb. Engl.* 128, 3253–3261.

Dillon, N. R. and Doe, C. Q. (2024). Castor is a temporal transcription factor that specifies early born central complex neuron identity. 2024.08.22.609207.

Dillon, N., Cocanougher, B., Sood, C., Yuan, X., Kohn, A. B., Moroz, L. L., Siegrist, S. E., Zlatic, M. and Doe, C. Q. (2022). Single cell RNA-seq analysis reveals temporally-regulated and quiescence-regulated gene expression in Drosophila larval neuroblasts. *Neural Develop.* 17, 7.

Dillon, N. R., Manning, L., Hirono, K. and Doe, C. Q. (2024). Seven-up acts in neuroblasts to specify adult central complex neuron identity and initiate neuroblast decommissioning. *Development* 151, dev202504.

Doe, C. Q. (1992). Molecular markers for identified neuroblasts and ganglion mother cells in the Drosophila central nervous system. *Development* 116, 855–863.

Doe, C. Q. (2017). Temporal Patterning in the Drosophila CNS. *Annu. Rev. Cell Dev. Biol.* 33, 219–240.

Ebens, A. J., Garren, H., Cheyette, B. N. R. and Zipursky, S. L. (1993). The Drosophila anachronism locus: A glycoprotein secreted by glia inhibits neuroblast proliferation. *Cell* 74, 15–27.

El-Danaf, R. N., Rajesh, R. and Desplan, C. (2023). Temporal regulation of neural diversity in Drosophila and vertebrates. *Semin. Cell Dev. Biol.* 142, 13–22.

Epiney, D., Chaya, G. M., Dillon, N., Lai, S.-L. and Doe, C. (2023). Transcriptional complexity in the insect central complex: single nuclei RNA sequencing of adult brain neurons derived from type 2 neuroblasts. 2023.12.10.571022.

Ewen-Campen, B., Yang-Zhou, D., Fernandes, V. R., González, D. P., Liu, L.-P., Tao, R., Ren, X., Sun, J., Hu, Y., Zirin, J., et al. (2017). Optimized strategy for in vivo Cas9-activation in Drosophila. *Proc. Natl. Acad. Sci.* 114, 9409–9414.

Fischer, J. A., Giniger, E., Maniatis, T. and Ptashne, M. (1988). GAL4 activates transcription in Drosophila. *Nature* 332, 853–856.

Fisher, Y. E. (2022). Flexible navigational computations in the *Drosophila* central complex. *Curr. Opin. Neurobiol.* 73, 102514.

Franconville, R., Beron, C. and Jayaraman, V. (2018). Building a functional connectome of the Drosophila central complex. *eLife* 7, e37017.

Green, J., Adachi, A., Shah, K. K., Hirokawa, J. D., Magani, P. S. and Maimon, G. (2017). A neural circuit architecture for angular integration in Drosophila. *Nature* 546, 101–106.

Green, J., Vijayan, V., Mussells Pires, P., Adachi, A. and Maimon, G. (2019). A neural heading estimate is compared with an internal goal to guide oriented navigation. *Nat. Neurosci.* 22, 1460–1468.

Grosskortenhaus, R. (2006). Pdm and Castor specify late-born motor neuron identity in the NB7-1 lineage. *Genes Dev.* 20, 2618–2627.

Grosskortenhaus, R., Pearson, B. J., Marusich, A. and Doe, C. Q. (2005). Regulation of Temporal Identity Transitions in Drosophila Neuroblasts. *Dev. Cell* 8, 193–202.

Hamid, A., Gattuso, H., Caglar, A. N., Pillai, M., Steele, T., Gonzalez, A., Nagel, K. and Syed, M. H. (2024). The conserved RNA-binding protein Imp is required for the specification and function of olfactory navigation circuitry in *Drosophila*. *Curr. Biol.* 34, 473-488.e6.

Hanesch, U., Fischbach, K.-F. and Heisenberg, M. (1989). Neuronal architecture of the central complex in Drosophila melanogaster. *Cell Tissue Res.* 257, 343–366.

Hartenstein, V. and Campos-Ortega, J. A. (1984). Early neurogenesis in wild-type Drosophila melanogaster. *Wilhelm Rouxs Arch. Dev. Biol.* 193, 308–325.

Hartenstein, V. and Wodarz, A. (2013). Initial neurogenesis in Drosophila. *Wiley Interdiscip. Rev. Dev. Biol.* 2, 701–721.

Hartenstein, V., Younossi-Hartenstein, A. and Lekven, A. (1994). Delamination and Division in the *Drosophila* Neurectoderm: Spatiotemporal Pattern, Cytoskeletal Dynamics, and Common Control by Neurogenic and Segment Polarity Genes. *Dev. Biol.* 165, 480–499.

Helfrich-Förster, C. (2018). Sleep in Insects. *Annu. Rev. Entomol.* 63, 69–86.

Hirono, K., Kohwi, M., Clark, M. Q., Heckscher, E. S. and Doe, C. Q. (2017). The Hunchback temporal transcription factor establishes, but is not required to maintain, early-born neuronal identity. *Neural Develop.* 12, 1.

Holguera, I. and Desplan, C. (2018). Neuronal specification in space and time. *Science*.

Homem, C. C. F., Steinmann, V., Burkard, T. R., Jais, A., Esterbauer, H. and Knoblich, J. A. (2014). Ecdysone and Mediator Change Energy Metabolism to Terminate Proliferation in Drosophila Neural Stem Cells. *Cell* 158, 874–888.

Hulse, B. K., Haberkern, H., Franconville, R., Turner-Evans, D. B., Takemura, S., Wolff, T., Noorman, M., Dreher, M., Dan, C., Parekh, R., et al. (2021). A connectome of the Drosophila central complex reveals network motifs suitable for flexible navigation and context-dependent action selection. *eLife* 10, e66039.

Ikeshima-Kataoka, H., Skeath, J. B., Nabeshima, Y., Doe, C. Q. and Matsuzaki, F. (1997). Miranda directs Prospero to a daughter cell during Drosophila asymmetric divisions. *Nature* 390, 625–629.

Isshiki, T., Takeichi, M. and Nose, A. (1997). The role of the msh homeobox gene during Drosophila neurogenesis: implication for the dorsoventral specification of the neuroectoderm. *Development* 124, 3099–3109.

Isshiki, T., Pearson, B., Holbrook, S. and Doe, C. Q. (2001). Drosophila Neuroblasts Sequentially Express Transcription Factors which Specify the Temporal Identity of Their Neuronal Progeny. *Cell* 106, 511–521.

Ito, K. and Hotta, Y. (1992). Proliferation pattern of postembryonic neuroblasts in the brain of Drosophila melanogaster. *Dev. Biol.* 149, 134–148.

Janssens, J., Aibar, S., Taskiran, I. I., Ismail, J. N., Spanier, K. I., González-Blas, C. B., Quan, X. J., Papasokrati, D., Hulselmans, G., Makhzami, S., et al. (2021). *Decoding gene regulation in the fly brain*.

Jenett, A., Rubin, G. M., Ngo, T.-T. B., Shepherd, D., Murphy, C., Dionne, H., Pfeiffer, B. D., Cavallaro, A., Hall, D., Jeter, J., et al. (2012). A GAL4-Driver Line Resource for *Drosophila* Neurobiology. *Cell Rep.* 2, 991–1001.

Kambadur, R., Koizumi, K., Stivers, C., Nagle, J., Poole, S. J. and Odenwald, W. F. (1998). Regulation of POU genes by castor and hunchback establishes layered compartments in the Drosophila CNS. *Genes Dev.* 12, 246.

Kanai, M. I., Okabe, M. and Hiromi, Y. (2005). seven-up Controls Switching of Transcription Factors that Specify Temporal Identities of Drosophila Neuroblasts. *Dev. Cell* 8, 203–213.

Kohwi, M., Hiebert, L. S. and Doe, C. Q. (2011). The pipsqueak-domain proteins Distal antenna and Distal antenna-related restrict Hunchback neuroblast expression and early-born neuronal identity. *Development* 138, 1727–1735.

Lai, S.-L. and Lee, T. (2006). Genetic mosaic with dual binary transcriptional systems in Drosophila. *Nat. Neurosci.* 9, 703–709.

Lane, M. E., Sauer, K., Wallace, K., Jan, Y. N., Lehner, C. F. and Vaessin, H. (1996). Dacapo, a cyclin-dependent kinase inhibitor, stops cell proliferation during Drosophila development. *Cell* 87, 1225–1235.

Larsen, C., Shy, D., Spindler, S. R., Fung, S., Pereanu, W., Younossi-Hartenstein, A. and Hartenstein, V. (2009). Patterns of growth, axonal extension and axonal arborization of neuronal lineages in the developing *Drosophila* brain. *Dev. Biol.* 335, 289–304.

Li, X., Erclik, T., Bertet, C., Chen, Z., Voutev, R., Venkatesh, S., Morante, J., Celik, A. and Desplan, C. (2013). Temporal patterning of Drosophila medulla neuroblasts controls neural fates. *Nature* 498, 456–462.

Li, X., Xie, Y. and Zhu, S. (2016). Notch maintains Drosophila type II neuroblasts by suppressing expression of the Fez transcription factor Earmuff. *Development* 143, 2511–2521.

Li, H., Horns, F., Wu, B., Xie, Q., Li, J., Li, T., Luginbuhl, D. J., Quake, S. R. and Luo, L. (2017a). Classifying Drosophila Olfactory Projection Neuron Subtypes by Single-Cell RNA Sequencing. *Cell* 171, 1206-1220.e22.

Li, X., Chen, R. and Zhu, S. (2017b). bHLH-O proteins balance the self-renewal and differentiation of Drosophila neural stem cells by regulating Earmuff expression. *Dev. Biol.* 431, 239–251.

Liu, Z., Yang, C.-P., Sugino, K., Fu, C.-C., Liu, L.-Y., Yao, X., Lee, L. P. and Lee, T. (2015). Opposing intrinsic temporal gradients guide neural stem cell production of varied neuronal fates. *Science* 350, 317–320.

Matsuzaki, M. and Saigo, K. (1996). hedgehog signaling independent of engrailed and wingless required for post-S1 neuroblast formation in Drosophila CNS. *Dev. Camb. Engl.* 122, 3567–3575.

Maurange, C., Cheng, L. and Gould, A. P. (2008). Temporal Transcription Factors and Their Targets Schedule the End of Neural Proliferation in Drosophila. *Cell* 133, 891–902.

McDonald, J. A. and Doe, C. Q. (1997). Establishing neuroblast-specific gene expression in the Drosophila CNS: huckebein is activated by Wingless and Hedgehog and repressed by Engrailed and Gooseberry. *Development* 124, 1079–1087.

McDonald, J. A., Holbrook, S., Isshiki, T., Weiss, J., Doe, C. Q. and Mellerick, D. M. (1998). Dorsoventral patterning in the Drosophila central nervous system: the vnd homeobox gene specifies ventral column identity. *Genes Dev.* 12, 3603–3612.

Meng, J. L., Marshall, Z. D., Lobb-Rabe, M. and Heckscher, E. S. (2019). How prolonged expression of Hunchback, a temporal transcription factor, re-wires locomotor circuits. *eLife* 8, e46089.

Meng, J. L., Wang, Y., Carrillo, R. A. and Heckscher, E. S. (2020). Temporal transcription factors determine circuit membership by permanently altering motor neuron-to-muscle synaptic partnerships. *eLife* 9, e56898.

Mettler, U., Vogler, G. and Urban, J. (2006). Timing of identity: spatiotemporal regulation of hunchback in neuroblast lineages of Drosophila by Seven-up and Prospero. *Development* 133, 429–437.

Michki, N. S., Li, Y., Sanjasaz, K., Zhao, Y., Shen, F. Y., Walker, L. A., Cao, W., Lee, C.-Y. and Cai, D. (2021). The molecular landscape of neural differentiation in the developing Drosophila brain revealed by targeted scRNA-seq and multi-informatic analysis. *Cell Rep.* 35, 109039.

Moris-Sanz, M., Estacio-Gómez, A., Alvarez-Rivero, J. and Díaz-Benjumea, F. J. (2014). Specification of neuronal subtypes by different levels of Hunchback. *Dev. Camb. Engl.* 141, 4366–4374.

Munroe, J. A. and Doe, C. Q. (2023). Imp is expressed in INPs and newborn neurons where it regulates neuropil targeting in the central complex. *Neural Develop.* 18, 9.

Munroe, J. A., Syed, M. H. and Doe, C. Q. (2022). Imp is required for timely exit from quiescence in Drosophila type II neuroblasts. *PLOS ONE* 17, e0272177.

Narbonne-Reveau, K., Lanet, E., Dillard, C., Foppolo, S., Chen, C.-H., Parrinello, H., Rialle, S., Sokol, N. S. and Maurange, C. (2016). Neural stem cell-encoded temporal patterning delineates an early window of malignant susceptibility in Drosophila. *eLife* 5, e13463.

Novotny, T., Eiselt, R. and Urban, J. (2002). Hunchback is required for the specification of the early sublineage of neuroblast 7-3 in the Drosophila central nervous system. *Dev. Camb. Engl.* 129, 1027–1036.

Omoto, J. J., Keleş, M. F., Nguyen, B.-C. M., Bolanos, C., Lovick, J. K., Frye, M. A. and Hartenstein, V. (2017). Visual Input to the Drosophila Central Complex by Developmentally and Functionally Distinct Neuronal Populations. *Curr. Biol.* 27, 1098–1110.

Otsuki, L. and Brand, A. H. (2018). Cell cycle heterogeneity directs the timing of neural stem cell activation from quiescence. *Science* 360, 99–102.

Otsuki, L. and Brand, A. H. (2019). Dorsal-Ventral Differences in Neural Stem Cell Quiescence Are Induced by p57KIP2/Dacapo. *Dev. Cell* 49, 293-300.e3.

Pearson, B. J. and Doe, C. Q. (2003). Regulation of neuroblast competence in Drosophila. *Nature* 425, 624–628.

Pearson, B. J. and Doe, C. Q. (2004). SPECIFICATION OF TEMPORAL IDENTITY IN THE DEVELOPING NERVOUS SYSTEM. *Annu. Rev. Cell Dev. Biol.* 20, 619–647.

Pereanu, W. and Hartenstein, V. (2006). Neural Lineages of the Drosophila Brain: A Three-Dimensional Digital Atlas of the Pattern of Lineage Location and Projection at the Late Larval Stage. *J. Neurosci.* 26, 5534–5553.

Pfeiffer, K. and Homberg, U. (2014). Organization and Functional Roles of the Central Complex in the Insect Brain. *Annu. Rev. Entomol.* 59, 165–184.

Pollington, H. Q., Seroka, A. Q. and Doe, C. Q. (2023). From temporal patterning to neuronal connectivity in Drosophila type I neuroblast lineages. *Semin. Cell Dev. Biol.* 142, 4–12.

Port, F. and Bullock, S. L. (2016). Augmenting CRISPR applications in Drosophila with tRNA-flanked sgRNAs. *Nat. Methods* 13, 852–854.

Port, F., Strein, C., Stricker, M., Rauscher, B., Heigwer, F., Zhou, J., Beyersdörffer, C., Frei, J., Hess, A., Kern, K., et al. (2020). A large-scale resource for tissue-specific CRISPR mutagenesis in Drosophila. *eLife* 9, e53865.

Prokop, A. and Technau, G. M. (1991). The origin of postembryonic neuroblasts in the ventral nerve cord of Drosophila melanogaster. *Development* 111, 79–88.

Reilly, M. B., Cros, C., Varol, E., Yemini, E. and Hobert, O. (2020). Unique homeobox codes delineate all the neuron classes of C. elegans. *Nature* 584, 595–601.

Ren, Q., Yang, C.-P., Liu, Z., Sugino, K., Mok, K., He, Y., Ito, M., Nern, A., Otsuna, H. and Lee, T. (2017). Stem Cell-Intrinsic, Seven-up-Triggered Temporal Factor Gradients Diversify Intermediate Neural Progenitors. *Curr. Biol.* 27, 1303–1313.

Renn, S. C., Armstrong, J. D., Yang, M., Wang, Z., An, X., Kaiser, K. and Taghert, P. H. (1999). Genetic analysis of the Drosophila ellipsoid body neuropil: organization and development of the central complex. *J. Neurobiol.* 41, 189–207.

Riebli, N., Viktorin, G. and Reichert, H. (2013). Early-born neurons in type II neuroblast lineages establish a larval primordium and integrate into adult circuitry during central complex development in Drosophila. *Neural Develop.* 8, 6.

Rives-Quinto, N., Komori, H., Ostgaard, C. M., Janssens, D. H., Kondo, S., Dai, Q., Moore, A. W. and Lee, C.-Y. (2020). Sequential activation of transcriptional repressors promotes progenitor commitment by silencing stem cell identity genes. *eLife* 9, e56187.

Robinow, S. and White, K. (1991). Characterization and spatial distribution of the ELAV protein during Drosophila melanogaster development. *J. Neurobiol.* 22, 443–461.

Rossi, A. M., Jafari, S. and Desplan, C. (2021). Integrated Patterning Programs During *Drosophila* Development Generate the Diversity of Neurons and Control Their Mature Properties. *Annu. Rev. Neurosci.* 44, annurev-neuro-102120-014813.

Samson, M.-L. and Chalvet, F. (2003). found in neurons, a third member of the Drosophila elav gene family, encodes a neuronal protein and interacts with elav. *Mech. Dev.* 120, 373–383.

San-Juán, B. P. and Baonza, A. (2011). The bHLH factor deadpan is a direct target of Notch signaling and regulates neuroblast self-renewal in Drosophila. *Dev. Biol.* 352, 70–82.

Scheffer, L. K., Xu, C. S., Januszewski, M., Lu, Z., Takemura, S., Hayworth, K. J., Huang, G. B., Shinomiya, K., Maitlin-Shepard, J., Berg, S., et al. (2020). A connectome and analysis of the adult Drosophila central brain. *eLife* 9, e57443.

Schmid, A., Chiba, A. and Doe, C. Q. (1999). Clonal analysis of Drosophila embryonic neuroblasts: neural cell types, axon projections and muscle targets. *Development* 126, 4653–4689.

Schmidt, H., Rickert, C., Bossing, T., Vef, O., Urban, J. and Technau, G. M. (1997). The Embryonic Central Nervous System Lineages of*Drosophila melanogaster*. *Dev. Biol.* 189, 186–204.

Seelig, J. D. and Jayaraman, V. (2013). Feature detection and orientation tuning in the Drosophila central complex. *Nature* 503, 262–266.

Sen, S. Q., Chanchani, S., Southall, T. D. and Doe, C. Q. (2019). Neuroblast-specific open chromatin allows the temporal transcription factor, Hunchback, to bind neuroblast-specific loci. *eLife* 8, e44036.

Seroka, A. Q. and Doe, C. Q. (2019). The Hunchback temporal transcription factor determines motor neuron axon and dendrite targeting in *Drosophila*. *Development* 146, dev175570.

Seroka, A., Yazejian, R. M., Lai, S.-L. and Doe, C. Q. (2020). A novel temporal identity window generates alternating Eve+/Nkx6+ motor neuron subtypes in a single progenitor lineage. *Neural Develop.* 15, 9.

Seroka, A., Lai, S.-L. and Doe, C. Q. (2022). Transcriptional profiling from whole embryos to single neuroblast lineages in Drosophila. *Dev. Biol.* 489, 21–33.

Siegrist, S. E., Haque, N. S., Chen, C.-H., Hay, B. A. and Hariharan, I. K. (2010). Inactivation of Both foxo and reaper Promotes Long-Term Adult Neurogenesis in Drosophila. *Curr. Biol.* 20, 643–648.

Skeath, J. B. and Thor, S. (2003). Genetic control of Drosophila nerve cord development. *Curr. Opin. Neurobiol.* 13, 8–15.

Skeath, J. B., Zhang, Y., Holmgren, R., Carroll, S. B. and Doe, C. Q. (1995). Specification of neuroblast identity in the Drosophila embryonic central nervous system by gooseberry-distal. *Nature* 376, 427–430.

Sousa-Nunes, R., Yee, L. L. and Gould, A. P. (2011). Fat cells reactivate quiescent neuroblasts via TOR and glial insulin relays in Drosophila. *Nature* 471, 508–512.

Strauss, R. (2002). The central complex and the genetic dissection of locomotor behaviour. *Curr. Opin. Neurobiol.* 12, 633–638.

Sullivan, L. F., Warren, T. L. and Doe, C. Q. (2019). Temporal identity establishes columnar neuron morphology, connectivity, and function in a Drosophila navigation circuit. *eLife* 8, e43482.

Syed, M. H., Mark, B. and Doe, C. Q. (2017). Steroid hormone induction of temporal gene expression in Drosophila brain neuroblasts generates neuronal and glial diversity. *eLife* 6, e26287.

Szüts, D. and Bienz, M. (2000). LexA chimeras reveal the function of Drosophila Fos as a context-dependent transcriptional activator. *Proc. Natl. Acad. Sci.* 97, 5351–5356.

Tang, J. L. Y., Hakes, A. E., Krautz, R., Suzuki, T., Contreras, E. G., Fox, P. M. and Brand, A. H. (2022). NanoDam identifies Homeobrain (ARX) and Scarecrow (NKX2.1) as conserved temporal factors in the Drosophila central brain and visual system. *Dev. Cell* 0,.

Timaeus, L., Geid, L., Sancer, G., Wernet, M. F. and Hummel, T. (2020). Parallel Visual Pathways with Topographic versus Nontopographic Organization Connect the Drosophila Eyes to the Central Brain. *iScience* 23, 101590.

Tran, K. D. and Doe, C. Q. (2008). Pdm and Castor close successive temporal identity windows in the NB3-1 lineage. *Dev. Camb. Engl.* 135, 3491–3499.

Truman, J. W. and Bate, M. (1988). Spatial and temporal patterns of neurogenesis in the central nervous system of Drosophila melanogaster. *Dev. Biol.* 125, 145–157.

Turner-Evans, D. B. and Jayaraman, V. (2016). The insect central complex. *Curr. Biol.* 26, R453–R457.

Turner-Evans, D., Wegener, S., Rouault, H., Franconville, R., Wolff, T., Seelig, J. D., Druckmann, S. and Jayaraman, V. (2017). Angular velocity integration in a fly heading circuit. *eLife*.

Turner-Evans, D. B., Jensen, K. T., Ali, S., Paterson, T., Sheridan, A., Ray, R. P., Wolff, T., Lauritzen, J. S., Rubin, G. M., Bock, D. D., et al. (2020). The Neuroanatomical Ultrastructure and Function of a Biological Ring Attractor. *Neuron* 108, 145-163.e10.

von Ohlen, T. and Doe, C. Q. (2000). Convergence of dorsal, dpp, and egfr signaling pathways subdivides the drosophila neuroectoderm into three dorsal-ventral columns. *Dev. Biol.* 224, 362–372.

Wagh, D. A., Rasse, T. M., Asan, E., Hofbauer, A., Schwenkert, I., Dürrbeck, H., Buchner, S., Dabauvalle, M.-C., Schmidt, M., Qin, G., et al. (2006). Bruchpilot, a Protein with Homology to ELKS/CAST, Is Required for Structural Integrity and Function of Synaptic Active Zones in Drosophila. *Neuron* 49, 833–844.

Walsh, K. T. and Doe, C. Q. (2017). *Drosophila* embryonic type II neuroblasts: origin, temporal patterning, and contribution to the adult central complex. *Development* 144, 4552–4562.

Wani, A. R., Chowdhury, B., Luong, J., Chaya, G. M., Patel, K., Isaacman-Beck, J., Shafer, O., Kayser, M. S. and Syed, M. H. (2023). Stem cell-specific ecdysone signaling regulates the development and function of a Drosophila sleep homeostat. 2023.09.29.560022.

Weiss, J. B., Von Ohlen, T., Mellerick, D. M., Dressler, G., Doe, C. Q. and Scott, M. P. (1998). Dorsoventral patterning in the Drosophila central nervous system: the intermediate neuroblasts defective homeobox gene specifies intermediate column identity. *Genes Dev.* 12, 3591–3602.

Wheeler, W. M. (1891). *Neuroblasts in the Arthropod Embryo*.

Wheeler, W. M. (1893). A contribution to insect embryology. *J. Morphol.* 8, 1–161.

Wolff, T. and Rubin, G. M. (2018). Neuroarchitecture of the Drosophila central complex: A catalog of nodulus and asymmetrical body neurons and a revision of the protocerebral bridge catalog. *J. Comp. Neurol.* 526, 2585–2611.

Wolff, T., Iyer, N. A. and Rubin, G. M. (2015). Neuroarchitecture and neuroanatomy of the Drosophila central complex: A GAL4-based dissection of protocerebral bridge neurons and circuits. *J. Comp. Neurol.* 523, 997–1037.

Wong, D. C., Lovick, J. K., Ngo, K. T., Borisuthirattana, W., Omoto, J. J. and Hartenstein, V. (2013). Postembryonic lineages of the *Drosophila* brain: II. Identification of lineage projection patterns based on MARCM clones. *Dev. Biol.* 384, 258–289.

Xiong, W. C., Okano, H., Patel, N. H., Blendy, J. A. and Montell, C. (1994). repo encodes a glial-specific homeo domain protein required in the Drosophila nervous system. *Genes Dev.* 8, 981–994.

Yang, J. S., Awasaki, T., Yu, H.-H., He, Y., Ding, P., Kao, J.-C. and Lee, T. (2013). Diverse neuronal lineages make stereotyped contributions to the *Drosophila* locomotor control center, the central complex: Lineage analysis of central complex neurons. *J. Comp. Neurol.* 521, 2645–2662.

Yang, C.-P., Samuels, T. J., Huang, Y., Yang, L., Ish-Horowicz, D., Davis, I. and Lee, T. (2017). Imp and Syp RNA-binding proteins govern decommissioning of Drosophila neural stem cells. *Development* 144, 3454–3464.

Yasugi, T., Umetsu, D., Murakami, S., Sato, M. and Tabata, T. (2008). Drosophila optic lobe neuroblasts triggered by a wave of proneural gene expression that is negatively regulated by JAK/STAT. *Dev. Camb. Engl.* 135, 1471–1480.

Young, J. M. and Armstrong, J. D. (2010). Building the central complex in Drosophila: the generation and development of distinct neural subsets. *J. Comp. Neurol.* 518, 1525–1541.

Younossi-Hartenstein, A., Nassif, C., Green, P. and Hartenstein, V. (1996). Early neurogenesis of the Drosophila brain. *J. Comp. Neurol.* 370, 313–329.

Zheng, Z., Lauritzen, J. S., Perlman, E., Robinson, C. G., Nichols, M., Milkie, D., Torrens, O., Price, J., Fisher, C. B., Sharifi, N., et al. (2018). A Complete Electron Microscopy Volume of the Brain of Adult Drosophila melanogaster. *Cell* 174, 730-743.e22.

Zhu, S., Barshow, S., Wildonger, J., Jan, L. Y. and Jan, Y.-N. (2011). Ets transcription factor Pointed promotes the generation of intermediate neural progenitors in Drosophila larval brains. *Proc. Natl. Acad. Sci.* 108, 20615–20620.

Zhu, S., Wildonger, J., Barshow, S., Younger, S., Huang, Y. and Lee, T. (2012). The bHLH Repressor Deadpan Regulates the Self-renewal and Specification of Drosophila Larval Neural Stem Cells Independently of Notch. *PLOS ONE* 7, e46724.

Chapter II

A single-cell RNA-seq analysis reveals temporally-regulated and quiescence-regulated gene expression in larval neuroblasts

Dillon, N., Cocanougher, B., Sood, C., Yuan, X., Kohn, A. B., Moroz, L. L., Siegrist, S. E., Zlatic, M. and Doe, C. Q. (2022). Single cell RNA-seq analysis reveals temporally-regulated and quiescence-regulated gene expression in Drosophila larval neuroblasts. *Neural Development* 17, 7.

Author contributions

ND performed all scRNAseq analysis, generated all figures, and wrote the manuscript. BC, LLM, ABK, and MZ generated the scRNAseq data; CS, XY, and SES generated Fig. 2.2H and provided comments on the manuscript. CQD supervised the project and edited figures and text. The authors read and approved the final manuscript.

Introduction

A major question in neuroscience is how neural diversity is generated, which underlies complex neural circuits and behavioral output of the central nervous system (CNS). In the past, neuronal diversity was commonly defined by morphological features (axon/dendrite processes), biochemical features (neurotransmitter choice), and physiological features (distinct ion channels and membrane properties) [1]. In addition, “low throughput” assays for molecular differences among neurons, typically for transcription factor (TF) expression, have been crucial for finding insights into the generation of neural diversity for decades [2, 3]. Taken together, these approaches resulted in the definition various classes or subtypes of motor neurons, interneurons, sensory neurons and peptidergic neurons, but they are ill-suited to address the question of how many unique types of neurons exist within the CNS, and the subsequent question of how each cell type contributes to the function of the CNS.

The advent of single cell RNA sequencing (scRNA-seq) allowed a more complete inventory of gene expression profiles within individual neurons, with the expression of “validated cell type

genes" used as a framework to identify transcriptionally related neurons [4–8]. Further analysis has revealed novel cell types based on common gene expression, but also that trajectories between cell types to be more gradual and less saltatory than previously appreciated, in part due to transcriptional priming [9–11].

In *Drosophila*, neuronal scRNA-seq has been done on adult brain [12–16], pupae [17–22], larvae [23–25], and blastoderm-stage embryos [26]. These experiments have provided valuable insight into the number of distinct neuronal types and identified gene candidates for regulating neural subtype function or connectivity. However, no studies to date have focused on identifying and characterizing the transcriptional diversity of neural progenitors, nor has any study mapped progenitor transcriptional profile at multiple larval stages. In this study, we identify multiple progenitor subtypes across several larval stages with differential gene expression to provide candidate genes as cell type specific markers and functional roles during development.

Results

Larval atlas shows distinct cell identities and differentiating neural progenitor axis

To identify single cell gene expression profiles throughout larval development, we used scRNA-seq data collected by [27] from dissociated brain and ventral nerve cord (VNC) – together termed the CNS – from larvae at 1h, 24h and 48h (all times in hours after larval hatching; ALH). We used the 10X Genomics pipeline for scRNA-seq analysis and used Cell Ranger Aggregation to aggregate multiple samples from the same timepoint. We used the standard Seurat integration pipeline to filter out low quality cells and clustered 97,845 cells from all larval stages (see methods; Fig. 2.1a). Within our atlas we identified clusters enriched for cell types in the CNS: neural progenitors, immature and mature neurons, glia, trachea, hemocytes and insulin-producing cells (IPCs; Fig. 2.1a; Supp. Table 2. 1). Representative examples of a progenitor marker (Deadpan; *dpn*), a new-born neuron marker (*Hey*), a maturing neuron marker (*nSyb*), and a glia marker (*repo*) are shown in Fig. 2.1b.

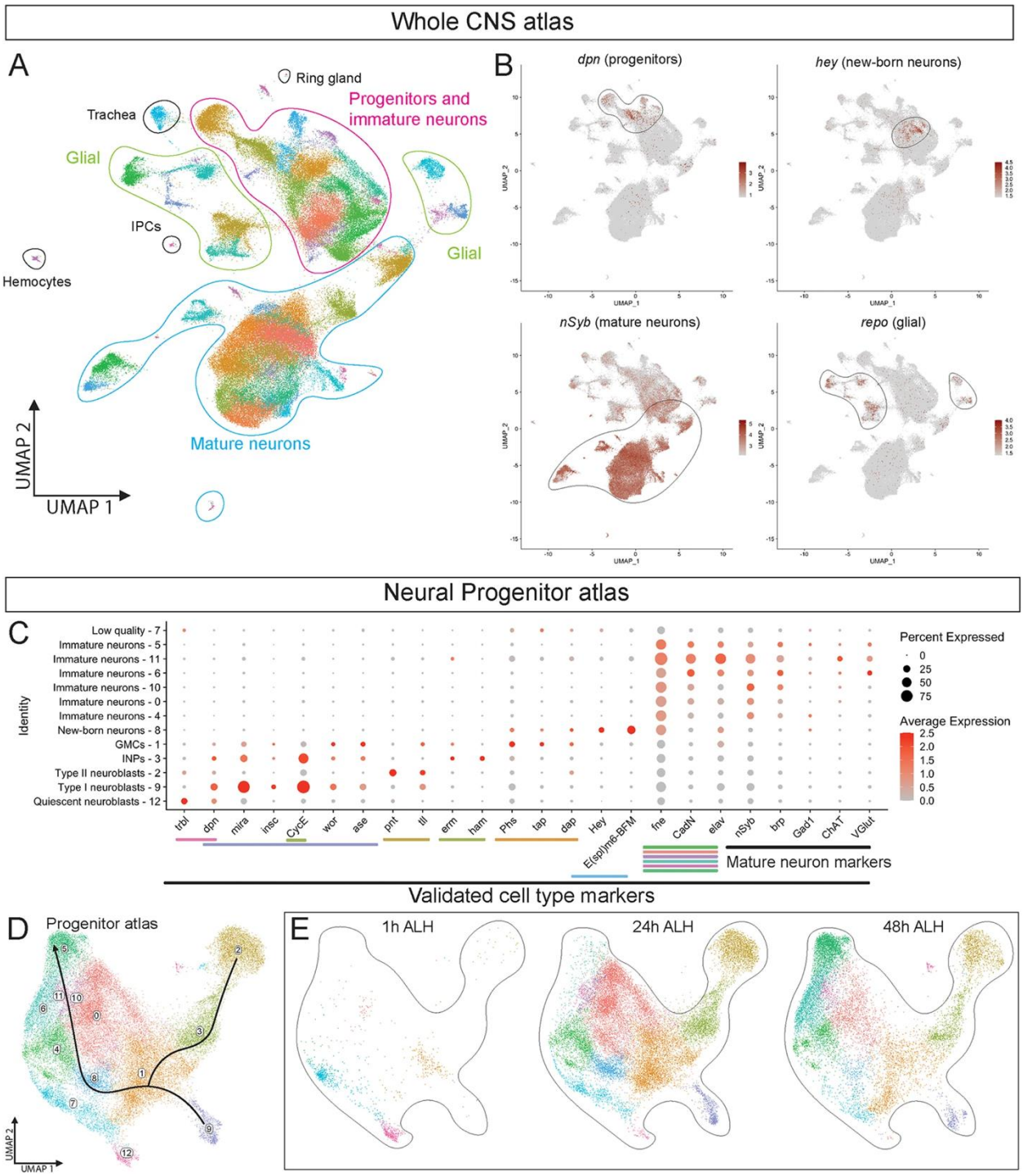

Fig. 2.1 Larval atlas shows distinct cell identities and differentiating neural progenitor axis. A An atlas of 97,845 cells collected from 1h, 24h and 48h ALH larvae was built. These cells were analyzed with Seurat and clustered to identify major cell types such as neural progenitors, glial, mature neurons and other features to validate the atlas in clustering by cell type. **B** Feature plots of *Dpn* and *Hey* show a differentiating neural progenitor axis. The mature neuronal marker *nSyb* shows limited expression in progenitors that extends into

(**Fig. 2.1 caption continued**) mature neuronal clusters. The glial marker *repo* shows glial cells separated from progenitors and mature neurons. **C** Validated cell identity markers label distinct progenitor cell types within a developmental axis. **D** Progenitor atlas was made with a subset from the whole atlas of 33,458 neural progenitor and immature neuron cells. Black line indicates expected developmental trajectory. **E** UMAPs of progenitor clusters from 1h-48h ALH.

We next focused on the progenitor and immature neuron cluster, sub-clustering only these cells. We found clear separation of the major progenitor cell types: quiescent neuroblasts (cluster 12), type I neuroblasts (cluster 9), type II neuroblasts (cluster 2), Intermediate Neural Progenitors (INPs, cluster 3), Ganglion Mother Cells (GMCs, cluster 1), new-born neurons (cluster 8), and immature neurons (clusters 0, 4–6, 10, and 11), plus one low quality cluster (7) that was excluded from subsequent analysis (Fig. 2.1c; Supp. Table 2.2). Clusters were assigned cell type designations based on enriched expression of experimentally validated cell type markers (Fig. 2.1c; Table 2.1). Interestingly, each class of progenitor formed a distinct cluster, creating a differentiation axis right to left in UMAP space (Fig. 2.1d). Not surprisingly, the quiescent neuroblast cluster was enriched at 1h when most neuroblasts are quiescent [28], followed by emergence of proliferating neuroblasts, INP and GMC clusters at 24h and 48h (Fig. 2.1e). Thus, we can identify and transcriptionally profile all known progenitor subtypes across larval development, including quiescent neuroblasts which have never been identified in RNA-seq experiments. We discuss each progenitor type in more detail below (Tables 2.2 and 2.3).

Table 2.1. Validated markers for progenitors and young neurons.

Cell type	Marker	References
Neuroblast, quiescent	Tribbles + Deadpan+ Worniu -	[29] [29] [29]
Neuroblast, Type I	Deadpan + Asense + Worniu + Miranda + Inscuteable + String + Cyclin E +	[30] [31] [32] [33] [34] [34] [35]
Neuroblast, Type II	Pointed + Tailless + Asense -	[36] [37] [31]
INP	Erm + Hamlet + Cyclin E +	[38] [37] [25, 39]
GMC	Target of Poxn +	[25]

Table 2.2. Validated markers for glial cell types.

Cell type	Marker	References
All glial	Repo +	[47, 48]
Astrocyte/neuropil glial	Gat + Alarm +	[49] [50]
Perineurial	CG6126 + Indy + CG4797 +	[51] [52] [12]
Subperineural	Moody + AdamTS-A +	[53] [52]
Cortex/chiasm glial	Wrapper + Hoe1 +	[54] [12]

Table 2.3. Validated markers for mature neuron cell types.

Cell type	Marker	References
Undifferentiated	Hdc+ Ncad+	[55] [43]
Cholinergic	Ace + ChAT +	[56]
GABAergic	Gad1 +	[57]
Glutamatergic	VGlut +	[58]
Monoaminergic	Vmat + Ddc + Trh +	[59] [60] [61]
vPeptidergic	Dimm + CCAP +	[62] [62]
	Burs +	[63]
	AstC +	[64]
Octopaminergic	Vmat + Tbh + Tdc2 +	[59] [65] [66]
Motor neurons	Twit +	[67]
Kenyon cells γ	Rgk1 Pka (R1/2, C1)	[68] [69]
Neurosecretory cells	ITP sNPF	[70] [70]

Quiescent neuroblasts and associated glia are enriched for expression of genes regulating the TOR and insulin pathways

The majority of neuroblasts enter quiescence before the end of embryogenesis and remain quiescent until 12-24h [71, 72]. We noticed that cluster 12 is clearly present at 1h but the number of cells drop at 24h and 48h (Fig. 2.2a-b); this timing coincides with neuroblasts exiting quiescence. We confirmed this cluster 12 identity as quiescent neuroblasts using the positive markers *dpn* and *trbls* in addition to the lack of expression of canonical proliferating neuroblast markers (Fig. 2.2c; Table 2.1; Supp. Table 2.2). The top cluster defining genes (i.e., genes that define the cluster as a distinct grouping of cells) represented cell growth, cell cycle progression and the insulin signaling pathway (Fig. 2.2c).

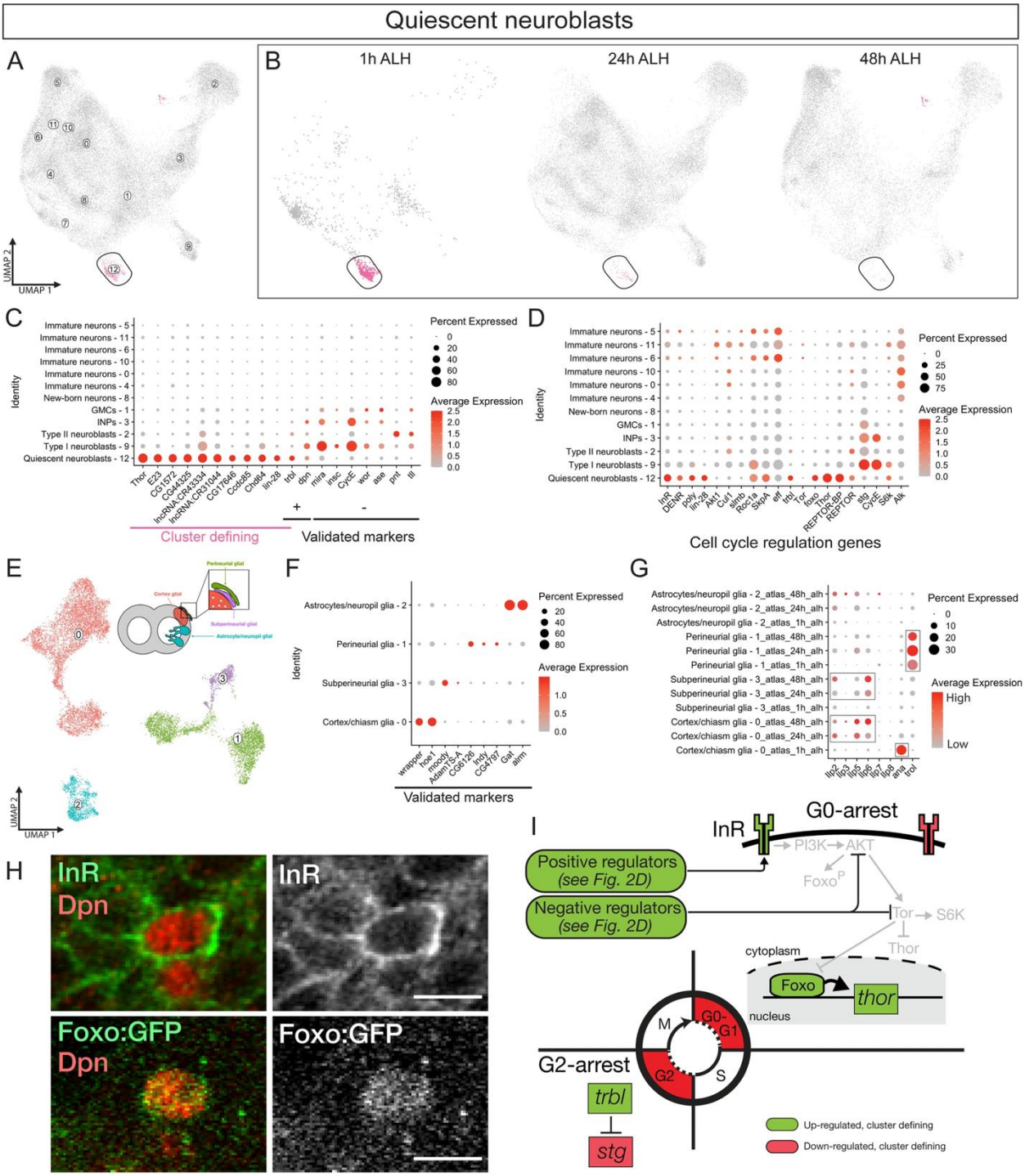

Fig 2.2 Quiescent neuroblasts and glial cells show enriched markers for regulating the TOR and insulin pathway. A UMAP of CNS cell types with quiescent neuroblasts in cluster 8 (circled). **B** UMAP of cluster from 1h-48h ALH. **C** Dot plot of top cluster defining genes alongside validated cell identity markers for quiescent neuroblasts. **D** Dot plot of genes involved with cell cycle regulation including the insulin signaling, AKT and TOR pathways. **E** UMAP re-clustered of 11,004 glia cells from a subset of the whole atlas. Diagram adapted from Kremer et al, 2017 [73]. **F** Validated glial cell type markers. **G** Temporal expression of

(Fig. 2.2 caption continued) signaling molecules involved in neuroblast quiescence within glial subtypes. **H** Validation of InR and Foxo expression in Dpn+ quiescent neuroblasts. Scale bar, 5 uM. **I** Model depicting cell growth and cell cycle genes identified as significantly enriched or depleted in the quiescent neuroblast cluster at 1h ALH, placed in the context of known signaling pathways.

To further investigate gene expression in this quiescent neuroblast population, we analyzed the expression of core elements regulating the insulin receptor (*InR*), AKT pathway, TOR pathway and general markers of cell growth. We were interested in *InR* regulation in quiescent neuroblasts because previous work has showed insulin signaling to be essential for neuroblasts to exit quiescence [28, 74]. We found upregulation of *InR* in addition to upregulation of positive regulators for InR (Fig. 2.2d). AKT and TOR genes showed lower expression (Fig. 2.2d), consistent with the lack of cellular growth in quiescent neuroblasts. Similarly, markers for cell cycle genes showed low expression (Fig. 2.2d). We conclude that quiescent neuroblasts are transcriptionally primed to receive insulin signaling but have yet to initiate proliferation and growth.

Previous work has found that insulin signaling from glia is required for neuroblasts to exit quiescence [28]. To investigate this connection, we explored glial gene expression related to neuroblast quiescent signaling pathways. We sub-clustered from the whole atlas 11,004 cells from clusters that were positive for the pan glial marker *repo* (Fig. 2.2e; Supp. Table 2.3) [47]. We found four glial subtypes: astrocytes, cortex/chiasm, perineurial, and subperineurial glia (Fig. 2.2f; Supp. Table 2.3). Known glial-quiescent neuroblast signaling molecules were differentially regulated in the cortex/chiasm glia and surface glia between 1h and 24h when quiescent neuroblasts are re-activated. Expression of these genes was maintained in glia along with proliferating neuroblasts at later stages of larval development (Fig. 2.2g; Supp. Tables 2.4, 2.5 and 2.6). For example, Ana, a glial secreted glycoprotein that inhibits neuroblast proliferation [75], was upregulated in cortex/chiasm glia at 1h (Fig. 2.2g; Supp. Table 2.4). Insulin-like peptides (Ilps), known to be secreted by glia and promote neuroblast exit from quiescence [28], were upregulated in cortex/chiasm glia and subperineurial glia at 24h and 48h (Fig. 2.2g; Supp. Tables 2.4 and 2.5). Trol, a secreted molecule acting downstream of Ana to promote neuroblast proliferation [76], was upregulated in perineurial glia at 24h (Fig. 2.2g; Supp. Table 2.6).

We validated two key regulators of quiescence, InR and Foxo, by antibody staining. Both proteins are enriched in Dpn + quiescent neuroblasts in newly hatched larvae (Fig. 2.2h). We conclude that known regulators of neuroblast quiescence are expressed in cortex and surface glia at times consistent with a role in regulating the timing of neuroblast exit from quiescence. We postulate testable models for this neuroblast cell state transition (Fig. 2.2i). Our data supports the notion that quiescent neuroblasts express some, but not all, elements of the insulin signaling pathway (Fig. 2.2i), thereby transcriptionally priming them for rapid exit from quiescence. Furthermore, both cortex/chiasm and surface glia express *Ilp* genes, suggesting a shared role in signaling neuroblasts to exit quiescence. Future work will be required to further validate these models and regulatory pathways within larval quiescent neuroblasts.

Proliferating neuroblasts shows candidate novel markers and temporal transcription factors

Here we focus on exploring gene expression in the proliferating type I and type II neuroblasts, beginning with the type I neuroblast population. We identified a type I neuroblast cluster (cluster 9; Fig. 2.3a,b) based on multiple validated progenitor and Type I neuroblast specific markers including: *CycE*, *str*, *wor*, *ase*, *dpn*, *mira* and *insc* plus lack of the type II specific marker *pointed* (Fig. 2.3c; Table 2.1; Supp. Table 2.2). The type I neuroblast cluster was most prominent at 24h and 48h (Fig. 2.3b), most likely due to neuroblasts at 1h being partitioned into the quiescence neuroblast cluster (see above). Not surprisingly, all markers except for *insc* were found to be cluster defining genes, demonstrating the robustness of the progenitor atlas in clustering by known cell type markers (Fig. 2.3c, right). The top cluster defining genes include known progenitor genes such as *Pen* (also called *oho31*), *grh* and *Syp* [39, 77–79]. In addition, we noticed novel genes in Type I neuroblasts that are uncharacterized such as several long non-coding RNAs and *CG13305* (Fig. 2.3c, left). These cluster defining genes are novel candidate markers for Type I neuroblasts.

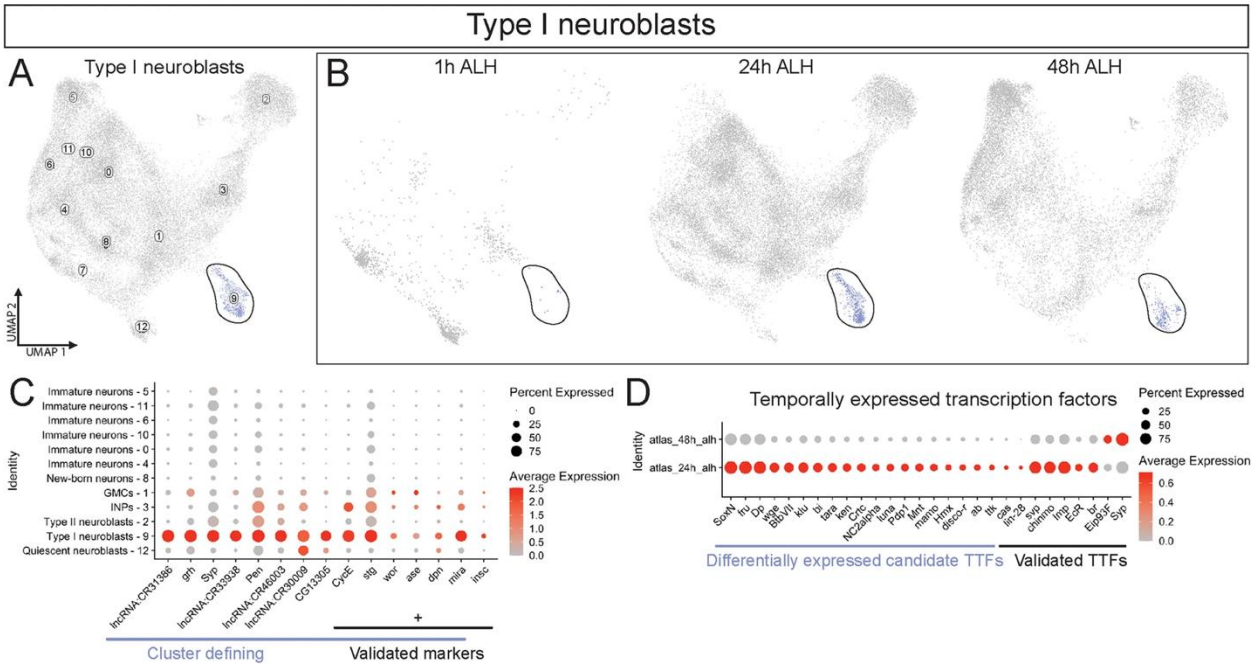

Fig. 2.3 Type I neuroblasts shows candidate novel markers and temporal transcription factors. A UMAP of type I neuroblasts highlighted. **B** UMAP of cluster from 1h-48h ALH. **C** Dot plot of top cluster defining genes and validated markers for type I neuroblasts. **D** Dot plot of differentially expressed transcription factors between 24h ALH and 48h ALH type I neuroblasts.

Neuroblasts are known to have temporal transcription factor (TTF) cascades [80]. To identify novel candidate TTFs, we identified differentially expressed transcription factors between 24h and 48h type I neuroblasts (Fig. 2.3d; Supp. Table 2.7). Surprisingly, we only found candidate transcription factors upregulated at 24h (24h > 48h), but not the opposite (48h > 24h). Validated TTFs for type II neuroblasts [81, 82] show their expected trend between 24h and 48h, with the exceptions of unexpected early expression of *EcR* and *Br* at 24h compared to their published expression only after 60h [81, 82]. This could be due to the presence of mRNA but not protein (i.e. post-transcriptional regulation) or due to detection of multiple isoforms with some isoforms only expressed after 60h. Our findings identify novel candidate type I neuroblast TTFs.

We identified a type II neuroblast cluster (cluster 2; Fig. 2.4a-b) based on the validated type II neuroblast markers *pnt* and *tll* with minimal expression of the negative marker *ase* (Fig. 2.4f; Supp. Table 2.2). As with the type I cluster, the type II cluster showed the most cells at 24h and 48h cells (Fig. 2.4b), consistent with the known type II neuroblast quiescent phase at 1h [28]. Further sub-division of cluster 2 showed two distinct clusters, one with substantially higher

expression of type II neuroblast markers *pnt*, *tll* and *dpn* (Fig. 2.4e; Supp. Table 2.8). We identified this sub cluster as type II neuroblasts and were unable to annotate the other progenitor cluster (Fig. 2.4c); the unknown subcluster is not enriched for optic lobe neuroblasts nor is it enriched for low quality cells. We suspect the unannotated cluster is also composed of type II progenitors given their similarity to the type II neuroblasts and slight expression of the INP markers *CycE* and *ase* expression (Fig. 2.4e). These type II neuroblasts had a similar trend to type I neuroblasts in being more prevalent at 24h and 48h than at 1h (Fig. 2.4d). Top cluster defining genes for cluster 2 included genes specific to type II neuroblasts but also expressed in type I neuroblasts and INPs (Fig. 2.4f). Interestingly, the uncharacterized gene *CG4250* was exclusive to type II and quiescent neuroblasts.

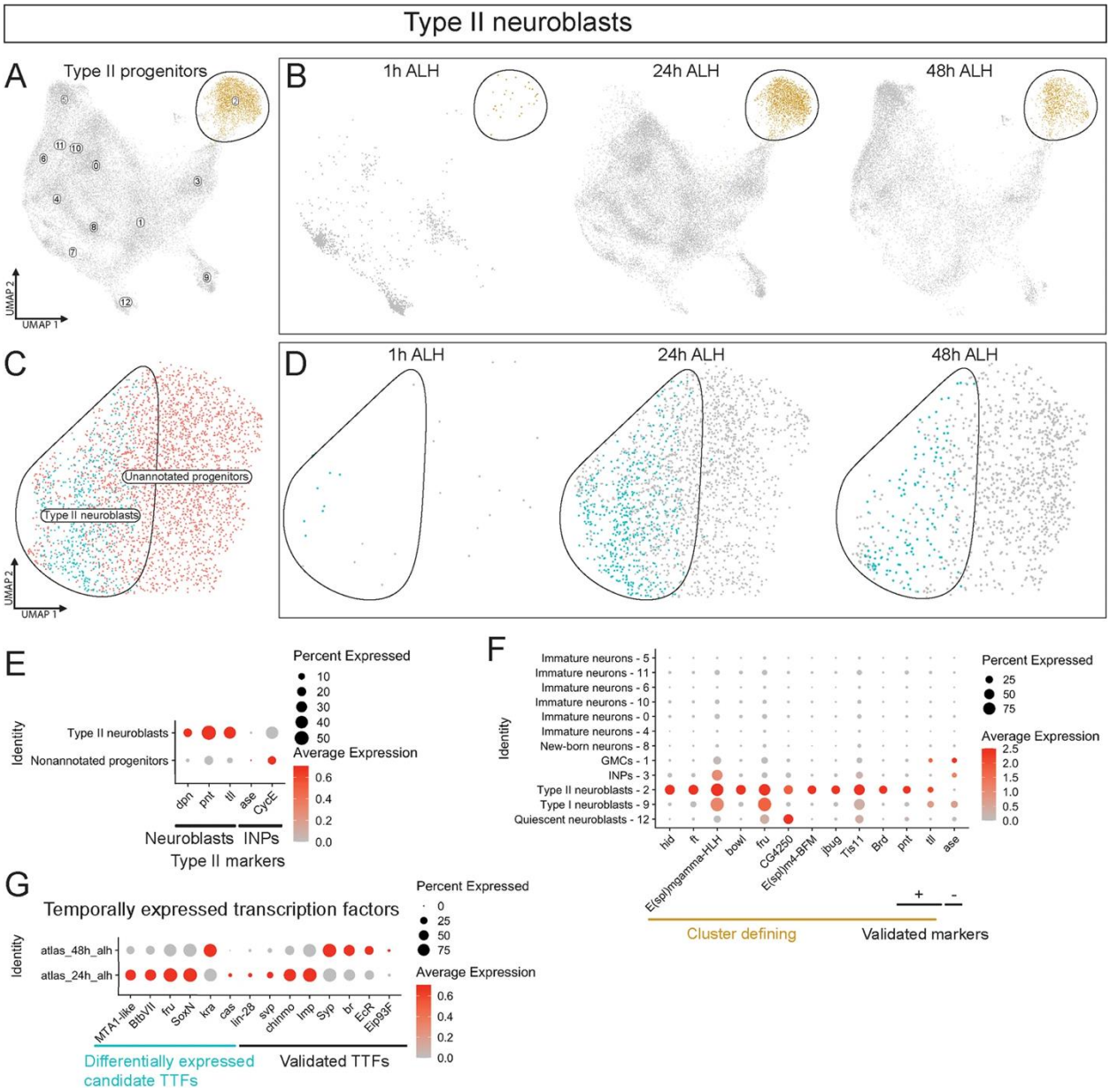

Fig. 2.4 Type II progenitor cluster contains type II neuroblasts that show candidate temporal transcription factors. A UMAP of type II progenitors highlighted. **B** UMAP of cluster from 1h-48h. **C** UMAP of sub clustered type II progenitors. **D** UMAP of type II neuroblasts from 1h-48h. **E** Dot plot of validated markers between type II neuroblasts and nonannotated progenitors. **F** Dot plot of top cluster defining genes and validated markers for type II neuroblasts. **G** Dot plot of differentially expressed TTFs between 24h alh and 48h type II neuroblasts.

We focused on identifying novel candidate TTFs between 24h and 48h in the sub-clustered type II neuroblast population. We found that validated TTFs (Fig. 2.4g; Supp. Table 2.9) followed the temporal trend previously described [80]. In addition, several novel candidate TTFs were

differentially expressed between 24h and 48h (Fig. 2.4g). The factors *BtbVII*, *fru* and *SoxN* show expression at 24h similar to the identified Type I neuroblast candidate TTFs. Our findings identify novel candidate type II neuroblast TTFs.

INPs express candidate novel cell type markers

Type II neuroblasts are unique among neuroblasts by producing INPs that generate a series of 4–6 GMCs, which each produce a pair of neurons. Type I neuroblasts in the VNC and optic lobe generate GMCs, which produce just two progeny neurons. In this way, INPs are more similar to type I neuroblasts than to GMCs. INPs can be identified by the expression of general progenitor markers (*dpn*, *ase*, *mira*, *wor*) and previously validated INP-specific gene expression of *erm* (also called *fezf2*) and *ham* (Fig. 2.5c; Table 2.1; Supp. Table 2.2). INPs were located near the type II neuroblasts on the UMAP plots, consistent with being derived from type II neuroblasts (Fig. 2.5a). As expected, we detected almost no INPs at 1h (Fig. 2.5b, left); these are likely to be INPs produced by embryonic type II neuroblasts [83] that are in quiescence at 1h. By 24h the type II neuroblasts have exited from quiescence and have generated a pool of INPs (Fig. 2.5b, center) which is maintained at 48h ALH (Fig. 2.5b, right). We identified a number of cluster defining genes including a proliferating INP marker *CycE* (Fig. 2.5c). These genes are excellent candidates for selective expression in INPs and could play a role in regulating INP-specific aspects of development and function; this hypothesis awaits validating gene expression and function.

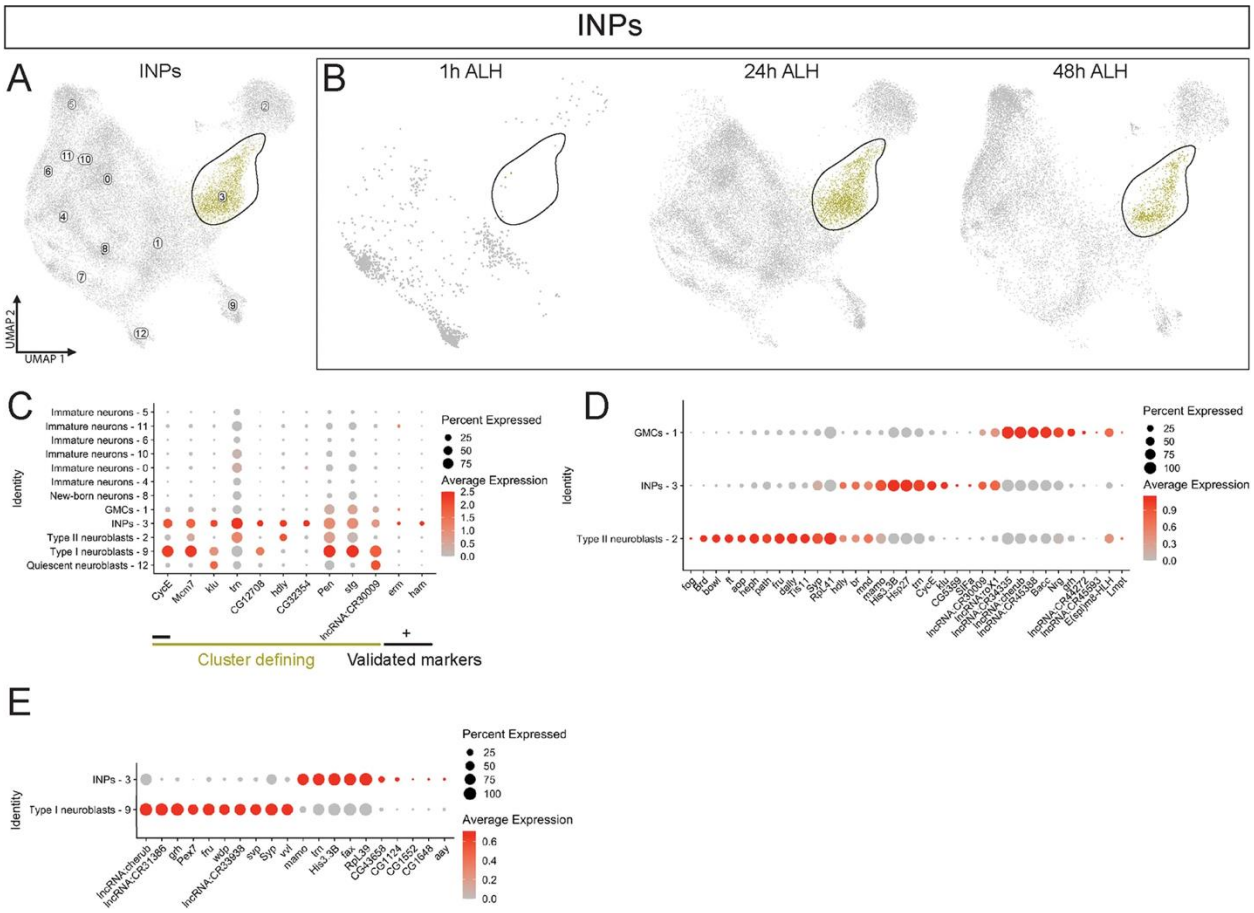

Fig. 2.5 INPs show candidate novel markers. A UMAP of INPs highlighted. **B** UMAP of cluster from 1h-48h alh. **C** Dot plot of top cluster defining genes and validated markers for INPs. **D** Dot plot of differentially expressed genes between type II neuroblasts, INPs and GMCs. **E** Dot plot of differentially expressed genes between type I neuroblasts and INPs.

INPs are located on the "progenitor" side of the UMAP plot, nestled between their progenitor (cluster 2, type II neuroblasts) and progeny (cluster 1, GMCs; Fig. 2.5a). Thus, we directly compared expression of cluster defining genes for all three cell types and found clear differences in gene expression (Fig. 2.5d; Supp. Tables 2.10 and 2.11). We hypothesize that these genes may play a role in distinguishing the fate of all three progenitor types. INPs share a cell division pattern that is similar to type I neuroblasts (both producing a series of GMCs) as well as share expression of many pan-neuroblast genes (e.g. *dpn*, *mira*, *insc*, *wor*, *ase*; Fig. 2.1c; Table 2.1). Thus, we wondered how different INPs and type I neuroblasts were by scRNA-seq. We found that while many genes shared expression profiles in the two cell types, we were able to identify a number of genes that showed selective expression in INPs or type I neuroblasts (Fig. 2.5e; Supp. Table 2.12). In particular, we found several long non-coding RNAs expressed specifically in type

I neuroblasts, and several previously uncharacterized genes expressed specifically in INPs. We note that *grainy head* (*grh*) is known to be expressed in both type I neuroblasts and late in some INP lineages [84–88], and it shows up as more strongly expressed in neuroblasts than INPs in our analysis (Fig. 2.5e). We conclude that INPs and type I neuroblasts have distinctive gene expression profiles, and that these differentially expressed genes are good candidates for distinguishing cell lineage and/or cell fate differences between these progenitors.

GMCs, new-born neurons and immature neurons express candidate novel cell type markers

Here we focus on the more fate-restricted GMCs, derived from type I neuroblasts and INPs, and their immature neuron progeny. GMCs were positive for the validated markers *dap* and *tap*; represented in cluster 1 (Fig. 2.6a,g; Table 2.1; Supp. Table 2.2). We identified new-born neurons by the Notch target *Hey*, which is expressed in new-born neurons following asymmetric division of GMCs into one $Notch^{ON}$ neuron (*Hey*+) and one $Notch^{OFF}$ neuron (*Hey*-) [41, 89]; new-born neurons are represented in cluster 8 and include both Hey + $Notch^{ON}$ neurons and Hey- presumptive $Notch^{OFF}$ neurons (Fig. 2.6c,h; Table 2.1). We annotated immature neurons by the expression of published immature neuron markers and absence of mature neuron markers, and markers, and are represented in clusters 0, 4–6, 8, 10, and 11 (Fig. 2.6e,i; Table 2.1). Clusters 0 and 4 are the first immature neuron clusters to appear at 24h, closest to the new-born neurons and show the weakest expression of mature neuron markers (Fig. 2.6e-f,i). Conversely, clusters 5, 6 and 11 appear at 48h, are further from the new-born neurons and have the highest expression of neurotransmitters. We hypothesize that these distinct immature neuron clusters provide a differential axis given their temporal, spatial and gene marker expression patterns.

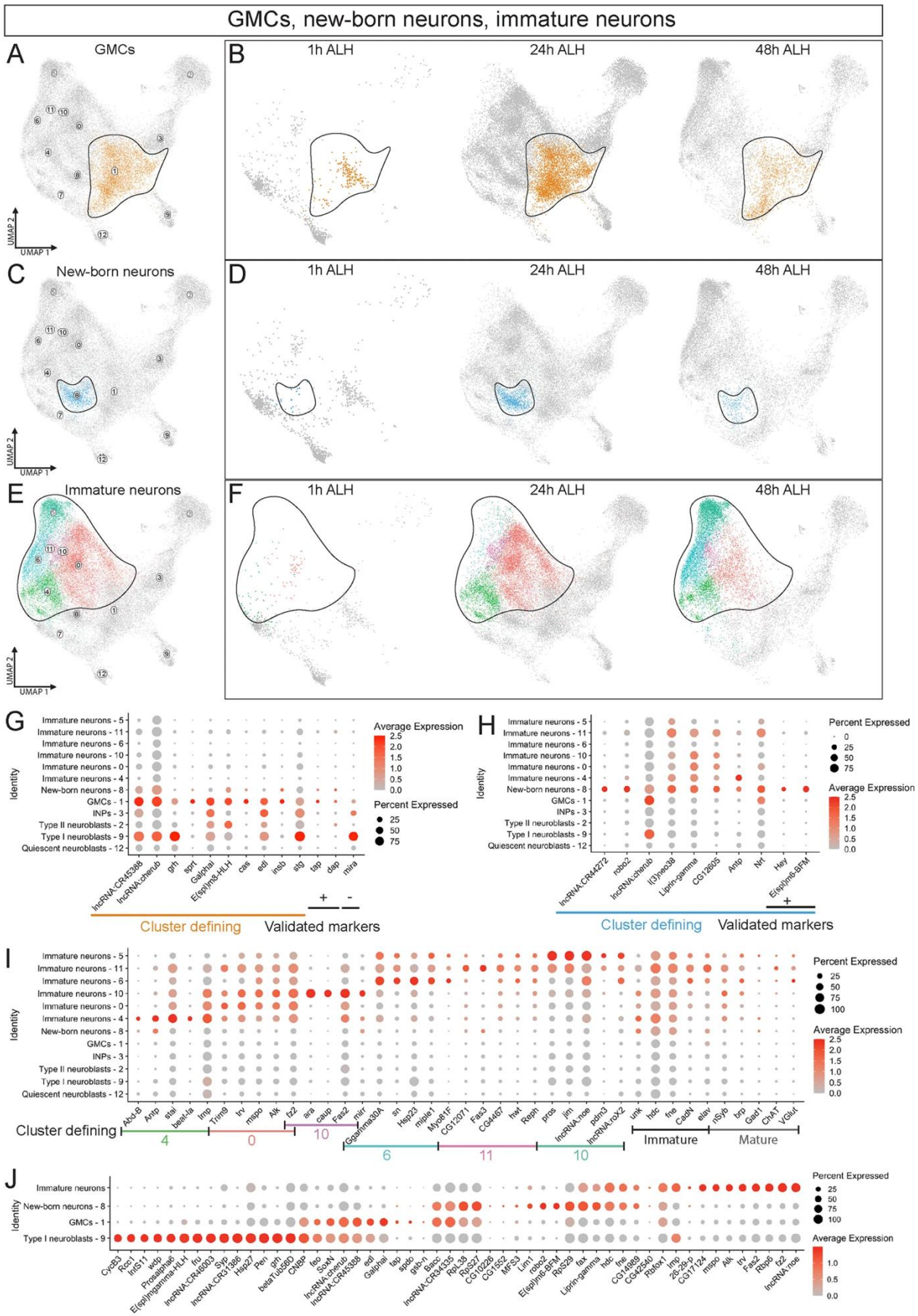
GMCs, new-born neurons, immature neurons
A
GMCs
B
1h ALH
24h ALH
48h ALH
C
New-born neurons
D
1h ALH
24h ALH
48h ALH
E
Immature neurons
F
1h ALH
24h ALH
48h ALH
UMAP 1
UMAP 2
G
Identity
Immature neurons - 5
Immature neurons - 11
Immature neurons - 6
Immature neurons - 10
Immature neurons - 0
Immature neurons - 4
New-born neurons - 8
GMCs - 1
INPs - 3
Type II neuroblasts - 2
Type I neuroblasts - 9
Quiescent neuroblasts - 12
lncRNA:CR45388
lncRNA:cherub
grh
sprt
Galphai
E(spl)m6-HLH
cas
edl
insb
stg
tap
dap
mira
Average Expression
Percent Expressed
Cluster defining
Validated markers
H
lncRNA:CR44272
robo2
lncRNA:cherub
l(3)neo38
Liprin-gamma
CG12605
Antp
Nrt
Hey
E(spl)m6-BFM
Percent Expressed
Average Expression
Cluster defining
Validated markers
I
Abd-B
Antp
stai
beat-Ia
Imp
TrimG
Irv
mspo
Alk
tz2
ara
caup
Fas2
mirr
Ggamma30A
sn
Hsp23
mipt1
Myo81F
CG12071
Fas3
CG4467
hwt
Reph
pros
jim
lncRNA:noe
pdm3
lncRNA:roX2
unk
hdc
fne
CadN
elav
nSyb
brp
Gad1
ChAT
VGlut
Cluster defining
4
0
10
6
11
10
Immature
Mature
Percent Expressed
Average Expression
J
Immature neurons
New-born neurons - 8
GMCs - 1
Type I neuroblasts - 9
CycB3
Rcd1
Intl11
lwdp
Prosalpha6
E(spl)mgamma-HLH
lncRNA:CR40603
Syp
lncRNA:CR31386
Hsp27
Pen
grh
betaTub56D
CNBP
fax
SoxN
lncRNA:cherub
lncRNA:CR45388
edl
Galphai
tap
sqd
gish-1
Bacc
lncRNA:CR34335
RpL38
RpS27
CG10226
CG11552
MFS3
Lim1
robo2
E(spl)m6-BFM
RpS29
fax
Liprin-gamma
hdc
fne
CG14989
CG42540
Rbfox1
Imp
26-29-p
CG17124
mspo
Alk
Irv
Fas2
Rbp6
tz2
lncRNA:noe
Percent Expressed
Average Expression

Fig. 2.6 (previous page) GMCs, new-born neurons and immature neurons show candidate novel markers. A UMAP of GMCs highlighted. **B** UMAP of GMCs from 1h-48h alh. **C** UMAP of new-born neurons highlighted. **D** UMAP of new-born neurons from 1h-48h alh. **E** UMAP of immature neurons highlighted. **F** UMAP of immature neurons from 1h-48h alh. **G-I** Dot plot of top cluster defining genes and validated markers for: **G** GMCs **H** New-born neurons **I** Immature neurons. **J** Differentially expressed genes between type I neuroblasts, GMCs, new-born neurons and immature neurons.

Interestingly, the three cell types (GMC, new-born neuron, and immature neuron) formed a differentiation axis from right to left in the UMAP plot (Fig. 2.6a,c,e); as expected, each of the three cell types were under-represented at 1h when most neuroblasts are quiescent and not producing progeny (Fig. 2.6b,d,f). We note that progenitors are dividing throughout larval life and add complexity to the data set given each timepoint will have each of these defined transitory cell types.

In addition to the validated cell type markers, we found potential novel markers for each cell type that drove cluster assignments. Top cluster defining genes for GMCs were shared with other progenitor cell types, but several were GMC specific including *sprt* and *cas* (Fig. 2.6g; Supp. Table 2.2). New-born neuron cluster defining genes included the validated markers *Hey* and a second putative Notch target gene *E(spl)m6-BFM* (Fig. 2.6h; Table 2.1; Supp. Table 2.2). The six immature neurons clusters were defined by expression of known immature neuron markers and absence of known mature neuron markers such as neurotransmitter biosynthetic genes (Fig.2. 6i; Table 2.1; Supp. Table 2.2).

To determine candidate novel markers that distinguish cell types along the differentiation axis, we compared each cluster for their top differentially expressed genes relative to the developmentally adjacent cell type. We grouped all 6 immature neuron clusters as a single cell type for comparison. We found distinct novel candidate markers that showed markers exclusive to individual cell types and shared between them (Fig. 2.6j; Supp. Tables 2.13, 2.14 and 2.15). Interestingly, we found type I neuroblasts and immature neurons had the most specific candidate markers (Fig. 2.6j, left and right) while GMCs and new-born neurons contained candidate markers shared more widely (Fig. 2.6j, middle). We conclude that our progenitor atlas reveals a

robust gene expression along a differential axis from progenitors to immature neurons with novel candidate markers and expression profiles present in each cell type.

Mature neurons show temporally distinct groups of transcription factors and cell surface molecules

To investigate temporal changes in mature neurons, we subclustered 51,596 cells from clusters positive for the mature neuron markers *brp* and *nSyb* from the whole atlas (Fig. 2.7a). Using validated markers and neurotransmitter genes, we annotated 11 out of the 14 mature neuron clusters (Fig. 2.7c; Supp. Table 2.16). Three clusters (clusters 1, 10 and 11) were left unannotated due to their lack of expression for known, validated markers (Fig. 2.7c, top). Surprisingly, we identified octopaminergic and neurosecretory neurons despite their relatively small cell number in the atlas of 126 and 79 respectfully. Interestingly, clusters 4 and 5 were temporally regulated, with cluster 4 enriched at 24h and cluster 5 enriched at 48h (Fig. 2.7b). These temporal clusters both expressed the immature neuronal markers *CadN* and *hdc*, suggesting that they are the least differentiated within this population of mature neurons (Fig. 2.7c, left). We further investigated the difference between the two clusters and found differential expression of cell surface molecules and neural differentiation genes such as *Toll-6/7*, *beat-IIa*, *jim* and *pros* (Fig. 2.7d; Supp. Table 2.17).

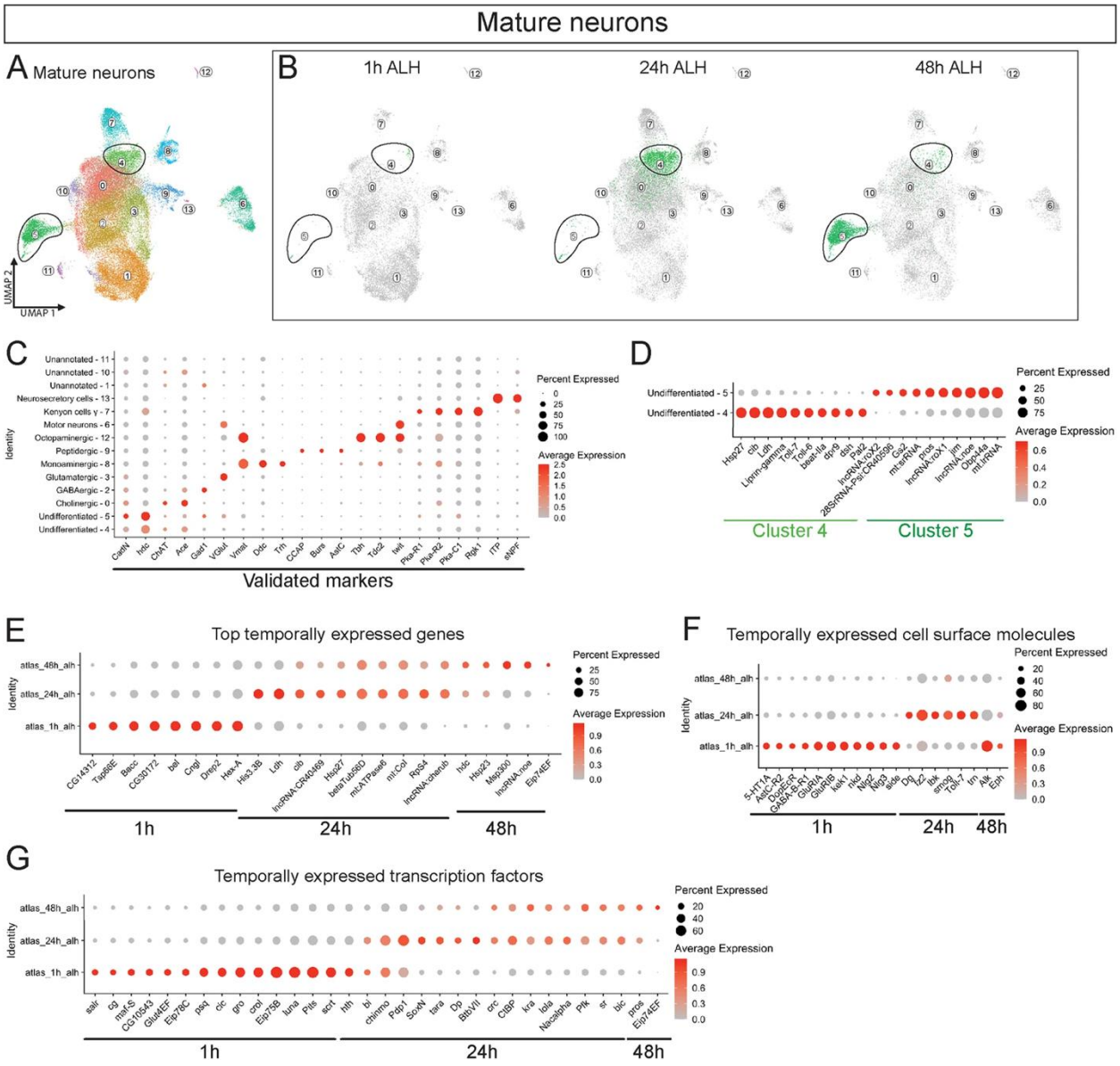

Fig. 2.7 Mature neuron conclusion. A An atlas of mature neurons (*Brp* and *nSyb* positive) was made with a subset of 51,596 cells from the whole atlas. **B** UMAP of atlas from 1h-48h alh with clusters 4 and 5 outlined. (**C**) Validated cell identity markers label distinct neuronal cell types. **D** Dot plot of differentially expressed factors between cluster 4 and 5. **E** Dot plot of top differentially* expressed genes between 1h alh, 24h alh and 48h alh in labeled mature neurons. **F** Dot plot of differentially* expressed cell surface molecules between 1h alh and 24h alh in labeled mature neurons. 48h alh contained no differentially expressed cell surface molecule genes. **G** Dot plot of differentially* expressed transcription factors between 1h alh, 24h alh and 48h alh in labeled mature neurons. *Genes found differentially expressed in at least 2 out of 9 annotated clusters of differentiated neuron cell types.

To identify temporally expressed genes within mature neurons, we focused on the remaining nine differentiated and annotated clusters within our mature neuron atlas. To circumvent the

differences in cell number between clusters that may weight gene expression of larger clusters disproportionately, we found the top temporally expressed genes for each cluster and only included genes found in more than one cluster to reduce noise. We identified the top temporally expressed genes between all three time points (Fig. 2.7e; Supp. Tables 2.18, 2.19, 2.20, 2.21, 2.22, 2.23, 2.24, 2.25, 2.26 and 2.27). Notably, 24h and 48h neurons are more similar to each other than 1h neurons (Fig. 2.7e, middle), perhaps due to most 1h mature neurons being produced during embryogenesis, whereas the other clusters likely contain neurons produced during larval stages.

We further explored stage-specific differences by finding temporally expressed cell surface molecules and transcription factors in at least three out of the nine clusters (Fig. 2.7f,g; Supp. Tables 2.28 and 2.29). At 1h, there was an upregulation of several neurotransmitter receptors and neuroligins (Fig. 2.7f, left). At 24h, there was an upregulation of several cell adhesion molecules, while 48h showed no upregulation of cell surface molecule genes (Fig. 2.7f, middle). Interestingly, *Alk* and *Eph* were downregulated at 48h (Fig. 2.7f, right). We identified over a dozen transcription factors upregulated at 1h (Fig. 2.7g, left). Not surprisingly, 24h and 48h also were enriched for distinct groups of similar transcription factors (Fig. 2.7g, right). These temporally expressed genes provide novel candidates for molecules involved with dynamic roles such as synaptic wiring and neuronal function.

We found that our mature neuron atlas contains a diversity of neuronal types across all time points. We provided evidence that 1h mature neurons had more differentially expressed genes compared to 24h and 48h across top markers and transcription factors, suggesting mature neuron gene expression is more temporally dynamic prior to 24h. We conclude that we have identified candidate temporal markers within mature larval neurons.

Discussion

Several scRNA-seq atlases of *Drosophila* larvae have been created [12, 15, 18, 20, 25, 90, 91]; however, few studies have offered multiple time points [21] but none to our knowledge have done so for the whole larval CNS as in our work (Fig. 2. 1). Although other scRNA-seq analyses have provided and validated cell type markers [12, 15, 18, 20, 25, 90, 91], we provide novel

candidate temporal factors within multiple cell types and lineages. It remains to be seen if the novel candidate markers we state here are validated *in vivo* and what their role is during development. Our work emphasizes the robustness of scRNA-seq data as supporting previously known gene expression profiles within specific cell types and providing strong candidate genes to explore. We provide access to our whole larval atlas and analysis as an easy to explore resource for the community (see Methods).

We note that some of our scRNA-seq samples had low sequencing depth and low read mapping (see Methods). Nevertheless, our whole atlas of 97,845 cells revealed a diversity of cell types: it identified all known progenitor cell types as well as many known mature neuronal types, including some that are quite rare (e.g. neurosecretory cells or insulin producing cells). The atlas contained three developmental time points (1h, 24h and 48h), and we still observed a robust differentiation axis within progenitors: from neuroblasts to neurons within UMAP plots. This further highlights the reliability of a scRNA-seq approach. In the future it would be beneficial to include additional time points across all developmental stages from embryo to adult.

Quiescent neuroblasts and glial signaling

Neuroblasts enter a quiescent state in the late embryo and exit in the early larvae [28]. A challenge in studying quiescent neuroblasts has been the lack of cell specific markers, given their loss of canonical neuroblast markers [28, 92]. We found that quiescent neuroblasts formed a distinct cluster in the UMAP plots, the first time scRNA-seq methods have identified quiescent neuroblasts. Interestingly, the RNA-binding protein Lin-28, known to be expressed in neuroblasts at early larval stages [81, 82, 93, 94] was a cluster defining gene for quiescent neuroblasts. *Lin-28* has been previously shown to play a role in regulating *InR* in intestinal stem cells [95]. This fits with our findings that quiescent neuroblasts are transcriptionally primed to respond to insulin signaling without expressing the cell cycle and cell growth genes that are activated upon exit from quiescence (Fig. 2.2h). It would be interesting to investigate other genes regulating the insulin signaling pathway as neuroblast early TTFs. It would also be interesting to test the function of the identified but uncharacterized neuroblast quiescence cluster defining genes.

Glia are known to maintain neuroblast quiescence as well as promote neuroblast reactivation via secreted signaling molecules [28, 75, 76]. As expected, we found both cortex and surface glia upregulate *ilps* at developmental times coinciding with exit from neuroblast quiescence (Fig. 2.2i). This provides evidence supporting the model that cortex glia express *ana* during early larval development to maintain quiescent neuroblasts while perineurial surface glia upregulate *trol* to signal an exit from quiescence. Future work should test if these glia subtypes are indeed responsible for regulating neuroblast quiescence.

TTFs in type I and type II neuroblasts

Embryonic neuroblasts have well characterized TTF cascades [80], but it is likely that only a fraction of larval neuroblast TTFs have been identified, and even fewer have been functionally characterized. Identifying larval TTFs is complicated by larvae containing both type I and type II neuroblasts that may have similar but not identical TTFs expressed synchronously in both neuroblast populations [81, 82]. Moreover, different TTFs may be used in each type of neuroblast due to their different cell lineage (type I neuroblasts bud off GMCs while type II neuroblasts bud off INPs). Our analysis of type I and type II neuroblasts identified novel candidate TTFs with some shared and other exclusive to one of these neuroblast types. We note that identifying temporally expressed genes is difficult with only two time points, but our work should narrow the time window for validating these candidate TTFs as early expressed factors. Future work should not only explore validating these TTFs but also probing scRNA-seq data to find additional TTFs at later time points in larval development.

Intermediate neural progenitors

INPs are produced from type II neuroblasts and add an additional TTF cascade in their divisions prior to producing GMCs [84]. Unfortunately, we were unable to provide candidate TTFs for INPs given the challenge of distinguishing INP specific TTFs from ones carried over from the type II neuroblast TTF cascade. Our analysis indicates transcriptional similarity between INPs and Type I neuroblasts with sharing common cluster defining genes (Fig. 2.5c). Despite the similarity between the cell types, we found differentially expressed genes that offer promising candidate genes that could underlie the different roles of these neural progenitors. This brings up an unexplored question of whether INPs and type I neuroblasts follow the same larval TTF

cascade given their similarity in lineage (both produce a series of GMCs). We hypothesize that common TTFs are likely but also expect transcriptional differences that could be tested for cell type specific functions.

The transition from progenitor to post-mitotic neurons

The transition from GMCs to newly born neurons marks a distinct developmental shift as a progenitor cell type becomes committed to a post-mitotic state. We noticed that cluster defining genes for GMCs were broadly expressed in progenitors while defining genes for new-born neurons were broadly expressed in immature neurons (Fig. 2.5g-h). This indicates a distinct transcriptional change captured in our analysis. We note that the GMC cluster was unexpectedly defined by *cas* expression, previously known for its expression and function in neuroblasts [96–98]; our results suggest *cas* should be re-evaluated for a functional role in GMCs. Future scRNA-seq work should keep in mind that candidate genes found represent transcripts not proteins; it is likely that these are not the same patterns for many genes due to post-transcriptional regulation.

Immature neurons represent an ambiguous cell identity that is poorly described in the literature, and there are few reliable markers [99, 100]. Our analysis found candidate markers that may bridge this gap. Curiously, our immature neurons were composed of six clusters; yet we were able to define it as a single cell type with the limited validated cell makers. Our cluster defining genes closely resemble those found in Michiki *et al.* [25] as novel neuronal markers differentially expressed over pseudotime. Additionally, our immature neuron clusters followed a developmental projection away from progenitors in both UMAP space and temporally (Fig. 2.1d-e). Thus, each of the six immature neuron clusters may represent discrete differentiation states within immature neurons. Alternatively, each cluster may represent neuroblast lineage-specific, segment-specific, or region-specific (e.g. central brain vs VNC). We did not observe differential expression of Hox genes in each cluster (data not shown), ruling out anterior/posterior regional clusters. Investigating how immature neurons form six discrete clusters is an interesting question for the future.

Mature neurons show novel temporal changes

Mature neurons have been extensively studied to understand their unique neurotransmitter expression down to rare subtypes [101–105], yet limited efforts have explored temporal changes within the same neuronal identities across development. We found significant changes in gene expression across early larval development within mature neurons. Most notably, we found one neuron cluster specifically only present at 24h and a different neuron cluster only expressed at 48h (Fig. 2.7b). We suspect that these clusters represent larval neurons born at different times and thus become differentiated at different times. If our suggestion is correct, it would show that larval born neurons can differentiate asynchronously, rather than differentiation being triggered for all larval born neurons at a single timepoint.

Previous larval scRNA-seq datasets have characterized temporally expressed neurons within specific cell types [20, 21]. In contrast, our analysis found global temporal changes shared across almost all differentiated neurons and provided interesting candidate genes for future functional assays (Fig. 2.7e-g). We noticed the most significant changes occurred between 1h and 24h. Surprisingly, we found many genes encoding "mature" neuron functions were upregulated at 1h. For example, various neurotransmitter receptors and the synaptic connectivity molecules Nlg2 and Nlg3. This is likely due to the presence of embryonic-born differentiated neurons at 1h after larval hatching. These findings suggest that establishing neuronal connectivity is persisting from late embryos into newly hatched larvae.

Conclusions

While much of the Drosophila genome has been extensively studied, there remains many uncharacterized genes. Our scRNA-seq analysis, similar to others [14, 24, 25, 81], can provide testable hypotheses for gene function based on cell type specific gene expression or co-expression with genes of a known function. We found many computational genes (CGs) with cell type-specific expression, as well as long noncoding RNAs. Both classes are likely to provide new insights into CNS development and function.

Materials and methods

Single cell isolation and sequencing

We analyzed a single-cell RNA-sequencing reads from dissociated cells collected from dissected Drosophila larval CNS tissue from 1h, 24h and 48h after larval hatching [27]. The raw sequencing data was obtained from GEO under the accession code GEO : GSE135810. In this study, we only used the following samples for analysis to enrich for larval neural progenitors: GSM4030593, GSM4030594, GSM4030597, GSM4030595, GSM4030596, GSM4030600, GSM4030601, GSM4030606, GSM4030602, GSM4030603, GSM4030604, GSM4030605, GSM4030607, GSM4030613, GSM4030614.

scRNA-seq analysis

Our bioinformatic analysis was performed using Cell Ranger software (Version 6.0.1, 10x Genomics, Pleasanton, CA, USA) and the Seurat R package version 4.0.4 [106]. Briefly, Cell Ranger was used to perform demultiplexing, alignment, filtering, and counting of barcodes and UMIs, with the output being a cell-by-genes matrix of counts. Additionally, Cell Ranger was used to aggregate cells from multiple samples for each time point into single feature-barcode matrices. To further ensure that only high-quality cells were retained, we removed any cells with fewer than 200 unique features and more than 20% mitochondrial RNA.

Principal component analysis was performed with cells as samples and gene expression levels as features. The top principal components (PCs) were retained as features for downstream analyses as determined by Elbow plots. We used 50 PCs for the main atlas and most of the following clusters as this provided a compromise of significant PCs and computational cost to run downstream analyses. Based on these top PCs, cells were clustered using the original Louvain algorithm approach in Seurat. Cluster resolution was determined by optimizing clusters to fit validated markers to ensure capturing an appropriate number of cell types. In order to visualize the results of the analysis, the top PCs were used to perform a nonlinear embedding into two dimensions using the UMAP algorithm.

Differentially expressed genes within clusters were determined to be expressed in at least 10% more cells within the cluster(s) of interest compared to other clusters. Additionally, the average log fold change of expression cut off was 0.1 or more. We kept differentially expressed genes only if the adjusted p-value in a Wilcoxon Rank Sum test was below a threshold of 0.05. Dot

plots show the average expression level of genes across all cells within the class. Temporally expressed genes were determined between time points in the atlas with similar number of cells. 1h cells were excluded from progenitor temporal analyses but kept with the mature neuron atlas given their approximately equal representation within the data sets.

Subclustering for further Seurat analysis

A total of 33,458 cells were identified as either neural progenitors or immature neurons within the whole atlas based on their cluster defining gene expression of validated markers specified in Table 2. 1. We reclustered these cells and kept 50 PCs as we did with the whole atlas and adjusted the cluster resolution to 0.49 as it provided biologically supported cell types as we identified all known progenitors with the fewest number of clusters. Differentially expressed genes were determined as described above. A total of 11,004 cells in *repo* positive clusters were labeled as glia and reclustered. We kept 50 PCs and adjusted the resolution to 0.045 as it provided the minimum number of clusters that strongly fitted known glia subtypes based on validated cell markers. We subclustered the progenitor atlas cluster 2, which we labeled as type II neuroblasts given *pnt* and *tll* expression. We kept 50 PCs and a resolution of 0.1 to show two clusters that were separated based on known cell type makers, e.g. a strong type II neuroblast cells and type II like progenitors were distinct. We subclustered 51,596 cells from *Brp* and *nSyb* positive clusters. Again, we kept 50 PCs but changed the cluster resolution to 0.37 as it provided the minimum number of clusters while capturing all known neuronal cell types that we could identify in the data.

Data and code availability

All code used for analyses with the corresponding Cell Ranger outputs and Seurat objects are available at (https://www.dropbox.com/sh/iilbqlqysgyocbu/AADar0UdyA1Ep5qsHtRhiq_da?dl=0). scRNA-seq data is accessible under the accession code GEO: GSE135810.

Protein localization

Standard methods were used for immunofluorescent staining [107]. The line for the foxo:GFP fusion protein is *MI00493-GFSTF.0* (BDSC#59,766) detected with anti-GFP immunofluoresence. Primary antibodies and sources: chicken anti-GFP (1:500; Abcam 13,970,

Cambridge, MA, USA), rat anti-Dpn (1:100; Abcam), guinea pig anti-InR (1:500; Siegrist lab). Secondary antibodies were from Jackson ImmunoResearech and used according to product recommendation. Images were collected on a Leica SP8 laser scanning confocal microscope (Leica, Wetzlar, Germany) equipped with a 63×, 1.4 NA oil-immersion objective.

Supplementary information

Supplementary information can be found in the online version of this work at https://doi.org /10.1186/s13064-022-00163-7.

Bridge

This chapter covered the published work of my co-authors and I where we used a large scRNAseq dataset to identify new features of the *Drosophila* larval CNS at key developmental timepoints. We identified all known major classes of neural progenitors and identified candidate markers for each. Surprisingly, we identified quiescent NBs and show that they are primed to respond to extrinsic signaling molecules from their adjacent glia. We propose several new TTF candidates for the larval NBs. Our work in this chapter demonstrates how large scRNAseq datasets allow for understanding temporally dynamic transcriptomes. Importantly, this work identified the genes: *seven-up* and *castor* in the T2NB lineages. I will cover these two genes in Chapters III and IV with regards to their roles in a) temporal progression of the T2NBs and b) temporal patterning to specify unique neuron identities.

References

1. Luo L. Principles of Neurobiology. 2. Boca Raton: Garland Science; 2020.

2. Skeath JB, Thor S. Genetic control of Drosophila nerve cord development. Curr Opin Neurobiol. 2003;13:8–15. doi: 10.1016/S0959-4388(03)00007-2.

3. Hobert O, Westphal H. Functions of LIM-homeobox genes. Trends Genet TIG. 2000;16:75–83. doi: 10.1016/S0168-9525(99)01883-1.

4. Clark BS, Stein-O'Brien GL, Shiau F, Cannon GH, Davis-Marcisak E, Sherman T, et al. Single-Cell RNA-Seq Analysis of Retinal Development Identifies NFI Factors as Regulating Mitotic Exit and Late-Born Cell Specification. Neuron. 2019;102:1111–1126.e5. doi: 10.1016/j.neuron.2019.04.010.

5. Johnson MB, Walsh CA. Cerebral cortical neuron diversity and development at single-cell resolution. Curr Opin Neurobiol. 2017;42:9–16. doi: 10.1016/j.conb.2016.11.001.

6. Li Z, Tyler WA, Haydar TF. Lessons from single cell sequencing in CNS cell specification and function. Curr Opin Genet Dev. 2020;65:138–43. doi: 10.1016/j.gde.2020.05.043.

7. Chang E, Ruan X, Zhu R, Wang Y, Zhang J. Values of Single-Cell RNA Sequencing in Development of Cerebral Cortex. Adv Exp Med Biol. 2020;1255:231–47. doi: 10.1007/978-981-15-4494-1_19.

8. Ying P, Huang C, Wang Y, Guo X, Cao Y, Zhang Y, et al. Single-Cell RNA Sequencing of Retina:New Looks for Gene Marker and Old Diseases. Front Mol Biosci. 2021;8:699906. doi: 10.3389/fmolb.2021.699906.

9. Meistermann D, Bruneau A, Loubersac S, Reignier A, Firmin J, François-Campion V, et al. Integrated pseudotime analysis of human pre-implantation embryo single-cell transcriptomes reveals the dynamics of lineage specification. Cell Stem Cell. 2021;S1934-5909(21):00185–5.

10. Zheng S, Papalexi E, Butler A, Stephenson W, Satija R. Molecular transitions in early progenitors during human cord blood hematopoiesis. Mol Syst Biol. 2018;14:e8041. doi: 10.15252/msb.20178041.

11. Zhou W, Yui MA, Williams BA, Yun J, Wold BJ, Cai L, et al. Single-Cell Analysis Reveals Regulatory Gene Expression Dynamics Leading to Lineage Commitment in Early T Cell Development. Cell Syst. 2019;9:321–337.e9. doi: 10.1016/j.cels.2019.09.008.

12. Konstantinides N, Kapuralin K, Fadil C, Barboza L, Satija R, Desplan C. Phenotypic Convergence: Distinct Transcription Factors Regulate Common Terminal Features. Cell. 2018;174:622–635.e13. doi: 10.1016/j.cell.2018.05.021.

13. Bates AS, Janssens J, Jefferis GS, Aerts S. Neuronal cell types in the fly: single-cell anatomy meets single-cell genomics. Curr Opin Neurobiol. 2019;56:125–34. doi: 10.1016/j.conb.2018.12.012.

14. Croset V, Treiber CD, Waddell S. Cellular diversity in the Drosophila midbrain revealed by single-cell transcriptomics. eLife. 2018;7:e34550. doi: 10.7554/eLife.34550.

15. Davie K, Janssens J, Koldere D, De Waegeneer M, Pech U, Kreft Ł, et al. A Single-Cell Transcriptome Atlas of the Aging Drosophila Brain. Cell. 2018;174:982–998.e20. doi: 10.1016/j.cell.2018.05.057.

16. Özel MN, Gibbs CS, Holguera I, Soliman M, Bonneau R, Desplan C. Coordinated control of neuronal differentiation and wiring by a sustained code of transcription factors [Internet]. bioRxiv; 2022 [cited 2022 May 2]. p. 2022.05.01.490216. Available from: https://www.biorxiv.org/content/10.1101/2022.05.01.490216v1

17. Özel MN, Simon F, Jafari S, Holguera I, Chen Y-C, Benhra N, et al. Neuronal diversity and convergence in a visual system developmental atlas. Nature. 2021;589:88–95. doi: 10.1038/s41586-020-2879-3.

18. Li H, Horns F, Wu B, Xie Q, Li J, Li T, et al. Classifying Drosophila Olfactory Projection Neuron Subtypes by Single-Cell RNA Sequencing. Cell. 2017;171:1206–1220.e22. doi: 10.1016/j.cell.2017.10.019.

19. Li H, Li T, Horns F, Li J, Xie Q, Xu C, et al. Single-Cell Transcriptomes Reveal Diverse Regulatory Strategies for Olfactory Receptor Expression and Axon Targeting. Curr Biol CB. 2020;30:1189–1198.e5. doi: 10.1016/j.cub.2020.01.049.

20. McLaughlin CN, Brbić M, Xie Q, Li T, Horns F, Kolluru SS, et al. Single-cell transcriptomes of developing and adult olfactory receptor neurons in Drosophila. eLife. 2021;10:e63856. doi: 10.7554/eLife.63856.

21. Xie Q, Brbic M, Horns F, Kolluru SS, Jones RC, Li J, et al. Temporal evolution of single-cell transcriptomes of Drosophila olfactory projection neurons. eLife. 2021;10:e63450. doi: 10.7554/eLife.63450.

22. Kurmangaliyev YZ, Yoo J, Valdes-Aleman J, Sanfilippo P, Zipursky SL. Transcriptional Programs of Circuit Assembly in the Drosophila Visual System. Neuron. 2020;108:1045–1057.e6. doi: 10.1016/j.neuron.2020.10.006.

23. Brunet Avalos C, Sprecher SG. Single-Cell Transcriptomic Reveals Dual and Multi-Transmitter Use in Neurons Across Metazoans. Front Mol Neurosci. 2021;14:623148. doi: 10.3389/fnmol.2021.623148.

24. Marques GS, Teles-Reis J, Konstantinides N, Brito PH, Homem CCF. Fate transitions in Drosophila neural lineages: a single cell road map to mature neurons [Internet]. 2021 Jun p.

2021.06.22.449317. Available from:
https://www.biorxiv.org/content/10.1101/2021.06.22.449317v1

25. Michki NS, Li Y, Sanjasaz K, Zhao Y, Shen FY, Walker LA, et al. The molecular landscape of neural differentiation in the developing Drosophila brain revealed by targeted scRNA-seq and multi-informatic analysis. Cell Rep. 2021;35:109039. doi: 10.1016/j.celrep.2021.109039.

26. Karaiskos N, Wahle P, Alles J, Boltengagen A, Ayoub S, Kipar C, et al. The Drosophila embryo at single-cell transcriptome resolution. Science. 2017;358:194–9. doi: 10.1126/science.aan3235.

27. Corrales M, Cocanougher BT, Kohn AB, Long XS, Lemire A, Cardona A, et al. A single-cell transcriptomic atlas of complete insect nervous systems across multiple life stages. Neural Dev. In press.

28. Chell JM, Brand AH. Nutrition-responsive glia control exit of neural stem cells from quiescence. Cell. 2010;143:1161–73. doi: 10.1016/j.cell.2010.12.007.

29. Otsuki L, Brand AH. Cell cycle heterogeneity directs the timing of neural stem cell activation from quiescence. Science. 2018;360:99–102. doi: 10.1126/science.aan8795.

30. Bier E, Vaessin H, Younger-Shepherd S, Jan LY, Jan YN. deadpan, an essential pan-neural gene in Drosophila, encodes a helix-loop-helix protein similar to the hairy gene product. Genes Dev. 1992;6:2137–51. doi: 10.1101/gad.6.11.2137.

31. Bowman SK, Rolland V, Betschinger J, Kinsey KA, Emery G, Knoblich JA. The tumor suppressors Brat and Numb regulate transit-amplifying neuroblast lineages in Drosophila. Dev Cell. 2008;14:535–46. doi: 10.1016/j.devcel.2008.03.004.

32. Ashraf SI, Ganguly A, Roote J, Ip YT. Worniu, a Snail family zinc-finger protein, is required for brain development in Drosophila. Dev Dyn. 2004;231:379–86. doi: 10.1002/dvdy.20130.

33. Ikeshima-Kataoka H, Skeath JB, Nabeshima Y, Doe CQ, Matsuzaki F. Miranda directs Prospero to a daughter cell during Drosophila asymmetric divisions. Nature. 1997;390:625–9. doi: 10.1038/37641.

34. Ashraf SI, Ip YT. The Snail protein family regulates neuroblast expression of inscuteable and string, genes involved in asymmetry and cell division in Drosophila. Development. 2001;128:4757–67. doi: 10.1242/dev.128.23.4757.

35. Caldwell MC, Datta S. Expression of cyclin E or DP/E2F rescues the G1 arrest of trol mutant neuroblasts in the Drosophila larval central nervous system. Mech Dev. 1998;79:121–30. doi: 10.1016/S0925-4773(98)00178-6.

36. Zhu S, Barshow S, Wildonger J, Jan LY, Jan YN. Ets transcription factor Pointed promotes the generation of intermediate neural progenitors in Drosophila larval brains. Proc Natl Acad Sci U A. 2011;108:20615–20. doi: 10.1073/pnas.1118595109.

37. Rives-Quinto N, Komori H, Ostgaard CM, Janssens DH, Kondo S, Dai Q, et al. Sequential activation of transcriptional repressors promotes progenitor commitment by silencing stem cell identity genes. Desplan C, Banerjee U, editors. eLife. eLife Sciences Publications, Ltd; 2020;9:e56187.

38. Li X, Xie Y, Zhu S. Notch maintains Drosophila type II neuroblasts by suppressing expression of the Fez transcription factor Earmuff. Dev Camb Engl. 2016;143:2511–21.

39. Yang C-P, Samuels TJ, Huang Y, Yang L, Ish-Horowicz D, Davis I, et al. Imp and Syp RNA-binding proteins govern decommissioning of Drosophila neural stem cells. Dev Camb Engl. 2017;144:3454–64.

40. Lane ME, Sauer K, Wallace K, Jan YN, Lehner CF, Vaessin H. Dacapo, a cyclin-dependent kinase inhibitor, stops cell proliferation during Drosophila development. Cell. 1996;87:1225–35. doi: 10.1016/S0092-8674(00)81818-8.

41. Monastirioti M, Giagtzoglou N, Koumbanakis KA, Zacharioudaki E, Deligiannaki M, Wech I, et al. Drosophila Hey is a target of Notch in asymmetric divisions during embryonic and larval neurogenesis. Development. 2010;137:191–201.

42. Robinow S, White K. Characterization and spatial distribution of the ELAV protein during Drosophila melanogaster development. J Neurobiol. 1991;22:443–61. doi: 10.1002/neu.480220503.

43. Young JM, Armstrong JD. Building the central complex in Drosophila: the generation and development of distinct neural subsets. J Comp Neurol. 2010;518:1525–41. doi: 10.1002/cne.22285.

44. Samson M-L, Chalvet F. found in neurons, a third member of the Drosophila elav gene family, encodes a neuronal protein and interacts with elav. Mech Dev. 2003;120:373–83. doi: 10.1016/S0925-4773(02)00444-6.

45. Wagh DA, Rasse TM, Asan E, Hofbauer A, Schwenkert I, Dürrbeck H, et al. Bruchpilot, a Protein with Homology to ELKS/CAST, Is Required for Structural Integrity and Function of Synaptic Active Zones in Drosophila. Neuron. 2006;49:833–44. doi: 10.1016/j.neuron.2006.02.008.

46. Deitcher DL, Ueda A, Stewart BA, Burgess RW, Kidokoro Y, Schwarz TL. Distinct requirements for evoked and spontaneous release of neurotransmitter are revealed by mutations in the Drosophila gene neuronal-synaptobrevin. J Neurosci Off J Soc Neurosci. 1998;18:2028–39. doi: 10.1523/JNEUROSCI.18-06-02028.1998.

47. Xiong WC, Okano H, Patel NH, Blendy JA, Montell C. repo encodes a glial-specific homeo domain protein required in the Drosophila nervous system. Genes Dev. 1994;8:981–94. doi: 10.1101/gad.8.8.981.

48. Campbell G, Goring H, Lin T, Spana E, Andersson S, Doe CQ, et al. RK2, a glial-specific homeodomain protein required for embryonic nerve cord condensation and viability in Drosophila. Development. 1994;120:2957–66. doi: 10.1242/dev.120.10.2957.

49. Stork T, Sheehan A, Tasdemir-Yilmaz OE, Freeman MR. Neuron-glia interactions through the Heartless FGF receptor signaling pathway mediate morphogenesis of Drosophila astrocytes. Neuron. 2014;83:388–403. doi: 10.1016/j.neuron.2014.06.026.

50. Doherty J, Logan MA, Tasdemir OE, Freeman MR. Ensheathing glia function as phagocytes in the adult Drosophila brain. J Neurosci. 2009;29:4768–81. doi: 10.1523/JNEUROSCI.5951-08.2009.

51. FlyBase Reference Report: Fisher et al., 2012, BDGP insitu homepage. [cited 2022 Apr 30]. Available from: http://beta.flybase.org/reports/FBrf0219073.html

52. DeSalvo MK, Hindle SJ, Rusan ZM, Orng S, Eddison M, Halliwill K, et al. The Drosophila surface glia transcriptome: evolutionary conserved blood-brain barrier processes. Front Neurosci. 2014;8:346. doi: 10.3389/fnins.2014.00346.

53. Bainton RJ, Tsai LT-Y, Schwabe T, DeSalvo M, Gaul U, Heberlein U. moody encodes two GPCRs that regulate cocaine behaviors and blood-brain barrier permeability in Drosophila. Cell. 2005;123:145–56. doi: 10.1016/j.cell.2005.07.029.

54. Noordermeer JN, Kopczynski CC, Fetter RD, Bland KS, Chen WY, Goodman CS. Wrapper, a novel member of the Ig superfamily, is expressed by midline glia and is required for them to ensheath commissural axons in Drosophila. Neuron. 1998;21:991–1001. doi: 10.1016/S0896-6273(00)80618-2.

55. Avet-Rochex A, Carvajal N, Christoforou CP, Yeung K, Maierbrugger KT, Hobbs C, et al. Unkempt is negatively regulated by mTOR and uncouples neuronal differentiation from growth control. PLoS Genet. 2014;10:e1004624. doi: 10.1371/journal.pgen.1004624.

56. Baqri R, Charan R, Schimmelpfeng K, Chavan S, Ray K. Kinesin-2 differentially regulates the anterograde axonal transports of acetylcholinesterase and choline acetyltransferase in Drosophila. J Neurobiol. 2006;66:378–92. doi: 10.1002/neu.20230.

57. Nässel DR, Enell LE, Santos JG, Wegener C, Johard HAD. A large population of diverse neurons in the Drosophila central nervous system expresses short neuropeptide F, suggesting multiple distributed peptide functions. BMC Neurosci. 2008;9:90. doi: 10.1186/1471-2202-9-90.

58. Daniels RW, Gelfand MV, Collins CA, DiAntonio A. Visualizing glutamatergic cell bodies and synapses in Drosophila larval and adult CNS. J Comp Neurol. 2008;508:131–52. doi: 10.1002/cne.21670.

59. Greer CL, Grygoruk A, Patton DE, Ley B, Romero-Calderon R, Chang H-Y, et al. A splice variant of the Drosophila vesicular monoamine transporter contains a conserved trafficking domain and functions in the storage of dopamine, serotonin, and octopamine. J Neurobiol. 2005;64:239–58. doi: 10.1002/neu.20146.

60. Beall CJ, Hirsh J. Regulation of the Drosophila dopa decarboxylase gene in neuronal and glial cells. Genes Dev. 1987;1:510–20. doi: 10.1101/gad.1.5.510.

61. Neckameyer WS, Coleman CM, Eadie S, Goodwin SF. Compartmentalization of neuronal and peripheral serotonin synthesis in Drosophila melanogaster. Genes Brain Behav. 2007;6:756–69. doi: 10.1111/j.1601-183X.2007.00307.x.

62. Hewes RS, Park D, Gauthier SA, Schaefer AM, Taghert PH. The bHLH protein Dimmed controls neuroendocrine cell differentiation in Drosophila. Dev Camb Engl. 2003;130:1771–81.

63. Lee GG, Kikuno K, Nair S, Park JH. Mechanisms of postecdysis-associated programmed cell death of peptidergic neurons in Drosophila melanogaster. J Comp Neurol. 2013;521:3972–91.

64. Díaz MM, Schlichting M, Abruzzi KC, Long X, Rosbash M. Allatostatin-C/AstC-R2 Is a Novel Pathway to Modulate the Circadian Activity Pattern in Drosophila. Curr Biol CB. 2019;29:13–22.e3. doi: 10.1016/j.cub.2018.11.005.

65. Koon AC, Ashley J, Barria R, DasGupta S, Brain R, Waddell S, et al. Autoregulatory and paracrine control of synaptic and behavioral plasticity by octopaminergic signaling. Nat Neurosci. 2011;14:190–9. doi: 10.1038/nn.2716.

66. Cole SH, Carney GE, McClung CA, Willard SS, Taylor BJ, Hirsh J. Two functional but noncomplementing Drosophila tyrosine decarboxylase genes: distinct roles for neural tyramine and octopamine in female fertility. J Biol Chem. 2005;280:14948–55. doi: 10.1074/jbc.M414197200.

67. Kim NC, Marqués G. The Ly6 neurotoxin-like molecule target of wit regulates spontaneous neurotransmitter release at the developing neuromuscular junction in Drosophila. Dev Neurobiol. 2012;72:1541–58. doi: 10.1002/dneu.22021.

68. Murakami S, Minami-Ohtsubo M, Nakato R, Shirahige K, Tabata T. Two Components of Aversive Memory in Drosophila, Anesthesia-Sensitive and Anesthesia-Resistant Memory, Require Distinct Domains Within the Rgk1 Small GTPase. J Neurosci Off J Soc Neurosci. 2017;37:5496–510. doi: 10.1523/JNEUROSCI.3648-16.2017.

69. Crittenden JR, Skoulakis EM, Han KA, Kalderon D, Davis RL. Tripartite mushroom body architecture revealed by antigenic markers. Learn Mem Cold Spring Harb N. 1998;5:38–51. doi: 10.1101/lm.5.1.38.

70. Kahsai L, Kapan N, Dircksen H, Winther AME, Nässel DR. Metabolic stress responses in Drosophila are modulated by brain neurosecretory cells that produce multiple neuropeptides. PloS One. 2010;5:e11480. doi: 10.1371/journal.pone.0011480.

71. Truman JW, Bate M. Spatial and temporal patterns of neurogenesis in the central nervous system of Drosophila melanogaster. Dev Biol. 1988;125:145–57. doi: 10.1016/0012-1606(88)90067-X.

72. Prokop A, Technau GM. The origin of postembryonic neuroblasts in the ventral nerve cord of Drosophila melanogaster. Dev Camb Engl. 1991;111:79–88.

73. Kremer MC, Jung C, Batelli S, Rubin GM, Gaul U. The glia of the adult Drosophila nervous system. Glia. 2017;65:606–38. doi: 10.1002/glia.23115.

74. Sousa-Nunes R, Yee LL, Gould AP. Fat cells reactivate quiescent neuroblasts via TOR and glial insulin relays in Drosophila. Nature. 2011;471:508–12. doi: 10.1038/nature09867.

75. Ebens AJ, Garren H, Cheyette BN, Zipursky SL. The Drosophila anachronism locus: a glycoprotein secreted by glia inhibits neuroblast proliferation. Cell. 1993;74:15–27. doi: 10.1016/0092-8674(93)90291-W.

76. Datta S. Control of proliferation activation in quiescent neuroblasts of the Drosophila central nervous system. Development. 1995;121:1173–82. doi: 10.1242/dev.121.4.1173.

77. Küssel P, Frasch M. Pendulin, a Drosophila protein with cell cycle-dependent nuclear localization, is required for normal cell proliferation. J Cell Biol. 1995;129:1491–507. doi: 10.1083/jcb.129.6.1491.

78. Török I, Strand D, Schmitt R, Tick G, Török T, Kiss I, et al. The overgrown hematopoietic organs-31 tumor suppressor gene of Drosophila encodes an Importin-like protein accumulating in the nucleus at the onset of mitosis. J Cell Biol. 1995;129:1473–89. doi: 10.1083/jcb.129.6.1473.

79. Uv AE, Harrison EJ, Bray SJ. Tissue-specific splicing and functions of the Drosophila transcription factor Grainyhead. Mol Cell Biol. 1997;17:6727–35. doi: 10.1128/MCB.17.11.6727.

80. Doe CQ. Temporal Patterning in the Drosophila CNS. Annu Rev Cell Dev Biol. 2017;33:in press.

81. Ren Q, Yan C-P, Liu Z, Sugino K, Mok K, He Y, et al. Stem cell intrinsic, Seven-up-triggered temporal factor gradients diversify intermediate neural progenitors. Curr Biol. 2017;in press.

82. Syed MH, Mark B, Doe CQ. Steroid hormone induction of temporal gene expression in Drosophila brain neuroblasts generates neuronal and glial diversity. Elife. 2017;6. Available from: https://www.ncbi.nlm.nih.gov/pubmed/28394252

83. Walsh KT, Doe CQ. Drosophila embryonic type II neuroblasts: origin, temporal patterning, and contribution to the adult central complex. Dev Camb Engl. 2017;144:4552–62.

84. Bayraktar OA, Doe CQ. Combinatorial temporal patterning in progenitors expands neural diversity. Nature. 2013;498:445–55. doi: 10.1038/nature12266.

85. Abdusselamoglu MD, Eroglu E, Burkard TR, Knoblich JA. The transcription factor odd-paired regulates temporal identity in transit-amplifying neural progenitors via an incoherent feed-forward loop. VijayRaghavan K, Wang H, Sen S, editors. eLife. 2019;8:e46566.

86. Almeida MS, Bray SJ. Regulation of post-embryonic neuroblasts by Drosophila Grainyhead. Mech Dev. 2005;122:1282–93. doi: 10.1016/j.mod.2005.08.004.

87. Sullivan LF, Warren TL, Doe CQ. Temporal identity establishes columnar neuron morphology, connectivity, and function in a Drosophila navigation circuit. eLife. 2019;8.

88. Farnsworth DR, Bayraktar OA, Doe CQ. Aging Neural Progenitors Lose Competence to Respond to Mitogenic Notch Signaling. Curr Biol. 2015;25:3058–68. doi: 10.1016/j.cub.2015.10.027.

89. Mark B, Lai S-L, Zarin AA, Manning L, Pollington HQ, Litwin-Kumar A, et al. A developmental framework linking neurogenesis and circuit formation in the Drosophila CNS. eLife. 2021;10.

90. Tan L, Zhang KX, Pecot MY, Nagarkar-Jaiswal S, Lee PT, Takemura SY, et al. Ig Superfamily Ligand and Receptor Pairs Expressed in Synaptic Partners in Drosophila. Cell. 2015;163:1756–69. doi: 10.1016/j.cell.2015.11.021.

91. Nguyen TH, Vicidomini R, Choudhury SD, Coon SL, Iben J, Brody T, et al. Single-Cell RNA Sequencing Analysis of the Drosophila Larval Ventral Cord. Curr Protoc. 2021;1:e38.

92. Lai SL, Doe CQ. Transient nuclear Prospero induces neural progenitor quiescence. Elife. 2014;3.

93. Narbonne-Reveau K, Lanet E, Dillard C, Foppolo S, Chen CH, Parrinello H, et al. Neural stem cell-encoded temporal patterning delineates an early window of malignant susceptibility in Drosophila. Elife. 2016;5. Available from: http://www.ncbi.nlm.nih.gov/pubmed/27296804

94. Liu Z, Yang CP, Sugino K, Fu CC, Liu LY, Yao X, et al. Opposing intrinsic temporal gradients guide neural stem cell production of varied neuronal fates. Science. 2015;350:317–20. doi: 10.1126/science.aad1886.

95. Chen C-H, Luhur A, Sokol N. Lin-28 promotes symmetric stem cell division and drives adaptive growth in the adult Drosophila intestine. Dev Camb Engl. 2015;142:3478–87.

96. Cui X, Doe CQ. ming is expressed in neuroblast sublineages and regulates gene expression in the Drosophila central nervous system. Development. 1992;116:943–52. doi: 10.1242/dev.116.4.943.

97. Kambadur R, Koizumi K, Stivers C, Nagle J, Poole SJ, Odenwald WF. Regulation of POU genes by castor and hunchback establishes layered compartments in the Drosophila CNS. Genes Dev. 1998;12:246–60. doi: 10.1101/gad.12.2.246.

98. Mellerick DM, Kassis JA, Zhang SD, Odenwald WF. castor encodes a novel zinc finger protein required for the development of a subset of CNS neurons in Drosophila. Neuron. 1992;9:789–803. doi: 10.1016/0896-6273(92)90234-5.

99. Dumstrei K, Wang F, Hartenstein V. Role of DE-cadherin in neuroblast proliferation, neural morphogenesis, and axon tract formation in Drosophila larval brain development. J Neurosci Off J Soc Neurosci. 2003;23:3325–35. doi: 10.1523/JNEUROSCI.23-08-03325.2003.

100. Young JM, Armstrong JD. Structure of the adult central complex in Drosophila: organization of distinct neuronal subsets. J Comp Neurol. 2010;518:1500–24. doi: 10.1002/cne.22284.

101. Hobert O, Kratsios P. Neuronal identity control by terminal selectors in worms, flies, and chordates. Curr Opin Neurobiol. 2019;56:97–105. doi: 10.1016/j.conb.2018.12.006.

102. Lodato S, Arlotta P. Generating neuronal diversity in the mammalian cerebral cortex. Annu Rev Cell Dev Biol. 2015;31:699–720. doi: 10.1146/annurev-cellbio-100814-125353.

103. Yasugi T, Nishimura T. Temporal regulation of the generation of neuronal diversity in Drosophila. Dev Growth Differ. 2016;58:73–87. doi: 10.1111/dgd.12245.

104. Williams EA, Jékely G. Neuronal cell types in the annelid Platynereis dumerilii. Curr Opin Neurobiol. 2019;56:106–16. doi: 10.1016/j.conb.2018.12.008.

105. Farnsworth DR, Saunders LM, Miller AC. A single-cell transcriptome atlas for zebrafish development. Dev Biol. 2020;459:100–8. doi: 10.1016/j.ydbio.2019.11.008.

106. Hao Y, Hao S, Andersen-Nissen E, Mauck WM, Zheng S, Butler A, et al. Integrated analysis of multimodal single-cell data. Cell. 2021;184:3573–3587.e29. doi: 10.1016/j.cell.2021.04.048.

107. Yuan X, Sipe CW, Suzawa M, Bland ML, Siegrist SE. Dilp-2-mediated PI3-kinase activation coordinates reactivation of quiescent neuroblasts with growth of their glial stem cell niche. PLoS Biol. 2020;18:e3000721. doi: 10.1371/journal.pbio.3000721.

Chapter III

The switching factor Seven-up acts in neuroblasts to specify adult neuron identity and initiate decommissioning

Dillon, N. R., Manning, L., Hirono, K. and Doe, C. Q. (2024). Seven-up acts in neuroblasts to specify adult central complex neuron identity and initiate neuroblast decommissioning. *Development* 151, dev202504.

Author contributions

Conceptualization: NRD, CQD. Design: NRD, LM (EdU drop out), KH (HCR RNA in situ), CQD. Investigation: NRD, LM (EdU drop out), KH (HCR RNA in situ). Analysis: NRD. Writing – original draft: NRD, CQD. Writing – review and editing: NRD, LM, KH, CQD.

Introduction

Developing a complex brain requires neural stem cells to generate both a large and diverse set of neuron subtypes. *Drosophila* neuroblasts (NBs) are neural stem cells that generate neuronal diversity through the initiation of spatial patterning that establishes lineage identities (Skeath and Thor, 2003; Erclik et al., 2017) and through the subsequent temporal patterning within a lineage to produce unique neuron subtypes (Doe, 2017; El-Danaf et al., 2023). These processes have been extensively studied in embryonic ventral nerve cord NB lineages (Isshiki et al., 2001; Novotny et al., 2002; Pearson and Doe, 2003; Tran and Doe, 2008; Moris-Sanz et al., 2014; Grosskortenhaus et al., 2005, 2006), but the role of temporal patterning mechanisms in larval central brain NB lineages remains understudied.

The larval central brain contains ∼100 NBs per hemibrain with spatially stereotyped lineages (Pereanu and Hartenstein, 2006). Type 2 neuroblast (T2NB) lineages are generated by eight T2NBs in each hemibrain, with unique spatially defined lineage identities (Pereanu and Hartenstein, 2006; Bello et al., 2008; Boone and Doe, 2008; Bowman et al., 2008). Lineage tracing shows that each T2NB lineage (DM1-6 and DL1-2) produces neurons with lineage-specific morphology (Riebli et al., 2013; Yang et al., 2013; Andrade et al., 2019). T2NBs

generate a series of intermediate neural progenitors (INPs), and each INP produces four to six ganglion mother cells, which each terminally divide to produce two post-mitotic neurons/glia (Fig. 3.1A). Notably, the T2NB division pattern is analogous to outer subventricular zone lineages in the primate cortex (Holguera and Desplan, 2018).

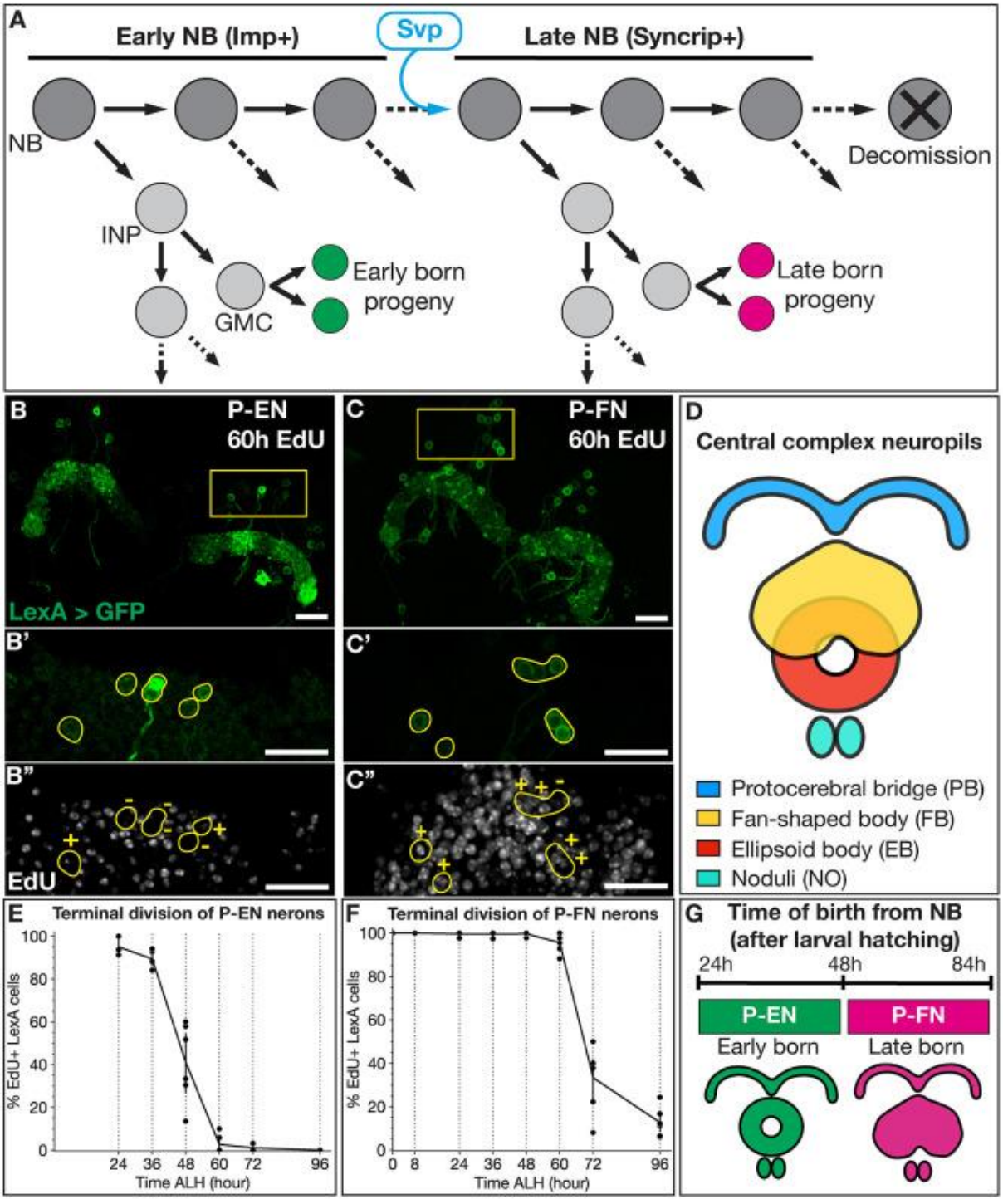

Fig. 3.1 (previous page) Columnar neuron subtypes are born from larval T2NBs at distinct temporal windows. (A) T2NBs express Imp during early larval stages and transition to Syncrip expression in late larvae due to Svp expression (Ren et al., 2017). All non-mushroom body NBs enter decommissioning in the early pupae (Ito and Hotta, 1992; Maurange et al., 2008; Siegrist et al., 2010; Homem et al., 2014; Yang et al., 2017). GMC, ganglion mother cell; INP, intermediate neural progenitor; NB, neuroblast. (B-C″) P-EN (B-B″) and P-FN (C-C″) adult neurons from EdU initiated feeding at 60 h ALH. Neurons are in green; EdU is in white. +, EdU-positive neuron; −, EdU-negative neuron. Yellow outlines in B′,B″,C′,C″ indicate cell bodies. Areas outlined in B and C are shown in more detail in images in B′,B″ and C′,C″, respectively. (D) Schematic of central complex neuropils of the adult brain. (E,F) Quantification of EdU drop out for P-EN neurons (E) and P-FN neurons (F) shown by percentage of neurons labeled by EdU. Each dot represents one adult brain. Error bars represent 95% confidence intervals. For both P-EN and P-FN neurons at each timepoint, *n*=3-7 brains. (G) Summary of P-EN and P-FN birth windows from larval T2NBs. Schematic of their neuropil targeting is shown. Scale bars: 5 μm.

The T2NBs have been shown to express several genes in a temporal-specific manner during larval stages. The IGF-II mRNA-binding protein (Imp) is expressed in a temporal gradient in T2NBs and other lineages, with high levels of Imp in early NBs and low levels in late NBs; this is the opposite of the low-to-high temporal gradient of the RNA-binding protein Syncrip (Liu et al., 2015; Ren et al., 2017; Syed et al., 2017). Previous work has identified the orphan nuclear hormone receptor Seven-up (Svp) as a switching factor to initiate this Imp-to-Syncrip transition within T2NBs (Fig. 3.1A) (Ren et al., 2017; Syed et al., 2017). Similarly, Svp in ventral nerve cord NB lineages is required to switch Type 1 NBs from producing early born neuron fates to producing late born fates (Kanai et al., 2005; Mettler et al., 2006; Benito-Sipos et al., 2011; Kohwi et al., 2011). Although Svp is required to switch from early to late temporal gene expression in T2NBs, it is unknown whether this has any effect on the specification of post-mitotic neurons.

T2NB lineages generate the majority of the central complex (CX) of the *Drosophila* adult brain, with recent connectomes showing the CX containing hundreds of morphologically distinct neuron subtypes (Franconville et al., 2018; Hulse et al., 2021). One group of interest is columnar neurons, which are members of neural circuits responsible for locomotion and spatial navigation behaviors that are integrated in the CX (Giraldo et al., 2018; Green et al., 2019; Turner-Evans et al., 2020). Columnar neurons target specific neuropils of the CX (Fig. 3.1D) and are named according to their dendrite-axon targeting to these regions (Wolff et al., 2015; Wolff and Rubin,

2018). For example, in this study we looked at the P-EN neurons, which are named according to their dendritic targeting to the protocerebral bridge (PB) and outputs to the ellipsoid body (EB) and noduli (NO). P-FN neurons are similarly named according to their dendritic targeting to the PB and outputs to the fan-shaped body (FB) and NO. Understanding the development of T2NB lineages may shed light on how complex circuits form and drive behavior.

Here, we characterize the function of Svp in specifying post-mitotic neuron identities within T2NB lineages. We find the birth windows of P-EN and P-FN columnar neurons are from early and late T2NBs, respectively. We find that Svp is transiently and asynchronously expressed in all eight larval T2NB lineages. We used CRISPR/Cas9 knockout lines to remove *svp* specifically from T2NB lineages and show that Svp is required for the late born P-FN fate while restricting the early born P-EN fate. Additionally, we discover a previously unreported role for Svp in terminating T2NB neurogenesis. We propose that Svp is essential for early-to-late transition in T2NB lineages, and that these changes propagate down to the level of altered identity in post-mitotic neurons. Finally, we document a previously unreported function for Svp in promoting T2NB decommissioning.

Results

Columnar neurons P-EN and P-FN are born from larval T2NBs in different temporal windows

Previous birth dating analysis of columnar neuron subtypes only assayed a subset of neurons, e.g. only 50-65% of the P-FN and P-EN neurons were birth dated (Sullivan et al., 2019). To obtain more-complete coverage, we developed a 5-ethynyl-2′-deoxyuridine (EdU) drop out approach to determine the temporal birth window for P-EN and P-FN neurons. Briefly, larvae were fed EdU, a thymidine analog that incorporates into DNA during DNA synthesis, at progressively later timepoints of larval life and maintained on EdU feeding until pupation. Thus, neurons born earlier will lose or ‘drop out’ of EdU labeling earlier than will neurons born later. We used LexA lines that specifically label the P-EN (R12D09-LexA) and P-FN (R16D01-LexA) neurons (Wolff et al., 2015; Wolff and Rubin, 2018; Sullivan et al., 2019). We found that P-EN neurons drop out from EdU labeling in early larvae by 60 h after larval hatching (ALH) (Fig. 3.1B-B″,E). In contrast, P-FN neurons remain EdU labeled at 60 h ALH and only drop out of

EdU labeling in the late larvae by 96 h ALH (Fig. 3.1C-C″,F). We conclude that P-EN neurons undergo their terminal division before P-FN neurons.

We took advantage of previous cell cycle data for NBs, INPs and ganglion mother cells to provide the points at which neurons went through terminal division to when their parental INP was birthed from the NB (Homem et al., 2013). Both P-EN and P-FN neurons are derived from young INPs (Sullivan et al., 2019), and neurons from young INPs are born from their parental NB ~12 h before terminal division (Homem et al., 2013). Therefore, we subtracted 12 h to reveal the time of origin from the T2NB. We conclude that P-EN neurons are born from T2NBs between 24 h and 48 h ALH, whereas P-FN neurons are born between 48 h and 84 h ALH (Fig. 3.1G). Thus, P-EN and P-FN neurons are derived from the same DM1-DM4 T2NB lineages (Yang et al., 2013) and the same young INP lineage (Sullivan et al., 2019), but differ in the timing of their birth window from the T2NB (this work). Next, we use these early and late born neuron identities to determine whether Svp, which is known for its role in regulating temporal gene expression in T2NBs (Ren et al., 2017; Syed et al., 2017), is also required for proper specification of post-mitotic neurons.

Svp is expressed transiently and asynchronously in all larval T2NB lineages between 18 h and 24 h ALH

Before assaying neuron identity after Svp knockout, we assayed for Svp protein expression in each of the eight T2NB lineages, primarily to confirm expression in the DM1-DM4 T2NB lineages known to generate the columnar neurons (Riebli et al., 2013; Yang et al., 2013; Andrade et al., 2019). T2NBs were identified by the co-expression of Pnt-Gal4 driving UAS membrane-bound GFP and the pan-neuroblast marker Deadpan in cells ≥5 μm in diameter. Individual T2NB lineages were identified based on the spatial position of the T2NBs within the brain lobes (Pereanu and Hartenstein, 2006; Izergina et al., 2009). We found that Svp was transiently expressed in all eight lineages with peak occurrence of expression in DM1-3 at 24 h ALH (Fig. 3.2A-C′,I) and for lineages DM4-6 and DL1-2 at 18 h (Fig. 3.2D-H′,I). Svp protein was restricted to the T2NB and absent in its progeny (Fig. 3.2A-H′). We saw a similar trend of Svp mRNA expression in all early T2NB lineages (Fig. 3.S1; see Appendix A for Chapter III supplements). We conclude that Svp is transiently expressed in all T2NB lineages.

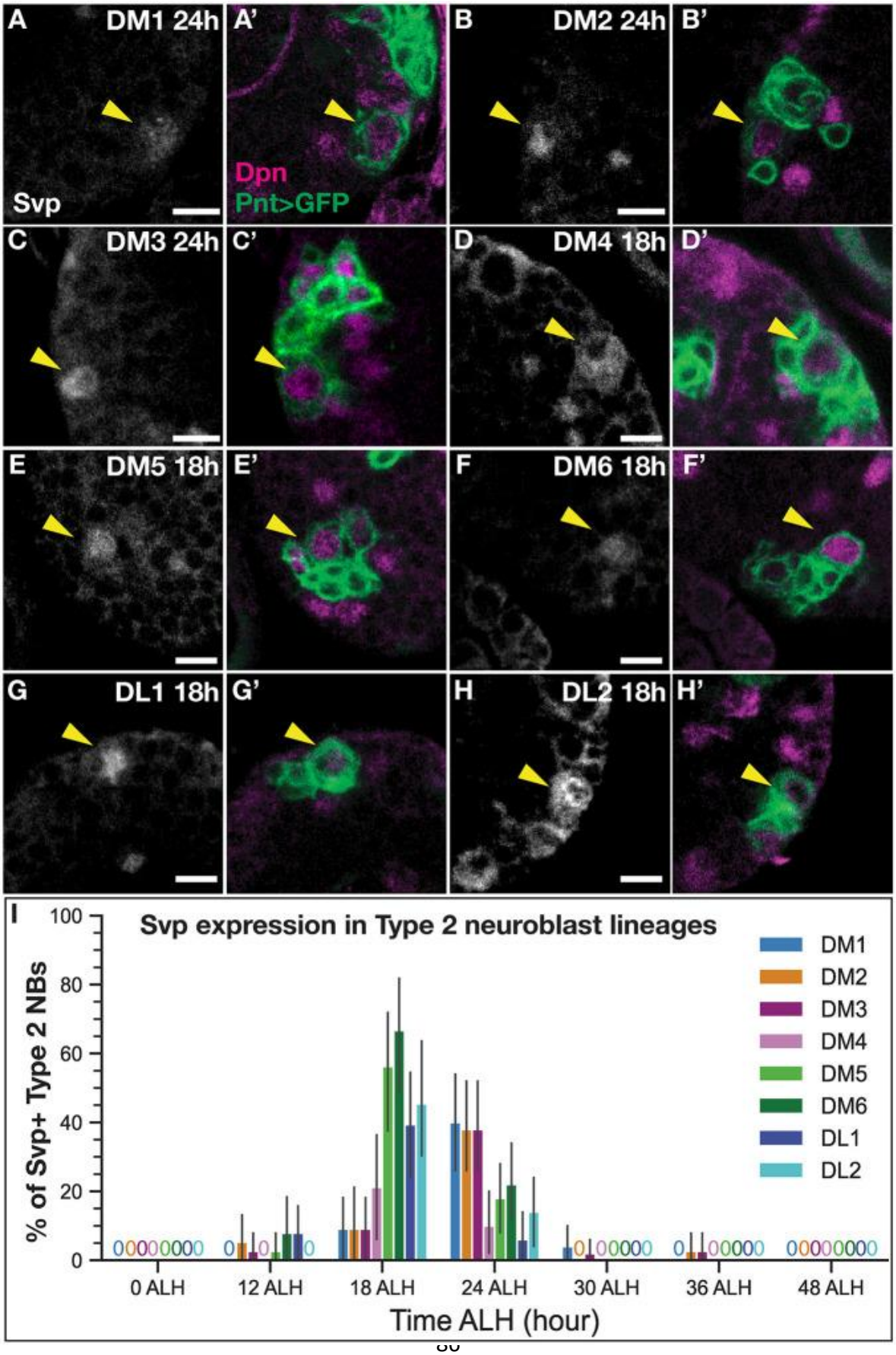
A
DM1 24h
Svp
A'
Dpn
Pnt>GFP
B
DM2 24h
B'
C
DM3 24h
C'
D
DM4 18h
D'
E
DM5 18h
E'
F
DM6 18h
F'
G
DL1 18h
G'
H
DL2 18h
H'
I
Svp expression in Type 2 neuroblast lineages
% of Svp+ Type 2 NBs
100
80
60
40
20
0
0 ALH
12 ALH
18 ALH
24 ALH
30 ALH
36 ALH
48 ALH
Time ALH (hour)
DM1
DM2
DM3
DM4
DM5
DM6
DL1
DL2

Fig. 3.2 (previous page) Svp is expressed early in all larval T2NB lineages. (A-C′) Svp is expressed 24 h after larval hatching (ALH) in T2NB lineages DM1-3. (D-H′) Svp is expressed at 18 h ALH in T2NB lineages DM4-6 and DL1-DL2. (A-H) In all images, Svp is in white and T2NBs are identified with Pnt-Gal4>GFP and Dpn. Yellow arrowheads indicate T2NB. (I) Quantification of Svp expression in T2NBs at 0 h-48 h ALH shown as a bar plot with 95% confidence interval. For each lineage, 0 ALH, *n*=34; 12 ALH, *n*=38; 18 h ALH, *n*=33; 24 h ALH, *n*=50; 30 h ALH, *n*=50; 36 h ALH, *n*=38; 48 h ALH, *n*=49 (DM lineages) or 42 (DL lineages) lobes. Scale bars: 5 μm.

We performed Svp loss-of-function experiments with the goal of making the most complete loss- and gain-of-function alterations to the T2NB temporal factor cascade as possible, thereby increasing the chance of seeing changes in P-EN and P-FN neuron identities. We chose to knockout *svp* specifically in T2NB lineages, which has been shown to extend the expression of early NB factors (e.g. Imp and Chinmo) at the expense of late NB factors (e.g. Syncrip, EcRB1, Broad and E93) (Ren et al., 2017; Syed et al., 2017); although changes in neuronal morphology were detected, adult post-mitotic neuron molecular identity was not assayed in these experiments. We hypothesize that if early NB factors play a role in neuronal specification, then loss of Svp should result in ectopic P-EN neurons due to failure to switch to late temporal factors, and, conversely, Svp knockout should reduce or eliminate late born identities such as P-FN neurons.

We generated Svp knockouts specifically in T2NB lineages. We used two independent CRISPR/Cas9 lines (Port et al., 2020), each with two Svp-specific sgRNAs to knockout *svp* in T2NBs. To determine the efficiency of our knockouts, we tested these lines for the loss of Svp expression and recapitulation of the loss of the late T2NB expression of E93 (Syed et al., 2017). We find that our knockout lines significantly reduce the occurrence of Svp expression in T2NBs but there are a minority of escaper NBs that have expression levels indistinguishable from wild type (Fig. 3.S2A-D); these are likely one or two T2NB lineages where CRISPR/Cas9-mediated *svp* knockout did not occur. Thus, our Svp knockouts had ‘all or none’ effects on Svp expression. T2NBs that exhibit loss of Svp also show a loss of E93 expression, as previously observed (Syed et al., 2017), further validating the Svp knockouts (Fig. 3.S2E-H). We conclude that our CRISPR/Cas9 lines effectively knockout *svp* completely within the majority of T2NB lineages, with only a few escapers that show wild-type levels of Svp expression. We conclude that these knockout lines can be used to test the role of Svp in specifying adult columnar neuron identity.

Cut expression distinguishes molecular identities of adult P-EN neurons from P-FN neurons

P-EN and P-FN neurons were first characterized based on their distinct axon projections into CX neuropils (P-EN sends axons to the EB; P-FN sends axons to the FB) (Wolff et al., 2015). Yet to date no molecular markers have been reported to distinguish these neurons, except for the LexA lines we use here. To address this, we used a single-cell RNA-sequencing atlas of adult T2NB-derived neurons to identify previously unreported molecular markers for P-EN and P-FN neurons (Epiney et al., 2023 preprint). We identified that the homeodomain transcription factor Cut was expressed in adult P-EN neurons but not in P-FN neurons (Fig. 3.3A-C), whereas Svp was in neither adult neuron type (Fig. 3.S3A-B″,C) and Runt was in both neuron types, as previously reported (Sullivan et al., 2019) (Fig. 3.3A′,B′; Fig. 3. S2A-B′). We conclude that Cut distinguishes the molecular identities of adult P-EN and P-FN neurons, and we use this marker in combination with subtype-specific LexA-driven V5 and Runt expression in our analysis of the Svp knockout phenotypes.

Fig. 3.3 (next page) Cut expression distinguishes P-EN and P-FN molecular identities. (A-A″) P-EN neurons labeled using a LexA driver co-express Runt and Cut. (B-B″) P-FN neurons labeled using a LexA driver express Runt but not Cut. (C) Quantification of molecular expression in P-EN and P-FN neurons. P-EN, *n*=13 brains; P-FN, *n*=6 brains. In all panels, $LexA^+$ neurons are in green, Runt is in magenta and Cut is in cyan. Neurons of interest are outlined in yellow. Scale bars: 10 μm.

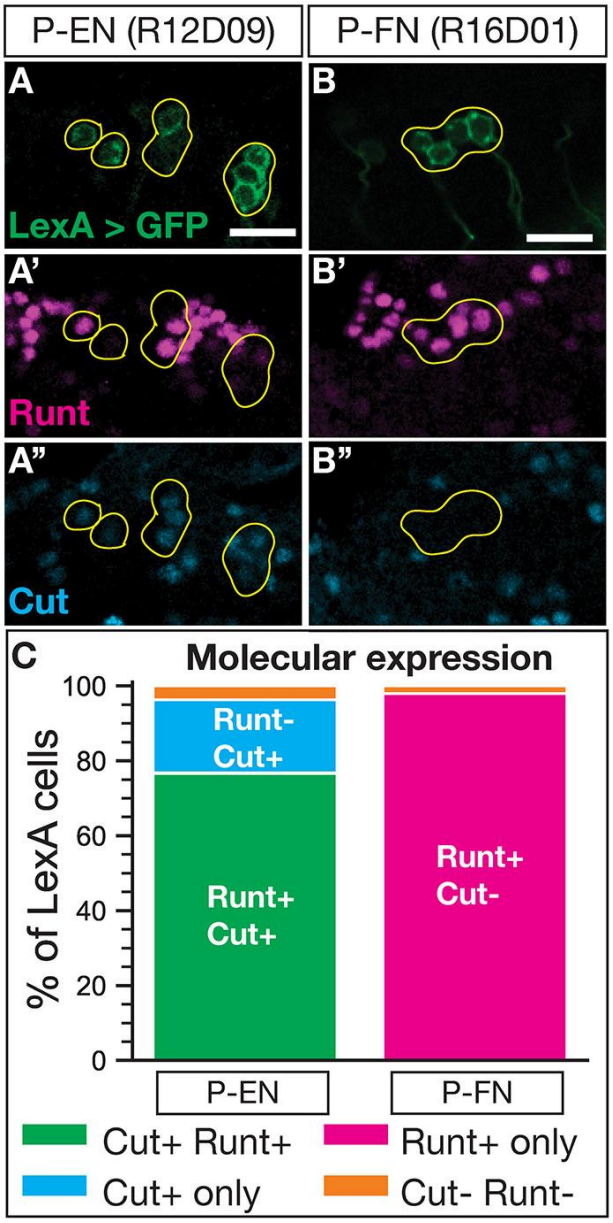

Loss of Svp decreases the number of late born P-FN adult neurons

Svp is required for the early-to-late switch in T2NB temporal gene expression (Ren et al., 2017; Syed et al., 2017). Here, we test whether this Svp-dependent switch in the T2NB gene expression extends to the specification of post-mitotic neurons. In this section, we ask whether Svp knockout reduces late born P-FN neurons. We used Pnt-Gal4 to drive our validated CRISPR/Cas9 lines to knock out Svp in the larval T2NB; additionally, we used a V5 membrane tag to visualize neuron specific LexA expression in the adult brain. We found Svp knockout leads to a highly penetrant loss of late born adult P-FN neurons (Fig. 3.4A-D). We note that there are

some P-FN neurons remaining; because the cell bodies are closely clustered, they likely reflect that the Svp knockout failed to remove *svp* within individual T2NB lineages (see Discussion). Further evidence that remaining P-FN neurons derived from Svp escaper NBs include their normal morphology (Fig. 3.4E-I; Movies 1 and 2; see online version for Movies) and normal birth date (Fig. 3.4J). We conclude that Svp is required for T2NBs to produce the late born P-FN neuron identity, likely due to either an extension of early born neuron identities blocking late born identities or a failure to initiate late born identity generation (Fig. 3.4K).

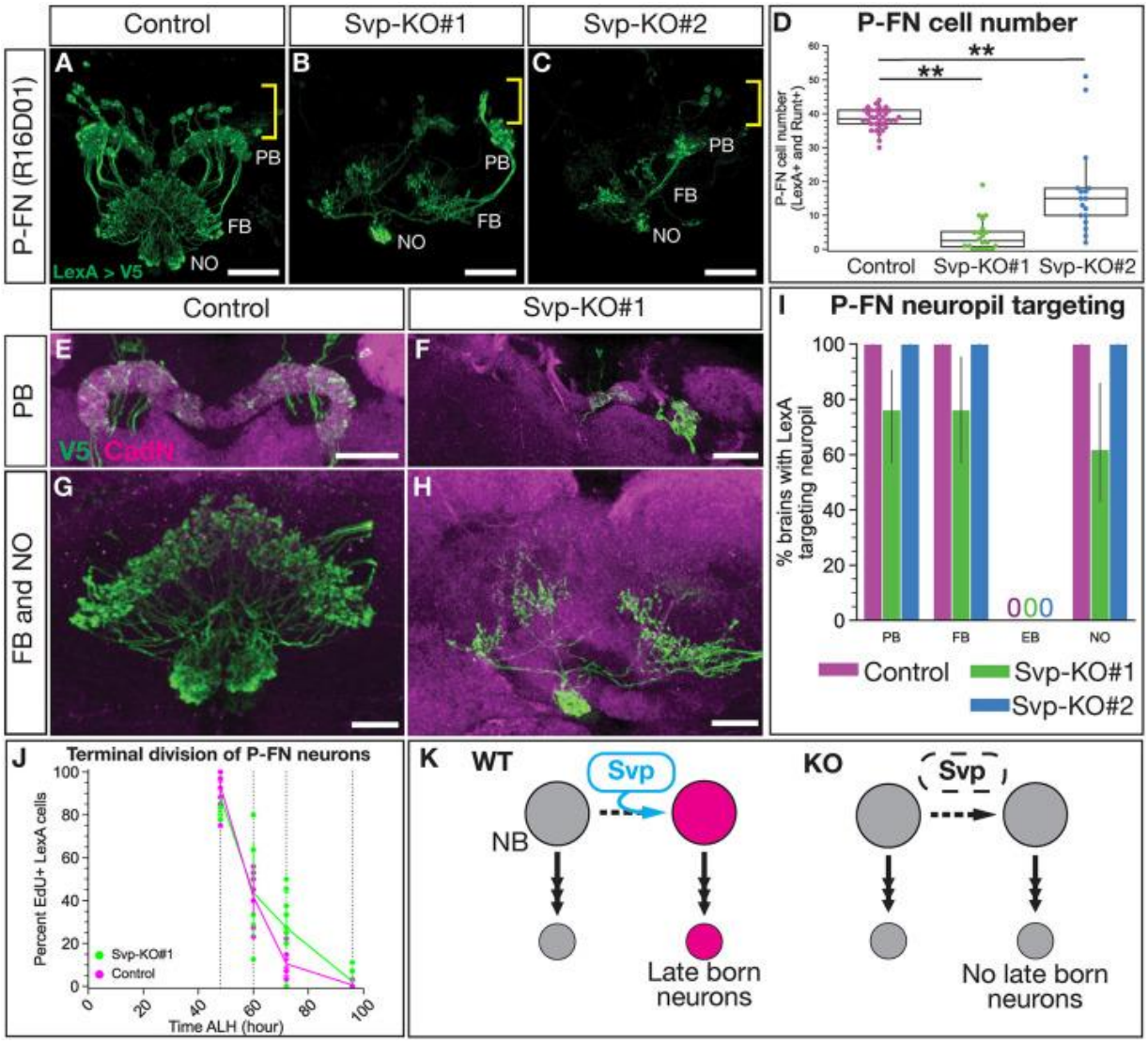

Fig. 3.4 Svp is required for the late born P-FN neuron identity. (A-C) P-FN neurons labeled using a LexA driver expressing membrane-bound V5 show that loss of Svp leads to the loss of P-FN neurons. Yellow brackets indicate the cell body region; white text labels the neuropils: protocerebral bridge (PB), fan-shaped body (FB) and noduli (NO). (D)

(Fig. 3.4 caption continued) Quantification of P-FN cell number identified with co-expression of LexA and Runt. Each dot represents one adult brain with box and whisker plot showing distribution. Whiskers display the minimum and maximum range for the data, excluding outliers (defined as data points outside of 1.5x interquartile range). Control, *n*=34; Svp-KO#1, *n*=20; Svp-KO#2, *n*=17. *P*-values were determined using one-way ANOVA with Tukey post-hoc test. Control versus Svp-KO#1, ***P*<0.001; Control versus Svp-KO#2, ***P*<0.001. (E,F) P-FN neuron PB morphology shows lack of targeting with loss of Svp. (G,H) P-FN neuron FB and NO morphology shows lack of targeting with loss of Svp. (I) Quantification of P-FN neuropil targeting scored based on LexA targeting to neuropils identified with nc82 or CadN shown as a bar plot with 95% confidence interval. Control, *n*=35 brains; Svp-KO#1, *n*=21 brains; Svp-KO#2, *n*=13 brains; 95% confidence interval. (J) P-FN EdU dropout shows that birth of P-FN neurons in Svp-KO escaper neuroblasts occurs in a normal NB birth window, as shown by the percentage P-FN neurons labeled by EdU. Each dot represents one adult brain. Error bars represent 95% confidence intervals. For all timepoints, control, *n*=11 or 12 brains; Svp-KO#1, *n*=5-12 brains. (K) Summary of Svp required for P-FN identity. In all images, $LexA^+$ neurons driving V5 are in green and CadN is in magenta. Scale bars: 20 μm in A-C; 30 μm in E; 20 μm in F; 10 μm in G,H.

Loss of Svp extends the production of early born P-EN adult neurons

We next tested whether Svp knockout in T2NBs extends early born P-EN neuron identity, using both molecular and morphological assays. We found that loss of Svp leads to the expansion of adult P-EN neurons, with projections into the protocerebral bridge, ellipsoid body and noduli (Fig. 3.5A-C). Furthermore, these ectopic P-EN neurons expressed the appropriate P-EN molecular markers: P-EN LexA-driven V5, Runt and Cut (Fig. 3.5D-F‴,G). We conclude that Svp is required to restrict the production of P-EN neurons.

Fig. 3.5 (next page) Svp restricts the early born P-EN neuron molecular identity and birth window. (A-C) P-FN neurons labeled using LexA drivers show loss of Svp produces ectopic P-EN neurons. Yellow brackets indicate the cell body region; white text labels neuropils: protocerebral bridge (PB), ellipsoid-body (EB) and noduli (NO). (D-F‴) Ectopic neurons maintain expression of P-EN LexA, Cut and Runt. (G) Quantification of P-EN cell numbers from A-F. Each dot represents one adult brain with box and whisker plot showing distribution. Whiskers display the minimum and maximum range for the data, excluding outliers (defined as data points outside of 1.5x interquartile range). Control, *n*=35 brains; Svp-KO#1, *n*=25 brains; Svp-KO#2, *n*=27 brains. *P*-values were determined using one-way ANOVA with Tukey's post-hoc test: control versus Svp-KO#1, ***P*<0.001; control versus Svp-KO#2, ***P*<0.001. (H) EdU dropout of P-EN neurons show an extended birth window with loss of Svp shown by percentage of P-EN neurons labeled by EdU. Each dot represents one adult brain. Error bars represent 95% confidence intervals. Control, *n*=6-10 brains; Svp-KO#1, *n*=8-13 brains. (I) Summary of Svp restricting P-EN neuron molecular identity and birth window. In all images, $LexA^+$ neurons driving V5 are in green, Runt is in magenta and Cut is in cyan. Scale bars: 40 μm in A-C; 10 μm in D-F‴.

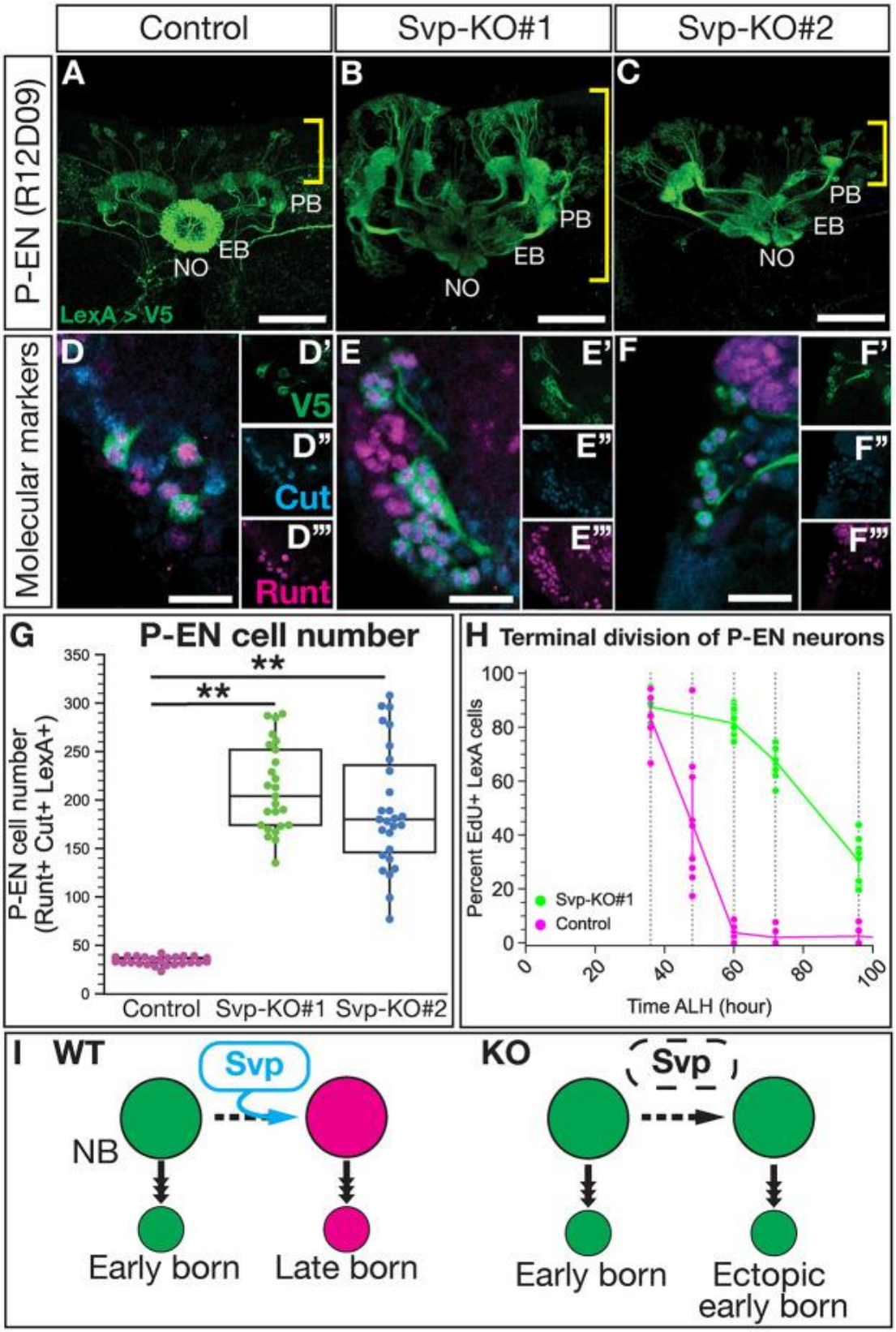
Control
Svp-KO#1
Svp-KO#2
P-EN (R12D09)
A
B
C
PB
EB
NO
LexA > V5
Molecular markers
D
D'
V5
D"
Cut
D"'
Runt
E
E'
E"
E"'
F
F'
F"
F"'
G
P-EN cell number
P-EN cell number (Runt+ Cut+ LexA+)
**
**
Control
Svp-KO#1
Svp-KO#2
H
Terminal division of P-EN neurons
Percent EdU+ LexA cells
Svp-KO#1
Control
Time ALH (hour)
I
WT
Svp
NB
Early born
Late born
KO
Svp
Early born
Ectopic early born

The ectopic P-EN neurons could arise from T2NBs generating more P-EN neurons at a normal early time, or they could arise from T2NBs generating P-EN neurons at abnormally late times in their lineage (replacing late born P-FN neurons). To distinguish these models, we performed EdU birth dating of P-EN neurons after Svp knockout. Whereas wild-type P-EN neurons are all born before 60 h ALH (Fig. 3.1B), we found that Svp knockout resulted in P-EN neurons still being born at 100 h ALH (Fig. 3.5H). Our data support a model in which loss of Svp extends the production of early born P-EN neurons at the expense of late born P-FN neurons (Fig. 3.5I).

We next wanted to know whether the ectopic P-EN neurons showed normal neuropil targeting. We reconstructed CX neuropils from anti-nc82 (Bruchpilot; a presynaptic marker) (Wagh et al., 2006) stains and assayed P-EN neuropil targeting (Fig. 3.6; Movies 3 and 4). We first quantified all CX neuropil volumes, which includes more neuron subtypes than only the P-EN and P-FN neurons. We found that after loss of Svp in the T2NB lineages, all CX neuropils increased in size (Fig. 3.S4A). This is due in part to ectopic P-EN neurons, which targeted all assayed CX neuropils but with increased targeting volume (Fig. 3.6A-H′; Fig. 3.S4B,C). Next, we assayed neuropil targeting of ectopic P-EN neurons in our T2NB Svp knockouts. We found that ectopic P-EN neurons target all the expected CX neuropils (e.g. protocerebral bridge, ellipsoid body and noduli) but with increased volume, likely reflecting the increase in neurons (Fig. 3.6A-F′; Fig. 3.S4B). We observed ectopic P-EN neurons abnormally target the fan-shaped body (Fig. 3.6G-H′,I, Fig. 3.S4B). We conclude that loss of Svp leads to the generation of ectopic P-EN neurons that show targeting to normal neuropil regions with increased volume and off-targeting to the fan-shaped body.

Fig. 3.6 (next page) Svp regulates the early born P-EN adult neuron morphology. (A-H′) Reconstruction of CX neuropils and P-EN neuron targeting for the protocerebral bridge (PB; A-B′), ellipsoid body (EB; C-D′), noduli (NO; E-F′) and fan-shaped body (FB; G-H′). (I) Quantification of P-EN neuropil targeting scored based on LexA targeting to neuropils identified with nc82 or CadN shown as a bar plot with 95% confidence interval. Control, *n*=8 brains; Svp-KO#1, *n*=20 brains; Svp-KO#2, *n*=16 brains. In all panels, nc82 reconstruction is in magenta and P-EN LexA targeting is in white. Scale bars: 10 μm.

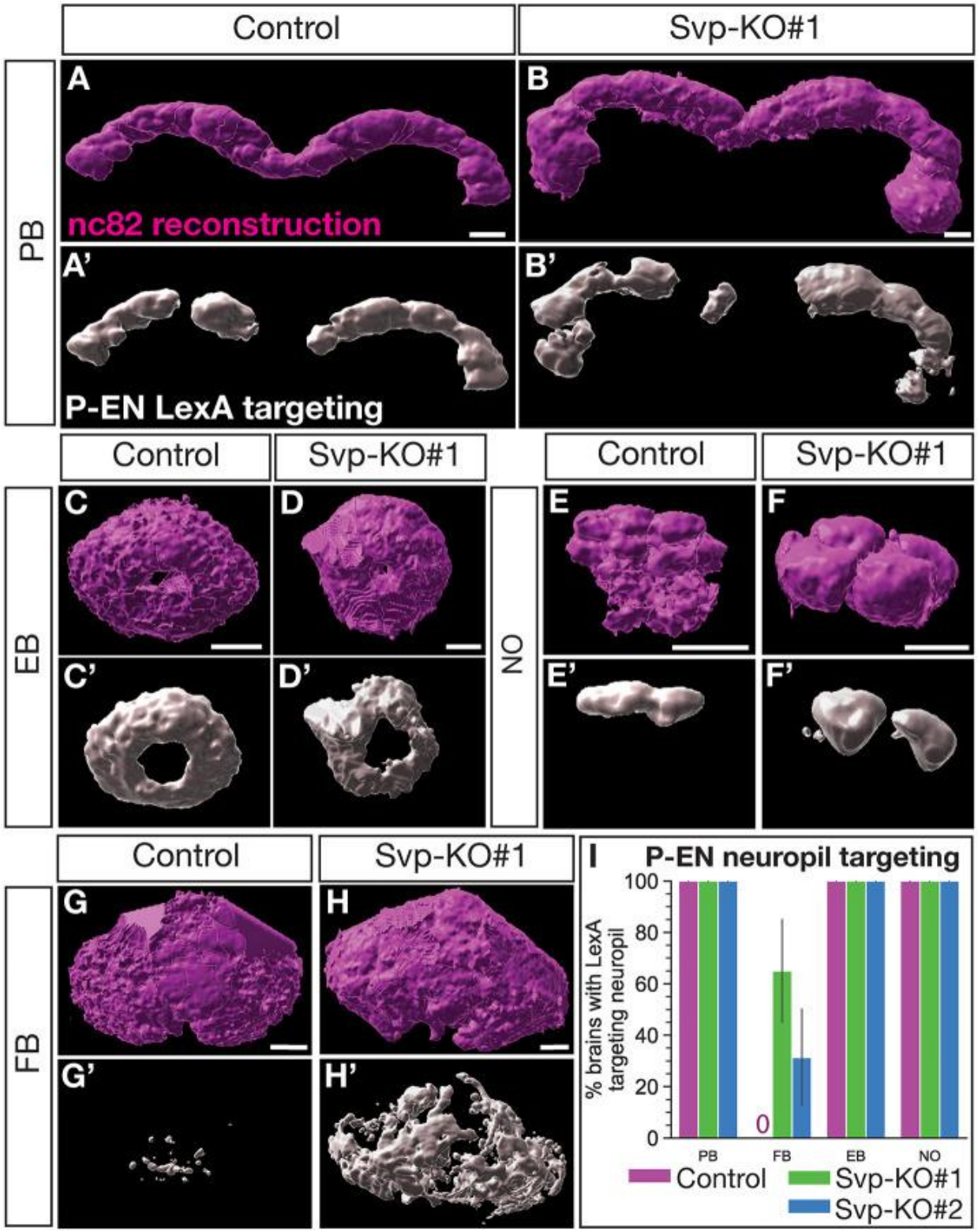
Control
Svp-KO#1
PB
A
B
nc82 reconstruction
A'
B'
P-EN LexA targeting
Control
Svp-KO#1
Control
Svp-KO#1
EB
C
D
NO
E
F
C'
D'
E'
F'
Control
Svp-KO#1
FB
G
H
G'
H'
I
P-EN neuropil targeting
% brains with LexA targeting neuropil
100
80
60
40
20
0
0
PB
FB
EB
NO
Control
Svp-KO#1
Svp-KO#2

Loss of Svp extends T2NB lineages into the adult

We note above that Svp knockout extended the production of P-EN neurons beyond the later part of larval life at 100 h ALH (Fig. 3.5H), raising the question of whether Svp is required for terminating neurogenesis in T2NBs? Previous work has demonstrated that Svp is required for decommissioning – characterized by loss of molecular markers, cell cycle arrest, death and/or differentiation – in Type 1 NB lineages (Maurange et al., 2008; Narbonne-Reveau et al., 2016). In wild-type animals, most NBs undergo decommissioning in late larval or early pupal stages (Ito and Hotta, 1992; Maurange et al., 2008; Siegrist et al., 2010; Yang et al., 2017). The time of T2NB decommissioning has been reported to be before 24 h after pupal formation (APF) (Homem et al., 2014). We confirmed that T2NBs have completed decommissioning by 24 h (Fig. 3.7A-A‴,E). In contrast, Svp knockout in T2NB lineages results in delayed decommissioning with persistence of proliferative T2NBs, marked by pH3, into 7-day-old adults (Fig. 3.7B-D‴,E-F). Remarkably, the persistent T2NBs after Svp knockout strongly express the early marker Imp and lack the late marker Syncrip (Fig. 3.7B-D″), consistent with previous work showing the Imp to Syncrip gradient regulates NB decommissioning (Yang et al., 2017). Thus, we conclude that Svp is required to initiate T2NB decommissioning (Fig. 3.7G). How these late functions of Svp, such as T2NB decommissioning in pupal stages, are triggered by transient expression of Svp many days earlier in first instar larvae remains an interesting unanswered question.

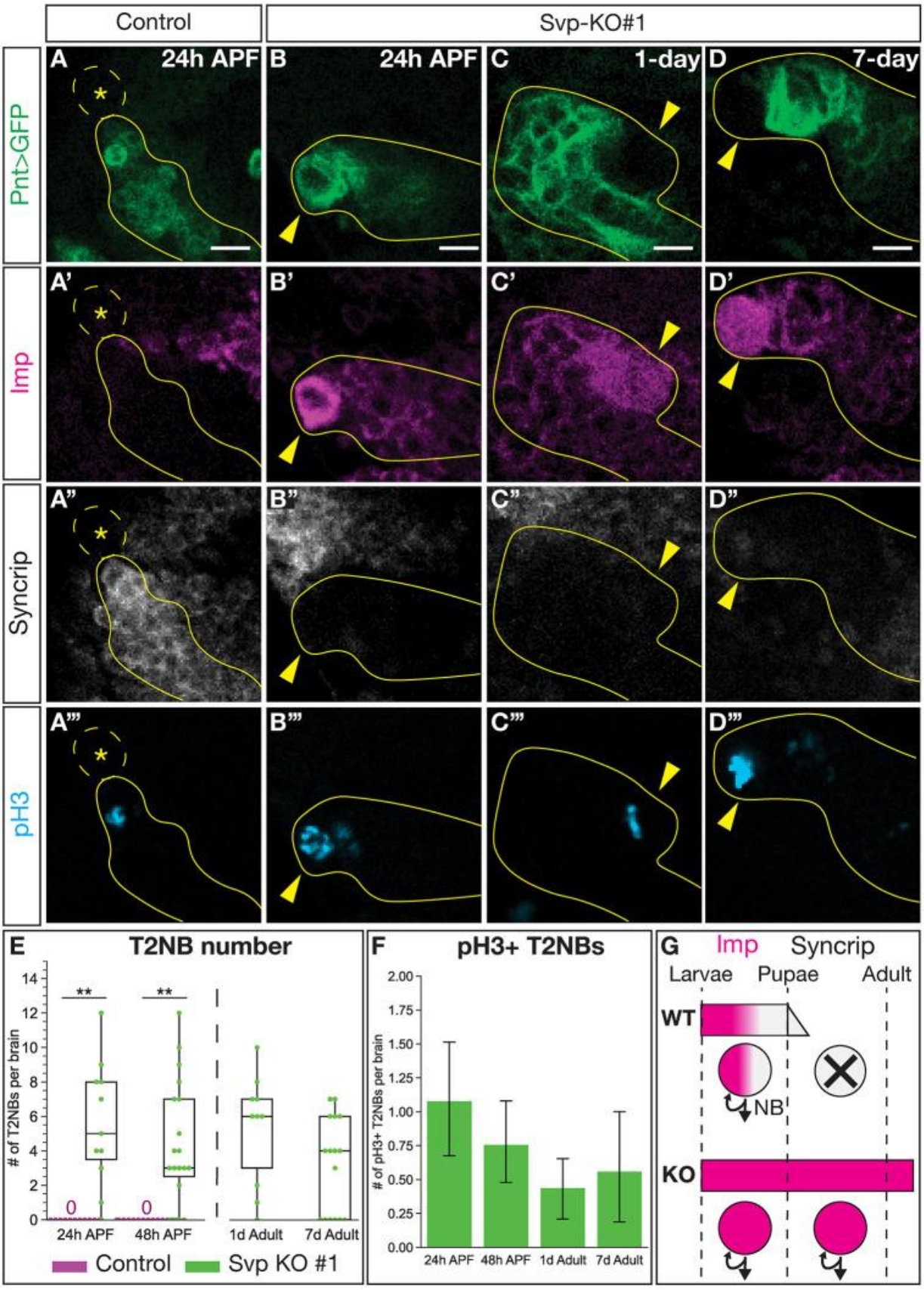
Control
Svp-KO#1
A 24h APF
B 24h APF
C 1-day
D 7-day
Pnt>GFP
Imp
Syncrip
pH3
A'
B'
C'
D'
A''
B''
C''
D''
A'''
B'''
C'''
D'''
E T2NB number
# of T2NBs per brain
24h APF
48h APF
1d Adult
7d Adult
Control
Svp KO #1
F pH3+ T2NBs
# of pH3+ T2NBs per brain
G Imp Syncrip
Larvae
Pupae
Adult
WT
NB
KO

Fig. 3.7 (previous page) Svp is required for timely onset of T2NB decommissioning. (A-A‴) T2NBs have decommissioned by 24 h after pupal formation (APF). (B-D‴) Loss of Svp led to the remaining T2NBs showing expression of the early factor Imp and no expression of the late factor Syncrip, while being mitotically active with expression of pH3 at 24 h APF (B-B‴), in 1-day-old adult (C-C‴) and in 7-day-old adult (D-D‴). (A-D‴) In all images, the Type 2 lineage can be identified by Pnt-Gal4 in green, Imp in magenta, Syncrip in white and pH3 in cyan. Dashed outline and asterisk indicate lack of T2NB. Solid yellow outline indicates a type 2 lineage. Yellow arrowheads indicate T2NB. (E) Quantification of T2NB number per brain. Each dot represents one brain with box and whisker plot showing distribution. Whiskers display the minimum and maximum range for the data, excluding outliers (defined as data points outside of 1.5x interquartile range). Control 24 h APF, *n*=16 brains; Svp-KO#1 24 h APF, *n*=11 brains; control 48 h APF, *n*=18 brains; Svp-KO#1 48 h APF, *n*=19 brains; Svp-KO#1 1-day-old adult, *n*=10 brains; Svp-KO#1 7-day-old adult, *n*=16 brains. *P*-values were determined by an independent, unpaired *t*-test: control versus Svp-KO#1 at 24 h APF, $^{**}P<0.001$; control versus Svp-KO#1 at 48 h APF, $^{**}P<0.001$. (F) Quantification of the number of $pH3^{+}$ ectopic T2NBs remaining in the pupae and adult stages shown as a bar plot with 95% confidence interval. Svp-KO#1 24 h APF, *n*=37 brains; Svp-KO#1 48 h APF, *n*=25 brains; Svp-KO#1 1-day-old adult, *n*=26 brains; Svp-KO#1 7-day-old adult, *n*=16 brains. (G) Summary of Svp required for transition of Imp to Syncrip expression in T2NBs for onset of neuroblast decommission. Scale bars: 5 μm.

Discussion

Columnar neurons are born at different times in the T2NB lineage

Our EdU birth dating revealed that P-EN neurons are born from early T2NBs, and P-FN neurons are born from late T2NBs, although previous work showed P-FN neurons are born from early T2NBs (Sullivan et al., 2019). Yet there is some overlap: Sullivan et al. (2019) mapped ∼10% of P-FN neurons to a 48-60 h ALH birth window, and we birth dated most P-FN neurons to a 48-84 h ALH window (Fig. 3.1F,G). Importantly, our approach tracks the terminal division of cells through EdU labeling, which accounts for all neurons within the population, whereas the previous genetic approach to immortalize INPs only accounted for 50-65% of the total P-EN and P-FN neurons (Sullivan et al., 2019). We propose that EdU birth dating is more comprehensive for assigning neurons to NB birth windows, as all neurons are reliably labeled with EdU, providing reproducible tracing of terminal divisions.

It remains an unanswered question how T2NBs are patterned to generate birth order-dependent neuronal identities. One hypothesis is that the lineage uses a temporal transcription factor cascade, similar to embryonic Type 1 NBs (Isshiki et al., 2001; Novotny et al., 2002; Pearson and Doe, 2003; Tran and Doe, 2008; Moris-Sanz et al., 2014). Alternatively, or in combination, the

lineage could use a temporal gradient of protein expression, such as mushroom body NBs (Liu et al., 2015). Several temporally expressed factors are known to cross-regulate in T2NBs (Ren et al., 2017; Syed et al., 2017). Our work with loss of Svp (i.e. changing expression of known temporal factors in T2NBs) shows that temporal patterning at the NB level is required to specify neuron subtypes. This is supported by recent work reporting knockdown of Imp levels in T2NB lineages results in altered CX neurons; however, it is unclear whether this is due to the role of Imp at the NB or INP level (Hamid et al., 2023 preprint). Additionally, the T2NB temporal factors EcR and E93 are required for specifying the CX neuron subtype dFB neurons (Wani et al., 2023 preprint). Our data do not distinguish between a model for a temporal transcription factor cascade and/or temporal gradients. Thus, it will be important to test individual temporal factors and expression levels in specifying birth order-dependent fates.

Svp expression in larval T2NB lineages

We report a comprehensive characterization of Svp in all eight T2NB lineages at stages that bracket Svp expression. Previous work has only observed Svp expression at either broad temporal windows or limited to a few lineages (Bayraktar and Doe, 2013; Ren et al., 2017; Syed et al., 2017). We show that Svp has a tight expression window between 18 and 24 h ALH in all T2NB lineages, with Svp protein restricted to the NB (Fig. 3.2). This finding is further supported by the *svp* mRNA showing a similar expression pattern in the T2NB lineages and restricted to the NB (Fig. 3.S1). Interestingly, *svp* mRNA was expressed before onset of protein expression and remained longer than protein expression (compare Fig. 3. 2 to Fig. 3.S1), which suggests post-transcriptional regulation of *svp* in the NB. We found evidence that indicates the posterior lineages (DM4-6, DL1-2) express Svp before the anterior lineages (DM1-3) (Fig. 3.2I). We speculate that the distinct onset of Svp expression between lineages may be determined by differential expression of spatial factors. Determining the upstream mechanism that initiates Svp expression remains an unanswered question. A further challenge will be resolving the orphan receptor status of Svp as it remains unknown whether Svp requires a ligand for activation.

Svp is required for late born fates in the T2NB lineages

We found that Svp knockout resulted in a loss of the late born P-FN neuron identity. The remaining P-FN neurons resemble wild-type neurons in cell body location, numbers,

morphology and birth window. We report that the Svp knockout lineages have a success rate of ~75%, with approximately one out of four T2NBs completely escaping *svp* knockout (Fig. 3.S2). Wild-type P-FN neurons contain ~40 cells, but in Svp knockouts we see ~5-15 cells remaining, which is the expected proportion based on the efficiency of our knockout lines (Fig. 3.4D). Moreover, the remaining P-FN neurons display lineage-appropriate morphology (Fig. 3.4E-H) and a wild-type birth window from the T2NBs (Fig. 3.4J). We conclude that the remaining P-FN neurons are derived from Svp knockout escaping NBs that maintain normal Svp expression and hence develop normally. Thus, our Svp knockout can be described as an 'all or none' knockout of Svp in ~75% of the T2NBs.

Svp specification of other CX neuron subtypes

Svp has previously been reported as either a switching factor in embryonic and larval NBs (Kanai et al., 2005; Mettler et al., 2006; Maurange et al., 2008; Benito-Sipos et al., 2011; Kohwi et al., 2011) or as a post-mitotic fate determinant in photoreceptor neuron subtypes (Mlodzik et al., 1990; Hiromi et al., 1993). Our work shows that Svp acts as a switching factor in T2NBs for specifying neuron identities, as Svp was not expressed in post-mitotic P-EN or P-FN neurons (Fig. 3.S3). However, we cannot rule out the possibility that Svp is required as a post-mitotic fate determinant for other CX subtypes.

We show that Svp is required to restrict the early born P-EN identity, as loss of Svp resulted in T2NBs extending production of P-EN neurons into an abnormally late temporal window (Fig. 3.5H). These ectopic P-EN neurons maintain wild-type molecular markers (e.g. LexA, Runt and Cut) (Fig. 3.5G). We note that these ectopic P-EN neurons have ectopic targeting to the fan-shaped body, a neuropil not extensively targeted by wild-type P-EN neurons (Hulse et al., 2021) (Fig. 3.6G-H′,I; Fig. 3.S4B,C). We speculate that this abnormal targeting may be compensation for the loss of P-FN neurons that normally target the region, suggesting that columnar neuron targeting may be promiscuous when subtypes are absent. Alternatively, the ectopic targeting to the fan-shaped body may be an expanded volume of neurites from the increased number of P-EN neurons as they pass through to target the ellipsoid body. We note that P-EN neurons are only one fate born from the early temporal window; other neurons born at a similar time are not visible with the P-EN/P-FN LexA markers used here. We hypothesize that these early born

populations will also be expanded with the loss of Svp. It will be vital for future work to identify additional CX neuron markers and their birth date from the T2NBs to test for functional temporal patterning factors.

We find that the loss of Svp resulted in significant changes to CX neuropil volumes. Although targeting from ectopic P-EN neurons accounts for some of this increase, it does not fully account for the global CX neuropil enlargement we report (Fig. 3.S4B,C). We speculate that either expanded populations of other T2NB-derived neuron subtypes and/or synaptic partners account for the ectopic targeting to these neuropils. For example, P-EN neurons form synapses with the T2NB-derived E-PG neurons (Green et al., 2017, 2019); thus, loss of Svp could lead to either E-PG compensation with increased targeting to ectopic P-EN neurons and/or an expanded E-PG neuron population. We are unable to account for the global CX changes that occurred with the loss of Svp due to the limitation in our assays of only the P-EN and P-FN neurons.

Svp-mediated regulation of Type 2 neuroblast temporal progression

Svp is expressed in early larval T2NBs prior to the Imp to Syncrip transition (Ren et al., 2017); thus, we were surprised by our findings that Svp is required for terminating neurogenesis in pupae. Previous work has shown the transition in central brain NBs from Imp to Syncrip expression initiates NB decommissioning (Yang et al., 2017). Interestingly, mushroom body NBs continue proliferating into pupal stages, when other NBs have decommissioned, owing to sustained Imp expression (Yang et al., 2017). Consistent with our work on T2NBs, previous work has also demonstrated that loss of Svp in the ventral nerve cord and central brain NB lineages leads to continued NB proliferation into the adult (Maurange et al., 2008; Narbonne-Reveau et al., 2016). We report that loss of Svp in early larval T2NBs had profound impacts on the lifespan of the NBs, where they survive into 7-day adults manifesting: (1) maintained Imp expression; (2) mitotic activation; and (3) maintenance of low levels of Syncrip (Fig. 3. 7). Thus, we propose that Svp initiating the switch of Imp-to-Syncrip in T2NBs is a NB-autonomous mechanism required for terminating neurogenesis within T2NB lineages. This is consistent with previous work showing that Svp is required for the progression of Imp to Syncrip expression in T2NBs (Ren et al., 2017). Two hypotheses are that Svp initiates a transcriptional cascade that executes a function ~24 h later, or that Svp alters the NB chromatin landscape to make it

responsive to a new input ~24 h later. It will be important future work to find the targets of Svp within the T2NBs.

Recently, Notch signaling has been shown to be required for central brain Type 1 NB decommissioning by disrupting temporal patterning progression; loss of Notch signaling produced prolonged expression of the early factor Imp and reduced expression of the late factor E93 (Sood et al., 2023). Additionally, Notch signaling appeared to be required in terminating expression of the early factors Castor and Svp (Sood et al., 2023). This indicates that Notch signaling acts upstream of NB temporal factors, and thus is also likely to act upstream of Svp. This is difficult to test because loss of Notch signaling in T2NBs results in loss of NB identity (San-Juán and Baonza, 2011; Zhu et al., 2012; Li et al., 2016, 2017).

Conserved role of Svp in vertebrate temporal patterning

Our work shows that Svp acts as a switching factor in T2NBs to switch from producing early born to late born neuronal identities. The mammalian orthologs of *svp*, *COUP-TFI* and *COUP-TFII* (*Nr2f1* and *Nr2f2*) have been characterized for a similar role as a switching factor in murine neural stem cells (Naka et al., 2008; Lodato et al., 2011). *COUP-TFI* and *COUP-TFII* are required for cultured neural stem cells to switch from producing early born neuron cell types to producing late born glia, because a loss of this molecular switch resulted in sustained neurogenesis (Naka et al., 2008). Additionally, *COUP-TFI* and *COUP-TFII* are required for switching cortical neural stem cells from producing early born interneuron fates to late born interneuron fates (Lodato et al., 2011). These findings, along with ours and others in *Drosophila*, suggest that Svp has a conserved role as a neural stem cell switching factor from fly to mammals (Mettler et al., 2006; Benito-Sipos et al., 2011; Ren et al., 2017).

Materials and methods

Animal preparation

Drosophila melanogaster was used in all experiments. All flies were kept and maintained at 25°C unless stated otherwise. Stocks used can be found in Table S3.1 and experimental genetic crosses in Table S3.2 (see Appendix A for supplementary tables).

EdU experiments

EDU (5-ethynyl-2′-deoxyuridine; Millipore-Sigma, 900584-50MG), a thymidine analog, was used to label proliferating cells starting at various sequential larvae ages. Larvae were fed food containing 20 µg/ml EdU nonstop from the initial age feeding started until the larvae pupated. Larvae fed on EdU were raised at temperatures between 18°C and 21°C until adults hatched and were dissected.

Larval experiments

Embryos were collected on 3% agar apple juice caps with yeast paste for 4 h and aged for 21 h. After aging, embryos were transferred to a fresh cap and aged 4 h for hatching. Hatched larvae were collected and dissected at the corresponding time after larval hatching (ALH).

Adult experiments

Males and virgin females were introduced in standard yeast medium vials and flipped every 2 days. Adult flies (2-5 days old) were dissected for all experiments unless stated otherwise. All animals dissected were a mixture of male and female, unless otherwise specified.

Hybridization chain reaction (HCR) RNA fluorescent in situ hybridization

Larval brains were dissected in Schneider's insect medium, fixed in 4% PFA (paraformaldehyde; Electron Microscopy Sciences, 15710) in PBS (phosphate-buffered saline; Sigma-Aldrich, P4417) for 7-15 min at room temperature, and washed in PBST (PBS with 0.3% Triton; Sigma-Aldrich, T8787). The fixed brains were stored in 70% ethanol in deionized water at 4°C until used. We followed the protocol from Duckhorn et al. (2022). A 20-probe set targeting all *svp* transcript isoforms was synthesized by Molecular Instruments and probes were added to a final concentration of 4 nM for hybridization. Amplifier B3-546 was also synthesized by Molecular Instruments and 6 pmol of each hairpin (h1 and h2) was added for amplification.

Larval brain sample preparation

Larval brains were dissected in PBS and mounted on poly-D-lysine coated coverslips (Neuvitro Corporation GG-12-PDL; primed in 100% ethanol). Samples fixed for 23 min in 4% PFA in PBST. Samples were washed in PBST and blocked with 2% normal donkey serum (Jackson

ImmunoResearch Laboratories) in PBST. Samples were incubated in a primary antibody mix diluted in PBST for overnight or for 1-2 days at 4°C. Primary antibodies were removed and samples thoroughly washed with PBST. Samples were incubated in secondary antibodies overnight at 4°C. Secondary antibodies were removed and samples washed in PBST. Samples were dehydrated with an ethanol series of 30%, 50%, 75% and 100% ethanol then incubated in xylene (Fisher Chemical, X5-1) for 2×10 min. Samples were mounted onto slides with DPX (Sigma-Aldrich 06552) and cured for 3-4 days then stored at 4°C until imaged.

Adult brain sample preparation

Adult brains were prepared in a similar way to larval brains, with the exception of 41 min for fixation in 4% PFA and 2×12 min xylene incubations.

EdU adult brain sample preparation

Adult brains from EdU-fed larvae were dissected in HL3.1 then fixed in 4% PFA for 30 min and incubated in block at 4°C overnight. Samples were incubated in primary and secondary mixes before Click-it-Reaction to label EdU. The Click-it-Reaction mix comprised PBS, Copper II sulfate (ThermoFisher, 033308.22), 555-Azide (ThermoFisher, A20012) in DSMO and ascorbic acid (Sigma-Aldrich, A4544-25G) for a 2 h incubation. Samples were dehydrated and washed in xylene before DPX mounting as described above.

Antibodies

Antibodies used can found in Table S3.3 (See Appendix A for supplementary tables).

Confocal microscopy

Fixed preparations were imaged with a Zeiss LSM 900 or 800 laser scanning confocal equipped with an Axio Imager.Z2 microscope. A 10×/0.3 EC Plan-Neofluar M27 or 40×/1.40 NA Oil Plan-Apochromat DIC M27 objective lens was used. The software program used was Zen 3.6 (blue edition) (Zeiss AG).

Image processing and analysis

Cell counting and neuropil target scoring. Confocal image stacks were loaded into Fiji (ImageJ 1.50d, https://imagej.net/Fiji). Cells were counted using the Cell Counter plug-in. Neuropil targeting was determined by colocalization of LexA expression with a neuropil marker that was not a filament bundle passing through the neuropil.

Imaris neuropil reconstructions. Confocal image stacks were loaded into Imaris 10.0.0 (Bitplane). Imaris Surface objects were created for each neuropil using nc82 staining and LexA expression followed by new objects designating overlap between neuropil and neurites. Briefly, the Surface tool was selected and a region of interest (ROI) was drawn to encompass a whole CX neuropil or LexA expression. The source channel was selected (nc82 in RRX for neuropils or LexA in 647 for neurites) and absolute threshold intensity was manually set slice by slice to outline fluorescent signal and morphologically split to separate regions. All Starting Points and Seed Points were kept, ensuring full coverage of signal. Surfaces were rendered and surfaces outside neuropil structures removed. To find the LexA targeting for each neuropil, Surface-Surface Overlap File XTension (Matthew Gastinger; https://imaris.oxinst.com/open/view/surface-surface-overlap) was used to find the volume (µm3) of overlap. A Smoothing Factor of 0.2 µm was kept for all surfaces.

Figure preparation. Images in figures were prepared either in Imaris 10.0.0 or Fiji. Scale bars are given for a single slice in all single slice images and from all stacks within maximum intensity projections images. Pixel brightness was adjusted in images for clearer visualization; all adjustments were made uniformly over the entire image, and uniformly across wild-type samples and corresponding control and experimental samples. Adobe Illustrator 2023 was used for formatting.

Statistical analyses

Statistics were computed using Python tests (see https://github.com/nrdDrosophila/Seven-up-specifies-neuron-identity). All statistical tests used are listed in the figure legends. *P*-values are reported in the figure legends. Plots display n.s.=not significant, **P*<0.05 and ***P*<0.01. Plots were generated using Seaborn and Matplotlib packages in Python. 95% confidence intervals and boxplot distributions were calculated when plotting the data.

Data availability

Code and corresponding data tables can be found at: https://github.com/nrdDrosophila/Seven-up-specifies-neuron-identity.

Supplementary information

Supplementary information can be found in Appendix A (Figures and Tables) or the online (Movies) version of this work at https://doi.org/10.1242/dev.202504.

Bridge

The previous chapter covered work that showed the temporal transcriptome dynamics of the developing larval CNS. This chapter covered the work of my co-authors and I where we studied the role of Seven-up as switching factor in larval T2NBs and its role in specifying CX neurons. In this work we: 1) birth dated the P-EN neurons to an early window and P-FN neurons to a late temporal window; 2) show that Seven-up is transiently expressed across all T2NB lineages; 3) Seven-up is required for the early-to-late switch in T2NB generation of CX neuron fates; 4) Seven-up is required for initiating the decommissioning of T2NBs. This work demonstrates the importance of transiently expressed factors such as Seven-up as regulatory mechanisms for NB temporal progression and specification of CX neurons. Importantly, this work showed that the temporal factors in T2NBs are required for neuron specification. The next chapter, Chapter IV, investigates the transiently expressed factor Castor as a candidate TTF in T2NB lineages for specifying CX neuron identities.

References

Andrade, I. V., Riebli, N., Nguyen, B.-C. M., Omoto, J. J., Cardona, A. and Hartenstein, V. (2019). Developmentally arrested precursors of pontine neurons establish an embryonic blueprint of the Drosophila central complex. Curr. Biol. 29, 412-425.e3. 10.1016/j.cub.2018.12.012

Bayraktar, O. A. and Doe, C. Q. (2013). Combinatorial temporal patterning in progenitors expands neural diversity. Nature 498, 449-455. 10.1038/nature12266

Bello, B. C., Izergina, N., Caussinus, E. and Reichert, H. (2008). Amplification of neural stem cell proliferation by intermediate progenitor cells in Drosophila brain development. Neural Dev. 3, 5. 10.1186/1749-8104-3-5

Benito-Sipos, J., Ulvklo, C., Gabilondo, H., Baumgardt, M., Angel, A., Torroja, L. and Thor, S. (2011). Seven up acts as a temporal factor during two different stages of neuroblast 5-6 development. Development 138, 5311-5320. 10.1242/dev.070946

Boone, J. Q. and Doe, C. Q. (2008). Identification of Drosophila type II neuroblast lineages containing transit amplifying ganglion mother cells. Dev. Neurobiol. 68, 1185-1195. 10.1002/dneu.20648

Bowman, S. K., Rolland, V., Betschinger, J., Kinsey, K. A., Emery, G. and Knoblich, J. A. (2008). The tumor suppressors brat and numb regulate transit-amplifying neuroblast lineages in Drosophila. Dev. Cell 14, 535-546. 10.1016/j.devcel.2008.03.004

Doe, C. Q. (2017). Temporal patterning in the Drosophila CNS. Annu. Rev. Cell Dev. Biol. 33, 219-240. 10.1146/annurev-cellbio-111315-125210

Duckhorn, J. C., Junker, I. P., Ding, Y. and Shirangi, T. R. (2022). Combined in situ hybridization chain reaction and immunostaining to visualize gene expression in whole-mount Drosophila central nervous systems. In Behavioral Neurogenetics (ed. Yamamoto D.), pp. 1-14. New York, NY: Springer US.

El-Danaf, R. N., Rajesh, R. and Desplan, C. (2023). Temporal regulation of neural diversity in Drosophila and vertebrates. Semin. Cell Dev. Biol. 142, 13-22. 10.1016/j.semcdb.2022.05.011

Epiney, D., Chaya, G. M., Dillon, N., Lai, S.-L. and Doe, C. (2023). Transcriptional complexity in the insect central complex: single nuclei RNA sequencing of adult brain neurons derived from type 2 neuroblasts. bioRxiv 2023.12.10.571022. 10.1101/2023.12.10.571022

Erclik, T., Li, X., Courgeon, M., Bertet, C., Chen, Z., Baumert, R., Ng, J., Koo, C., Arain, U., Behnia, R.et al. (2017). Integration of temporal and spatial patterning generates neural diversity. Nature 541, 365-370. 10.1038/nature20794

Franconville, R., Beron, C. and Jayaraman, V. (2018). Building a functional connectome of the Drosophila central complex. eLife 7, e37017. 10.7554/eLife.37017

Giraldo, Y. M., Leitch, K. J., Ros, I. G., Warren, T. L., Weir, P. T. and Dickinson, M. H. (2018). Sun navigation requires compass neurons in Drosophila. Curr. Biol. 28, 2845-2852.e4. 10.1016/j.cub.2018.07.002

Green, J., Adachi, A., Shah, K. K., Hirokawa, J. D., Magani, P. S. and Maimon, G. (2017). A neural circuit architecture for angular integration in Drosophila. Nature 546, 101-106. 10.1038/nature22343

Green, J., Vijayan, V., Mussells Pires, P., Adachi, A. and Maimon, G. (2019). A neural heading estimate is compared with an internal goal to guide oriented navigation. Nat. Neurosci. 22, 1460-1468. 10.1038/s41593-019-0444-x

Grosskortenhaus, R., Pearson, B. J., Marusich, A. and Doe, C. Q. (2005). Regulation of temporal identity transitions in Drosophila neuroblasts. Dev. Cell 8, 193-202. 10.1016/j.devcel.2004.11.019

Grosskortenhaus, R., Robinson, K. J. and Doe, C. Q. (2006). Pdm and Castor specify late-born motor neuron identity in the NB7-1 lineage. Genes Dev. 20, 2618-2627. 10.1101/gad.1445306

Hamid, A., Gattuso, H., Caglar, A. N., Pillai, M., Steele, T., Gonzalez, A., Nagel, K. and Syed, M. H. (2023). The RNA-binding protein, Imp specifies olfactory navigation circuitry and behavior in Drosophila. bioRxiv 2023.05.26.542522. 10.1101/2023.05.26.542522

Hiromi, Y., Mlodzik, M., West, S. R., Rubin, G. M. and Goodman, C. S. (1993). Ectopic expression of seven-up causes cell fate changes during ommatidial assembly. Development 118, 1123-1135. 10.1242/dev.118.4.1123

Holguera, I. and Desplan, C. (2018). Neuronal specification in space and time. Science 362, 176-180. 10.1126/science.aas9435

Homem, C. C. F., Reichardt, I., Berger, C., Lendl, T. and Knoblich, J. A. (2013). Long-term live cell imaging and automated 4D analysis of Drosophila neuroblast lineages. PLoS ONE 8, e79588. 10.1371/journal.pone.0079588

Homem, C. C. F., Steinmann, V., Burkard, T. R., Jais, A., Esterbauer, H. and Knoblich, J. A. (2014). Ecdysone and mediator change energy metabolism to terminate proliferation in Drosophila neural stem cells. Cell 158, 874-888. 10.1016/j.cell.2014.06.024

Hulse, B. K., Haberkern, H., Franconville, R., Turner-Evans, D. B., Takemura, S., Wolff, T., Noorman, M., Dreher, M., Dan, C., Parekh, R.et al. (2021). A connectome of the Drosophila central complex reveals network motifs suitable for flexible navigation and context-dependent action selection. eLife 10, e66039. 10.7554/eLife.66039

Isshiki, T., Pearson, B., Holbrook, S. and Doe, C. Q. (2001). Drosophila neuroblasts sequentially express transcription factors which specify the temporal identity of their neuronal progeny. Cell 106, 511-521. 10.1016/S0092-8674(01)00465-2

Ito, K. and Hotta, Y. (1992). Proliferation pattern of postembryonic neuroblasts in the brain of Drosophila melanogaster. Dev. Biol. 149, 134-148. 10.1016/0012-1606(92)90270-Q

Izergina, N., Balmer, J., Bello, B. and Reichert, H. (2009). Postembryonic development of transit amplifying neuroblast lineages in the Drosophila brain. Neural Dev. 4, 44. 10.1186/1749-8104-4-44

Kanai, M. I., Okabe, M. and Hiromi, Y. (2005). seven-up controls switching of transcription factors that specify temporal identities of Drosophila neuroblasts. Dev. Cell 8, 203-213. 10.1016/j.devcel.2004.12.014

Kohwi, M., Hiebert, L. S. and Doe, C. Q. (2011). The pipsqueak-domain proteins Distal antenna and Distal antenna-related restrict Hunchback neuroblast expression and early-born neuronal identity. Development 138, 1727-1735. 10.1242/dev.061499

Li, X., Xie, Y. and Zhu, S. (2016). Notch maintains Drosophila type II neuroblasts by suppressing the expression of the Fez transcription factor Earmuff. Development 143, 2511-2521. 10.1242/dev.136184

Li, X., Chen, R. and Zhu, S. (2017). bHLH-O proteins balance the self-renewal and differentiation of Drosophila neural stem cells by regulating Earmuff expression. Dev. Biol. 431, 239-251. 10.1016/j.ydbio.2017.09.011

Liu, Z., Yang, C.-P., Sugino, K., Fu, C.-C., Liu, L.-Y., Yao, X., Lee, L. P. and Lee, T. (2015). Opposing intrinsic temporal gradients guide neural stem cell production of varied neuronal fates. Science 350, 317-320. 10.1126/science.aad1886

Lodato, S., Tomassy, G. S., De Leonibus, E., Uzcategui, Y. G., Andolfi, G., Armentano, M., Touzot, A., Gaztelu, J. M., Arlotta, P., Menendez de la Prida, L.et al. (2011). Loss of COUP-TFI alters the balance between caudal ganglionic eminence- and medial ganglionic eminence-derived cortical interneurons and results in resistance to epilepsy. J. Neurosci. 31, 4650-4662. 10.1523/JNEUROSCI.6580-10.2011

Maurange, C., Cheng, L. and Gould, A. P. (2008). Temporal transcription factors and their targets schedule the end of neural proliferation in Drosophila. Cell 133, 891-902. 10.1016/j.cell.2008.03.034

Mettler, U., Vogler, G. and Urban, J. (2006). Timing of identity: spatiotemporal regulation of hunchback in neuroblast lineages of Drosophila by Seven-up and Prospero. Development 133, 429-437. 10.1242/dev.02229

Mlodzik, M., Hiromi, Y., Weber, U., Goodman, C. S. and Rubin, G. M. (1990). The Drosophila seven-up gene, a member of the steroid receptor gene superfamily, controls photoreceptor cell fates. Cell 60, 211-224. 10.1016/0092-8674(90)90737-Y

Moris-Sanz, M., Estacio-Gómez, A., Álvarez-Rivero, J. and Díaz-Benjumea, F. J. (2014). Specification of neuronal subtypes by different levels of Hunchback. Development 141, 4366-4374. 10.1242/dev.113381

Naka, H., Nakamura, S., Shimazaki, T. and Okano, H. (2008). Requirement for COUP-TFI and II in the temporal specification of neural stem cells in CNS development. Nat. Neurosci. 11, 1014-1023. 10.1038/nn.2168

Narbonne-Reveau, K., Lanet, E., Dillard, C., Foppolo, S., Chen, C.-H., Parrinello, H., Rialle, S., Sokol, N. S. and Maurange, C. (2016). Neural stem cell-encoded temporal patterning delineates an early window of malignant susceptibility in Drosophila. eLife 5, e13463. 10.7554/eLife.13463

Novotny, T., Eiselt, R. and Urban, J. (2002). Hunchback is required for the specification of the early sublineage of neuroblast 7-3 in the Drosophila central nervous system. Development 129, 1027-1036. 10.1242/dev.129.4.1027

Pearson, B. J. and Doe, C. Q. (2003). Regulation of neuroblast competence in Drosophila. Nature 425, 624-628. 10.1038/nature01910

Pereanu, W. and Hartenstein, V. (2006). Neural lineages of the Drosophila brain: a three-dimensional digital atlas of the pattern of lineage location and projection at the late larval stage. J. Neurosci. 26, 5534-5553. 10.1523/JNEUROSCI.4708-05.2006

Port, F., Strein, C., Stricker, M., Rauscher, B., Heigwer, F., Zhou, J., Beyersdörffer, C., Frei, J., Hess, A., Kern, K.et al. (2020). A large-scale resource for tissue-specific CRISPR mutagenesis in Drosophila. eLife 9, e53865. 10.7554/eLife.53865

Ren, Q., Yang, C.-P., Liu, Z., Sugino, K., Mok, K., He, Y., Ito, M., Nern, A., Otsuna, H. and Lee, T. (2017). Stem cell-intrinsic, seven-up-triggered temporal factor gradients diversify intermediate neural progenitors. Curr. Biol. 27, 1303-1313. 10.1016/j.cub.2017.03.047

Riebli, N., Viktorin, G. and Reichert, H. (2013). Early-born neurons in type II neuroblast lineages establish a larval primordium and integrate into adult circuitry during central complex development in Drosophila. Neural Dev. 8, 6. 10.1186/1749-8104-8-6

San-Juán, B. P. and Baonza, A. (2011). The bHLH factor deadpan is a direct target of Notch signaling and regulates neuroblast self-renewal in Drosophila. Dev. Biol. 352, 70-82. 10.1016/j.ydbio.2011.01.019

Siegrist, S. E., Haque, N. S., Chen, C.-H., Hay, B. A. and Hariharan, I. K. (2010). Inactivation of both foxo and reaper promotes long-term adult neurogenesis in Drosophila. Curr. Biol. 20, 643-648. 10.1016/j.cub.2010.01.060

Skeath, J. B. and Thor, S. (2003). Genetic control of Drosophila nerve cord development. Curr. Opin. Neurobiol. 13, 8-15. 10.1016/S0959-4388(03)00007-2

Sood, C., Nahid, M. A., Branham, K. R., Pahl, M. C., Doyle, S. E. and Siegrist, S. E. (2023). Delta-dependent Notch activation closes the early neuroblast temporal program to promote lineage progression and neurogenesis termination in Drosophila. eLife 12. 10.7554/eLife.88565.1

Sullivan, L. F., Warren, T. L. and Doe, C. Q. (2019). Temporal identity establishes columnar neuron morphology, connectivity, and function in a Drosophila navigation circuit. eLife 8, e43482. 10.7554/eLife.43482

Syed, M. H., Mark, B. and Doe, C. Q. (2017). Steroid hormone induction of temporal gene expression in Drosophila brain neuroblasts generates neuronal and glial diversity. eLife 6, e26287. 10.7554/eLife.26287

Tran, K. D. and Doe, C. Q. (2008). Pdm and Castor close successive temporal identity windows in the NB3-1 lineage. Development 135, 3491-3499. 10.1242/dev.024349

Turner-Evans, D. B., Jensen, K. T., Ali, S., Paterson, T., Sheridan, A., Ray, R. P., Wolff, T., Lauritzen, J. S., Rubin, G. M., Bock, D. D.et al. (2020). The neuroanatomical ultrastructure and function of a biological ring attractor. Neuron 108, 145-163.e10. 10.1016/j.neuron.2020.08.006

Wagh, D. A., Rasse, T. M., Asan, E., Hofbauer, A., Schwenkert, I., Dürrbeck, H., Buchner, S., Dabauvalle, M.-C., Schmidt, M., Qin, G.et al. (2006). Bruchpilot, a protein with homology to ELKS/CAST, is required for structural integrity and function of synaptic active zones in Drosophila. Neuron 49, 833-844. 10.1016/j.neuron.2006.02.008

Wani, A. R., Chowdhury, B., Luong, J., Chaya, G. M., Patel, K., Isaacman-Beck, J., Shafer, O., Kayser, M. S. and Syed, M. H. (2023). Stem cell-specific ecdysone signaling regulates the development and function of a Drosophila sleep homeostat. bioRxiv 2023.09.29.560022. 10.1101/2023.09.29.560022

Wolff, T. and Rubin, G. M. (2018). Neuroarchitecture of the Drosophila central complex: a catalog of nodulus and asymmetrical body neurons and a revision of the protocerebral bridge catalog. J. Comp. Neurol. 526, 2585-2611. 10.1002/cne.24512

Wolff, T., Iyer, N. A. and Rubin, G. M. (2015). Neuroarchitecture and neuroanatomy of the Drosophila central complex: A GAL4-based dissection of protocerebral bridge neurons and circuits. J. Comp. Neurol. 523, 997-1037. 10.1002/cne.23705

Yang, J. S., Awasaki, T., Yu, H.-H., He, Y., Ding, P., Kao, J.-C. and Lee, T. (2013). Diverse neuronal lineages make stereotyped contributions to the Drosophila locomotor control center, the central complex. J. Comp. Neurol. 521, 2645-2662. 10.1002/cne.23339

Yang, C.-P., Samuels, T. J., Huang, Y., Yang, L., Ish-Horowicz, D., Davis, I. and Lee, T. (2017). Imp and Syp RNA-binding proteins govern decommissioning of Drosophila neural stem cells. Development 144, 3454-3464. 10.1242/dev.149500

Zhu, S., Wildonger, J., Barshow, S., Younger, S., Huang, Y. and Lee, T. (2012). The bHLH repressor deadpan regulates the self-renewal and specification of Drosophila larval neural stem cells independently of Notch. PLoS ONE 7, e46724. 10.1371/journal.pone.0046724

Chapter IV

Castor is a temporal transcription factor that specifies early born central complex neuron identity

Dillon, N. R. and Doe, C. Q. (2024). Castor is a temporal transcription factor that specifies early born central complex neuron identity. 2024.08.22.609207. *In review at Development.*

Author contributions

Conceptualization: N.R.D.; Methodology: N.R.D.; Validation: N.R.D.; Formal analysis: N.R.D.; Investigation: N.R.D.; Resources: N.R.D.; Data curation: N.R.D.; Writing – original draft: N.R.D.; Writing – review & editing: N.R.D., C.Q.D.; Visualization: N.R.D.; Supervision: C.Q.D.

Introduction

Generating a complex brain requires neural stem cells to generate a large and diverse set of cell types. The neural stem cells in *Drosophila*, known as neuroblasts (NBs), generate neuronal diversity through a combination of spatial and temporal patterning mechanisms (Doe, 2017; El-Danaf et al., 2023). Similar results have been observed in mammals (Alsio et al., 2013; Clark et al., 2019; Elliott et al., 2008; Frith et al., 2024; Javed et al., 2020; Liu et al., 2020; Mattar and Cayouette, 2015; Mattar et al., 2021), highlighting the importance of temporal patterning in generating neuronal diversity across species. In *Drosophila*, these processes have been most extensively studied in embryonic NB lineages where narrow windows of temporal transcription factors (TTFs) specify distinct neuronal identities (Cleary and Doe, 2006; Grosskortenhaus et al., 2006; Isshiki et al., 2001; Meng et al., 2019; Meng et al., 2020; Moris-Sanz et al., 2015; Novotny et al., 2002; Pearson and Doe, 2003; Seroka and Doe, 2019; Tran and Doe, 2008). Whether larval NBs undergo similar TTF windows remains understudied.

The larval central brain contains ~100 NB lineages per hemibrain (Pereanu and Hartenstein, 2006). There are two types of NBs based on their lineages: Type 1 NBs generate a series of ganglion mother cells that divide once to produce a pair of post-

mitotic neurons, whereas Type 2 NBs (T2NBs) generate a series of intermediate neural progenitors (INPs) that each generate 4-6 ganglion mother cells that divide to produce a pair of post-mitotic neurons (Bello et al., 2008; Boone and Doe, 2008; Bowman et al., 2008). This T2NB division pattern is analogous to the outer subventricular zone lineages of the primate cortex (Holguera and Desplan, 2018; El-Danaf et al., 2023); thus, it is important to understand how these larval lineages, which closely resemble mammalian neural stem cells, are patterned to generate neuronal diversity. There are only eight T2NBs per hemibrain, with each lineage having a unique spatial identity that generates neurons with lineage-specific morphology (Andrade et al., 2019; Pereanu and Hartenstein, 2006; Riebli et al., 2013; Yang et al., 2013). Previous work has suggested that temporal patterning in both the T2NBs and INPs act in combination to generate neuronal diversity (Bayraktar and Doe, 2013).

Larval NBs express broad and opposing temporal gradients of two RNA-binding proteins: high levels of IGF-II mRNA-binding protein (Imp) in early stages and high levels of Syncrip in late stages (Fig. 4.1A) (Liu et al., 2015; Ren et al., 2017; Syed et al., 2017). The short burst of Seven-up (Svp) expression has been identified as a switching factor to initiate the temporal Imp-to-Syncrip transition in larval T2NBs (Fig. 4.1A) (Ren et al., 2017; Syed et al., 2017). We have previously shown that Svp acts in T2NBs to initiate a switch for transitioning the generation of early born fates to late born fates (Dillon et al., 2024); thus, temporally expressed factors in T2NBs are required for specifying neuronal identities. Previous work has demonstrated the importance of TTFs in the INPs to generate neuron subtype diversity (Bayraktar and Doe, 2013; Sullivan et al., 2019). Several candidate TTFs have been shown to have narrow temporal windows of expression in the T2NBs (Castor, Chinmo, Broad, and E93) (Ren et al., 2017; Syed et al., 2017) but whether these factors are required to specify different neuronal subtypes remains unknown.

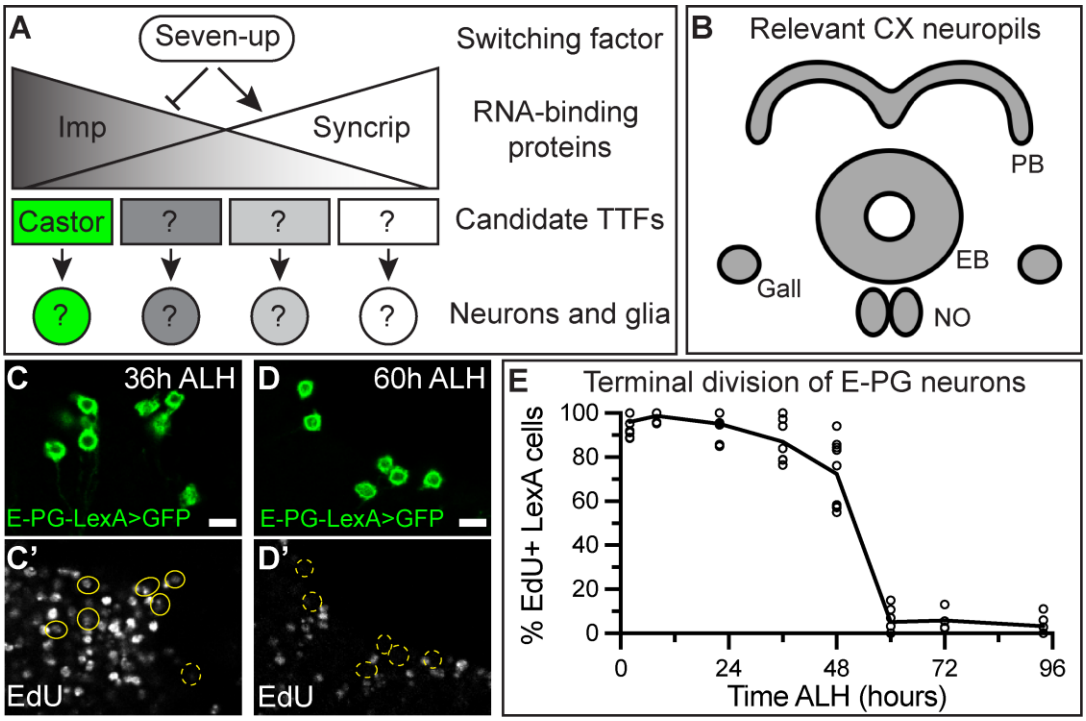

Figure 4.1. E-PG neurons are born early in Type 2 neuroblast lineages. (A) Larval neuroblasts express broad temporal gradients of the RNA-binding proteins Imp and Syncrip and shorter temporal windows of candidate temporal transcription factors (TTFs) such as Castor in the early larval T2NBs (Ren et al., 2017; Syed et al., 2017). (B) Schematic of central complex (CX) neuropils of the adult brain relevant to this study. PB, protocerebral bridge; EB, ellipsoid body; NO, noduli. (C-E) EdU labeling shows nearly all E-PG neurons are being generated prior to 36h ALH (EdU-positive) (C-C') but are post-mitotic (EdU-negative) by 60h ALH (D-D'). Similar results are seen for P-EN neurons (Dillon et al., 2024). (E) Quantification. Each dot represents one adult brain. Lines connected at mean for each timepoint. For each timepoint, n = 4-11 brains. In all images, LexA+ neurons driving membrane-bound GFP are in green and outlined in yellow; solid line indicates positive for EdU, dashed line indicates negative for EdU. All scale bars: 5 μm.

T2NB lineages generate the majority of the adult *Drosophila* central complex (CX) with connectomes showing this region of the central brain to contain hundreds of morphologically distinct neuron subtypes (Franconville et al., 2018; Hulse et al., 2021). One group of CX neurons of interest have been the columnar neurons, which form neural circuits responsible for locomotion and spatial navigation (Giraldo et al., 2018; Green et al., 2017; Green et al., 2019; Turner-Evans et al., 2020). Columnar neurons are characterized by their axonal and dendritic projections into CX neuropils (Fig. 4.1B). For example, in this study we focused on E-PG neurons that send dendrites to the ellipsoid body (EB) and axons to the protocerebral bridge (PB) and gall; and P-EN neurons that

send dendrites to the PB and axons to the EB and noduli (NO) (Wolff and Rubin, 2018; Wolff et al., 2015). Notably, the E-PG and P-EN neurons are within the same navigational circuit (Green et al., 2017; Green et al., 2019). Understanding the development of these neurons may shed light on how NB lineages generate complex behavioral circuits.

In this study, we show that Castor is a TTF in Type 2 (T2) lineages that specify early born CX neuronal identity. We find that E-PG neurons are born in an early T2NB window and have molecularly distinct markers that distinguish their identity from another group of early born neurons, the P-EN neurons. We find that Svp is required to restrict the generation of E-PG and P-EN neurons (this work and (Dillon et al., 2024)). We define the expression of the candidate TTF Castor in T2NBs to be transiently expressed in T2 lineages. We use T2NB lineage-specific manipulations of Castor during larval development to perform CRISPR/Cas9 knockouts of *castor* or ectopically extend the temporal expression of Castor in T2NBs to assay the impacts on adult CX neuron identities. We show that Castor is required to specify the early born E-PG and P-EN neuron identities. Additionally, we show Castor is sufficient to produce extra adult P-EN neurons but not E-PG neurons. This is the first study to identify a T2NB lineage TTF, Castor, expressed in a narrow T2NB temporal window that subdivides the previously known broad RNA-binding protein gradients, and to show it is necessary and sufficient to temporally specify columnar neurons in the adult CX.

Results

E-PG neurons are born early in Type 2 neuroblast lineages

We previously birth dated the columnar subtype of P-EN neurons to the early temporal window in the T2NB lineages (Dillon et al., 2024) and derived from young INPs (Sullivan et al., 2019). To identify additional early born neurons, we performed our 5-ethynyl-2′-deoxyuridine (EdU) drop out birth dating to find an additional early born columnar identity. We found that E-PG (R60D05-LexA) neurons become postmitotic, thus do not incorporate EdU, between 36 h and 60 h ALH (after larval hatching, Fig. 4.1C-E). We utilized cell cycle data for T2NBs, INPs and ganglion mother cells to determine the time from E-PG terminal division to birth from the parental T2NB (Bello et

al., 2008; Bowman et al., 2008; Homem et al., 2013). E-PG neurons are derived from old INPs (Sullivan et al., 2019), which divide every 2 h for 4-6 divisions (Bello et al., 2008; Bowman et al., 2008) and are birthed from the parental T2NB 12 h before producing neurons (Homem et al., 2013); thus, neurons born from old INPs are derived from the parental T2NB 16-18 h prior to terminal division. We conclude that E-PG neurons are born from T2NBs between 20 h and 44 h ALH; this is similar to previous birth dating approaches for E-PG neurons (Sullivan et al., 2019) and is during the Castor expression window in T2NBs (Ren et al., 2017; Syed et al., 2017).

E-PG and P-EN neurons have distinct molecular identities

Here, we focus on the E-PG and P-EN neurons as both are generated early from the same T2NBs but in different INP lineages (Dillon et al., 2024; Sullivan et al., 2019; Yang et al., 2013). Previous work has shown that P-EN neurons have a distinct molecular identity based on the expression of R12D09-LexA (Wolff et al., 2015) and the transcription factors Cut (Dillon et al., 2024; Epiney et al., 2023) and Runt (Sullivan et al., 2019). In contrast, E-PG neurons express the R60D05-LexA (Wolff et al., 2015) and the transcription factor Toy (Sullivan et al., 2019). To determine additional markers to distinguish E-PG neurons, we used a single-cell RNA-sequencing atlas of adult T2NB-derived neurons to identify markers that distinguish E-PG and P-EN neurons (Epiney et al., 2023). We found the transcription factor Dac was expressed in adult E-PG neurons (Fig. 4.2A-A'', C) but not in adult P-EN neurons (Fig. 4.2B-B'', C). We conclude that E-PG and P-EN neurons have multiple markers that distinguish their molecular identities (Fig. 4.2D). We use these markers in subsequent analyses as readouts of neuronal identities.

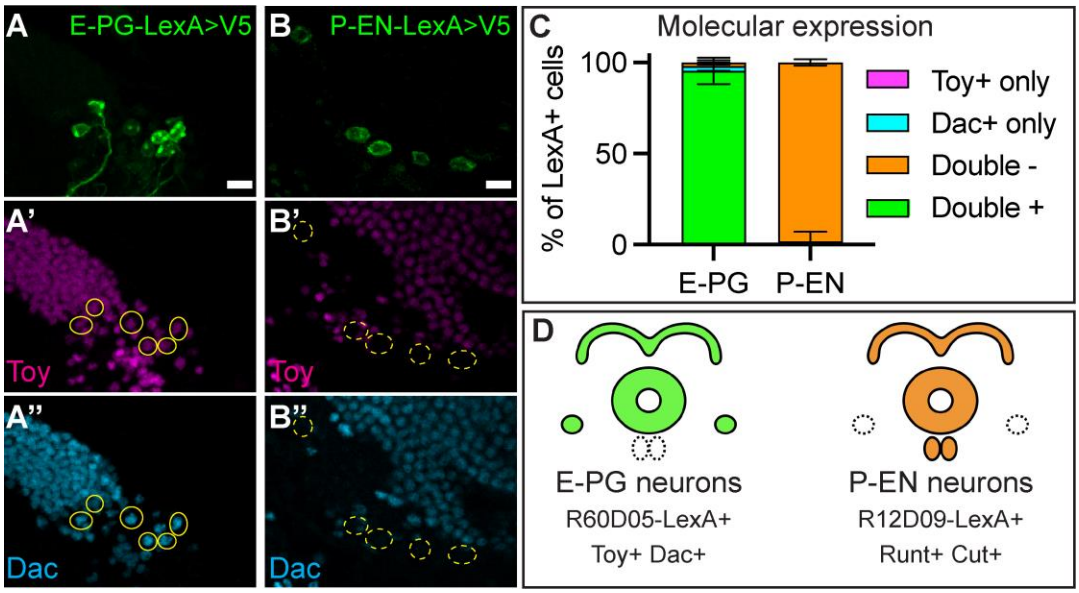

Figure 4.2. E-PG and P-EN neurons have distinct molecular identities. (A-C) Adult E-PG neurons express Toy and Dac (A-A'') whereas adult P-EN neurons do not express Toy or Dac. (B-B''). (C) Quantification. Error bars show standard error of the mean. For each genotype, *n* = 4-6 brains. (D) Summary. E-PG and P-EN are both early born from T2NBs but differ in neuropil targeting and molecular markers (Dillon et al., 2024). In all images, LexA+ neurons driving membrane-bound V5 are in green and outlined in yellow; solid line indicates double positive for markers, dashed line indicates double negative for markers; Toy, magenta; Dac, cyan. All scale bars: 5 μm.

Seven-up is required to restrict E-PG production in early Type 2 neuroblast lineages

Previous work has shown that the loss of Svp in T2NB lineages leads to the production of extra early born neuron identities, such as P-EN neurons, by extending the early temporal window (Dillon et al., 2024; Ren et al., 2017). To confirm that early temporal factors are similarly required to specify E-PG neurons, we tested if loss of Svp in the T2NBs could produce extra E-PG neurons. We used previously validated, lineage specific CRISPR/Cas9 lines (Dillon et al., 2024) to generate Svp knockouts (Svp-KO) in the T2NBs with the T2NB driver Pnt-Gal4 (Zhu et al., 2011) in combination with the R60D05-LexA driver expressing a membrane-bound V5 epitope to label adult E-PGs neurons. We found that loss of Svp leads to an expansion of E-PG neuron numbers (Fig. 4.3A-B, E). Additionally, Svp-KOs led to defective EB morphology, with an incomplete closure of the EB neuropil (Fig. 4.3A-B; Fig. S1). The ectopic E-PG neurons expressed the appropriate wildtype E-PG markers: R60D05-LexA, Toy, and Dac (Fig. 4.3C-D''', F). We conclude that Svp is required to restrict E-PG neuron production to the early T2NB

window. We hypothesize that an early TTF may be required to generate the early born E-PG and P-EN neuron identities. We subsequently focus on the candidate TTF Castor.

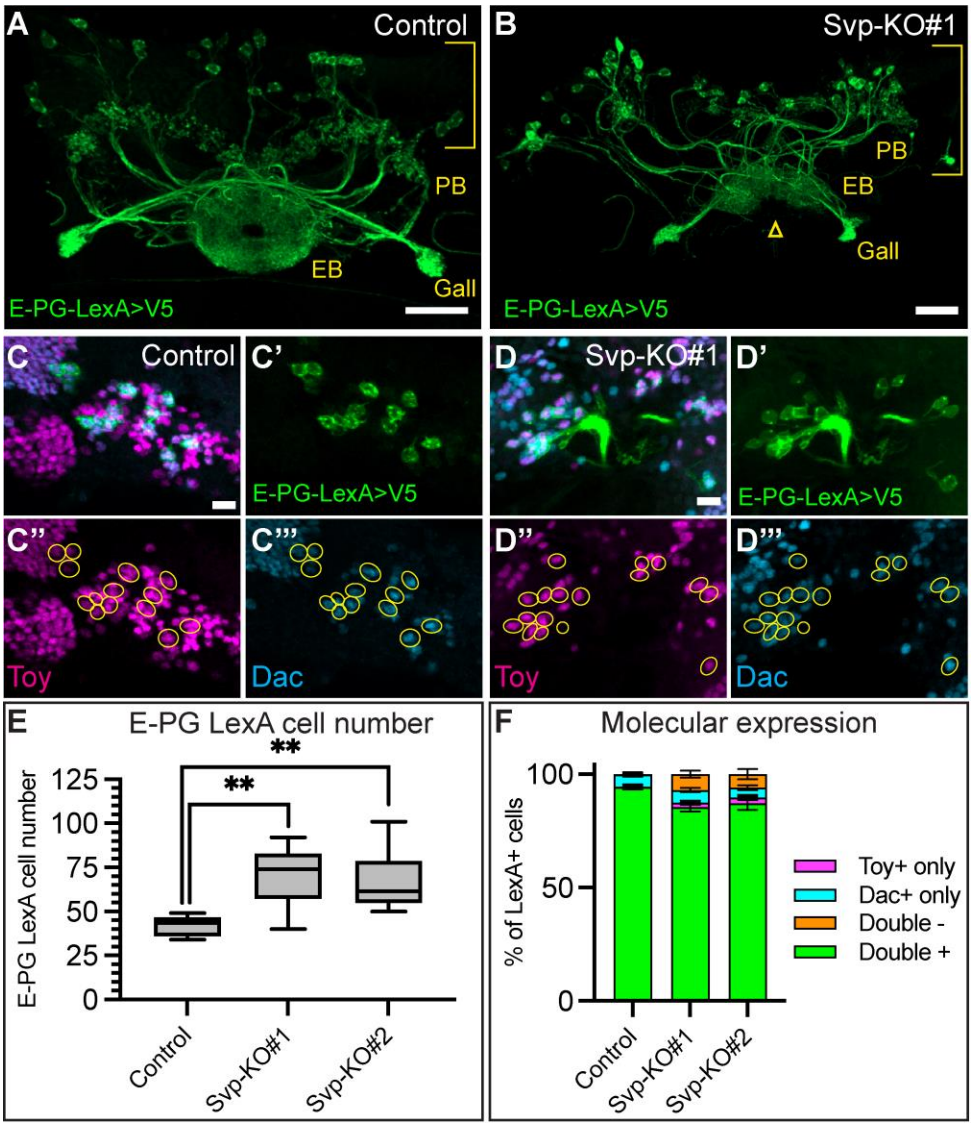

Figure 4.3 Seven-up is required to restrict E-PG production in early Type 2 neuroblast lineages. (A,B) Control (A) and Seven-up (Svp) knockout (B). There is an expansion of R60D05-LexA+ E-PG neurons in the Svp knockout. Brackets indicate cell body region; yellow text labels central complex neuropils: protocerebral bridge (PB), ellipsoid body (EB), and gall. Yellow arrowhead indicates morphological defect in the EB. (C-D) Control (C) and Svp knockout (D). Ectopic R60D05-LexA+ E-PG neurons maintain expression of molecular markers: R60D05-LexA, Toy, and Dac. (E) Quantification of LexA cell numbers from A,B. Box and whisker plots display the minimum and maximum range of the data with interquartile range. Control, *n*=16; Svp-KO#1, *n*=15; Svp-KO#2, *n*=14. *P*-values were determined using a one-way ANOVA, $^{**}P<0.001$, followed by unpaired *t*-tests between the control and Svp-KOs: Control versus Svp-KO#1, $^{**}P<0.001$; Control versus Svp-**(Fig. 4.3**

caption continued) KO#2, ***P*<0.001. (F) Quantification of the molecular expression of E-PG neurons. Error bars show standard error of the mean. *n* the same as in E. In all images, LexA+ neurons driving membrane-bound V5 are in green. Neurons outlined in yellow in C-D'''; Toy, magenta; Dac, cyan. Scale bars: 20 μm in A-B; 5 μm in C-D'''.

Castor expression is transient in the Type 2 larval neuroblast lineages

The early expression window of Castor in larval T2NBs makes it an ideal candidate as a TTF that specifies early born CX neuron identities. Before assaying neuron identity with Castor manipulations, we characterized the expression of Castor in the larval T2 lineage. We used Pnt-Gal4 to label the T2 lineage in larval stages (Zhu et al., 2011), Dpn to label NBs and INPs (NBs identified as ≥ 5 μm in diameter; INPs identified as < 5 μm) (Boone and Doe, 2008; Bowman et al., 2008), and Elav to label post-mitotic neurons (Robinow and White, 1991). We found that Castor was expressed in T2NBs only prior to 48 h ALH (Fig. 4.4A-D). INPs expressed Castor across 24-96 h ALH (Fig. 4.4E-H). T2 larval neurons expressed Castor starting at 48 h ALH with peak occurrence of Castor positive neurons at 72 h ALH before decreasing in occurrence at 96 h ALH (Fig. 4.4I-L). Castor expression was not maintained into the adult E-PG or P-EN neurons (Fig. 4.4M-O). We conclude that Castor is expressed in an early and narrow T2NB temporal window with transient expression across the larval T2 lineage and is not maintained in the adult P-EN and E-PG neurons (Fig. 4.4P). The Castor expression in T2NBs aligns with our birth dating of E-PG and P-EN neurons to the early temporal window (Fig. 4.1) (Dillon et al., 2024); thus, we focus on Castor in subsequent experiments.

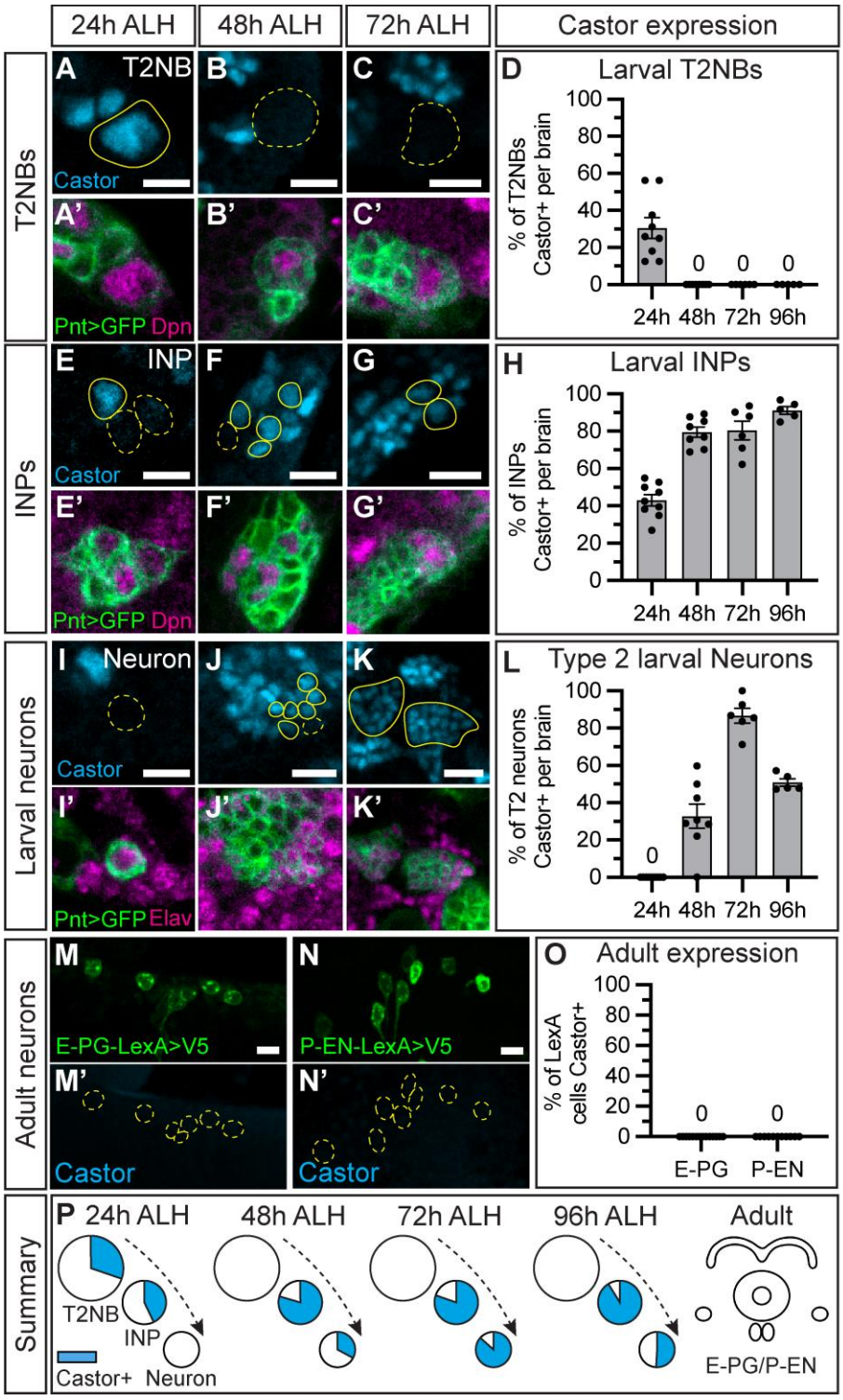

Figure 4.4. Castor expression is transient in Type 2 neuroblast lineages. (A-D) Castor expression in wild-type T2NBs at 24 h (A), 48 h (B), and 72 h ALH (C). Castor expression was seen at 24 h and at no later timepoints. (D) Quantification. Bar plot shows mean with error bars showing standard error of the mean (SEM). Each dot represents one brain. 24 h, *n*=9; 48 h, *n*=8; 72 h, *n*=7; 96 h, *n*=5. (E-H) Castor expression in wild-type INPs at 24 h (E), 48 h (F), and 72 h ALH (G). (H)

(Fig. 4.4 caption continued) Quantification. Bar plot shows mean with SEM. Each dot represents one brain. *n* the same as in D. (I-L) Castor expression in wild-type INPs at 24 h (I), 48 h (J), and 72 h ALH (K). (L) Quantification. Bar plot shows mean with SEM. Each dot represents one brain. *n* the same as in D. (M-O) Adult E-PG neurons (M-M') and adult P-EN neurons do not express Castor (N-N'). LexA neurons driving membrane-bound V5, green. (O) Quantification. Bar plot. Each dot represents one brain. E-PG, *n*=14; P-EN, *n*=11. (P) Summary of Castor expression in the larval Type 2 neuroblast lineage and adult neurons shows transient expression across time and cell types. In all images, Pnt-Gal4>GFP+ cells in green, A-K'; LexA+ neurons in green M-N'; cells outlined in yellow; solid line indicates positive for Castor, dashed line indicates negative for Castor; Dpn or Elav, magenta; Castor, cyan. All scale bars: 5 μm.

Generating Type 2 lineage specific Castor knockout and misexpression lines

To test if Castor is required and/or sufficient to specify CX neuron identities, we validated a Castor knockout (Castor-KO) line and two UAS-Castor misexpression (Castor ME) lines expressed with the Pnt-Gal4 driver. We generated a Castor-KO specific to the T2NB lineages. We used a CRISPR/Cas9 line (Port et al., 2020) with two Castor-specific sgRNAs to knockout *castor* in T2NBs. Similar to our previously reported Svp-KO lines (Dillon et al., 2024), we found that Castor-KO effectively knocks out *castor* in the majority of T2NBs by 24 h ALH, when the P-EN and E-PG neurons are first being born, with a few escaper T2NBs that show wild-type expression of Castor (Fig. 4.S2A-C). We found two Castor misexpression lines (Castor-ME) (Kambadur et al., 1998) that ectopically extend Castor expression into 48 h ALH T2NBs (Fig. 4.S2D-F). We conclude that these Castor-KO and Castor-ME lines are sufficient to test the role of Castor in specifying adult CX neuron identities.

To determine if Castor and Svp cross-regulate in the larval T2NB lineage, we used our Castor-KO and Svp-KO lines to assay the resulting expression of each temporal factor within the T2NB lineages. We found that Castor-KO did not disrupt the expression of Svp in 24 h ALH T2NBs (Fig. 4.S3A-C). Additionally, we found that Svp-KO did not result in prolonged expression of Castor in T2NBs at 48 h ALH (Fig. 4.S3D-F). These data support previous findings that Castor and Svp are not cross regulatory in the larval T2NBs (Ren et al., 2017; Syed et al., 2017).

Castor is required to specify early born P-EN and E-PG adult neuron molecular identities

To determine if Castor is required as a TTF to specify early born neuron identities, we expressed Castor-KO in larval T2NB lineages and assayed P-EN and E-PG neuron identities in the adult. We found that a loss of Castor led to a loss of R12D09-LexA P-EN neurons (Fig. 4.5A-C). Additionally, Castor-KO led to a loss of the molecular markers Runt and Cut in the remaining P-EN neurons (Fig. 4.5D-F). We found similar phenotypes in E-PG neurons with Castor-KO resulting in a loss of R60D05-LexA E-PG neurons (Fig. 4.5G-I). Furthermore, Castor-KO showed a loss of the E-PG molecular markers Toy and Dac in the remaining E-PG neurons (Fig. 4.5J-L). We conclude that Castor is required for specifying the molecular identities of the adult P-EN and E-PG neurons.

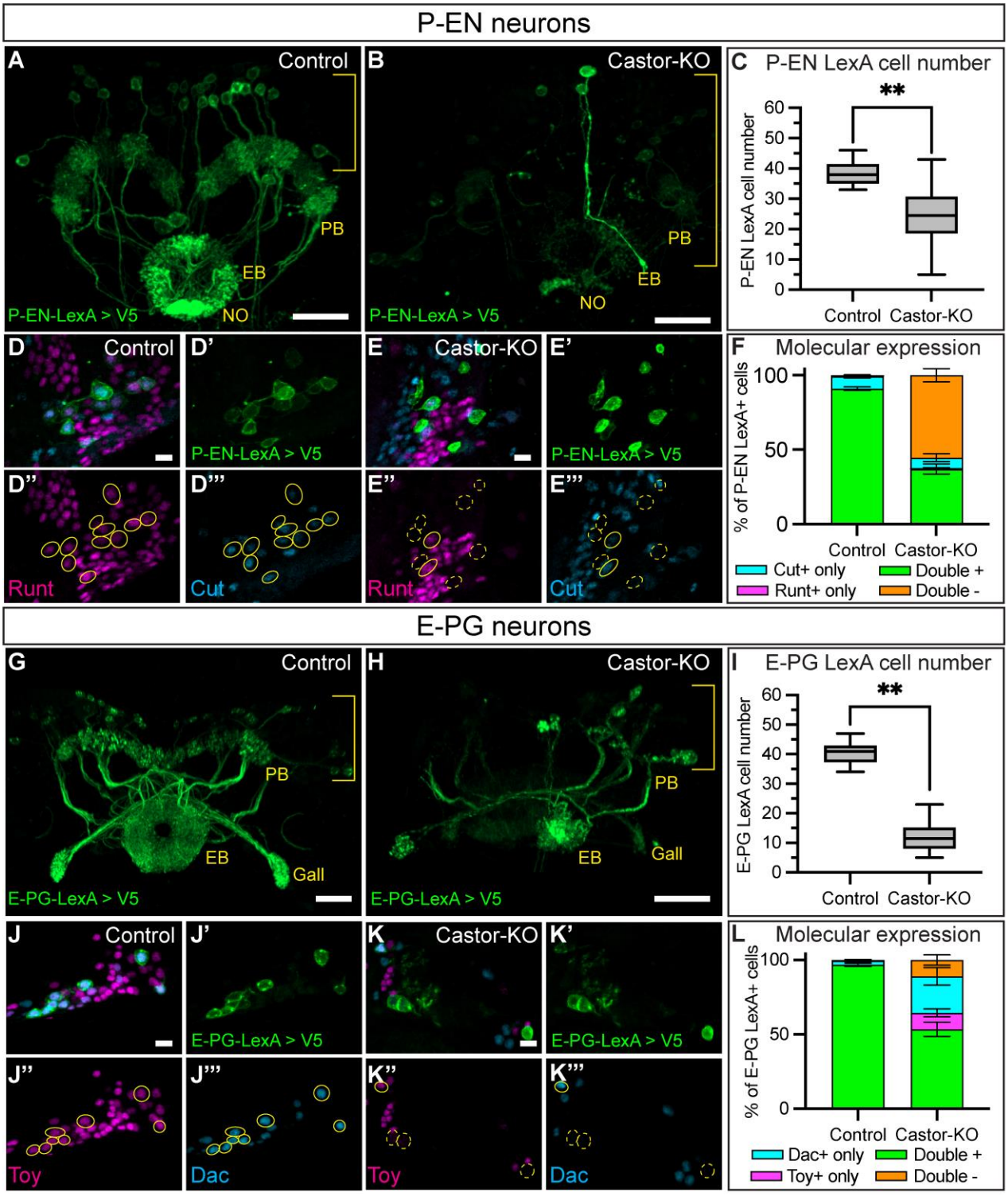

Figure 4.5 Castor is required to specify early born P-EN and E-PG adult neuron molecular identities. (A-C) Control (A) and Castor knockout (B) show a loss of R12D09-LexA+ P-EN neurons in the Castor knockout. Brackets indicate cell body region; yellow text labels central complex neuropils: protocerebral bridge (PB), ellipsoid body (EB), and noduli (NO). (C) Quantification. Box and whisker plots display the minimum and maximum range of the data with interquartile range.

(Fig. 4.5 caption continued) Control, *n*=17; Castor-KO, *n*=16. *P*-value was determined using an unpaired *t*-test, ***P*<0.001. (D-F) Control (D-D’’’) and Castor knockout (E-E’’’) show a loss of P-EN molecular markers with the loss of Castor. (F) Quantification. Bar plot shows mean with error bars showing standard error of the mean (SEM). *n* the same as in C. (G-I) Control (G) and Castor knockout (H). R60D05-LexA+ E-PG neurons are reduced in the Castor knockout. Brackets indicate cell body region; yellow text labels central complex neuropils: protocerebral bridge (PB), ellipsoid body (EB), and gall. (I) Quantification. Box and whisker plots display the minimum and maximum range of the data with interquartile range. Control, *n*=16; Castor-KO, *n*=18. *P*-value was determined using an unpaired *t*-test, ***P*<0.001. (J-L) Control (J-J’’’) and Castor knockout (K-K’’’) show a loss of E-PG molecular markers with the loss of Castor. (L) Quantification. Bar plot shows mean with SEM. *n* the same as in I. In all images, LexA+ neurons driving membrane-bound V5 are in green and outlined in yellow; solid line indicates double positive for markers, dashed line indicates not double positive for markers, Runt or Toy, magenta; Cut or Dac, cyan. Scale bars: 20 μm in A-B,G-H; 5 μm in D-E’’’, J-K’’’.

Castor is sufficient to produce ectopic adult P-EN neurons but not E-PG neurons

To determine if Castor is sufficient to produce ectopic early born identities, we used our two Castor-ME lines in the T2NB lineage and assayed for adult P-EN and E-PG neurons. We found that Castor-ME led to an increase in R12D09-LexA P-EN neuron number (Fig. 4.6A-C). Additionally, these ectopic P-EN neurons maintained wild-type expression of the P-EN markers Runt and Cut (Fig. 4.6D-F). We found no noticeable phenotype with Castor-ME in R60D05-LexA E-PG neurons with no change in neuron number (Fig. 4.6G-I) or molecular expression (Fig. 4.6J-L). We conclude that Castor is sufficient to produce ectopic adult P-EN neurons but not E-PG neurons.

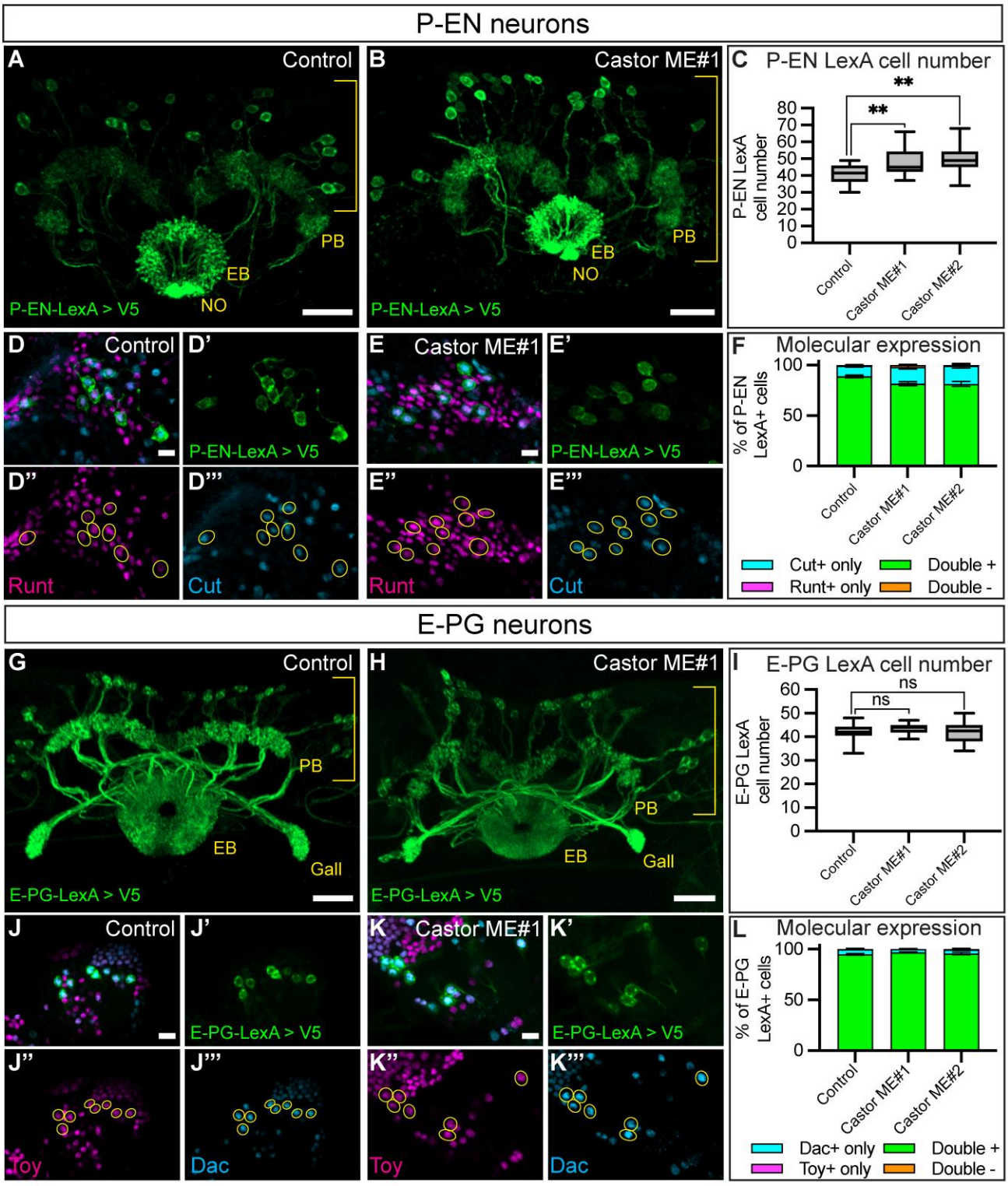

Figure 4.6 Castor is sufficient to produce ectopic adult P-EN neurons but not EPG neurons. (A-C) Control (A) and Castor misexpression (B) show a gain of R12D09-LexA+ P-EN neurons in the Castor misexpression (ME). Brackets indicate cell body region; yellow text labels central complex neuropils: protocerebral bridge (PB), ellipsoid body (EB), and noduli (NO). (C) Quantification. Box and whisker

(Fig. 4.6 caption continued) plots display the minimum and maximum range of the data with interquartile range. Control, *n*=16; Castor ME#1, *n*=16; Castor ME#2, *n*=18. *P*-values were determined using a one-way ANOVA, ***P*=0.005, followed by unpaired *t*-tests between the control and Castor misexpressions: Control versus Castor ME#1, ***P*=0.009; Control versus Castor ME#2, ***P*=0.002. (D-F) Control (D-D'') and Castor ME#1 (E-E'') shows a maintenance of P-EN molecular markers with the misexpression of Castor. (F) Quantification. Bar plot shows mean with standard error of the mean (SEM). *n* the same as in C. (G-I) Control (G) and Castor misexpression (H). R60D05-LexA+ E-PG neurons are unchanged in Castor ME. Brackets indicate cell body region; yellow text labels central complex neuropils: protocerebral bridge (PB), ellipsoid body (EB), and gall. (I) Quantification. Box and whisker plots display the minimum and maximum range of the data with interquartile range. Control, *n*=18; Castor ME#1, *n*=18; Castor-ME#2, *n*=18. *P*-value was determined using a one-way ANOVA, *P*=0.33. (J-L) Control (J-J'') and Castor-ME#1 (K-K'') show a no change in E-PG molecular markers with Castor-ME. (L) Quantification. Bar plot shows mean with SEM. *n* the same as in I. In all images, LexA+ neurons driving membrane-bound V5 are in green and outlined in yellow; Runt or Toy, magenta; Cut or Dac, cyan. Scale bars: 20 μm in A-B,G-H; 5 μm in D-E'', J-K''.

Discussion

Castor expression in larval Type 2 neuroblast lineages

We report a characterization of Castor across larval development and in most stages of the T2 lineage (NB, INP, and neurons). Previous work has only reported the T2NB expression window of Castor (Bayraktar and Doe, 2013; Ren et al., 2017; Syed et al., 2017). We confirmed previous findings that Castor expression in T2NBs is restricted to the early temporal window (Fig. 4.4A-D) (Bayraktar and Doe, 2013; Ren et al., 2017; Syed et al., 2017). We show that Castor is expressed outside of T2NBs in INPs and postmitotic larval neurons at later stages (Fig. 4.4E-H). Notably, the adult E-PG and P-EN neurons do not express Castor (Fig. 4.4M-O). These data are consistent with a TTF pattern of transient expression within a narrow temporal window in the parental NB, and inheritance of expression by progeny cells, as seen for embryonic TTFs (Cleary and Doe, 2006; Grosskortenhaus et al., 2006; Isshiki et al., 2001; Meng et al., 2019; Meng et al., 2020; Moris-Sanz et al., 2015; Novotny et al., 2002; Pearson and Doe, 2003; Seroka and Doe, 2019; Tran and Doe, 2008). This indicates that Castor may play a role in specifying identities but is not required to maintain neuron identity. Determining Castor target genes in these transient stages remains an unanswered question. Future work is needed to identify the DNA-binding targets of Castor.

Castor is a narrowly expressed early temporal transcription factor in larval Type 2 lineages

It remains an open question of how T2NBs generate diverse, birth order-dependent identities. The two hypotheses are that the lineage could use: (1) broad temporal gradients of protein expression similar to mushroom body neurons (Liu et al., 2015); or (2) a TTF cascade similar to the embryonic NB lineages (Cleary and Doe, 2006; Grosskortenhaus et al., 2006; Isshiki et al., 2001; Meng et al., 2019; Meng et al., 2020; Moris-Sanz et al., 2015; Novotny et al., 2002; Pearson and Doe, 2003; Seroka and Doe, 2019; Tran and Doe, 2008). Here, we show that Castor acts as an early TTF in the larval T2NB lineage for specifying early-born neuron identities (Fig. 4.5; Fig. 4.6). Additionally, previous work has shown that Castor and the switching factor Svp act upstream of these protein gradients (Ren et al., 2017). Recent work has also shown that these broadly expressed protein gradients are required for proper CX neuron specification in both T2NBs and INPs (Hamid et al., 2024; Munroe and Doe, 2023). These data are consistent with a model that the T2NB lineage is patterned by both briefly expressed TTFs and lengthy gradients of RNA-binding proteins (Fig. 4.1A). In the future, it will be important to determine whether other TTFs exist in T2NBs and how these temporal patterning genes are regulated.

One hallmark of TTFs have been their ability to form cross regulatory TTF cascades as seen in the embryonic lineages (Cleary and Doe, 2006; Grosskortenhaus et al., 2006; Isshiki et al., 2001; Meng et al., 2019; Meng et al., 2020; Moris-Sanz et al., 2015; Novotny et al., 2002; Pearson and Doe, 2003; Seroka and Doe, 2019; Tran and Doe, 2008). We, and others, report that Castor and Svp do not cross regulate in the larval T2NBs (Fig. 4.S3) (Ren et al., 2017; Syed et al., 2017). This raises an open question of whether T2NBs use a TTF cascade or another mechanism of patterning to regulate temporal progression. Additional TTFs will need to be identified to test these hypotheses.

We show that Castor is required for the early born P-EN and E-PG adult neurons (Fig. 4.5); conversely, we show that Castor is sufficient to produce additional adult P-EN

neurons, but not E-PG neurons (Fig. 4.6). These data, along with Castor's early expression window, are consistent with Castor acting as an early TTF in the T2NB lineage. Interestingly, loss of Svp does not extend the Castor window (Fig. 4.S3) (Ren et al., 2017; Syed et al., 2017) but does extend the production of early born neuron identities (Fig. 3) (Dillon et al., 2024). This could be due to a difference in the INP window in which P-EN and E-PG neurons are born (young vs old). Alternatively, additional early factors may be required for specifying fates and could explain the lack of Castor sufficiency to produce additional E-PG neurons. Future work should aim to determine additional molecular mechanisms for specifying these CX neuron identities.

Columnar neurons born in the same Type 2 neuroblast window have distinct adult molecular identities

This work and previous work have shown that columnar neurons express distinct molecular markers that differentiate their identities (Dillon et al., 2024; Epiney et al., 2023; Sullivan et al., 2019). We show that E-PG and P-EN neurons are born within the same T2NB early window but have distinct molecular identities (Fig. 4.1C-E; Fig. 4.2) (Dillon et al., 2024). Interestingly, previous work has shown that columnar neurons born in the same INP windows share common markers: for example, young INP derived P-EN and P-FN neurons express Runt while old INP derived E-PG and PF-R neurons express Toy, even when these fates are born in different NB windows (Sullivan et al., 2019; Dillon et al., 2024). It remains an open question whether columnar neurons born in the same NB window share common molecular markers specified within the T2NB regardless of their INP birth window.

Conserved role of Castor in vertebrate neurogenesis

Our work shows that Castor acts as a TTF in the early larval T2NBs. Previous work has shown Castor is a late TTF in embryonic NB lineages (Grosskortenhaus et al., 2006; Tran and Doe, 2008), although it has not been identified as a TTF in optic lobe NB lineages (El-Danaf et al., 2023). The mammalian ortholog of *castor*, *Casz1*, has been shown in mammalian models of the mouse retina and dorsal root ganglion to be temporally expressed in progenitors to control the generation of neuronal subtypes (Mattar et al.,

2015; Mattar et al., 2018; Mattar et al., 2021; Monteiro et al., 2016). Furthermore, Casz1 has been shown in retinal progenitor cells to be regulated by Ikzf1 (Mattar et al., 2015), an ortholog of the *Drosophila* TTF Hunchback in embryonic NB lineages (Cleary and Doe, 2006; Grosskortenhaus et al., 2006; Isshiki et al., 2001; Meng et al., 2019; Meng et al., 2020; Moris-Sanz et al., 2015; Novotny et al., 2002; Pearson and Doe, 2003; Seroka and Doe, 2019; Tran and Doe, 2008). These findings suggest that Castor has a conserved role as a temporal patterning gene from fly to mammals (Frith et al., 2024; Liu et al., 2023; Sagner and Briscoe, 2019).

Materials and Methods

Animal Preparation

Drosophila melanogaster was used in all experiments. All flies were kept and maintained at 25°C unless stated otherwise. Stocks used can be found in Table. 4.S1 and experimental genetic crosses in Table. 4.S2 (See Appendix B for supplementary tables).

EdU experiment

EDU (5-ethynyl-2′-deoxyuridine; Millipore-Sigma, 900584-50MG) was used to label proliferating cells starting at various sequential larval ages. Larvae were fed food containing 20 μg/ml EdU nonstop from the initial age feeding started until pupation. Larvae fed on EdU were raised at temperatures between 18°C and 21°C until adults hatched and were dissected.

Larval experiments

Embryos were collected on 3% agar apple juice caps with yeast paste for 4 hours and aged for the equivalent time after larval hatching (ALH). Hatched larvae were collected and dissected.

Adult experiments

Males and virgin females were introduced in standard yeast medium vials and flipped every two days. 2-5 day old adult flies were dissected for all experiments unless stated

otherwise. All animals dissected were a mixture of male and female unless otherwise specified.

Immunohistochemistry

Antibodies used with supporting notes can found in Table. 4.S3 (See Appendix B for supplementary tables).

Larval brain sample preparation

Larval brains were dissected in PBS and mounted on poly-L-lysine coated coverslips (Corning BioCoat 354085). Samples fixed for 23 minutes in 4% PFA in PBST. Samples were washed in PBST and blocked with 2% normal donkey serum (Jackson ImmunoResearch Laboratories, Inc. 017-000-121) in PBST. Samples incubated in a primary antibody mix diluted in PBST at room temperature for 4 h or at 4°C overnight. Primary antibodies were removed, and samples thoroughly washed with PBST. Samples were incubated in secondary antibodies at room temperature for 4 h or overnight at 4°C. Secondary antibodies were removed, and samples washed in PBST. Samples were dehydrated with an ethanol series of 30%, 50%, 75%, and 100% ethanol then incubated in xylene (Fisher Chemical X5-1) for 2x10 minutes. Samples were mounted onto slides with DPX (Sigma-Aldrich 06552) and cured for 3-4 days then stored at 4°C until imaged.

Adult brain sample preparation

Adult brains were prepared similar to larval brains with the exception of 38 minutes for fixation in 4% PFA and 2x12 minute xylene incubations.

EdU adult brain sample preparation

Adult brains from EdU-fed larvae were dissected in HL3.1 then fixed in 4% PFA for 30 min and incubated in block at 4°C overnight. Samples were incubated in primary and secondary mixes before Click-it-Reaction to label EdU. The Click-it-Reaction mix comprised PBS, Copper II sulfate (ThermoFisher, 033308.22), 555-Azide (ThermoFisher, A20012) in DSMO and ascorbic acid (Sigma-Aldrich, A4544-25G) for a 2h incubation.

Samples were dehydrated and washed in xylene before DPX mounting as described above.

Confocal Microscopy

Fixed preparations were imaged with a Zeiss LSM 900 laser scanning confocal (Carl Zeiss AG, Oberkochen, Germany) equipped with an Axio Imager.Z2 microscope. A 10x/0.3 EC Plan-Neofluar M27 or 40x/1.40 NA Oil Plan-Apochromat DIC M27 objective lens were used. Software program used was Zen 3.6 (blue edition) (Carl Zeiss AG, Oberkochen, Germany).

Image processing and analysis

Figure preparation

Images in figures were prepared either in Imaris 10.0.1 or FIJI. Scale bars are given for a single slice in all single slice images and from all stacks within maximum intensity projections images. Pixel brightness was adjusted in images for clearer visualization; all adjustments were made uniformly over the entire image, and uniformly across wild-type samples and corresponding control and experimental samples. Adobe Illustrator 2024 (Adobe, Mountain View, CA) was used for figure formatting.

Statistical analyses

Statistics were computed using Prism 10 (GraphPad Software, Boston, MA). All statistical tests used are listed in the figure legends. *P*-values are reported in the figure legends. Plots display ns=not significant with $P>0.05$, *$P<0.05$, **$P<0.01$. Plots were generated using Prism with standard error of the mean bars shown and box and whisker plots display the minimum and maximum range of the data with interquartile range.

Supplementary information

Supplementary information can be found in Appendix B (Figures and Tables) or the online (Supplemental Table 4) version of this work at https://www.biorxiv.org/content/10.1101/2024.08.22.609207v1.

Data availability

All relevant data can be found within the article and its supplementary information.

Bridge

The previous chapter covered work that showed that the temporal progression of T2NB is required for specifying CX neuron identities. In this chapter, I showed that the early factor Castor acts as a TTF to specify the early born CX neuron identities. I showed that 1) E-PG neurons are from early larval T2NBs, the same as the P-EN neurons; 2) Castor is transiently expressed in the T2NBs when both E-PG and P-EN neurons are born; 3) Castor is required for specifying the early born E-PG and P-EN neurons. This demonstrates TTFs, narrow expression windows of transient factors, could be a mechanisms of temporal patterning in larval T2NBs. It remains to be seen if other TTFs exist in the lineage. The next chapter, Chapter V, will be a discussion on future direction inspired by the work presented in Chapters II, III, and IV. I will also cover how neurogenesis in *Drosophila* is similar and different to that of mammals.

References

Alsio, J. M., Tarchini, B., Cayouette, M. and Livesey, F. J. (2013). Ikaros promotes early-born neuronal fates in the cerebral cortex. *Proc. Natl. Acad. Sci. U. S. A.* 110, E716-25.

Andrade, I. V., Riebli, N., Nguyen, B.-C. M., Omoto, J. J., Cardona, A. and Hartenstein, V. (2019). Developmentally Arrested Precursors of Pontine Neurons Establish an Embryonic Blueprint of the Drosophila Central Complex. *Curr. Biol. CB* 29, 412-425.e3.

Bayraktar, O. A. and Doe, C. Q. (2013). Combinatorial temporal patterning in progenitors expands neural diversity. *Nature* 498, 445–455.

Bello, B. C., Izergina, N., Caussinus, E. and Reichert, H. (2008). Amplification of neural stem cell proliferation by intermediate progenitor cells in Drosophila brain development. *Neural Dev* 3, 5.

Boone, J. Q. and Doe, C. Q. (2008). Identification of Drosophila type II neuroblast lineages containing transit amplifying ganglion mother cells. *Dev Neurobiol* 68, 1185–95.

Bowman, S. K., Rolland, V., Betschinger, J., Kinsey, K. A., Emery, G. and Knoblich, J. A. (2008). The tumor suppressors Brat and Numb regulate transit-amplifying neuroblast lineages in Drosophila. *Dev Cell* 14, 535–46.

Clark, B. S., Stein-O'Brien, G. L., Shiau, F., Cannon, G. H., Davis-Marcisak, E., Sherman, T., Santiago, C. P., Hoang, T. V., Rajaii, F., James-Esposito, R. E., et al. (2019). Single-Cell RNA-Seq Analysis of Retinal Development Identifies NFI Factors as Regulating Mitotic Exit and Late-Born Cell Specification. *Neuron* 102, 1111-1126.e5.

Cleary, M. D. and Doe, C. Q. (2006). Regulation of neuroblast competence: multiple temporal identity factors specify distinct neuronal fates within a single early competence window. *Genes Dev* 20, 429–34.

Dillon, N. R., Manning, L., Hirono, K. and Doe, C. Q. (2024). Seven-up acts in neuroblasts to specify adult central complex neuron identity and initiate neuroblast decommissioning. *Dev. Camb. Engl.* 151, dev202504.

Doe, C. Q. (2017). Temporal Patterning in the Drosophila CNS. *Annu Rev Cell Dev Biol* 33, 219–240.

El-Danaf, R. N., Rajesh, R. and Desplan, C. (2023). Temporal regulation of neural diversity in Drosophila and vertebrates. *Semin. Cell Dev. Biol.* 142, 13–22.

Elliott, J., Jolicoeur, C., Ramamurthy, V. and Cayouette, M. (2008). Ikaros confers early temporal competence to mouse retinal progenitor cells. *Neuron* 60, 26–39.

Epiney, D., Chaya, G. M., Dillon, N., Lai, S.-L. and Doe, C. (2023). Transcriptional complexity in the insect central complex: single nuclei RNA sequencing of adult brain neurons derived from type 2 neuroblasts. 2023.12.10.571022.

Franconville, R., Beron, C. and Jayaraman, V. (2018). Building a functional connectome of the Drosophila central complex. *eLife* 7, e37017.

Frith, T. J. R., Briscoe, J. and Boezio, G. L. M. (2024). From signalling to form: the coordination of neural tube patterning. *Curr. Top. Dev. Biol.* 159, 168–231.

Giraldo, Y. M., Leitch, K. J., Ros, I. G., Warren, T. L., Weir, P. T. and Dickinson, M. H. (2018). Sun Navigation Requires Compass Neurons in Drosophila. *Curr. Biol. CB* 28, 2845-2852.e4.

Green, J., Adachi, A., Shah, K. K., Hirokawa, J. D., Magani, P. S. and Maimon, G. (2017). A neural circuit architecture for angular integration in Drosophila. *Nature* 546, 101–106.

Green, J., Vijayan, V., Mussells Pires, P., Adachi, A. and Maimon, G. (2019). A neural heading estimate is compared with an internal goal to guide oriented navigation. *Nat. Neurosci.* 22, 1460–1468.

Grosskortenhaus, R., Pearson, B. J., Marusich, A. and Doe, C. Q. (2005). Regulation of temporal identity transitions in Drosophila neuroblasts. *Dev Cell* 8, 193–202.

Grosskortenhaus, R., Robinson, K. J. and Doe, C. Q. (2006). Pdm and Castor specify late-born motor neuron identity in the NB7-1 lineage. *Genes Dev* 20, 2618–27.

Hamid, A., Gattuso, H., Caglar, A. N., Pillai, M., Steele, T., Gonzalez, A., Nagel, K. and Syed, M. H. (2024). The conserved RNA-binding protein Imp is required for the specification and function of olfactory navigation circuitry in Drosophila. *Curr. Biol. CB* 34, 473-488.e6.

Holguera, I. and Desplan, C. (2018). Neuronal specification in space and time. *Science* 362, 176–180.

Homem, C. C., Reichardt, I., Berger, C., Lendl, T. and Knoblich, J. A. (2013). Long-term live cell imaging and automated 4D analysis of drosophila neuroblast lineages. *PLoS One* 8, e79588.

Hulse, B. K., Haberkern, H., Franconville, R., Turner-Evans, D., Takemura, S., Wolff, T., Noorman, M., Dreher, M., Dan, C., Parekh, R., et al. (2021). A connectome of the Drosophila central complex reveals network motifs suitable for flexible navigation and context-dependent action selection. *eLife* 10, e66039.

Isshiki, T., Pearson, B., Holbrook, S. and Doe, C. Q. (2001). Drosophila neuroblasts sequentially express transcription factors which specify the temporal identity of their neuronal progeny. *Cell* 106, 511–21.

Javed, A., Mattar, P., Lu, S., Kruczek, K., Kloc, M., Gonzalez-Cordero, A., Bremner, R., Ali, R. R. and Cayouette, M. (2020). Pou2f1 and Pou2f2 cooperate to control the timing of cone photoreceptor production in the developing mouse retina. *Dev. Camb. Engl.* 147, dev188730.

Kambadur, R., Koizumi, K., Stivers, C., Nagle, J., Poole, S. J. and Odenwald, W. F. (1998). Regulation of POU genes by castor and hunchback establishes layered compartments in the Drosophila CNS. *Genes Dev* 12, 246–60.

Liu, Z., Yang, C. P., Sugino, K., Fu, C. C., Liu, L. Y., Yao, X., Lee, L. P. and Lee, T. (2015). Opposing intrinsic temporal gradients guide neural stem cell production of varied neuronal fates. *Science* 350, 317–20.

Liu, S., Liu, X., Li, S., Huang, X., Qian, H., Jin, K. and Xiang, M. (2020). Foxn4 is a temporal identity factor conferring mid/late-early retinal competence and involved in retinal synaptogenesis. *Proc. Natl. Acad. Sci. U. S. A.* 117, 5016–5027.

Liu, T., Li, T. and Ke, S. (2023). Role of the CASZ1 transcription factor in tissue development and disease. *Eur. J. Med. Res.* 28, 562.

Mattar, P. and Cayouette, M. (2015). Mechanisms of temporal identity regulation in mouse retinal progenitor cells. *Neurogenesis Austin Tex* 2, e1125409.

Mattar, P., Ericson, J., Blackshaw, S. and Cayouette, M. (2015). A conserved regulatory logic controls temporal identity in mouse neural progenitors. *Neuron* 85, 497–504.

Mattar, P., Stevanovic, M., Nad, I. and Cayouette, M. (2018). Casz1 controls higher-order nuclear organization in rod photoreceptors. *Proc. Natl. Acad. Sci. U. S. A.* 115, E7987–E7996.

Mattar, P., Jolicoeur, C., Dang, T., Shah, S., Clark, B. S. and Cayouette, M. (2021). A Casz1-NuRD complex regulates temporal identity transitions in neural progenitors. *Sci. Rep.* 11, 3858.

Meng, J. L., Marshall, Z. D., Lobb-Rabe, M. and Heckscher, E. S. (2019). How prolonged expression of Hunchback, a temporal transcription factor, re-wires locomotor circuits. *Elife* 8,.

Meng, J. L., Wang, Y., Carrillo, R. A. and Heckscher, E. (2020). Temporal transcription factors determine circuit membership by permanently altering motor neuron-to-muscle synaptic partnerships. *eLife* 9,.

Monteiro, C. B., Midão, L., Rebelo, S., Reguenga, C., Lima, D. and Monteiro, F. A. (2016). Zinc finger transcription factor Casz1 expression is regulated by homeodomain transcription factor Prrxl1 in embryonic spinal dorsal horn late-born excitatory interneurons. *Eur. J. Neurosci.* 43, 1449–1459.

Moris-Sanz, M., Estacio-Gomez, A., Sanchez-Herrero, E. and Diaz-Benjumea, F. J. (2015). The study of the Bithorax-complex genes in patterning CCAP neurons reveals a temporal control of neuronal differentiation by Abd-B. *Biol Open* 4, 1132–42.

Munroe, J. A. and Doe, C. Q. (2023). Imp is expressed in INPs and newborn neurons where it regulates neuropil targeting in the central complex. *Neural Develop.* 18, 9.

Novotny, T., Eiselt, R. and Urban, J. (2002). Hunchback is required for the specification of the early sublineage of neuroblast 7-3 in the Drosophila central nervous system. *Development* 129, 1027–36.

Pearson, B. J. and Doe, C. Q. (2003). Regulation of neuroblast competence in Drosophila. *Nature* 425, 624–8.

Pereanu, W. and Hartenstein, V. (2006). Neural lineages of the Drosophila brain: a three-dimensional digital atlas of the pattern of lineage location and projection at the late larval stage. *J. Neurosci. Off. J. Soc. Neurosci.* 26, 5534–53.

Port, F., Strein, C., Stricker, M., Rauscher, B., Heigwer, F., Zhou, J., Beyersdörffer, C., Frei, J., Hess, A., Kern, K., et al. (2020). A large-scale resource for tissue-specific CRISPR mutagenesis in Drosophila. *eLife* 9, e53865.

Ren, Q., Yang, C.-P., Liu, Z., Sugino, K., Mok, K., He, Y., Ito, M., Nern, A., Otsuna, H. and Lee, T. (2017). Stem Cell-Intrinsic, Seven-up-Triggered Temporal Factor Gradients Diversify Intermediate Neural Progenitors. *Curr. Biol. CB* 27, 1303–1313.

Riebli, N., Viktorin, G. and Reichert, H. (2013). Early-born neurons in type II neuroblast lineages establish a larval primordium and integrate into adult circuitry during central complex development in Drosophila. *Neural Dev* 8, 6.

Robinow, S. and White, K. (1991). Characterization and spatial distribution of the ELAV protein during Drosophila melanogaster development. *J Neurobiol* 22, 443–61.

Sagner, A. and Briscoe, J. (2019). Establishing neuronal diversity in the spinal cord: a time and a place. *Development* 146,.

Seroka, A. Q. and Doe, C. Q. (2019). The Hunchback temporal transcription factor determines motor neuron axon and dendrite targeting in Drosophila. *Development* 137,.

Sullivan, L. F., Warren, T. L. and Doe, C. Q. (2019). Temporal identity establishes columnar neuron morphology, connectivity, and function in a Drosophila navigation circuit. *eLife* 8,.

Syed, M. H., Mark, B. and Doe, C. Q. (2017). Steroid hormone induction of temporal gene expression in Drosophila brain neuroblasts generates neuronal and glial diversity. *Elife* 6,.

Tran, K. D. and Doe, C. Q. (2008). Pdm and Castor close successive temporal identity windows in the NB3-1 lineage. *Development* 135, 3491–9.

Turner-Evans, D. B., Jensen, K. T., Ali, S., Paterson, T., Sheridan, A., Ray, R. P., Wolff, T., Lauritzen, J. S., Rubin, G. M., Bock, D. D., et al. (2020). The Neuroanatomical Ultrastructure and Function of a Biological Ring Attractor. *Neuron* 108, 145-163.e10.

Wolff, T. and Rubin, G. M. (2018). Neuroarchitecture of the Drosophila central complex: A catalog of nodulus and asymmetrical body neurons and a revision of the protocerebral bridge catalog. *J. Comp. Neurol.* 526, 2585–2611.

Wolff, T., Iyer, N. A. and Rubin, G. M. (2015). Neuroarchitecture and neuroanatomy of the Drosophila central complex: A GAL4-based dissection of protocerebral bridge neurons and circuits. *J Comp Neurol* 523, 997–1037.

Yang, J. S., Awasaki, T., Yu, H. H., He, Y., Ding, P., Kao, J. C. and Lee, T. (2013). Diverse neuronal lineages make stereotyped contributions to the Drosophila locomotor control center, the central complex. *J Comp Neurol* 521, 2645–62.

Zhu, S., Barshow, S., Wildonger, J., Jan, L. Y. and Jan, Y. N. (2011). Ets transcription factor Pointed promotes the generation of intermediate neural progenitors in Drosophila larval brains. *Proc Natl Acad Sci U A* 108, 20615–20.

Chapter V

Discussion

Future directions in understanding neuroblast quiescence and reactivation

How is neurogenesis regulated for producing the proper number of cells at appropriate times? Understanding how stem cells initiate proliferation, enter quiescence (cell cycle arrest), and then reactivate presents an exciting direction for understanding neural development. These basic mechanisms are conserved between flies to mammals (reviewed in Homem et al., 2015). Thus, understanding reactivation in *Drosophila* may provide insight into the regenerative properties of the neural stem cells found in the adult mammalian CNS (reviewed in Ma et al., 2009). My work in *Drosophila* may be relevant for understanding neural developmental stem cell diseases like microcephaly (too few cells) and megalencephaly (too many cells). This section will discuss future directions to pursue in understanding how neuroblasts (NBs) exit quiescence and resume proliferation.

Insulin signaling and cell cycle in quiescence

Previous studies have identified extrinsic signaling pathways that lead to NB exit from quiescence. Early work found that reactivation was coupled to nutrition via signaling from the fat body in response to newly hatched larvae eating (Britton and Edgar, 1998). Subsequent studies identifed that fat body-derived mitogens induce insulin-like peptide (Ilp) release from glial cell niches to activate cell cycle progression in adjacent quiescent NBs (qNBs) (Chell and Brand, 2010; Sousa-Nunes et al., 2011; Yuan et al., 2020). My work with single-cell RNA sequencing (scRNAseq) analyses supported these findings with glial cells upregulating *ilps* during the window of reactivation and qNBs expressing high levels of *insulin-receptor* (Dillon et al., 2022). These studies provide an understanding of which extrinsic cues are required for qNBs to resume proliferation.

It remains unknown how qNBs become competent to receive and appropriately respond to extrinsic signals. This is important as there is heterogeneity in qNBs in both cell arrest state (G_0 or G_2) and time of reactivation between NB lineages (Munroe et al., 2022; Otsuki and Brand,

2018; Otsuki and Brand, 2019; Prokop and Technau, 1991; Truman and Bate, 1988) (reviewed in Otsuki and Brand, 2020). These studies suggest that the competency of qNBs to respond to extrinsic cues remains an open direction to investigate.

Recent work has revealed some intrinsic mechanisms that maintains quiescent states and re-entry into the cell cycle. Trbl, a pseudo kinase, was shown to be required for both entry into G_2 quiescence by degradation of Cdc25 and maintenance of quiescence by inhibiting Akt (Otsuki and Brand, 2018). Additionally, Dacapo, a kinase inhibitor, was identified to promote G_0 cell arrest for NB quiescence (Otsuki and Brand, 2019). This work also demonstrated that the spatial factor Msh promotes Dacapo for dorsal NBs to undergo G_0 cell arrest and that ventral NBs preferentially undergo G_2 cell arrest (Otsuki and Brand, 2019). Furthermore, G_0 NBs (dorsal) reactivate prior to G_2 NBs (ventral) (Otsuki and Brand, 2019). These studies suggest that heterogeneity in cell cycle arrest may be important for intrinsic competency to respond to reactivation cues. Future work will require identifying the cell arrest state for each NB lineage. Do lineages that wire together reactivate at the same time? Do the first NBs to reactivate generate more progeny with an extended lineage time? My scRNAseq study (Dillon et al., 2022) was unable to identify separate lineages so could not address these questions. Understanding the differences between the cell cycle arrested state of qNBs would provide insight into whether these mechanisms of reactivation regulate circuit formation and generation of neuron number.

My work demonstrated that qNBs express high levels of both positive and negative regulators of the insulin signaling pathway and cell cycle progression (see Chapter II) (Dillon et al., 2022). This suggests that qNBs are primed to receive and respond to Ilps while maintaining a non-proliferative state. One limitation of my work was an insufficiency to distinguish cell cycle arrested states of qNBs (G_0 or G_2). Thus, we were unable to analyze the heterogeneity of qNBs. Additionally, my work only showed the mRNA of qNBs in newly hatched larvae at a single timepoint. Future work will require understanding how mRNA may be regulated in different populations of qNBs. Combining proteomics with scRNAseq for several timepoints of qNBs would provide a useful dataset for understanding the post-translational regulation in qNBs.

Ongoing work has focused on the transcription factor Foxo in qNBs (see Dr. Sarah Siegrist's lab: https://siegristlab.org/research/; personal communication). My work, along with collaborators in the Siegrist lab, identified through mRNA and immunohistochemistry that Foxo is expressed in qNBs (Dillon et al., 2022). This finding was not surprising as Foxo is a regulator of the insulin signaling pathway that limits proliferation (reviewed in Nijhout, 2003). Additionally, Foxo is required in pupal NBs for terminating neurogenesis by ending NB cell cycle (Siegrist et al., 2010). Thus, it is expected for a negative regulator of proliferation to be enriched in qNBs. It would be interesting to follow up on whether Foxo expression is expressed in all qNBs or specific to G_0 or G_2 arrested qNBs. Identifying the DNA-binding targets of Foxo will be important for determining its role in qNBs.

Connecting quiescence to the temporal cascade

Early larval NBs initiate two important developmental steps: i) re-entry into the cell cycle and ii) expressing a series of transient temporal factors. This raises the question: Is reactivation and the temporal series dependent on each other? The last canonical embryonic TTF (temporal transcription factor), Grainy head (Grh), is expressed in embryonic NBs entering quiescence and persists into larval NBs (Brody and Odenwald, 2000; Prokop et al., 1998). Grh limits abdominal NB proliferation while suppressing thoracic NB proliferation in early larval stages (Almeida and Bray, 2005). This suggests that the competency to respond to Grh may differ between lineages (abdominal versus thoracic). Interestingly, Grh is sufficient to increase E-Cadherin expression, which promotes NB proliferation in glial cell niches (Almeida and Bray, 2005; Dumstrei et al., 2003). These studies provide support that NB lineages may have different mechanisms to initiate reactivation and subsequent temporal progression in response to the same intrinsic (Grh) and extrinsic (glial signaling molecules) cues. My scRNAseq work found that Grh was enriched in actively proliferating NBs compared to qNB (Dillon et al., 2022). This suggests that there may be components upstream of Grh regulating its role in qNB reactivation. Future work will require investigating the expression patterns of Grh across qNB lineages with markers for G_0 and G_2 to understand if there is an underlining pattern.

Two of the earliest larval NB temporal factors are IGF-II mRNA-binding protein (Imp) and Lin-28 (reviewed in Doe, 2017). Imp expression shows a temporal protein gradient with high levels

in early larvae and lower levels in later stages across the mushroom body and Type 2 NB lineages (Liu et al., 2015; Munroe et al., 2022; Ren et al., 2017). The early expression of Imp in Type 2 lineages promotes NB exit from quiescence (Munroe et al., 2022). Additionally, Imp levels (high versus low) are required for proper specification of adult neuron morphology (Hamid et al., 2024; Ren et al., 2017). These studies indicate that temporal factors may play a dual role in NB reactivation and specification of neuronal fates.

Lin-28 is another RNA-binding protein identified as an early factor in larval NB lineages but has yet to be functionally tested (Syed et al., 2017a). Interestingly, Lin-28 in adult *Drosophila* intestinal stem cells reactivates proliferation in response to insulin signaling and provides a hint for how it may function in larval CNS NBs (Chen et al., 2015). Does Lin-28 play a role in NB reactivation in response to Ilps? My previous work captured the known temporally dynamic expression of Imp and Lin-28 in both qNBs and early reactivated NBs (Dillon et al., 2022). Future work should identify the regulatory mechanisms of these factors in addition to functionally testing Lin28 in neuron specification. One challenge will be decoupling the role of these factors in reactivation from specification of neuronal identities.

Future directions in understanding larval neuroblast temporal progression

Larval born neurons are generated in a birth-order dependent manner (Jefferis et al., 2001; Kao et al., 2012) (reviewed in Doe, 2017). What mechanisms specify these temporally defined identities? This section will discuss future directions for understanding how larval NBs temporally progress to generate neuron diversity. Temporal progression is defined as NBs transitioning from expressing early factors to later factors with subsequent NB decommissioning (i.e., NBs differentiate or undergo cell death).

Extrinsic signaling over time

Extrinsic cues have been shown to regulate temporal progression of larval NBs towards eventual decommissioning. Hedgehog signaling is expressed in late NBs to promote cell cycle exit during early pupal stages (Chai et al., 2013). Interestingly, the early TTF Castor is required for this Hedgehog mediated termination of NB cell cycle (Chai et al., 2013). It remains unknown how transient expression of Castor in an early window acts upstream of Hedgehog activity in a late

window. More recently, Ecdysone signaling was shown to act in middle-staged NBs to repress early factors and promote late factors (Syed et al., 2017a). This early-to-late transition is known to require the early transient expression of Seven-up (Ren et al., 2017; Syed et al., 2017a). These studies suggest that the early expression of Castor and Seven-up may change the competency of NBs to extrinsic cues well after these intrinsic factors are no longer expressed. This is supported studies showing that loss of Seven-up (early) or Ecdysone receptor (EcR, mid) leads to continuous expression of early factors at the expense of late ones (Dillon et al., 2024; Ren et al., 2017; Syed et al., 2017a). One future approach will be characterizing the chromatin landscape and transcriptome of NBs across all larval stages. My scRNAseq work is limited to early larval NBs prior to any known transitional stages (Dillon et al., 2022). Additional data will provide a resource for screening the transcriptional state and gene accessibility of NBs to postulate testable hypotheses about how temporal transitions are regulated.

Recent work has shown Notch signaling to regulate progression in larval NBs. Delta expression in glia was found to promote Notch in central brain NBs to initiate the repression of early factors (Sood et al., 2023). Additionally, early factors further promoted Notch activity while Delta was repressed by late factors (Sood et al., 2023). Loss of Notch leads to prolonged NB proliferation into adults as Notch activity is required during an early window, prior to NB decommissioning, for progression (Sood et al., 2023). My work showed a similar result with early transient Seven-up required for Type 2 NB decommissioning (Dillon et al., 2024). These data from Sood *et al.* and my work (Dillon et al., 2024) indicate that Notch and Seven-up act to progress NBs towards decommissioning through mechanisms regulated days prior. One limitation of the Sood *et al.* study was an inability to manipulate the specific levels of Notch activity as experiments relied on the partial knockdowns of Notch and Delta in a few cell types (glia or NBs but no other adjacent cells positive for Delta). What mechanism does Notch regulate for NB progression? Identifying Notch targets across larval NB stages would provide useful candidates to pursue.

Previous studies of Notch in larval NBs showed that it was required for maintaining Type 2 NB identity and proliferation (Li et al., 2016; Li et al., 2017; San-Juán and Baonza, 2011; Zhu et al., 2012). Does Notch act differently between Type 1 and Type 2 NB lineages? Do individual NB lineages respond differently to extrinsic cues such as Delta for progression? Mushroom body

NBs go through decommissioning later than other lineages due to sustained high levels of the early factor Imp (Yang et al., 2017). Both Notch and Ecdysone signaling have been shown to repress Imp levels in NBs (Sood et al., 2023; Syed et al., 2017a). This suggests that lineages could respond differently to signaling cues. No study to date has compared the temporal progression of NBs to extrinsic signals with lineage specificity. Future work will be needed to understand these lineage differences in temporal progression.

The epistatic relationship between Notch, Ecdysone, and Hedgehog signaling for promoting NB progression remains unknown. These signaling cues may be in the same pathway as previous studies have shown each required for timely progression (described above). This suggests little to no redundancy between the pathways. I hypothesize that Notch acts upstream of Ecdysone, which acts upstream of Hedgehog (Fig. 5.1). Notch is supported to be first as it: a) has the earliest onset of expression, b) inhibits the earliest temporal factors Castor and Seven-up, and c) loss of Notch prior to 72h in larvae and re-expression after 72h is sufficient to inhibit NB decommissioning (Sood et al., 2023). These findings show that Notch regulates Seven-up, known to be upstream of EcR (Syed et al., 2017a), and Castor, known to be upstream of Hedgehog (Chai et al., 2013). Additionally, loss of Notch in the early window, prior to Ecdysone or Hedgehog, is sufficient to produce NB progression defects (Sood et al., 2023). The Ecdysone window starts mid in larval stages while Hedgehog begins in late larvae and into early pupa through decommissioning (Chai et al., 2013; Syed et al., 2017a). Thus, Ecdysone and then Hedgehog may act downstream of Notch signaling. Future work will be required to test these epistatic relationships.

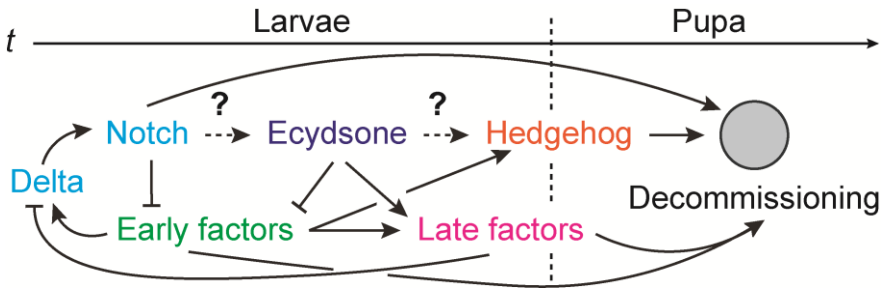

Fig. 5.1 Model of temporal progression in larval neuroblasts by regulation from extrinsic signaling pathways. Larval neuroblasts progress from expressing early factors (Castor, Seven-up, Chinmo, Imp) to late factors (EcR-B1, Broad, E93, Syncrip) before they initiate decommissioning. Solid lines represent regulatory relationships, direct and indirect,

(Fig. 5.1 caption continued) supported from previous studies (Chai et al., 2013; Dillon et al., 2024; Maurange et al., 2008; Ren et al., 2017; Sood et al., 2023; Syed et al., 2017a; Yang et al., 2017). Dashed lines with question marks represent proposed relationships to be tested.

Switching factors and the shifting of competence

The transcription factor Seven-up is an intriguing temporal factor for several reasons. First, it is an orphan receptor with no known ligand identified to date. Early work on Seven-up identified that the ligand binding domain is not required but enhances its function as a fate determinant (Hiromi et al., 1993). Secondly, Seven-up was initially identified as a fate determinate in photoreceptor neurons (Hiromi et al., 1993; Mlodzik et al., 1990) and later as a switching factor in NBs (Benito-Sipos et al., 2011; Dillon et al., 2024; Kanai et al., 2005; Kohwi et al., 2011; Maurange et al., 2008; Mettler et al., 2006; Ren et al., 2017; Syed et al., 2017a). Switching factors are transiently expressed and act to transition a NB from an early TTF window that generates early born identities to a NB expressing a later TTF window that generates later born identities. For example, Seven-up in embryonic NB 7-1 is required to switch from the early Hb+ window generating U1/2 motor neurons to the later Kr+ window to produce the U3 motor neuron (Kanai et al., 2005). Lastly, Seven-up is expressed in a short burst of protein in an early window but phenotypes from Seven-up manipulations are reported much later in lineages (Dillon et al., 2024; Maurange et al., 2008; Narbonne-Reveau et al., 2016; Ren et al., 2017; Syed et al., 2017a). My work showed Seven-up protein in Type 2 NBs was transiently present from 18-24h after larval hatching and loss of Seven-up resulted in Type 2 NBs persisting in the week old adult (Dillon et al., 2024). These studies indicate that the downstream effectors of Seven-up are poorly understood. I describe below future directions to understanding the mechanism of Seven-up in larval NB progression.

How Seven-up is regulated in larval NBs remains unknown. My work showed that *seven-up* mRNA is present prior to and after Seven-up protein in Type 2 lineages (Dillon et al., 2024). I found both mRNA and protein is restricted exclusively to the NB and onset of protein has a spatial pattern with peak expression in posterior lineages prior to anterior lineages (Dillon et al., 2024). These data indicate that Seven-up is regulated both post-transcriptionally (broader mRNA window compared to protein) and transcriptionally by cell type (present in NBs but not progeny cells). A candidate upstream regulator of Seven-up is Castor, which is expressed prior to Seven-

up (Ren et al., 2017). However, my work and others have shown that Castor is not required for Seven-up expression and that Seven-up is not required to restrict the expression of Castor (Dillon and Doe, 2024; Ren et al., 2017; Syed et al., 2017a). Thus, there is no cross-regulation of these factors as would be expected in a TTF cascade. The spatial pattern of Seven-up protein suggests that either extrinsic cues or an unidentified intrinsic factor initiates *seven-up* expression. One challenge will be resolving the orphan receptor status of Seven-up to help identity upstream candidates. Future work may want to investigate how NB proliferation could regulate Seven-up given the timing of expression is shortly after reactivation.

The loss of Seven-up shows phenotypes in larval NBs that maintain expression of early factors, no expression of late factors, and continued proliferation of NBs into the adult (Dillon et al., 2024; Maurange et al., 2008; Narbonne-Reveau et al., 2016). How can a highly transient factor control NB progression days after expression is over? The known switching functions of Seven-up in Type 2 NBs is the Imp to Syncrip transition and expression of EcR >24h after Seven-up (Ren et al., 2017; Syed et al., 2017a). Two hypotheses are i) Seven-up initiates a temporal cascade of TTFs, similar to its function in the embryonic NB lineages (Kanai et al., 2005), and/or ii) Seven-up alters the chromatin landscape to enable NBs to become competent to a signal such as Ecdysone. Identifying the DNA-binding targets of Seven-up would provide insight into these two models by identifying downstream targets in the Seven-up switching pathway. Characterizing the NB chromatin landscape between developmental stages would provide additional candidate genes and identify how NB competency to extrinsic cues, like Ecdysone, changes across development.

Temporal factors and the Central Complex

Understanding larval neurogenesis has presented more challenges compared to embryonic neurogenesis. First, the embryonic stage is shorter, so larval stages require additional timepoints to assay. Secondly, embryonic NB lineages generally produce a unique cell type with each division. For example, the NB 7-1 lineage generates motor neurons U1-5 and VO over the course of six NB divisions (Seroka and Doe, 2019). Larval NB lineages produce multiple neurons of the same cell type over several divisions. For example, the four Type 2 lineages DM1-4 produce dozens of the same columnar neuron identities that are currently indistinguishable (Andrade et

al., 2019; Ito and Hotta, 1992; Pereanu and Hartenstein, 2006; Riebli et al., 2013; Yang et al., 2017). Connectome and transcriptomic datasets show these neuron populations to be homogenous cell types (Epiney et al., 2023; Hulse et al., 2020). Thus, it has been difficult to trace single neuron identities to single lineages in discrete birth windows. Future work will require resource-intensive approaches for single neuron lineage tracing experiments to better understand the Type 2 derived neuron populations.

Type 2 NBs generate the majority of the Central Complex (CX) (Riebli et al., 2013; Yang et al., 2013). Thus, understanding the development of these lineages will provide insight into how diverse neurons are generated to form complex circuits. My work and others have established that temporal factors in Type 2 NBs are required for establishing neuron molecular and morphological features (Dillon and Doe, 2024; Dillon et al., 2024; Hamid et al., 2024; Ren et al., 2017; Syed et al., 2017a; Wani et al., 2023). For example, the loss of Seven-up, and subsequently extended window of early factors, results in excess early neuron identities born at ectopically late timepoints (Dillon et al., 2024). Likewise, the absence of late temporal factors results in a loss of late identity neurons (Dillon et al., 2024). I have shown the early TTF Castor to specify early CX neuron identities (Dillon and Doe, 2024). Additional work has shown temporal factors Imp (early) and E93 (late) to specify CX neurons born at early and late windows (Hamid et al., 2024; Munroe and Doe, 2023; Ren et al., 2017; Wani et al., 2023). These studies demonstrate that temporally transient factors are a mechanism for generating diverse CX neurons in the Type 2 NBs. Previous work has shown that intermediate neural progenitors (INPs; the stem cell-like progeny derived from Type 2 NBs) are patterned through a cross-regulatory TTF cascade (Bayraktar and Doe, 2013; Sullivan et al., 2019; Tang et al., 2022). Ongoing work is focused on identifying novel candidate NB TTFs as the known factors are insufficient to produce the neuron diversity seen in the adult CX (Dillon and Morales Chaya et al, unpublished).

There are two proposed models for how Type 2 NBs generate CX neurons. The temporal gradient model: broad temporal gradients of protein expression specify unique neuron identities based on the level of proteins expressed at the time of neuronal birth (Fig. 5.2, top). This is a similar mechanism to how mushroom body neurons are specified with opposing gradients of Imp and Syncrip (Liu et al., 2015). Previous work supports this model as manipulations of Imp or

Syncrip levels results in disrupted CX neuron morphology and molecular identity (Hamid et al., 2024; Munroe and Doe, 2023; Ren et al., 2017). The temporal cascade model: transient expression of cross-regulatory factors specifies neuron identities born within discrete temporal windows (Fig. 5.2, bottom). This is similar to the embryonic NB TTF cascades (Cleary and Doe, 2006; Grosskortenhaus, 2006; Isshiki et al., 2001; Meng et al., 2019; Meng et al., 2020; Moris-Sanz et al., 2014; Novotny et al., 2002; Pearson and Doe, 2003; Seroka and Doe, 2019; Tran and Doe, 2008). Previous work supports this model as the TTFs Castor (early) and E93 (late) are required to specify early and late neuron identities (Dillon and Doe, 2024; Wani et al., 2023). These studies indicate that both temporal gradients and TTFs play a role in Type 2 NBs to generate the CX neurons. Future work will be needed to understand how these factors activate, or inhibit, neuron identities with temporal precision.

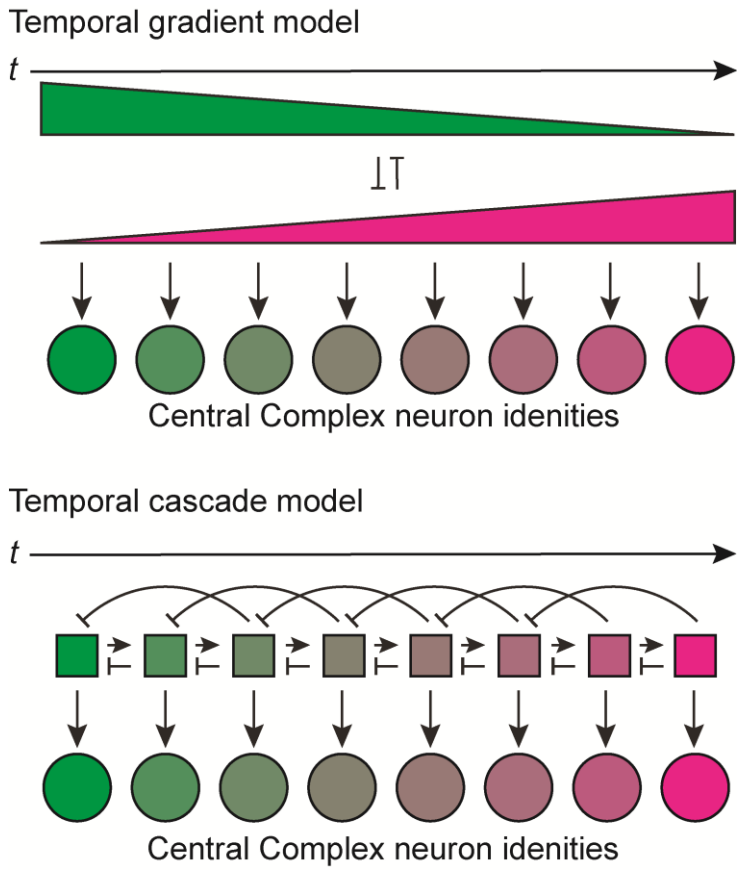

Fig. 5.2 Model for Type 2 neuroblast generation of Central Complex neuron identities. Temporal gradients of proteins (colored triangles) specify neuron identities (top). Temporal cascade of cross-regulatory temporal factors (squares) specifies neuron identities in discrete

(Fig. 5.2 caption continued) temporal windows (bottom). Temporal patterning from the intermediate neural progenitors (INPs) not depicted here.

The current understanding of how CX neurons are specified is incomplete. There are an estimated ~250 unique CX neuron subtypes based on transcriptome and connectome datasets (Epiney et al., 2023; Franconville et al., 2018; Hulse et al., 2020). To understand the development of these CX neuron identities, it will require characterizing: i) the lineage neurons are derived from, ii) the NB birth window, and iii) the INP birth window. Lineage tracings of Type 2 NBs have established which neuronal classes are derived from each of the eight Type 2 lineages (Riebli et al., 2013; Yang et al., 2013). Thus, birth dating has been a limiting factor. My work, along with others, have identified all three developmental aspects for only the P-EN, P-FN, and E-PG neurons (Dillon and Doe, 2024; Dillon et al., 2024; Sullivan et al., 2019; Yang et al., 2013) (Fig. 5.3). When are each of the distinct CX neuron identities specified? What mechanisms specify these unique identities? Are there additional temporal factors to be discovered? Answering these questions will provide a greater understanding of underlining patterns for how complex neural circuits are generated.

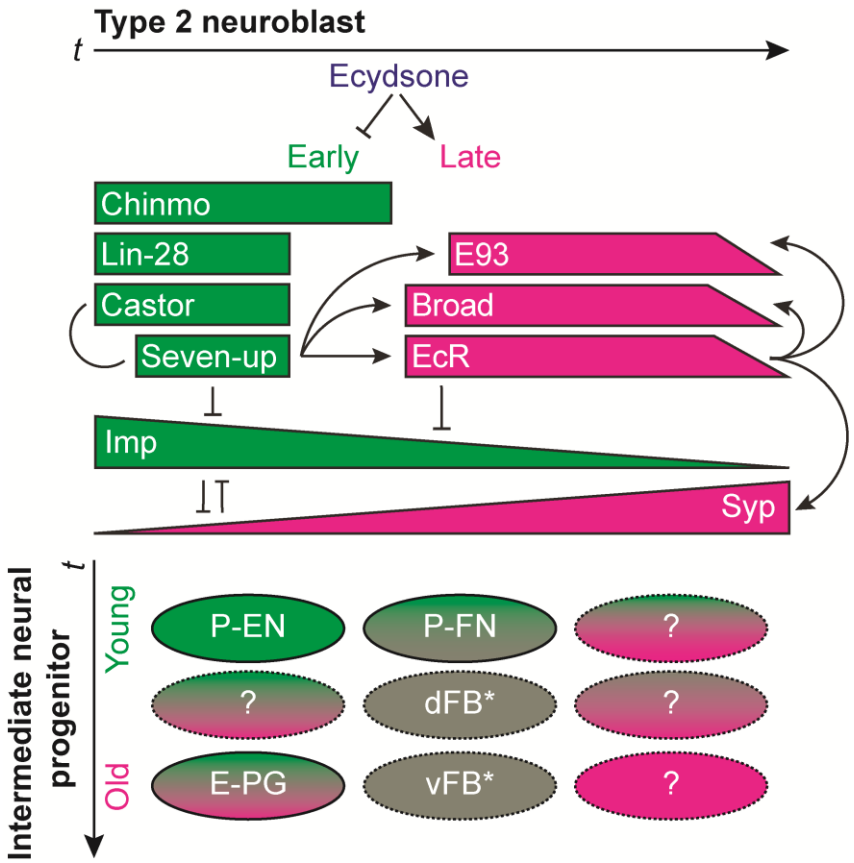

Fig. 5.3 Current understanding of temporal patterning in the Type 2 lineages generating Central Complex neurons. Temporal gradients of proteins and restricted windows of transcription factors show partial cross regulation. Several Central Complex (CX) neuron identities have been mapped to a NB and INP birth window. Dashed lines indicate unknown neuron identity or incomplete birth dating. *, unknown INP birth window. Temporal transcription factors (TTFs) from the intermediate neural progenitors (INPs) not depicted in detail here.

Type 2 NB divisions generate INPs, which then divide additional times to produce ganglion mother cells (GMCs). Both NB and INPs are temporally patterned (Bayraktar and Doe, 2013). Thus, it is important to birth date when neurons are derived from each window. My work used an EdU dropout birth dating approach to determine the NB birth window (see Chapters III and IV) (Dillon and Doe, 2024; Dillon et al., 2024). Other studies have used genetic approaches to conditionally label neurons for birth dating (Hamid et al., 2024; Sullivan et al., 2019; Wani et al., 2023). Both approaches yield discrete NB birth windows. INP birth dating is less studied and is broadly defined as neurons derived from either "young" or "old" INPs (Bayraktar and Doe, 2013; Sullivan et al., 2019). Knowing the NB and INP window allows for directed experiments to determine if temporal factors expressed during those windows are required for specifying

identities. Active investigation aims to discover novel factors across the Type 2 lineage and functionally test them for specifying CX neurons (Dillon and Morales Chaya et al, unpublished).

Which temporal factors are required for specifying neuron identities? My work and others have determined NB temporal factors are required for specifying CX neuron identities (Dillon and Doe, 2024; Dillon et al., 2024; Hamid et al., 2024; Ren et al., 2017; Wani et al., 2023). Less work has been done determining the requirement of INP temporal factors (Bayraktar and Doe, 2013; Munroe and Doe, 2023; Sullivan et al., 2019). To date, only the E-PG neurons have been shown to require both a specific NB TTF, Castor (early NB), and specific INP TTF, Eyeless (old INP) (Dillon and Doe, 2024; Sullivan et al., 2019). It remains unclear how Castor and Eyeless act in combination to specify the E-PG identity. Is the combination of NB and INP TTFs required for all CX neurons, as previously purposed (Bayraktar and Doe, 2013)? Discovering and testing additional TTFs will provide an underlining mechanism for how CX identities are specified.

What are the downstream mechanisms for how TTFs initiate identity features? The manipulation of several factors (Seven-up, Castor, Imp, Syncrip, and Eyeless) in the developing Type 2 lineage has shown to disrupt neuron morphology and neuron cell numbers (Hamid et al., 2024; Munroe and Doe, 2023; Ren et al., 2017; Sullivan et al., 2019). For example, loss of Eyeless leads to the loss of old INP derived neurons (Sullivan et al., 2019). Additionally, the molecular marker for old INPs, Toy (Twin of Eyeless; a suspected downstream target of Eyeless), is required for proper E-PG neuron morphology (Sullivan et al., 2019). My work has shown the NB TTF Castor is required for specifying E-PG and P-EN neuron molecular identities (Dillon and Doe, 2024). Castor knockout leads to the loss of E-PG markers Toy and Dac and P-EN markers Cut and Runt (Dillon and Doe, 2024). These data suggests that NB and INP factors specify CX identity features such as molecular expression and neuropil targeting (neuron morphology). The lack of fully investigated CX neuron identities with both NB and INP TTFs necessary for specification makes it impossible to draw further conclusions.

Conservation of temporal patterning mechanisms in *Drosophila* and mammalian central nervous systems

Previous reviews have highlighted conserved features between the genes and regulatory mechanisms found in the developing *Drosophila* central nervous systems and their mammalian orthologs (Doe, 2017; El-Danaf et al., 2023; Holguera and Desplan, 2018; Pollington et al., 2023; Santos-França et al., 2022; Syed et al., 2017b). This section will provide an overview of cortical and retinal development in mammals followed by a comparison between fly and mammalian neural stem cells. The comparison will cover aspects that are conserved and features that differ. The intention is to highlight the mechanisms found in model organisms that may inform how the relatively large and complex human brain develops.

An introduction to mammalian neural stem cells that generate the cortex

How does the human brain develop? This is a driving question for many neurobiologists who rely on model organisms to indirectly test developmental mechanisms likely to be present in humans. One of the most prominent hypotheses relating to this question has been the radial-unit hypothesis. The hypothesis proposes that the cerebral neocortex is generated by neural stem cells producing progeny that form a unit of cells in a radial column to populate the cortical layers (Rakic, 1988). Importantly, an increased starting pool of "units" will increase the overall cell numbers even if the number of divisions for each stem cell remains the same (Rakic, 1988). More stem cells equal bigger brain. Early work proposed that small evolutionary changes to the number of stem cells could explain the rapid increase in the human cortex compared to other primates (Rakic, 1995). Lineage tracing in radial glial cells (RGCs) in the ventricular and subventricular zones determined these cells to be the proliferative units generating the neurons and glia that populate the cerebral cortex (Noctor et al., 2001). Furthermore, RGCs were found to be the primary stem cells that give rise to the majority of the cortex (Noctor et al., 2002). Outer RGCs (oRGCs) were discovered in the outer subventricular zone, not found in rodents (Hansen et al., 2010). oRGCs are found exclusively in gyrencephalic (brains with folds) mammals and provide an expanded proliferative capacity with novel features that distinguish them from RGCs (Reillo et al., 2011) (detailed below). These landmark studies show that understanding the molecular mechanisms of RGCs and oRGCs will be vital for understanding mammalian (especially human) corticogenesis.

Classic work used thymidine injection tracings, a method where radioactive thymidine is incorporated into dividing cells for labeling, to characterize how the developing neocortex. The mouse neocortex forms in an inside-out fashion with the inner layers populated by early born progeny and outer layers populated by late born progeny (Angevine and Sidman, 1961). Tracings in the rhesus monkey cortex found this patterning to be conserved in primates (Schmechel and Rakic, 1979). Interestingly, RGCs have a unique morphology with a glial fiber, a long process that extends from the cell body to the pial surface, in which neurons were found to closely remain in contact with the fiber; raising the question if progeny cells use this structure to guide their migration to layered positions (Mission et al., 1991). Live imaging studies confirmed this as RGCs asymmetrically divide with the renewed RGC retaining the glial fiber as the progeny cell "climbs" up the fiber towards a final layer (Miyata et al., 2001; Noctor et al., 2001). It is important to note that these studies report columnar migration where the progeny cells remain in their proliferative unit. Subsequent work identified some neuron subtypes, such as Cajal-Retzius neurons, tangentially migrate across several glial fibers to form more complex neuroarchitecture (Bielle et al., 2005; Borrell and Marín, 2006; Takiguchi-Hayashi et al., 2004; Yoshida et al., 2006). These studies show that RGCs are highly dynamic neural stem cells that not only produce progeny but also guide cell migration.

Are neuron identities determined by their birth order or by extrinsic factors? An early transplant study found extrinsic cues are partially required for determining neuron identity. RGCs in an early S phase of cell cycle transplanted to a later staged embryo will follow the normal host neuron layer migration (i.e., early RGC producing a late born identity when in a late staged environment) (McConnell and Kaznowski, 1991). When RGCs were transplanted later in the cell cycle, they produced neurons normal for the donor and not the host (McConnell and Kaznowski, 1991). These data suggest a competency window for RGCs to produce progeny determined by extrinsic signals before being restricted to generate a specific identity. Subsequent work identified the G1 cell cycle stage as the main competency window for extrinsic cues to determine layer identity (Takahashi et al., 1995). Interestingly, cell cycle progression is different across primate cortical regions (Lukaszewicz et al., 2005). These studies show that RGCs are highly regulated by their cell cycle state that provide a window for which environmental cues determine layer identity.

RGCs have been shown to generate distinct identities over time (reviewed in Miller and Gauthier, 2007; Molyneaux et al., 2007). RGCs generate neurons and then transition to generating astrocytes (Malatesta et al., 2000; Qian et al., 2000). Later work demonstrated that RGCs generated not only layer specific neurons but also molecularly distinct neurons in a predictable order (Shen et al., 2006). Furthermore, the timing of this birth order was maintained *in vitro* (Shen et al., 2006). This work demonstrates that RGCs will be interesting models for understanding how intrinsic temporal patterning genes determine neuron identities.

A brief introduction to mammalian retinal progenitor cells

Retinal progenitor cells (RPCs) provide another model to study how neural stem cells generate complex tissues such as the eye. The retina is comprised of seven distinct cell types (six neuron identities and one glial) (reviewed in Bassett and Wallace, 2012). Similar to classic work in the cortex, thymidine injection tracing in mouse retinas found neuron identities to be sequentially generated by RPCs over the course of development (Young, 1985). These neurons have been well characterized for being generating in a predictable series (Cherry et al., 2009; Morrow et al., 2008; Rapaport et al., 2004; Turner and Cepko, 1987; Voinescu et al., 2009). Additionally, this birth order is maintained *in vitro* with cultured RPCs generating the expected number and diversity of cell types (Belliveau and Cepko, 1999). These studies suggest that RPCs undergo an intrinsic temporal patterning to generate a set diversity of cell types (reviewed in Cepko, 2014; Santos-França et al., 2023). Several temporal transcription factors (TTFs), including Ikaros, Pou2f1/2, FoxN4, Nfia/b/x, and Casz1 (ordered early to late), have been identified as being required and sufficient to specify distinct retinal identities (Clark et al., 2019; Elliott et al., 2008; Javed et al., 2020; Liu et al., 2020; Mattar et al., 2015). These TTFs have *Drosophila* orthologs involved with temporal patterning (see below). These studies demonstrate that retinal development is controlled by similar temporal patterning mechanisms found in the mammalian cortex and *Drosophila* central nervous system.

A comparison between the fly and mammalian neurogenesis

The mammalian RGCs and *Drosophila* neuroblasts (NBs) share similar division patterns (reviewed in Doe, 2017; Taverna et al., 2014). RGCs divide asymmetrically to generate a self-

renewed RGC and produce either a neuron for direct neurogenesis or an intermediate progenitor cell that divides symmetrically to produce two neurons for indirect neurogenesis (glia are also generated in these lineages) (Noctor et al., 2004). These divisions are similar to *Drosophila* NB Type 0 (direct neurogenesis) and Type 1 (indirect neurogenesis) divisions where the ganglion mother cell (GMC) is the intermediate cell type (Baumgardt et al., 2014; Spana and Doe, 1995) (see Chapter I). oRGCs divide either asymmetrically to produce an intermediate progenitor or symmetrically to produce two oRGCs that increase proliferative capacity (Hansen et al., 2010). This division pattern is similar to the *Drosophila* Type 2 NB divisions that generate intermediate neural progenitors (INPs) that then divide several times (Bello et al., 2008; Boone and Doe, 2008; Bowman et al., 2008). The key difference is that oRGCs generate another identical oRGC that remains proliferative while the *Drosophila* INP disappears after several division. Both oRGCs and Type 2 NBs have an increased neurogenic capacity relative to their starting number (reviewed in Taverna et al., 2014) (see Chapter I). These findings suggest that *Drosophila* NBs can be used as models for understanding cell division mechanisms of neurogenesis that may be conserved in mammals.

Mammalian RPCs, RGCs, and *Drosophila* NBs show asymmetrical localization of proteins as a mechanism for fate determining neuron identities. In *Drosophila* NBs, Numb asymmetrically localizes in daughter cells to specify neuron identities (Rhyu et al., 1994; Spana et al., 1995). This asymmetric segregation of Numb is conserved in RPCs as fate determinant (Cayouette et al., 2001). Similarly Numb localization in RGCs of the ventricular zone is asymmetrical while subventricular zone RGCs show symmetrically localized Numb (Zhong et al., 1996; Zhong et al., 1997). Interestingly, the division pattern of RGCs is highly correlated to location to where these progenitors divide. Apical RGCs show a preference for asymmetrical divisions while basal progenitors tend to divide symmetrically (Haubensak et al., 2004; Kowalczyk et al., 2009). These findings suggest that conversed mechanisms such as protein segregation may a useful model to study in NBs and applied to understanding mammalian stem cells. However, these studies also indicate that mammalian neural stem cells may have unique features not suitable to study in NBs.

To date, no discernable morphological features or evidence of migration has been identified in *Drosophila* NBs. RGCs and oRGCs have been extensively studied for their unique cellular

morphology and migration patterns. RGCs were originally characterized based on their unique cell morphology in addition to molecular markers (Levitt and Rakic, 1980; Rakic, 1972). RGCs have two main processes: i) the basal process extending to the ventricular border and ii) the glial fiber that extends through the cortical layers to the pial surface. These RGC glial fibers have a primarily radial direction and direct neuron migration (Malatesta et al., 2000; Mission et al., 1991). oRGCs lack a basal projection but maintain a glial fiber with more tangential paths to the pial surface (Hansen et al., 2010). These oRGC glial fibers are hypothesized to allow more complex neuroarchitecture by directing tangential cell migration (Reillo et al., 2011). Interesting, recent work has shown that the end feet of glial fibers to have unique transcriptional dynamics (compared to the soma) and is required for organizing the interneurons of the marginal zone (D'Arcy et al., 2023; Pilaz et al., 2016). Live imaging studies have shown that RGCs and oRGCs migrate in their respective zones (ventricular, subventricular, and outer subventricular) extensively during divisions (Hansen et al., 2010; Haubensak et al., 2004; Noctor et al., 2001; Noctor et al., 2004). The mechanisms behind these cell movements and if they have a functional purpose remains unknown. These findings indicate that *Drosophila* NBs cannot be used as models for understanding these RGC/oRGC features of morphology and migration.

Drosophila NBs are models for understanding temporal patterning mechanisms that may be conserved in mammals. My work with Seven-up has shown it to be a switching factor for Type 2 NBs to transition from producing early born fates to late born fates (Dillon and Doe, 2024; Dillon et al., 2024). COUP-TFI/II, orthologs of Seven-up, act as switching factors in corticogenesis. COUP-TFI/II are required for switching from neurogenesis to gliogenesis and COUP-TFI is required to balance the generation of early and late GABAergic interneurons (Lodato et al., 2011; Naka et al., 2008). These findings suggest that identifying the mechanisms of Seven-up in NBs will provide testable candidates for understanding the COUP-TFI/II switching function in mammalian RGCs.

Previous work in *Drosophila* NBs provided candidates for temporal patterning genes to explore in mammalian cortical and retinal neurogenesis. My work has shown the TTF Castor is required and sufficient for specifying neuron identities of the adult *Drosophila* central brain (Dillon and Doe, 2024). The role of Casz1, the mammalian ortholog of Castor, has yet to be tested in

corticogenesis. However, Casz1 has been extensively studied in RPCs as a temporal patterning gene required for specifying the late born rod cell identity (Mattar et al., 2015; Mattar et al., 2018; Mattar et al., 2021; Monteiro et al., 2016). Additionally, Ikaros, ortholog to the *Drosophila* TTF Hunchback, is required and sufficient to generate early born neuron identities in both cortical (deep layer neurons) and retinal (horizontal, amacrine, and retinal ganglion cells) development (Alsiö et al., 2013; Elliott et al., 2008). These results demonstrate that TTFs in *Drosophila* NBs provide suitable candidates to test their function in mammalian cortical and retinal progenitors. Future studies should focus on identifying the expression patterns of *Drosophila* temporal patterning genes in available scRNAseq datasets of the neocortex and developing retina.

Concluding remarks

Over the past four years, I am proud to have contributed to the field of developmental neurobiology. My work has touched on several aspects across the developing *Drosophila* central nervous system. I have provided a useful scRNAseq dataset as a tool for the community and investigated the temporal patterning mechanisms for how Central Complex neurons are generated. I have taken away from my work more questions than answers. Much remains to be explored for how complex brains are made and I look forward to making further contributions.

References

Almeida, M. S. and Bray, S. J. (2005). Regulation of post-embryonic neuroblasts by Drosophila Grainyhead. *Mech. Dev.* 122, 1282–1293.

Alsiö, J. M., Tarchini, B., Cayouette, M. and Livesey, F. J. (2013). Ikaros promotes early-born neuronal fates in the cerebral cortex. *Proc. Natl. Acad. Sci.* 110, E716–E725.

Andrade, I. V., Riebli, N., Nguyen, B.-C. M., Omoto, J. J., Cardona, A. and Hartenstein, V. (2019). Developmentally Arrested Precursors of Pontine Neurons Establish an Embryonic Blueprint of the Drosophila Central Complex. *Curr. Biol.* 29, 412-425.e3.

Angevine, J. B. and Sidman, R. L. (1961). Autoradiographic Study of Cell Migration during Histogenesis of Cerebral Cortex in the Mouse. *Nature* 192, 766–768.

Bassett, E. A. and Wallace, V. A. (2012). Cell fate determination in the vertebrate retina. *Trends Neurosci.* 35, 565–573.

Baumgardt, M., Karlsson, D., Salmani, B. Y., Bivik, C., MacDonald, R. B., Gunnar, E. and Thor, S. (2014). Global Programmed Switch in Neural Daughter Cell Proliferation Mode Triggered by a Temporal Gene Cascade. *Dev. Cell* 30, 192–208.

Bayraktar, O. A. and Doe, C. Q. (2013). Combinatorial temporal patterning in progenitors expands neural diversity. *Nature* 498, 449–455.

Belliveau, M. J. and Cepko, C. L. (1999). Extrinsic and intrinsic factors control the genesis of amacrine and cone cells in the rat retina. *Development* 126, 555–566.

Bello, B. C., Izergina, N., Caussinus, E. and Reichert, H. (2008). Amplification of neural stem cell proliferation by intermediate progenitor cells in Drosophila brain development. *Neural Develop.* 3, 5.

Benito-Sipos, J., Ulvklo, C., Gabilondo, H., Baumgardt, M., Angel, A., Torroja, L. and Thor, S. (2011). Seven up acts as a temporal factor during two different stages of neuroblast 5-6 development. *Development* 138, 5311–5320.

Bielle, F., Griveau, A., Narboux-Nême, N., Vigneau, S., Sigrist, M., Arber, S., Wassef, M. and Pierani, A. (2005). Multiple origins of Cajal-Retzius cells at the borders of the developing pallium. *Nat. Neurosci.* 8, 1002–1012.

Boone, J. Q. and Doe, C. Q. (2008). Identification of *Drosophila* type II neuroblast lineages containing transit amplifying ganglion mother cells. *Dev. Neurobiol.* 68, 1185–1195.

Borrell, V. and Marín, O. (2006). Meninges control tangential migration of hem-derived Cajal-Retzius cells via CXCL12/CXCR4 signaling. *Nat. Neurosci.* 9, 1284–1293.

Bowman, S. K., Rolland, V., Betschinger, J., Kinsey, K. A., Emery, G. and Knoblich, J. A. (2008). The Tumor Suppressors Brat and Numb Regulate Transit-Amplifying Neuroblast Lineages in Drosophila. *Dev. Cell* 14, 535–546.

Britton, J. S. and Edgar, B. A. (1998). Environmental control of the cell cycle in Drosophila: nutrition activates mitotic and endoreplicative cells by distinct mechanisms. *Development* 125, 2149–2158.

Brody, T. and Odenwald, W. F. (2000). Programmed transformations in neuroblast gene expression during Drosophila CNS lineage development. *Dev. Biol.* 226, 34–44.

Cayouette, M., Whitmore, A. V., Jeffery, G. and Raff, M. (2001). Asymmetric Segregation of Numb in Retinal Development and the Influence of the Pigmented Epithelium. *J. Neurosci.* 21, 5643–5651.

Cepko, C. (2014). Intrinsically different retinal progenitor cells produce specific types of progeny. *Nat. Rev. Neurosci.* 15, 615–627.

Chai, P. C., Liu, Z., Chia, W. and Cai, Y. (2013). Hedgehog Signaling Acts with the Temporal Cascade to Promote Neuroblast Cell Cycle Exit. *PLoS Biol.* 11, e1001494.

Chell, J. M. and Brand, A. H. (2010). Nutrition-Responsive Glia Control Exit of Neural Stem Cells from Quiescence. *Cell* 143, 1161–1173.

Chen, C.-H., Luhur, A. and Sokol, N. (2015). Lin-28 promotes symmetric stem cell division and drives adaptive growth in the adult Drosophila intestine. *Development* 142, 3478–3487.

Cherry, T. J., Trimarchi, J. M., Stadler, M. B. and Cepko, C. L. (2009). Development and diversification of retinal amacrine interneurons at single cell resolution. *Proc. Natl. Acad. Sci.* 106, 9495–9500.

Clark, B. S., Stein-O'Brien, G. L., Shiau, F., Cannon, G. H., Davis-Marcisak, E., Sherman, T., Santiago, C. P., Hoang, T. V., Rajaii, F., James-Esposito, R. E., et al. (2019). Single-Cell RNA-Seq Analysis of Retinal Development Identifies NFI Factors as Regulating Mitotic Exit and Late-Born Cell Specification. *Neuron* 102, 1111-1126.e5.

Cleary, M. D. and Doe, C. Q. (2006). Regulation of neuroblast competence: multiple temporal identity factors specify distinct neuronal fates within a single early competence window. *Genes Dev.* 20, 429–434.

D'Arcy, B. R., Lennox, A. L., Manso Musso, C., Bracher, A., Escobar-Tomlienovich, C., Perez-Sanchez, S. and Silver, D. L. (2023). Non-muscle myosins control radial glial basal endfeet to mediate interneuron organization. *PLOS Biol.* 21, e3001926.

Dillon, N. R. and Doe, C. Q. (2024). Castor is a temporal transcription factor that specifies early born central complex neuron identity. 2024.08.22.609207.

Dillon, N., Cocanougher, B., Sood, C., Yuan, X., Kohn, A. B., Moroz, L. L., Siegrist, S. E., Zlatic, M. and Doe, C. Q. (2022). Single cell RNA-seq analysis reveals temporally-regulated and quiescence-regulated gene expression in Drosophila larval neuroblasts. *Neural Develop.* 17, 7.

Dillon, N. R., Manning, L., Hirono, K. and Doe, C. Q. (2024). Seven-up acts in neuroblasts to specify adult central complex neuron identity and initiate neuroblast decommissioning. *Development* 151, dev202504.

Doe, C. Q. (2017). Temporal Patterning in the Drosophila CNS. 25.

Dumstrei, K., Wang, F. and Hartenstein, V. (2003). Role of DE-Cadherin in Neuroblast Proliferation, Neural Morphogenesis, and Axon Tract Formation in DrosophilaLarval Brain Development. *J. Neurosci.* 23, 3325–3335.

El-Danaf, R. N., Rajesh, R. and Desplan, C. (2023). Temporal regulation of neural diversity in Drosophila and vertebrates. *Semin. Cell Dev. Biol.* 142, 13–22.

Elliott, J., Jolicoeur, C., Ramamurthy, V. and Cayouette, M. (2008). Ikaros Confers Early Temporal Competence to Mouse Retinal Progenitor Cells. *Neuron* 60, 26–39.

Epiney, D., Chaya, G. M., Dillon, N., Lai, S.-L. and Doe, C. (2023). Transcriptional complexity in the insect central complex: single nuclei RNA sequencing of adult brain neurons derived from type 2 neuroblasts. 2023.12.10.571022.

Franconville, R., Beron, C. and Jayaraman, V. (2018). Building a functional connectome of the Drosophila central complex. *eLife* 7, e37017.

Grosskortenhaus, R. (2006). Pdm and Castor specify late-born motor neuron identity in the NB7-1 lineage. *Genes Dev.* 20, 2618–2627.

Hamid, A., Gattuso, H., Caglar, A. N., Pillai, M., Steele, T., Gonzalez, A., Nagel, K. and Syed, M. H. (2024). The conserved RNA-binding protein Imp is required for the specification and function of olfactory navigation circuitry in *Drosophila*. *Curr. Biol.* 34, 473-488.e6.

Hansen, D. V., Lui, J. H., Parker, P. R. L. and Kriegstein, A. R. (2010). Neurogenic radial glia in the outer subventricular zone of human neocortex. *Nature* 464, 554–561.

Haubensak, W., Attardo, A., Denk, W. and Huttner, W. B. (2004). Neurons arise in the basal neuroepithelium of the early mammalian telencephalon: A major site of neurogenesis. *Proc. Natl. Acad. Sci.* 101, 3196–3201.

Hiromi, Y., Mlodzik, M., West, S. R., Rubin, G. M. and Goodman, C. S. (1993). Ectopic expression of seven-up causes cell fate changes during ommatidial assembly. *Development* 118, 1123–1135.

Holguera, I. and Desplan, C. (2018). Neuronal specification in space and time. *Science*.

Homem, C. C. F., Repic, M. and Knoblich, J. A. (2015). Proliferation control in neural stem and progenitor cells. *Nat. Rev. Neurosci.* 16, 647–659.

Hulse, B. K., Haberkern, H., Franconville, R., Turner-Evans, D. B., Takemura, S., Wolff, T., Noorman, M., Dreher, M., Dan, C., Parekh, R., et al. (2020). *A connectome of the* Drosophila

central complex reveals network motifs suitable for flexible navigation and context-dependent action selection. Neuroscience.

Isshiki, T., Pearson, B., Holbrook, S. and Doe, C. Q. (2001). Drosophila Neuroblasts Sequentially Express Transcription Factors which Specify the Temporal Identity of Their Neuronal Progeny. *Cell* 106, 511–521.

Ito, K. and Hotta, Y. (1992). Proliferation pattern of postembryonic neuroblasts in the brain of Drosophila melanogaster. *Dev. Biol.* 149, 134–148.

Javed, A., Mattar, P., Lu, S., Kruczek, K., Kloc, M., Gonzalez-Cordero, A., Bremner, R., Ali, R. R. and Cayouette, M. (2020). Pou2f1 and Pou2f2 cooperate to control the timing of cone photoreceptor production in the developing mouse retina. *Development* 147, dev188730.

Jefferis, G. S. X. E., Marin, E. C., Stocker, R. F. and Luo, L. (2001). Target neuron prespecification in the olfactory map of Drosophila. *Nature* 414, 204–208.

Kanai, M. I., Okabe, M. and Hiromi, Y. (2005). seven-up Controls Switching of Transcription Factors that Specify Temporal Identities of Drosophila Neuroblasts. *Dev. Cell* 8, 203–213.

Kao, C.-F., Yu, H.-H., He, Y., Kao, J.-C. and Lee, T. (2012). Hierarchical Deployment of Factors Regulating Temporal Fate in a Diverse Neuronal Lineage of the Drosophila Central Brain. *Neuron* 73, 677–684.

Kohwi, M., Hiebert, L. S. and Doe, C. Q. (2011). The pipsqueak-domain proteins Distal antenna and Distal antenna-related restrict Hunchback neuroblast expression and early-born neuronal identity. *Development* 138, 1727–1735.

Kowalczyk, T., Pontious, A., Englund, C., Daza, R. A. M., Bedogni, F., Hodge, R., Attardo, A., Bell, C., Huttner, W. B. and Hevner, R. F. (2009). Intermediate Neuronal Progenitors (Basal Progenitors) Produce Pyramidal–Projection Neurons for All Layers of Cerebral Cortex. *Cereb. Cortex* 19, 2439–2450.

Levitt, P. and Rakic, P. (1980). Immunoperoxidase localization of glial fibrillary acidic protein in radial glial cells and astrocytes of the developing rhesus monkey brain. *J. Comp. Neurol.* 193, 815–840.

Li, X., Xie, Y. and Zhu, S. (2016). Notch maintains Drosophila type II neuroblasts by suppressing expression of the Fez transcription factor Earmuff. *Development* 143, 2511–2521.

Li, X., Chen, R. and Zhu, S. (2017). bHLH-O proteins balance the self-renewal and differentiation of Drosophila neural stem cells by regulating Earmuff expression. *Dev. Biol.* 431, 239–251.

Liu, Z., Yang, C.-P., Sugino, K., Fu, C.-C., Liu, L.-Y., Yao, X., Lee, L. P. and Lee, T. (2015). Opposing intrinsic temporal gradients guide neural stem cell production of varied neuronal fates. *Science* 350, 317–320.

Liu, S., Liu, X., Li, S., Huang, X., Qian, H., Jin, K. and Xiang, M. (2020). Foxn4 is a temporal identity factor conferring mid/late-early retinal competence and involved in retinal synaptogenesis. *Proc. Natl. Acad. Sci.* 117, 5016–5027.

Lukaszewicz, A., Savatier, P., Cortay, V., Giroud, P., Huissoud, C., Berland, M., Kennedy, H. and Dehay, C. (2005). G1 Phase Regulation, Area-Specific Cell Cycle Control, and Cytoarchitectonics in the Primate Cortex. *Neuron* 47, 353–364.

Ma, D. K., Bonaguidi, M. A., Ming, G. and Song, H. (2009). Adult neural stem cells in the mammalian central nervous system. *Cell Res.* 19, 672–682.

Malatesta, P., Hartfuss, E. and Götz, M. (2000). Isolation of radial glial cells by fluorescent-activated cell sorting reveals a neuronal lineage. *Development* 127, 5253–5263.

Mattar, P., Ericson, J., Blackshaw, S. and Cayouette, M. (2015). A Conserved Regulatory Logic Controls Temporal Identity in Mouse Neural Progenitors. *Neuron* 85, 497–504.

Mattar, P., Stevanovic, M., Nad, I. and Cayouette, M. (2018). Casz1 controls higher-order nuclear organization in rod photoreceptors. *Proc. Natl. Acad. Sci. U. S. A.* 115, E7987–E7996.

Mattar, P., Jolicoeur, C., Dang, T., Shah, S., Clark, B. S. and Cayouette, M. (2021). A Casz1–NuRD complex regulates temporal identity transitions in neural progenitors. *Sci. Rep.* 11, 3858.

Maurange, C., Cheng, L. and Gould, A. P. (2008). Temporal Transcription Factors and Their Targets Schedule the End of Neural Proliferation in Drosophila. *Cell* 133, 891–902.

McConnell, S. and Kaznowski, C. (1991). Cell cycle dependence of laminar determination in developing neocortex. *Science* 254, 282–285.

Meng, J. L., Marshall, Z. D., Lobb-Rabe, M. and Heckscher, E. S. (2019). How prolonged expression of Hunchback, a temporal transcription factor, re-wires locomotor circuits. *eLife* 8, e46089.

Meng, J. L., Wang, Y., Carrillo, R. A. and Heckscher, E. S. (2020). Temporal transcription factors determine circuit membership by permanently altering motor neuron-to-muscle synaptic partnerships. *eLife* 9, e56898.

Mettler, U., Vogler, G. and Urban, J. (2006). Timing of identity: spatiotemporal regulation of hunchback in neuroblast lineages of Drosophila by Seven-up and Prospero. *Development* 133, 429–437.

Miller, F. D. and Gauthier, A. S. (2007). Timing Is Everything: Making Neurons versus Glia in the Developing Cortex. *Neuron* 54, 357–369.

Mission, J.-P., Austin, C. P., Takahashi, T., Cepko, C. L. and Caviness, V. S. (1991). The Alignment of Migrating Neural Cells in Relation to the Murine Neopallial Radial Glial Fiber System. *Cereb. Cortex*.

Miyata, T., Kawaguchi, A., Okano, H. and Ogawa, M. (2001). Asymmetric Inheritance of Radial Glial Fibers by Cortical Neurons. *Neuron* 31, 727–741.

Mlodzik, M., Hiromi, Y., Weber, U., Goodman, C. S. and Rubin, G. M. (1990). The Drosophila seven-up gene, a member of the steroid receptor gene superfamily, controls photoreceptor cell fates. *Cell* 60, 211–224.

Molyneaux, B. J., Arlotta, P., Menezes, J. R. L. and Macklis, J. D. (2007). Neuronal subtype specification in the cerebral cortex. *Nat. Rev. Neurosci.* 8, 427–437.

Monteiro, C. B., Midão, L., Rebelo, S., Reguenga, C., Lima, D. and Monteiro, F. A. (2016). Zinc finger transcription factor Casz1 expression is regulated by homeodomain transcription factor Prrxl1 in embryonic spinal dorsal horn late-born excitatory interneurons. *Eur. J. Neurosci.* 43, 1449–1459.

Moris-Sanz, M., Estacio-Gómez, A., Alvarez-Rivero, J. and Díaz-Benjumea, F. J. (2014). Specification of neuronal subtypes by different levels of Hunchback. *Dev. Camb. Engl.* 141, 4366–4374.

Morrow, E. M., Chen, C.-M. A. and Cepko, C. L. (2008). Temporal order of bipolar cell genesis in the neural retina. *Neural Develop.* 3, 2.

Munroe, J. A. and Doe, C. Q. (2023). Imp is expressed in INPs and newborn neurons where it regulates neuropil targeting in the central complex. *Neural Develop.* 18, 9.

Munroe, J. A., Syed, M. H. and Doe, C. Q. (2022). Imp is required for timely exit from quiescence in Drosophila type II neuroblasts. *PLOS ONE* 17, e0272177.

Naka, H., Nakamura, S., Shimazaki, T. and Okano, H. (2008). Requirement for COUP-TFI and II in the temporal specification of neural stem cells in CNS development. *Nat. Neurosci.* 11, 1014–1023.

Narbonne-Reveau, K., Lanet, E., Dillard, C., Foppolo, S., Chen, C.-H., Parrinello, H., Rialle, S., Sokol, N. S. and Maurange, C. (2016). Neural stem cell-encoded temporal patterning delineates an early window of malignant susceptibility in Drosophila. *eLife* 5, e13463.

Nijhout, H. F. (2003). The control of growth. *Development* 130, 5863–5867.

Noctor, S. C., Flint, A. C., Weissman, T. A., Dammerman, R. S. and Kriegstein, A. R. (2001). Neurons derived from radial glial cells establish radial units in neocortex. *Nature* 409, 714–720.

Noctor, S. C., Flint, A. C., Weissman, T. A., Wong, W. S., Clinton, B. K. and Kriegstein, A. R. (2002). Dividing precursor cells of the embryonic cortical ventricular zone have morphological and molecular characteristics of radial glia. *J. Neurosci. Off. J. Soc. Neurosci.* 22, 3161–3173.

Noctor, S. C., Martínez-Cerdeño, V., Ivic, L. and Kriegstein, A. R. (2004). Cortical neurons arise in symmetric and asymmetric division zones and migrate through specific phases. *Nat. Neurosci.* 7, 136–144.

Novotny, T., Eiselt, R. and Urban, J. (2002). Hunchback is required for the specification of the early sublineage of neuroblast 7-3 in the Drosophila central nervous system. *Dev. Camb. Engl.* 129, 1027–1036.

Otsuki, L. and Brand, A. H. (2018). Cell cycle heterogeneity directs the timing of neural stem cell activation from quiescence. *Science* 360, 99–102.

Otsuki, L. and Brand, A. H. (2019). Dorsal-Ventral Differences in Neural Stem Cell Quiescence Are Induced by p57KIP2/Dacapo. *Dev. Cell* 49, 293-300.e3.

Otsuki, L. and Brand, A. H. (2020). Quiescent Neural Stem Cells for Brain Repair and Regeneration: Lessons from Model Systems. *Trends Neurosci.* 43, 213–226.

Pearson, B. J. and Doe, C. Q. (2003). Regulation of neuroblast competence in Drosophila. *Nature* 425, 624–628.

Pereanu, W. and Hartenstein, V. (2006). Neural Lineages of the Drosophila Brain: A Three-Dimensional Digital Atlas of the Pattern of Lineage Location and Projection at the Late Larval Stage. *J. Neurosci.* 26, 5534–5553.

Pilaz, L.-J., Lennox, A. L., Rouanet, J. P. and Silver, D. L. (2016). Dynamic mRNA Transport and Local Translation in Radial Glial Progenitors of the Developing Brain. *Curr. Biol.* 26, 3383–3392.

Pollington, H. Q., Seroka, A. Q. and Doe, C. Q. (2023). From temporal patterning to neuronal connectivity in Drosophila type I neuroblast lineages. *Semin. Cell Dev. Biol.* 142, 4–12.

Prokop, A. and Technau, G. M. (1991). The origin of postembryonic neuroblasts in the ventral nerve cord of Drosophila melanogaster. *Development* 111, 79–88.

Prokop, A., Bray, S., Harrison, E. and Technau, G. M. (1998). Homeotic regulation of segment-specific differences in neuroblast numbers and proliferation in the *Drosophila* central nervous system. *Mech. Dev.* 74, 99–110.

Qian, X., Shen, Q., Goderie, S. K., He, W., Capela, A., Davis, A. A. and Temple, S. (2000). Timing of CNS Cell Generation: A Programmed Sequence of Neuron and Glial Cell Production from Isolated Murine Cortical Stem Cells. *Neuron* 28, 69–80.

Rakic, P. (1972). Mode of cell migration to the superficial layers of fetal monkey neocortex. *J. Comp. Neurol.* 145, 61–83.

Rakic, P. (1988). Specification of Cerebral Cortical Areas. *Science* 241, 170–176.

Rakic, P. (1995). A small step for the cell, a giant leap for mankind: a hypothesis of neocortical expansion during evolution. *Trends Neurosci.* 18, 383–388.

Rapaport, D. H., Wong, L. L., Wood, E. D., Yasumura, D. and LaVail, M. M. (2004). Timing and topography of cell genesis in the rat retina. *J. Comp. Neurol.* 474, 304–324.

Reillo, I., de Juan Romero, C., García-Cabezas, M. Á. and Borrell, V. (2011). A Role for Intermediate Radial Glia in the Tangential Expansion of the Mammalian Cerebral Cortex. *Cereb. Cortex* 21, 1674–1694.

Ren, Q., Yang, C.-P., Liu, Z., Sugino, K., Mok, K., He, Y., Ito, M., Nern, A., Otsuna, H. and Lee, T. (2017). Stem Cell-Intrinsic, Seven-up-Triggered Temporal Factor Gradients Diversify Intermediate Neural Progenitors. *Curr. Biol.* 27, 1303–1313.

Rhyu, M. S., Jan, L. Y. and Jan, Y. N. (1994). Asymmetric distribution of numb protein during division of the sensory organ precursor cell confers distinct fates to daughter cells. *Cell* 76, 477–491.

Riebli, N., Viktorin, G. and Reichert, H. (2013). Early-born neurons in type II neuroblast lineages establish a larval primordium and integrate into adult circuitry during central complex development in Drosophila. *Neural Develop.* 8, 6.

San-Juán, B. P. and Baonza, A. (2011). The bHLH factor deadpan is a direct target of Notch signaling and regulates neuroblast self-renewal in Drosophila. *Dev. Biol.* 352, 70–82.

Santos-França, P. L., David, L. A., Kassem, F., Meng, X. Q. and Cayouette, M. (2022). Time to see: How temporal identity factors specify the developing mammalian retina. *Semin. Cell Dev. Biol.* S1084952122002117.

Santos-França, P. L., David, L. A., Kassem, F., Meng, X. Q. and Cayouette, M. (2023). Time to see: How temporal identity factors specify the developing mammalian retina. *Semin. Cell Dev. Biol.* 142, 36–42.

Schmechel, D. E. and Rakic, P. (1979). A golgi study of radial glial cells in developing monkey telencephalon: Morphogenesis and transformation into astrocytes. *Anat. Embryol. (Berl.)* 156, 115–152.

Seroka, A. Q. and Doe, C. Q. (2019). The Hunchback temporal transcription factor determines motor neuron axon and dendrite targeting in *Drosophila*. *Development* 146, dev175570.

Shen, Q., Wang, Y., Dimos, J. T., Fasano, C. A., Phoenix, T. N., Lemischka, I. R., Ivanova, N. B., Stifani, S., Morrisey, E. E. and Temple, S. (2006). The timing of cortical neurogenesis is encoded within lineages of individual progenitor cells. *Nat. Neurosci.* 9, 743–751.

Siegrist, S. E., Haque, N. S., Chen, C.-H., Hay, B. A. and Hariharan, I. K. (2010). Inactivation of Both foxo and reaper Promotes Long-Term Adult Neurogenesis in Drosophila. *Curr. Biol.* 20, 643–648.

Sood, C., Nahid, M. A., Branham, K. R., Pahl, M. C., Doyle, S. E. and Siegrist, S. E. (2023). Delta-dependent Notch activation closes the early neuroblast temporal program to promote lineage progression and neurogenesis termination in Drosophila. 2023.03.28.534626.

Sousa-Nunes, R., Yee, L. L. and Gould, A. P. (2011). Fat cells reactivate quiescent neuroblasts via TOR and glial insulin relays in Drosophila. *Nature* 471, 508–512.

Spana, E. P. and Doe, C. Q. (1995). The prospero transcription factor is asymmetrically localized to the cell cortex during neuroblast mitosis in Drosophila. *Development* 121, 3187–3195.

Spana, E. P., Kopczynski, C., Goodman, C. S. and Doe, C. Q. (1995). Asymmetric localization of numb autonomously determines sibling neuron identity in the Drosophila CNS. *Development* 121, 3489–3494.

Sullivan, L. F., Warren, T. L. and Doe, C. Q. (2019). Temporal identity establishes columnar neuron morphology, connectivity, and function in a Drosophila navigation circuit. *eLife* 8, e43482.

Syed, M. H., Mark, B. and Doe, C. Q. (2017a). Steroid hormone induction of temporal gene expression in Drosophila brain neuroblasts generates neuronal and glial diversity. *eLife* 6, e26287.

Syed, M. H., Mark, B. and Doe, C. Q. (2017b). Playing Well with Others: Extrinsic Cues Regulate Neural Progenitor Temporal Identity to Generate Neuronal Diversity. *Trends Genet.* 33, 933–942.

Takahashi, T., Nowakowski, R. and Caviness, V. (1995). The cell cycle of the pseudostratified ventricular epithelium of the embryonic murine cerebral wall. *J. Neurosci.* 15, 6046–6057.

Takiguchi-Hayashi, K., Sekiguchi, M., Ashigaki, S., Takamatsu, M., Hasegawa, H., Suzuki-Migishima, R., Yokoyama, M., Nakanishi, S. and Tanabe, Y. (2004). Generation of Reelin-Positive Marginal Zone Cells from the Caudomedial Wall of Telencephalic Vesicles. *J. Neurosci.* 24, 2286–2295.

Tang, J. L. Y., Hakes, A. E., Krautz, R., Suzuki, T., Contreras, E. G., Fox, P. M. and Brand, A. H. (2022). NanoDam identifies Homeobrain (ARX) and Scarecrow (NKX2.1) as conserved temporal factors in the Drosophila central brain and visual system. *Dev. Cell* 0,.

Taverna, E., Götz, M. and Huttner, W. B. (2014). The Cell Biology of Neurogenesis: Toward an Understanding of the Development and Evolution of the Neocortex. *Annu. Rev. Cell Dev. Biol.* 30, 465–502.

Tran, K. D. and Doe, C. Q. (2008). Pdm and Castor close successive temporal identity windows in the NB3-1 lineage. *Development* 135, 3491–3499.

Truman, J. W. and Bate, M. (1988). Spatial and temporal patterns of neurogenesis in the central nervous system of Drosophila melanogaster. *Dev. Biol.* 125, 145–157.

Turner, D. L. and Cepko, C. L. (1987). A common progenitor for neurons and glia persists in rat retina late in development. *Nature* 328, 131–136.

Voinescu, P. E., Kay, J. N. and Sanes, J. R. (2009). Birthdays of retinal amacrine cell subtypes are systematically related to their molecular identity and soma position. *J. Comp. Neurol.* 517, 737–750.

Wani, A. R., Chowdhury, B., Luong, J., Chaya, G. M., Patel, K., Isaacman-Beck, J., Shafer, O., Kayser, M. S. and Syed, M. H. (2023). Stem cell-specific ecdysone signaling regulates the development and function of a Drosophila sleep homeostat. 2023.09.29.560022.

Yang, J. S., Awasaki, T., Yu, H.-H., He, Y., Ding, P., Kao, J.-C. and Lee, T. (2013). Diverse neuronal lineages make stereotyped contributions to the Drosophila locomotor control center, the central complex. *J. Comp. Neurol.* 521, 2645–2662.

Yang, C.-P., Samuels, T. J., Huang, Y., Yang, L., Ish-Horowicz, D., Davis, I. and Lee, T. (2017). Imp and Syp RNA-binding proteins govern decommissioning of Drosophila neural stem cells. *Development* 144, 3454–3464.

Yoshida, M., Assimacopoulos, S., Jones, K. R. and Grove, E. A. (2006). Massive loss of Cajal-Retzius cells does not disrupt neocortical layer order. *Development* 133, 537–545.

Young, R. W. (1985). Cell differentiation in the retina of the mouse. *Anat. Rec.* 212, 199–205.

Yuan, X., Sipe, C. W., Suzawa, M., Bland, M. L. and Siegrist, S. E. (2020). Dilp-2–mediated PI3-kinase activation coordinates reactivation of quiescent neuroblasts with growth of their glial stem cell niche. *PLOS Biol.* 18, e3000721.

Zhong, W., Feder, J. N., Jiang, M.-M., Jan, L. Y. and Jan, Y. N. (1996). Asymmetric Localization of a Mammalian Numb Homolog during Mouse Cortical Neurogenesis. *Neuron* 17, 43–53.

Zhong, W., Jiang, M.-M., Weinmaster, G., Jan, L. Y. and Jan, Y. N. (1997). Differential expression of mammalian Numb, Numblike and Notch1 suggests distinct roles during mouse cortical neurogenesis. *Development* 124, 1887–1897.

Zhu, S., Wildonger, J., Barshow, S., Younger, S., Huang, Y. and Lee, T. (2012). The bHLH Repressor Deadpan Regulates the Self-renewal and Specification of Drosophila Larval Neural Stem Cells Independently of Notch. *PLOS ONE* 7, e46724.

Appendices

Appendix A. Chapter III supplementary figures and tables

Supplemental Figure 3.1 (next page). Svp mRNA is expressed early in all larval T2NB lineages similar to protein expression. (A-H) In all images, Svp mRNA is in white and T2NBs identified with Pnt-Gal4>GFP. Svp mRNA is detected at high levels in the T2NB nucleus and at very low levels in the cytoplasm, possibly due to our probe labeling a large intronic region of the svp RC isoform. Dashed yellow lines, T2NB. (A-C',G-G') Svp mRNA is expressed at 24h after larval hatching (ALH) in T2NB lineages DM1-3 and DL1. (D-H') Svp is expressed at 18h ALH in T2NB lineages DM4-6 and DL2. (I) Quantification of Svp mRNA expression in T2NBs across 12h-30h ALH shown as a bar plot with 95% confidence interval. For each lineage, 12 ALH, n = 10; 18h ALH, n = 18; 24h ALH, n = 17; 30h ALH, n = 20 lobes. Scale bars: 5 μm.

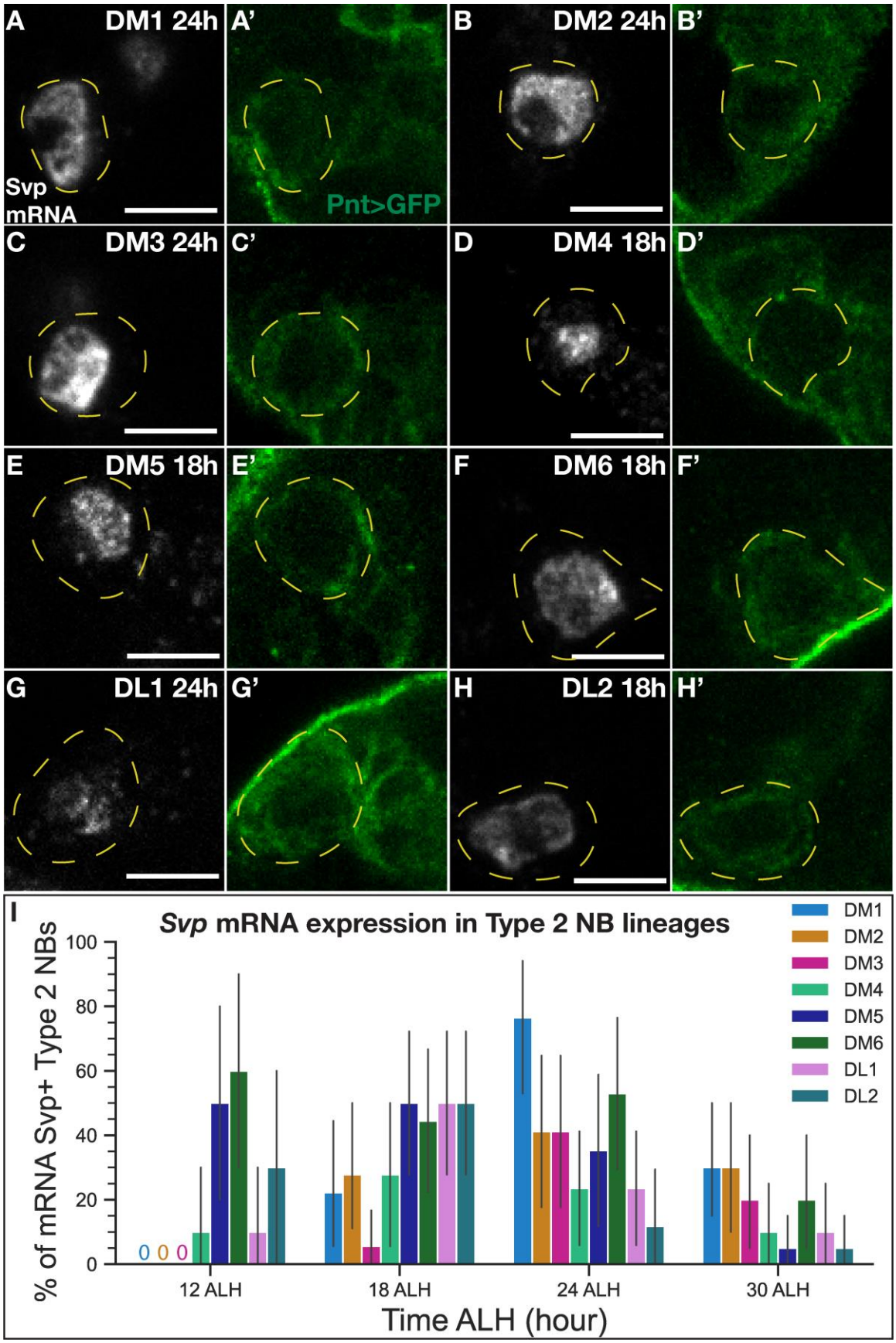
A
DM1 24h
Svp
mRNA
A'
Pnt>GFP
B
DM2 24h
B'
C
DM3 24h
C'
D
DM4 18h
D'
E
DM5 18h
E'
F
DM6 18h
F'
G
DL1 24h
G'
H
DL2 18h
H'
I
Svp mRNA expression in Type 2 NB lineages
% of mRNA Svp+ Type 2 NBs
100
80
60
40
20
0
0 0 0
12 ALH
18 ALH
24 ALH
30 ALH
Time ALH (hour)
DM1
DM2
DM3
DM4
DM5
DM6
DL1
DL2

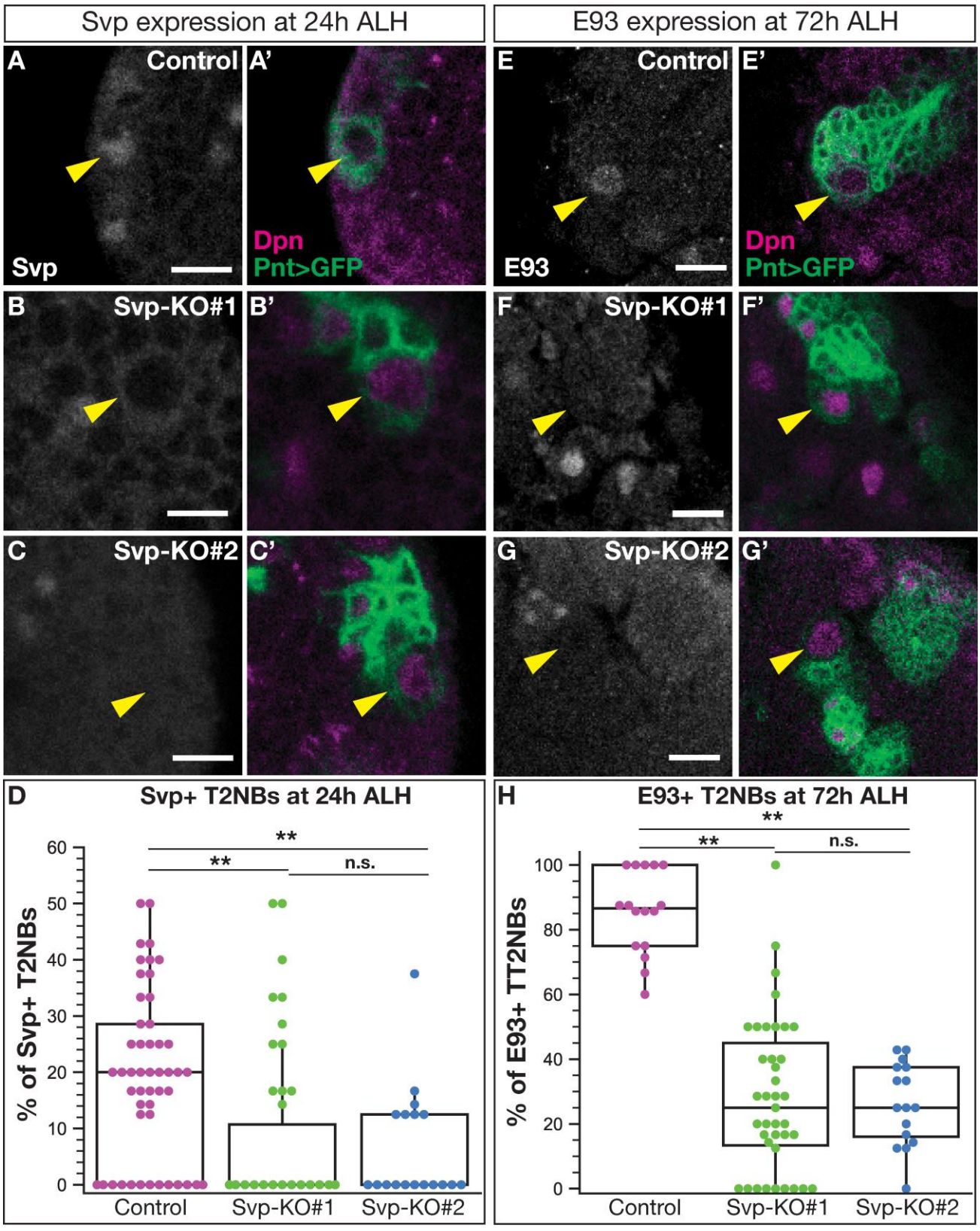

Supplemental Figure 3.2. Svp CRISPR/Cas9 knockout Svp in T2NBs and prevents temporal expression of the late factor E93. (A-C') Svp-KO reduces occurrence of Svp

(continued from previous page) in 24h after larval hatching (ALH) T2NBs. (D) Quantification of Svp expression in T2NBs at 24h ALH. Each dot represents one larval brain lobe with box and whisker plot showing distribution. Control = 49, Svp-KO#1 = 46, Svp-KO#2 = 18 lobes. *P*-values determined by One-way ANOVA, $P < 0.001$, with Tukey post-hoc test: Control versus Svp-KO#1 $P < 0.001$, Control versus Svp-KO#2 $P = 0.004$. (E-G') Svp-KO reduces occurrence of E93 expression in T2NBs at 72h ALH. (H) Quantification of E93 expression in T2NBs at 72h ALH. Each dot represents one larval brain lobe with box and whisker plot showing distribution. Control = 16, Svp-KO#1 = 39, Svp-KO#2 = 16. *P*-values determined by One-way ANOVA, $P < 0.001$, with Tukey post-hoc test: Control versus Svp-KO#1 $P < 0.001$, Control versus Svp-KO#2 $P < 0.001$. In all panels, transcription factor of interest is in white and T2NBs identified with Pnt-Gal4>GFP and Dpn. Scale bars: 5 μm.

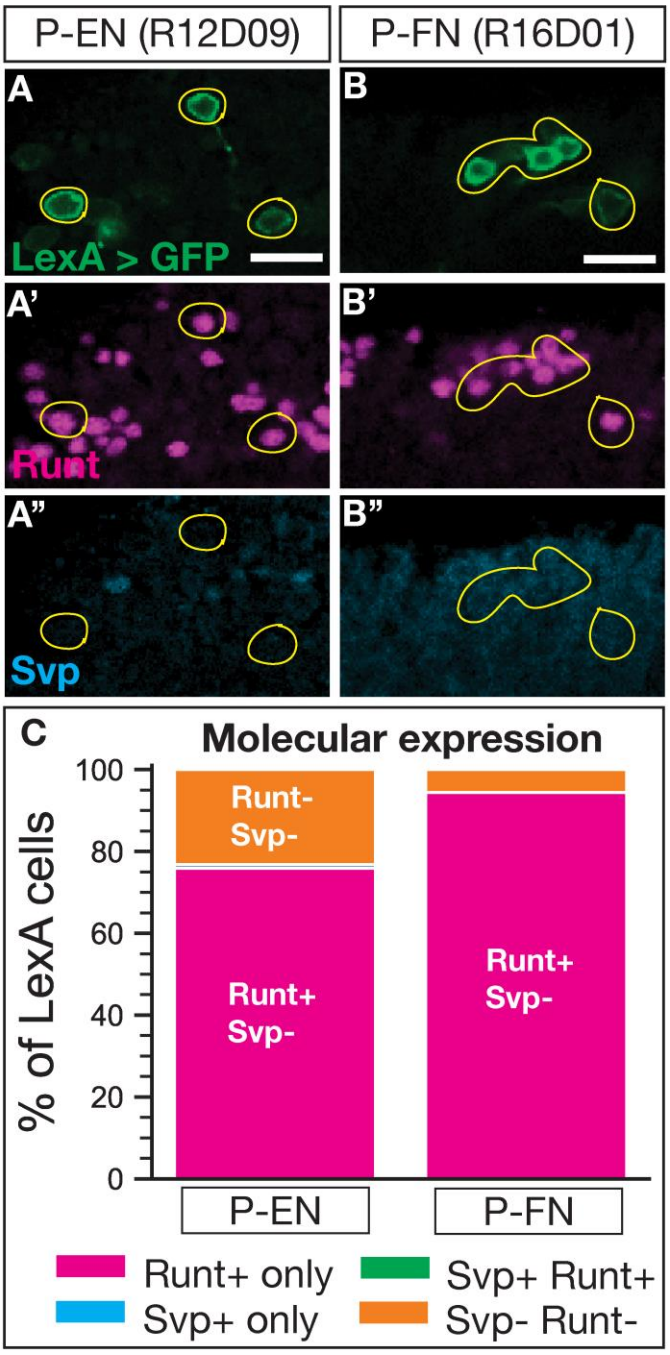

Supplemental Figure 3.3. Adult P-EN and P-FN neurons do not express Svp. (A-B'') P-EN and P-FN neurons labeled by LexA driver lines express Runt but do not Svp. (C) Quantification of molecular expression in P-EN and P-FN neurons. P-EN and P-FN, n = 6 brains. In all panels, LexA+ neurons in green, Runt in magenta, and Svp in cyan. Yellow outline, neurons of interest. Scale bars: 10 μm.

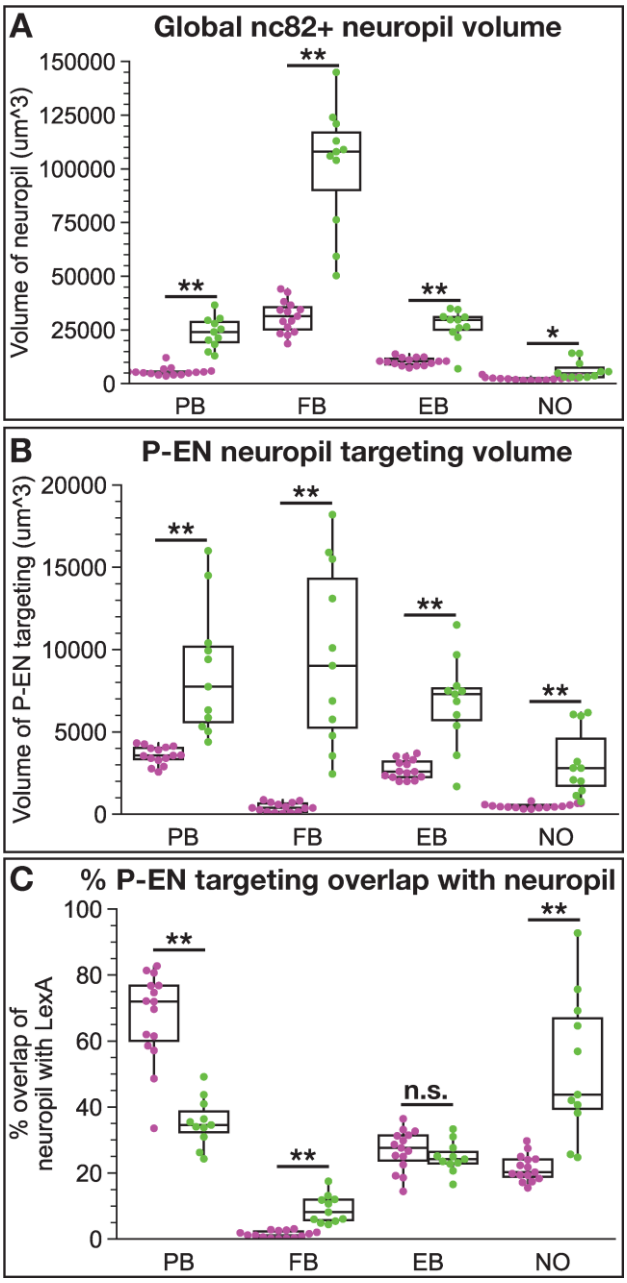

Supplemental Figure 3.4. Svp in T2NBs regulates adult CX neuropil development. (A-C) Quantifications of neuropil volumes between Controls and Svp-KO#1. All plots show each dot representing one adult brain with box and whisker plot showing distribution. For all panels, Control, n = 15; Svp-KO#1, n = 11 brains, and *P*-values determined by independent t-tests. (A) Quantification of CX neuropil volume (μm^3) from nc82 reconstruction. Control versus Svp-KO#1 for PB $P < 0.001$, for FB $P < 0.001$, for EB $P < 0.001$, for NO $P = 0.012$. (B) P-EN LexA neuron targeting volume (μm^3) to CX neuropils. Control versus Svp-KO#1 for PB $P = 0.002$, for FB $P < 0.001$, for EB $P < 0.001$, for NO $P < 0.001$. (C) Percent of CX neuropil volume (μm^3) targeted by P-EN LexA neurons. Control versus Svp-KO#1 for PB $P < 0.001$, for FB $P < 0.001$, for EB $P = 0.34$, for NO $P < 0.001$.

Supplementary table 3.1. Transgenes and *Drosophila melanogaster* stock lines used in Dillon et al., 2024.

Genotype	Source and identifier	Additional information
R12D09-LexA	BDSC #54419	Expressed in P-EN neurons
R16D01-LexA	BDSC #52503	Expressed in P-FN neurons
13xLexAop-myr::GFP	BDSC #32210	Expresses membrane bound GFP under LexAop control
10XUAS-IVS-myr::GFP	BDSC #32198	Expresses membrane bound GFP under UAS control
Pointed-Gal4	*PMID:* 22143802 *14-94*	Expressed in Type 2 lineage starting in the neuroblast
10xUAS-IVS-myr::smGdP::HA, 13xLexAop2-IVS-myr::smGdP::V5	BDSC #64092	Expresses HA membrane tag under UAS control, V5 membrane tag under LexAop control
hsFLP; ;UAS-Cas9.P2	BDSC #58986	Expresses Cas9 under UAS control
hsFLP; UAS-sgRNA::svp ;	VDRC #341527	Expresses two short guide RNAs against Svp under UAS control; Svp-KO#1
hsFLP; UAS-sgRNA::svp ;	VDRC #341390	Expresses two short guide RNAs against Svp under UAS control; Svp-KO#2

Supplementary table 3.2. Genetic crosses for each experiment in Dillon et al., 2024.

Figures	Summary	Genetic cross
Figure 1;	(i) Labels adult P-EN neurons (ii) Labels adult P-FN neurons	Females containing *13xLexAop-myr::GFP* were crossed to males containing either (i) *R12D09-LexA* or (ii) *R16D01-LexA*
Figure 2; Supplemental Figure 1	Labels larval Type 2 lineage	Self-cross of females and males containing *10XUAS-IVS-myr::GFP ; Pointed-Gal4*
Figure 3; Supplemental Figure 3	(i) Labels adult P-EN neurons (ii) Labels adult P-FN neurons	Self-cross of females and males containing (i) *10xUAS-IVS-myr::smGdP::HA, 13xLexAop2-IVS-myr::smGdP::V5*; *R16D01-LexA*; *Pointed-Gal4* or (ii) *10xUAS-IVS-myr::smGdP::HA, 13xLexAop2-IVS-myr::smGdP::V5* ; *R12D09-LexA* ; *Pointed-Gal4*
Figure 4	(i) Control (ii) Svp-KO#1 (iii) Svp-KO#2	Females containing *10xUAS-IVS-myr::smGdP::HA, 13xLexAop2-IVS-myr::smGdP::V5*; *R16D01-LexA*; *Pointed-Gal4* were crossed to males containing either (i) *hsFLP* or + ; *UAS-Cas9.P2*, (ii) *hsFLP* or + ; *UAS-sgRNA::svp* (VDRC #341527) ; *UAS-Cas9.P2* , or (iii) *hsFLP* or + ; *UAS-sgRNA::svp* (VDRC #341390) ; *UAS-Cas9.P2*
Figure 5; Figure 6; Supplement Figure 4	(i) Control (ii) Svp-KO#1 (iii) Svp-KO#2	Females containing *10xUAS-IVS-myr::smGdP::HA, 13xLexAop2-IVS-myr::smGdP::V5* ; *R12D09-LexA* ; *Pointed-Gal4* were crossed to males containing either (i) *hsFLP* or + ; + ; *UAS-Cas9.P2*, (ii) *hsFLP* or + ; *UAS-sgRNA::svp* (VDRC #341527) ; *UAS-Cas9.P2,* or (iii) *hsFLP* or + ; *UAS-sgRNA::svp* (VDRC #341390) ; *UAS-Cas9.P2*
Figure 7; Supplemental Figure 2	(i) Control (ii) Svp-KO#1 (iii) Svp-KO#2	Females containing *10XUAS-IVS-myr::GFP; Pointed-Gal4* were crossed to males containing either (i) *hsFLP ; ; UAS-Cas9.P2* , (ii) *hsFLP* or + ; *UAS-sgRNA::svp* (VDRC #341527) ; *UAS-Cas9.P2* , or (iii) *hsFLP* or + ; *UAS-sgRNA::svp* (VDRC #341390) ; *UAS-Cas9.P2*

Supplementary table 3.3. Antibodies used in Dillon et al., 2024.

Antibody	Source and identifier	Additional information
Chicken anti-GFP	Aves: 1020	(1:1000)
Mouse anti-Seven-up 6F7	DSHB: Hiromi, Y. / Hondo, T. / Kanda, H.	(1:4)
Rat anti-Deadpan	Abcam: 11D1 BC7.1B	(1:20)
Guinea pig anti-Runt	Claude Desplan lab (NYU)	(1:1000)
Mouse -anti-Cut 2B10	DSHB: Rubin, G.M.	(1:10)
Mouse anti-V5 tag	ThermoFisher: R960-25 (previously Invitrogen 46-0705)	(1:1000)
Rabbit anti-V5 tag	Cell signaling: 13202S	(1:1000)
Rat anti-CadN DN-Ex #8	DSHB: Uemura, T	(1:50)
Mouse anti-nc82	DSHB: Buchner, E.	(1:100)
Rat anti-Imp	Claude Desplan lab (NYU)	(1:200)
Rabbit anti-Imp	Paul Macdonald	(1:500)
Rabbit anti-Syncrip	Claude Desplan lab (NYU)	(1:200)
Rabbit anti-pHH3	Millipore Sigma: MC463	(1:1000)
Mouse anti-pHH3	Abcam: 14955	(1:1000)
Guinea pig anti-Eip93	GenScript: 542604-33	(1:500)
Alexa Fluor® 488 AffiniPure Donkey Anti-Chicken IgY (IgG) (H+L)	Jackson ImmunoResearch, West Grove, PA: 703-545-155	(1:400)
Rhodamine Red™-X (RRX) AffiniPure Donkey Anti-Rat IgG (H+L)	Jackson ImmunoResearch, West Grove, PA: 712-295-153	(1:400)
Alexa Fluor® 647 AffiniPure Donkey Anti-Mouse IgG (H+L)	Jackson ImmunoResearch, West Grove, PA: 715-605-151	(1:400)
Rhodamine Red™-X (RRX) AffiniPure Donkey Anti-Guinea pig IgG (H+L)	Jackson ImmunoResearch, West Grove, PA: 706-295-148	(1:400)
Alexa Fluor® 488 AffiniPure Donkey Anti-Mouse IgG (H+L)	Jackson ImmunoResearch, West Grove, PA: 715-295-151	(1:400)
Alexa Fluor® 488 AffiniPure Donkey Anti-Rabbit IgG (H+L)	Jackson ImmunoResearch, West Grove, PA: 711-295-152	(1:400)
Rhodamine Red™-X (RRX) AffiniPure Donkey Anti-Mouse IgG (H+L)	Jackson ImmunoResearch, West Grove, PA: 715-295-151	(1:400)
Alexa Fluor® 405 AffiniPure Donkey Anti-Rabbit IgG (H+L)	Jackson ImmunoResearch, West Grove, PA: 711-475-152	(1:400)

Appendix B. Chapter IV supplementary figures and tables

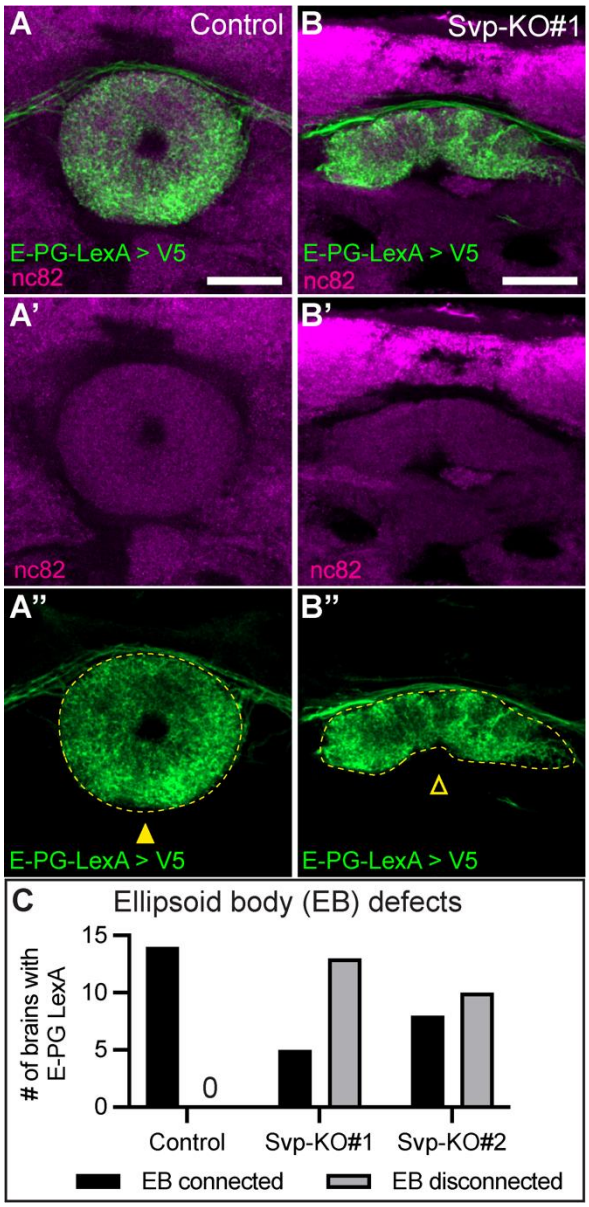

Supplemental Fig 4.1. Loss of Seven-up in Type 2 neuroblasts leads to altered E-PG ellipsoid body morphology. (A-B) Control (A) and Seven-up (Svp) knockout (B). There is altered morphology of R60D05-LexA+ E-PG neurons in the Svp knockout with a disconnected ellipsoid body (EB). (C) Quantification. Control, n = 14; Svp-KO#1, n = 18; Svp-KO#2, n = 18. P-value determined by Chi-square analysis ** P<0.001. In all images, LexA+ neurons driving V5 expression are in green, neuropil nc82 in magenta, and EB outlined in yellow dashed line. Closed arrowhead indicates a connected EB; open arrowhead indicates a disconnected EB. Scale bars: 20 μm.

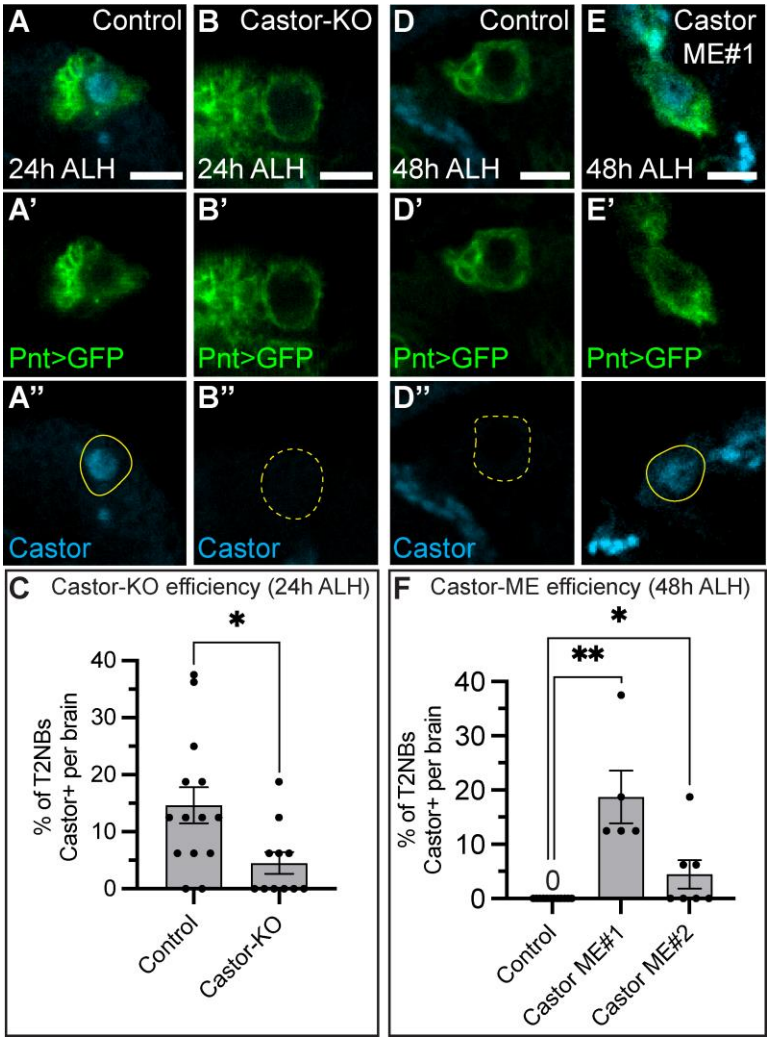

Supplemental Fig 4.2. Generating Type 2 lineage specific Castor knockout and misexpression lines. (A-C) Control (A) and Castor-KO (B) show a loss of Castor in Type 2 neuroblasts (T2NB) in the Castor-KO at 24h after larval hatching (ALH). (C) Quantification. Bar plot shows mean with standard error of the mean (SEM). Each dot represents one brain. Control, *n*=14; Castor-KO, *n*=11. *P*-value was determined using an unpaired *t*-test, **P*=0.017. (D-F) Control (A) and Castor misexpression (ME) (B) show ectopic expression of Castor in Type 2 neuroblasts (T2NB) in the Castor-ME at 48h after larval hatching (ALH). (F) Quantification. Bar plot shows mean with SEM. Each dot represents one brain. Control, *n*=12; Castor 2nd, *n*=5; Castor 3rd, *n*=7. *P*-values were determined using a one-way ANOVA, ***P*<0.001, followed by unpaired *t*-tests between the control and Castor-MEs: Control versus Castor 2nd, ***P*<0.001; Control versus Castor 3rd, **P*=0.036. In all images, Pnt-Gal4 driving GFP in green and T2NBs outlined in yellow; solid line indicates positive for Castor, dashed line indicates negative for Castor; Castor, cyan. Scale bars: 5 μm.

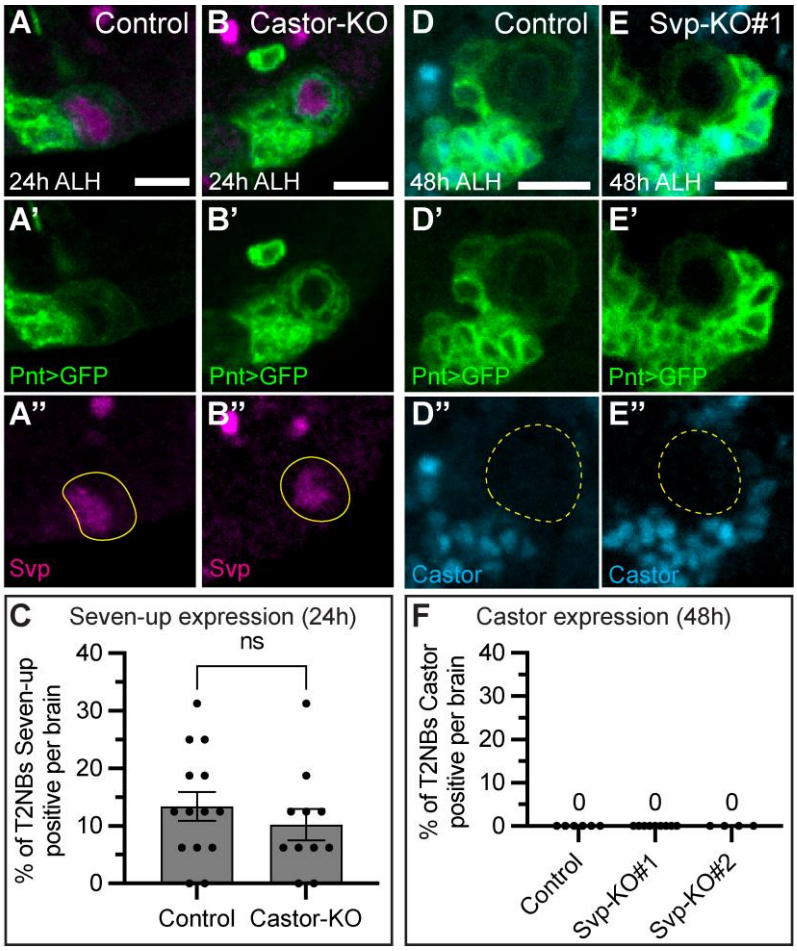

Supplemental Fig 4.3. Castor and Seven-up do not cross regulate in Type 2 neuroblasts. (A-C) Control (A) and Castor-KO (B) shows no change in Seven-up (Svp) expression in Type 2 neuroblasts (T2NB) in the Castor-KO at 24 h ALH. (C) Quantification. Bar plot shows mean with standard error of the mean. Each dot represents one brain. Control, *n*=14; Castor-KO, *n*=11. *P*-value was determined using an unpaired *t*-test, **P*=0.40. (D-E) Control (D) and Svp-KO#1 (E) shows no extended expression of Castor in Type 2 neuroblasts (T2NB) in the Svp-KO at 48 h ALH. (F) Quantification. Bar plot shows mean with no error bars due to no differential values. Each dot represents one brain. Control, *n*=6; Svp-KO#1, *n*=9; Svp-KO#2, *n*=4. *P*-value was not determined due to no differential values reported between conditions. In all images, Pnt-Gal4 driving GFP in green and T2NBs outlined in yellow; solid line indicates positive for transcription factor of interest, dashed line indicates negative for transcription factor of interest; Svp, magenta; Castor, Cyan. Scale bars: 5 μm.

Supplementary table 1. Transgenes and *Drosophila melanogaster* stock lines used in Dillon and Doe 2024.

Genotype	Source and identifier	Additional information
R12D09-LexA	BDSC #54419	Expressed in P-EN neurons
R60D05-LexA	BDSC # 52867	Expressed in E-PG neurons
13xLexAop-myr::GFP	BDSC #32210	Expresses membrane bound GFP under LexAop control
10XUAS-IVS-myr::GFP	BDSC #32198	Expresses membrane bound GFP under UAS control
Pointed-Gal4	*PMID:* 22143802 *14-94*	Expressed in Type 2 lineage starting in the neuroblast
10xUAS-IVS-myr::smGdP::HA, 13xLexAop2-IVS-myr::smGdP::V5	BDSC #64092	Expresses HA membrane tag under UAS control, V5 membrane tag under LexAop control
hsFLP; ;UAS-Cas9.P2	BDSC #58986	Expresses Cas9 under UAS control
hsFLP; UAS-sgRNA::svp ;	VDRC #341527	Expresses two short guide RNAs against Svp under UAS control; Svp-KO#1
hsFLP; UAS-sgRNA::svp ;	VDRC #341390	Expresses two short guide RNAs against Svp under UAS control; Svp-KO#2
hsFLP; UAS-sgRNA::castor ;	VDRC #341386	Expresses two short guide RNAs against Castor under UAS control
; UAS-LacZ ;	BDSC #8529	Expresses LacZ under UAS control
; UAS-Castor ;	Odenwald, W.	Expresses Castor under UAS control
; ; UAS-Castor	Odenwald, W.	Expresses Castor under UAS control

Supplementary table 2. Genetic crosses for each experiment in Dillon and Doe 2024.

Figures	Summary	Genetic cross
Figure 1C-E	Labels adult E-PG neurons for EdU birth dating	Females containing *13xLexAop-myr::GFP* were crossed to males containing R60D05-*LexA*
Figure 2A-C Figure 4M-O	Labels adult E-PG (i) and P-EN (ii) neurons for molecular markers	Self-cross of females and males containing (i) *10xUAS-IVS-myr::smGdP::HA, 13xLexAop2-IVS-myr::smGdP::V5*; *R60D05-LexA*; *Pointed-Gal4* or (ii) *10xUAS-IVS-myr::smGdP::HA, 13xLexAop2-IVS-myr::smGdP::V5* ; *R12D09-LexA* ; *Pointed-Gal4*
Figure 3A-F Figure S1A-C	Labels adult E-PG neurons and drives UAS constructs in the Type 2 progenitors for: Cas9.P2 control (i) Svp-KO#1 (ii) Svp-KO#2 (iii)	Females containing *10xUAS-IVS-myr::smGdP::HA, 13xLexAop2-IVS-myr::smGdP::V5*; *R60D05-LexA*; *Pointed-Gal4* were crossed to males containing either (i) *; ; UAS-Cas9.P2*, (ii) ; *UAS-sgRNA::svp* (VDRC #341527) ; *UAS-Cas9.P2* , or (iii) ; *UAS-sgRNA::svp* (VDRC #341390) ; *UAS-Cas9.P2*
Figure 4A-L	Labels larval Type 2 lineage	Self-cross of females and males containing *10XUAS-IVS-myr::GFP ; Pointed-Gal4*
Figure 5A-F	Labels adult P-EN neurons and drives UAS constructs in the Type 2 progenitors for: Cas9.P2 control (i) Castor-KO#1 (ii)	Females containing *10xUAS-IVS-myr::smGdP::HA, 13xLexAop2-IVS-myr::smGdP::V5*; *R12D09-LexA*; *Pointed-Gal4* were crossed to males containing either (i) *; ; UAS-Cas9.P2*, (ii) ; *UAS-sgRNA::castor*; *UAS-Cas9.P2*
Figure 5G-L	Labels adult E-PG neurons and drives UAS constructs in the Type 2 progenitors for: Cas9.P2 control (i) Castor-KO#1 (ii)	Females containing *10xUAS-IVS-myr::smGdP::HA, 13xLexAop2-IVS-myr::smGdP::V5*; *R60D05-LexA*; *Pointed-Gal4* were crossed to males containing either (i) *; ; UAS-Cas9.P2*, (ii) ; *UAS-sgRNA::castor*; *UAS-Cas9.P2*
Figure 6A-F	Labels adult P-EN neurons and drives UAS constructs in	Females containing *10xUAS-IVS-myr::smGdP::HA, 13xLexAop2-IVS-myr::smGdP::V5*; *R12D09-LexA*; *Pointed-Gal4* were crossed to males containing

	the Type 2 progenitors for: LacZ control (i) Castor ME#1 (ii) Castor ME#2 (iii)	either (i) *; UAS-LacZ ;* (ii) ; *UAS-Castor* ; (iii) ; ; *UAS-Castor*
Figure 6G-L	Labels adult E-PG neurons and drives UAS constructs in the Type 2 progenitors for: LacZ control (i) Castor ME#1 (ii) Castor ME#2 (iii)	Females containing *10xUAS-IVS-myr::smGdP::HA, 13xLexAop2-IVS-myr::smGdP::V5*; *R60D05-LexA*; *Pointed-Gal4* were crossed to males containing either (i) *; UAS-LacZ ;* (ii) ; *UAS-Castor* ; (iii) ; ; *UAS-Castor*
Figure S2A-F	Labels larval Type 2 lineage and drives UAS constructs in the Type 2 progenitors for: Cas9.P2 control (i) Castor-KO#1 (ii) LacZ control (iii) Castor ME#1 (iv) Castor ME#2 (v)	Females containing *10XUAS-IVS-myr::GFP ; Pointed-Gal4* were crossed to males containing either (i) *; ; UAS-Cas9.P2*, (ii) ; *UAS-sgRNA::castor*; *UAS-Cas9.P2* (iii) *; UAS-LacZ ;* (iv) ; *UAS-Castor* ; (v) ; ; *UAS-Castor*
Figure S3A-C	Labels larval Type 2 lineage and drives UAS constructs in the Type 2 progenitors for: Cas9.P2 control (i) Castor-KO (ii)	Females containing *10XUAS-IVS-myr::GFP ; Pointed-Gal4* were crossed to males containing either (i) *; ; UAS-Cas9.P2*, (ii) ; *UAS-sgRNA::castor*; *UAS-Cas9.P2*
Figure S3D-F	Labels larval Type 2 lineage and drives UAS constructs in the Type 2 progenitors for: Cas9.P2 control (i) Svp-KO#1 (ii) Svp-KO#2 (iii)	Females containing *10XUAS-IVS-myr::GFP ; Pointed-Gal4* were crossed to males containing either (i) *; ; UAS-Cas9.P2*, (ii) ; *UAS-sgRNA::svp* (VDRC #341527) ; *UAS-Cas9.P2* , or (iii) ; *UAS-sgRNA::svp* (VDRC #341390) ; *UAS-Cas9.P2*

Supplementary table 3. Antibodies used in Dillon and Doe 2024.

Antibody	Source and identifier	Additional information
Chicken anti-GFP	Aves: 1020	(1:1000)
Rabbit anti-Castor	PMID:1418995; W. Odenwald	(1:1000)
Mouse anti-Seven-up 6F7	DSHB: Hiromi, Y. / Hondo, T. / Kanda, H.	(1:4)
Rat anti-Deadpan	Abcam: 11D1 BC7.1B	(1:20)
Guinea pig anti-Runt	Claude Desplan lab (NYU)	(1:1000)
Guinea pig anti-Toy	Genscripts U1806FG070_27/DC0126	(1:1000)
Mouse anti-Cut 2B10	DSHB: Rubin, G.M.	(1:10)
Mouse anti-Dac mAbdac1-1	DSHB: Rubin, G.M.	(1:50)
Mouse anti-Elav 9F8A9	DSHB: Rubin, G.M.	(1:50)
Mouse anti-V5 tag	ThermoFisher: R960-25 (previously Invitrogen 46-0705)	(1:1000)
Rabbit anti-V5 tag	Cell signaling: 13202S	(1:1000)
Mouse anti-nc82	DSHB: Buchner, E.	(1:100)
Alexa Fluor® 488 AffiniPure Donkey Anti-Chicken IgY (IgG) (H+L)	Jackson ImmunoResearch, West Grove, PA: 703-545-155	(1:400)
Rhodamine Red™-X (RRX) AffiniPure Donkey Anti-Rat IgG (H+L)	Jackson ImmunoResearch, West Grove, PA: 712-295-153	(1:400)
Alexa Fluor® 647 AffiniPure Donkey Anti-Mouse IgG (H+L)	Jackson ImmunoResearch, West Grove, PA: 715-605-151	(1:400)
Rhodamine Red™-X (RRX) AffiniPure Donkey Anti-Guinea pig IgG (H+L)	Jackson ImmunoResearch, West Grove, PA: 706-295-148	(1:400)

Alexa Fluor® 488 AffiniPure Donkey Anti-Mouse IgG (H+L)	Jackson ImmunoResearch, West Grove, PA: 715-295-151	(1:400)
Alexa Fluor® 488 AffiniPure Donkey Anti-Rabbit IgG (H+L)	Jackson ImmunoResearch, West Grove, PA: 711-295-152	(1:400)
Rhodamine Red™-X (RRX) AffiniPure Donkey Anti-Mouse IgG (H+L)	Jackson ImmunoResearch, West Grove, PA: 715-295-151	(1:400)
Alexa Fluor® 405 AffiniPure Donkey Anti-Mouse IgG (H+L)	Jackson ImmunoResearch, West Grove, PA: 715-475-150	(1:200)